Université de Montréal

# Deciphering mRNP – nuclear pore interactions: Study of basket protein dynamics in budding yeast

*Par*

Pierre Bensidoun

Département de biochimie et médecine moléculaire, Faculté de médecine

Thèse présentée en vue de l'obtention du grade de doctorat en biochimie

Août 2021

Université de Montréal

Département de biochimie et médecine moléculaire, Faculté de médecine

---

Cette thèse est intitulée

# Deciphering mRNP – nuclear pore interactions: Study of basket protein dynamics in budding yeast

*Présentée par*

Pierre Bensidoun

*A été évaluée par un jury composé des personnes suivantes*

Mohan Malleshaiah
Président-rapporteur

Marlene Oeffinger & Daniel Zenklusen
Co-Directeurs de recherche

Lea Harrington
Membre du jury

Anita Corbett
Examinateur externe

Alain Verreault
Représentant de la Doyenne

# Résumé

L'exportation des ARN messagers du noyau vers le cytoplasme est l'une des nombreuses étapes de la voie d'expression des gènes et est fondamentale pour que les ARNm rencontrent les ribosomes pour être traduits dans le cytoplasme. Les échanges entre le noyau et le cytoplasme se font par l'intermédiaire du complexe du pore nucléaire, qui est un grand complexe multiprotéique enchâssé dans la membrane nucléaire et assemblé par 30 protéines différentes, les nucléoporines. Le versant nucléoplasmique du pore orchestre de nombreux processus nucléaires fondamentaux. En effet, un nombre croissant d'études suggère que le pore nucléaire est impliqué dans un large éventail d'activités, notamment la modulation de la topologie de l'ADN, la réparation de l'ADN, la régulation épigénétique de l'expression des gènes et l'accès sélectif aux molécules candidates à l'export. Le composant structurel nécessaire pour orchestrer ces fonctions nucléoplasmiques est appelé le panier une structure de ~60 à 80 nm de long faisant saillie dans le nucléoplasme. Une vision consensuelle dépeint le panier comme une structure assemblée par des protéines filamenteuses convergeant en un anneau distal, TPR (Translocated Promoter Region protein) chez l'homme et par ses deux paralogues Mlp1 et Mlp2 (myosin-like proteins) chez la levure.

Dans la première partie de cette thèse, nous avons caractérisé le mouvement d'ARNm spécifiques au voisinage de la périphérie nucléaire. Nous avons observé que les transcrits scannent l'enveloppe nucléaire, probablement pour trouver un pore nucléaire afin d'être exportés. Nous avons également montré que ce comportement était affecté par la délétion ou la troncation de Mlp1 ainsi que par la mutation de la protéine de liaison aux queues poly(A) Nab2. Ces observations indiquent que Mlp1 et donc les paniers, ainsi que des protéines liant l'ARN, facilitent l'interaction des ARNm avec la périphérie nucléaire.

Alors que la structure canonique du pore nucléaire est bien établie, notre compréhension des conditions et des facteurs contribuant à l'assemblage du panier, ainsi que de la stœchiométrie de ses composants, reste incomplète. Bien que les protéines du panier soient impliquées dans la régulation de l'expression des gènes par l'ancrage des gènes à la périphérie nucléaire et dans le recrutement des ARNm avant leur export, la manière dont le panier intervient dans ce processus est mal comprise. De plus, la dynamique des protéines du panier chez la levure semble obéir à des

règles différentes de celles des autres nucléoporines, car leur renouvellement (turn over) au niveau du pore est plus rapide que celui des autres composants du NPC. De plus, il a été observé que lors d'un choc thermique, Mlp1 et Mlp2 se dissocient des pores nucléaires et forment des granules intra-nucléaires, séquestrant les ARNm et les facteurs d'exportation d'ARN. Pourtant, le mécanisme de formation de ces granules ou leur rôle pendant le choc thermique est mal compris. Chez la levure, le panier nucléaire n'est pas associé à tous les pores nucléaires, et les paniers sont absents des pores adjacents au nucléole. La manière dont les cellules établissent ces pores sans paniers et s'ils représentent des pores nucléaires spécialisés ayant des fonctions différentes des pores contenant des corbeilles n'est pas connue.

Pour comprendre la dynamique de l'assemblage des paniers et la pertinence biologique de former de deux types de pores distincts, nous avons disséqué les processus biologiques menant à la formation des paniers. De plus, afin de mettre en évidence les différences fonctionnelles potentielles entre les deux types de pores nous avons étudié les protéines associées aux pores contenant un panier nucléaire et des pores sans panier. Nous avons montré que l'assemblage d'un panier n'est pas un mode par défaut pour un pore dans le nucléoplasme et que la formation et la maturation des ARNm est nécessaire pour maintenir l'intégrité des paniers. Alors que l'ARNm peut être trouvé associé aux deux types de pores, nos résultats suggèrent que la cinétique d'export peut être différente sur les pores avec et sans panier.

Les eucaryotes organisent leur noyau en régions fonctionnelles discrètes et l'enveloppe nucléaire a été envisagée comme pouvant être une organelle à part entière. Nos analyses indiquent que les ARNm et Mlp1 participent à un degré supplémentaire de compartimentation nucléaire en permettant la formation d'une structure dynamique : le panier. Mon projet apporte un nouvel éclairage sur l'organisation des compartiments nucléaire et met en évidence l'intrication surprenante entre l'export des ARNm et la plasticité des pores nucléaires.

Mots-clés : Pores nucléaires, Paniers nucléaires, Dynamiques des protéines Mlp1, métabolisme des ARN messager

# Abstract

The export of mRNAs from the nucleus to the cytoplasm is one of many steps along the gene expression pathway and is fundamental for mRNAs to meet with ribosomes for translation in the cytoplasm. Exchanges between nucleus and cytoplasm occur through the nuclear pore complex (NPC), which is a large multi-protein complex embedded in the nuclear membrane and assembled by 30 different proteins the nucleoporins. The nucleoplasmic side of the pore is believed to orchestrate many fundamental nuclear processes. Indeed, a growing body of evidence suggests that the nuclear pore is involved in a broad range of activities including modulation of DNA topology, DNA repair, epigenetic regulation of gene expression, and selective access to exporting molecules. The structural component required for orchestrating those nucleoplasmic functions is the basket, a ~60- to 80-nm-long structure protruding into the nucleoplasm. The consensus view depicts the basket as a structure assembled by filamentous proteins, TPR (Translocated Promoter Region protein) in humans and by its two paralogues Mlp1 and Mlp2 (myosin-like proteins) in yeast, converging into a distal ring.

In the first part of this thesis, we characterized the motion of specific mRNAs at the vicinity of the nuclear periphery. We observed that transcripts scan along the nuclear envelope, likely to find a nuclear pore to be exported. We also showed the scanning behavior was affected upon Mlp1 deletion or truncation as well as upon mutation of the nuclear poly(A) binding protein Nab2. These observations indicated that Mlp1 and hence baskets, as well as specific RNA binding proteins, facilitate the interaction of mRNA with the nuclear periphery.

While the canonical structure of the NPC is well established, our understanding of the conditions and factors contributing to the assembly of a basket, as well as the stoichiometry of its components, remains incomplete. Although basket proteins have been implicated in the regulation of gene expression through gene anchoring to the nuclear periphery and in mRNA scanning before export, how this is mediated by Mlp1/2 is poorly understood. Moreover, the dynamics of basket proteins in yeast seem to obey different rules than those of other nucleoporins as their turnover at the pore is faster than any other NPC components. Furthermore, it has been observed that during heat shock Mlp1 and Mlp2 dissociate from nuclear pores and form intra-nuclear granules, sequestering mRNAs and RNA export factors. Yet the mechanism for the formation of these

granules or their role during heat shock is poorly understood. In yeast, the nuclear baskets are not associated with all NPCs, as no baskets assemble on the pores adjacent to the nucleolus. Yet, how cells establish these basket-less pores and whether they represent specialized nuclear pores with different functions from basket-containing pores is still unknown.

To understand the dynamics of basket assembly and the biological relevance of establishing distinct sets of pores, we dissected the biological processes leading to the formation of baskets. In addition, to highlight potential functional differences between the two types of pores, we identified the interactors of nuclear basket-containing and nucleolar basket-less pores. We showed that assembling a basket is not a default mode for a pore in the nucleoplasm and that active mRNA processing is required to maintain baskets integrity. While mRNA can be found associated with both types of pores, our results suggest that export kinetics may be different on basket-containing and basket-less pores.

The eukaryotes organize their nucleus in discrete functional regions and the nuclear envelope has been envisioned as an organelle by and of itself. Our analyzes indicate that mRNAs and Mlp1 participate in an additional degree of nuclear compartmentalization by enabling the formation of a dynamic structure: the basket. Overall, my project sheds new light on the nuclear organization and highlights the surprising entanglement between mRNA export and NPC plasticity.

Keywords: Nuclear pore complexes, Nuclear basket, Mlp1 protein dynamic(s) , mRNA metabolisms

# Table des matières

# Liste des tableaux

# Liste des figures

# Liste des sigles et abréviations

3’ UTR: 3’ untranslated region

3C : Chromosome conformation capture

AP : Affinity purification

ChIP : Chromatin immunoprecipitation

CIHR : Canadian Institute of Health Research

CPF : cleavage/polyadenylation factors

CTD : C-terminal domain

DDR : DNA damage response

DSB : Double strand break

EM : Electron microscopy

FISH : fluorescent hybridization *in situ*

FRQS : Fonds de Recherche Québec Santé

H2A : Histone H2A

IDD : intrinsically disordered domain

lncRNA : long non-coding RNA

m6A : N6-methyladenosine

MAX : maximum intensity projection

MGL : Memory gene loop

mRNA : messenger RNA

mRNP : messenger ribonucleoprotein

MS: mass spectrometry

NE : Nuclear envelope

NEAT1 : Nuclear Enriched Abundant Transcript 1

NHEJ : non-homologous end-joining

NPC : nuclear pore complex

Pol II : Polymerase II

Poly(A) RNA : Polyadenylated RNA

PTM : Post-translational modification

QC : Quality control

R-Loop : RNA loop

rARN : ribosomal ARN

RBP : RNA binding protein

RNA : Ribonucleic acid

RNAi : RNA interference

RNP : Ribonucleoprotein

SDS-PAGE : Sodium dodecyl sulfate polyacrylamide gel electrophoresis

Ser : Serine

SIM : structured illumination microscopy

snoRNA : Small nucleolar RNA

SUMO : Small ubiquitin-like modifier

TADs : Topologically associated domains

TREX :Transcription and Export

WT : Wild type

*Pluralitas non est ponenda sine necessitate*

(les multiples ne doivent pas être utilisés sans nécessité)
(Plurality should not be posited without necessity)

Guillaume d'Ockham *Quaestiones et decisiones in quatuor libros Sententiarum cum centilogio theologico*, livre II (1319).

# Remerciements

Je voudrais en premier lieu remercier mes directeurs de recherche, Marlene Oeffinger et Daniel Zenklusen. Merci de m'avoir accueilli au sein de vos laboratoires, de m'avoir formé, appris à disséquer les articles avec un regard critique. Merci pour les conseils sur l'écriture et les présentations, toujours délivrés avec beaucoup de patience et de bienveillance.

Merci à tous les membres des Labos Oeffinger et Zenklusen. Particulièrement Pascal et Carolina tout ce je sais des levures je l'ai appris d'eux, (je n'ai pas tout retenu, mais c'est déjà beaucoup). Merci à Christian et Vatsi pour le soutien moral, les blagues et le gros coup de main pour les designs expérimentaux. Vatsi est une des rares personnes capables d'écouter une phrase jusqu'au bout, et c'est bien moins fréquent qu'on ne le pense. Certains footballeurs disent qu'ils ont eu la chance de jouer avec Zidane, je pourrai dire que j'ai eu la chance de faire de la science avec Vatsi.

Merci aux membres de mon comité de thèse, Dr Pascal Chartrand et Dr Stephen Michnick ainsi qu'aux nombreux chercheurs qui m'ont encouragé au long de mon projet au Canada et en France, particulièrement Stéphanie Weber, Martin Sauvageau, François Robert, Celia Jeronimo, François Bachand, Rodrigo Reyes-Lamothe, Pierre-Emmanuel Gleizes, Jérôme Cavaillé, Marie-Line Bortolin et Nicole Francis. Merci également aux membres de mon jury de thèse pour avoir accepté d'évaluer mes travaux, Mohan Malleshaiah, Lea Harrington, Anita Corbett et Alain Verreault.

Merci à mes parents pour m'avoir transmis le gout des questions et l'envie d'essayer d'y répondre, et à Rémi avec qui je partage lesdites questions.

Merci à tous les amis de l'université, Maxime, Charline, Aurélien, Hadrien, Camille pour les voyages et les fêtes et les apéros. Ainsi que pour les théories les plus tabous concernant les hybridations ARNm-ARNm dans la cellule. On en reparle bientôt en Europe. Merci aux amis en dehors de la fac pour toutes les années de vie communes, Nai, Thib et Nico, Iri, Elo, Luis, Léo. Merci à Vivi pour sa confiance et son soutien indéfectible et les heures (indues) de partages autour de sujets passionnants que je n'aurai pas découvert sans toi. Merci aux Monks. Thomas, Marc,

Saminou, Pilou, Pierre-Manu, Elise, Manu, Steph, Mariama, Dude, Léa, Yaya, Quentin. Un immense merci à Flore pour m'avoir supporté, écouté, et encouragé pendant toutes ces années.

Finalement merci à Bob Dylan, Vincent Moscato, Eric Di Meco, Trent Reznor et Mike Patton cela n'aurait jamais été possible sans eux.

# Acknowledgements

First, I would like to thank my research supervisors, Marlene Oeffinger and Daniel Zenklusen. Thank you for hiring me in your laboratories, training us, and teaching me to dissect articles with a critical eye. Thank you for the advice on writing and presentation, always delivered with great patience and kindness.

Thanks to all the members of the Oeffinger and Zenklusen Labs. Especially Pascal and Carolina, everything I know about yeast came from them (I didn't remember everything about it, but it is already a lot). Thanks to Christian and Vatsi for the moral support, the jokes, and the experimental designs' help. Vatsi is one of the few people able to listen to a sentence until the end, and it's much rarer than you think. Some soccer players said they had the chance to play with Zidane; I could say I had the opportunity to do science with Vatsi.

Thanks to the members of my thesis committee, Dr Pascal Chartrand and Dr Stephen Michnick, and to the many researchers who encouraged me throughout my project in Canada and France, especially Stephanie Weber, Martin Sauvageau, François Robert, Celia Jeronimo, Nicole Francis, François Bachand, Rodrigo Reyes-Lamothe, Pierre-Emmanuel Gleizes, Jérôme Cavaillé and Marie-Line Bortolin. Thanks also to the jury members for accepting to evaluate my work, Mohan Malleshaiah, Lea Harrington, Anita Corbett and Alain Verreault.

Thanks to my parents for giving me a taste for questions and the desire to answer them and Remi with whom I share those questions.

Thanks to all the university friends, Maxime, Charline, Aurélien, Hadrien, Camille, for the trips and the parties and for coming up with the tabooest theories about mRNA-mRNA hybridization in the cell. We will talk about it soon in Europe.

Thanks to my friends outside of university for all the years together, Nai, Thib and Nico, Iri. Elo, Luis, Léo. Thanks to Vivi for his trust, his unwavering support, and the (undue) hours of sharing around fascinating subjects that I wouldn't have discovered without you. Thanks to the Monks.

Thomas, Marc, Pilou, Pierre-Manu, Manu, Steph, Saminou, Elise, Mariama, Quentin, Dude, Léa, Yaya. A huge thank you to Flore for supporting me, listening to me, and encouraging me during all these years.

Finally, thanks to Bob Dylan, Vincent Moscato, Eric Di Meco, Trent Reznor and Mike Patton, without whom this would never have been possible.

# 1. Introduction

## 1.1 A brief history of mRNA export

### 1.1.1 RNA pioneers and the central dogma

*'Despite tremendous effort in the last decade to characterize heterogeneous nuclear RNA, several basic questions concerning its formation, metabolism, and relation to cytoplasmic messenger RNA still remain unanswered. The greatest obstacles to such studies include an extensive size heterogeneity and complexity in physical and metabolic states, as well as large variations in chemical composition […] There are also completed hnRNA molecules, processed or unprocessed, with or without post-transcriptionally added poly(A) segments at the 3' terminal end, and finished hnRNA molecules lacking poly(A). Attempts to characterize hnRNA are further complicated by the fact that molecules destined for transportation to cytoplasmic polysome are mixed with molecules accumulating and turning over within the nucleus*[1]*.'*

It is amusing to note the amazing insight of the questions raised by the author E.Engyhazi while he was introducing his review entitled "Quantitation of Turnover and Export to the Cytoplasm of hnRNA Transcribed in the Balbiani Rings" published in Cell in 1976. Reading this foreword, one can only wonder about the current state of progress in the field and the distance covered since then. While methods advanced beyond comparison, did we significantly improve our understanding of mRNA processing and export -designated at the time as hnRNA - over the last 50 years?

Ten years before the publication of this review, F.Jacob and J.Monod in the laboratory of A. Wolf laid the foundations for understanding the transcription of a gene into RNA, then termed factor X, in *Escherichia coli*. They also demonstrated that transcription also requires the presence of several so-called regulatory proteins (the transcription factors), associating with DNA regions located upstream of the gene to be transcribed (the promoters!). They reported their discoveries in a work whose universal significance was well understood at the time since it led them to Stockholm in 1965 where they received the Nobel Prize. The exact nature of Jacob and Monod's factor X was elucidated, contemporaneously with their work, by M. Nirenberg who demonstrated that the addition of a messenger RNA (mRNA) consisting only of uridine to a bacterial extract was sufficient to trigger the synthesis of a phenylalanine chain. H.G Kohrnana then established a correspondence between the 64 potential codons and the 20 amino acids of the living world while

Robert Holley proposed a theory of information detailing the notion of "code" where the genes determine the nature of the proteins produced. Nirenberg, Holley, and Kohrnana were also awarded the Nobel Prize in 1968. Thus, the essential steps of the central dogma were laid down at the end of the 1960s. The following years were also fruitful for the understanding of gene expression organization, in particular, thanks to the progress of electron microscopy (EM) which allowed O.Miller in 1969 to acquire the first images of transcription in the form of the well-known “Christmas trees”. In addition, pioneer studies led by Darnell and colleagues in the '70s also brought a new notion: the maturation of transcripts. Indeed, the use of $^{3}H$, $^{14}C$, $^{32}P$-labeled messenger RNA revealed the presence of 3′ unitary-sized polyadenylated segments of mRNAs (the poly(A) tails) and was followed by the discovery in 1974- 1975 of the addition of the 5′-methylated GpppXmp cap at the 5′ end. Following up on Darnell’s work, the laboratories of R. Roberts, P. Sharp, and P. Chambon, also awarded a Nobel Prize, independently observed that eukaryotic genes have a mosaic structure, alternating a coding minority found in mRNA (the exons) and non-coding regions "intruders" (the introns), thus characterizing thanks to EM images the revolutionary concepts of splicing and alternative splicing (For reviews detailing the history of molecular biology see [2,3,4,5]).

Initially, pulse-chase labeling experiments carried out at the end of the 1950s showed that RNA molecules were unstable in the nucleus and, therefore, mainly cytoplasmic, however, questions of nucleocytoplasmic trafficking and RNA export through the nuclear pore were not addressed until the late 1960s[5]. Thanks to cryoEM, an accumulation of large mRNPs could be described on the nuclear side of the nuclear membrane and provided one of the first images showing the detailed structure of the nuclear pore by negative staining in Amphibian Oocytes[6] (Fig.1a,b). Concomitantly, it was suggested that specific mRNPs, the particularly large Balbiani Rings(BR) of *Chironomus tentans* salivary glands, unfold and discard most or all of their proteins when passing through the pore[7].

Thus, by the mid-1970s, all of the major steps in the central dogma and maturation of RNA had been exposed or suggested and the first images of the translocation through a pore came much later in 1992. Those cryoEM tomograms showed export events of BR transcribed from characteristic giant puffs on chromosome IV in mosquitos[8] (Fig.1c). The overall picture of

transcription, splicing, 3' and 5' processing, association with proteins, and translocation through a pore correlating with mRNP rearrangements, remains the same today. It is interesting to note that, in addition to requiring almost unreasonable quantities of radioactivity, this model could be established thanks to methods studying entire RNA populations with a limited resolution and without being able to study specific transcripts/genes unless they presented unusual characteristics such as Miller's Christmas trees or BR. It is thus necessary to pay homage to the extraordinary observation and interpretation skills of the pioneer groups who established our knowledge of mRNA maturation and export starting from images of cryoEM, then in its beginnings, autoradiography and pulse-chase labeling experiments.

*Figure 1 Nuclear envelope ultrastructure.*

*(a) The top panel presents an obliquely grazing section to an out pocketing of the nuclear envelope. Note the difference in stainability between the ribosomes upon the outer membrane (arrows) and the annular material and also the finely fibrillar strands in the upper left (arrows). x 64,000. (46) the intracisternal dense material, which sometimes appears as a lamellar sheet can be recognized. Note also the strand-like material which is preferentially associated with the inner annulus of the pore complexes in*

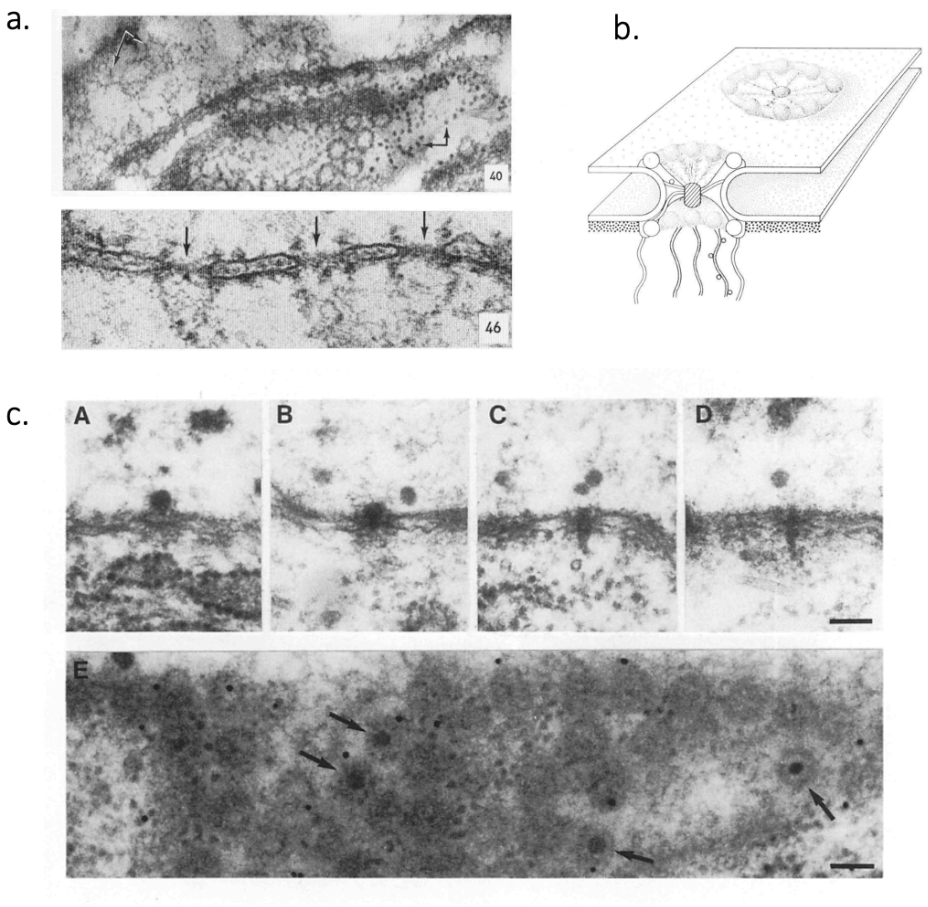

*Fig.a 46-bottom image (arrows). Both, x 100,000. (b) Diagram illustrating the structural components of the nuclear pore complex of the amphibian oocyte. Annuli lie upon the cytoplasmic and nucleoplasmic margin of the nuclear pore which consists of eight symmetrically distributed granules and some amorphous material. Amorphous material extends also into the pore interior in which the central granule and the internal fibrils appear as particulate structures. Similar fibrils often studded with small granules, are attached to the nucleoplasmic annulus. Peripheral chromatin underlies the inner nuclear membrane. (c) Balbiani Ring RNP particles in various stages of translocation through the nuclear pore. The pore complex with its densely stained spoke assembly in the middle can be discerned. The RNP particle is first bound to thin filaments projecting into nucleoplasm from the rim of the pore complex (A). Subsequently, the particle is translocated through the pre and concomitantly changes conformation to a rod-like structure (B-D). Particles in transit can also be seen in the middle of the pore complex in a tangential section (arrow in E) The bar corresponds to 100 nm. These data have been published in*[6,8].

### 1.1.2 Some adds-on to the central dogma

It would not be realistic to try to provide a comprehensive narrative of all the innovations and discoveries made in recent years in the field of mRNA metabolism. However, some technical breakthroughs highlighted here have been historically key for Dr Zenklusen and Dr Oeffinger's laboratories and were, therefore, central during my Ph.D. The model for mRNA general metabolism has been refined by bringing a spatio-temporal framework for studying the expression of specific genes. Notably, the use of probes hybridized to specific genes or transcripts has made it possible to observe the position of transcription sites by fluorescence microscopy, revealing a biased distribution of genes in the nucleus according to their transcriptional activity[9]. RNA fish approaches developed by the R. Singer group, ex post-doc in Darnell lab, allowed to detect single mRNA molecules by 'simply' (quoting Rob Singer himself [10]) multiplexing probes to the RNA template. This new strategy enabled other research groups to show that RNAs are not necessarily dispersed randomly in cells but can be preferentially localized according to a precise topology depending on the compartment in which they are retained, matured, or translated[11].

The study of RNA distribution has also known major advances thanks to techniques for labeling and tracking single RNA molecules developed in 1998, also by R.Singer laboratory and detailed in

Chapter 2 of this thesis. This labeling system using a capsid protein from MS2 viruses fused to GFP to bind to MS2 stem-loops inserted into an mRNA of interest launched numerous studies in living cells describing mRNA expression in a native environment, showing polymerase II (Pol II) transcription dynamics and its bursting behavior, mRNP transport through NPC, and even translation at the single-molecule level[12,13]. Using this strategy, the path and diffusion of mRNPs in the nucleus have been dissected allowing R. Singer to reject his own hypothesis of a motor-driven mRNP transport on the nuclear skeleton or matrix[14,15,16,17]. In addition, our understanding of RBP behavior has been significantly improved by the development of fluorescent ligands and particle tracking analysis tools allowing us to follow single proteins[18,19,20]. This major progress in particle visualization revealed that mRNP composition may be very dynamic as some RBPs exchange and display transient interaction with the transcript[21].

Likewise, different methods of extraction and affinity purification for dissection of molecular complexes considerably improved our understanding of the mRNA maturation pathway, and today we have probably identified most factors involved in the process. Those biochemical approaches applied to mRNP purification were often coupled with stabilization steps for capturing interactomes at their vicinity and followed by mass spectrometry analysis, next-generation sequencing [22,23]. Hence, an mRNP's exact composition, stoichiometry, and precise position of the factors assembling the particles are now within our reach. Numerous details were brought to the description of the mRNP maturation pathway providing a more dynamic picture, both describing the mRNP path from the transcription site towards the cytoplasm, but also regarding the fine-tuning of their composition along the processing pathway. Nevertheless, the overall picture of mRNP production remains globally unchanged and we can wonder where the next conceptual breakthroughs will come from?

### 1.1.3 A revisiting of mRNP maturation in subcellular spaces

A recent and fascinating research field has opened up in an attempt to understand how cells organize complex biochemical reactions orchestrating gene expression outcome in space. Some aspects of the answer were brought by biophysics, which then described the formation of non-membrane-bound compartments driven by phase transition phenomena sometimes described as simple drops of liquid enclosing localized biochemical reactions[24,25]. The most emblematic example

of these compartments is probably the nucleolus that self-organizes around rRNA synthesis, where molecules diffuse freely so that biochemical reactions for ribosomal biogenesis can take place[26,25,27]. mRNAs also encounter such compartments several times during their journey toward the cytoplasm. Indeed, it has been suggested that polymerase II and transcription factors themselves participate in the regulation of transcription through phase separation[28,29,30]. Furthermore, entire clusters of active genes and transcription factors (e.g., super-enhancers, topologically associating domains or lamina-associated domains) are now believed to be organized into liquid compartments, similar to nucleoli[31,32]. Once released from the transcription sites, transcripts can depend on the maturation pathway they follow, pass through other membrane-less mRNP granules, including paraspeckles, P-bodies, Cajal bodies, or stress granules[33,24,34]. Finally, to access the cytoplasm, the transcripts cross the pore, passing through a phase assembled by the proteins of the central channel[35,36]. In short, the formation of those compartments seems driven by a low-affinity interactions network of multivalent proteins and/or proteins containing intrinsically disordered domains (IDDs)[37,38].

Captivating investigations are now emerging: RNAs, as long multivalent charged polymers, arise as an architectural element that can, in synergy with RBPs, seed and modulates the biophysical properties of droplets[39,40]. This has been particularly well described for lncRNA-based nuclear body formation such as paraspeckle assembly and its structural RNA scaffold NEAT1_2[39,41]. These fascinating observations suggest that in addition to carrying the message for protein production, transcripts could also 'encode' for the cellular compartmentalization, therefore, ultimately organizing their own processing in space. This postulate has been at the center of some of the most interesting and lively debates during my Ph.D., mostly because it has provided one of the possible conceptual frameworks for interpreting some of our data, developed in the last part of the discussion.

## 1.2 The current model of mRNA export

The following sections are intended to describe the mRNA export pathway with a specific emphasis on mRNP-NPC and pore-associated factor interactions. Some sections and figures, have been published in April 2021 in *WIREs RNA* as an advanced review, present in the annex 1 of this

thesis, entitled *"Choosing the right exit: How functional plasticity of the nuclear pore drives selective and efficient mRNA export"*[42]. To provide a better context for the following chapters, the maturation pathway described here is mostly centered on studies in *S. cerevisiae*, unless mentioned otherwise. However, the general stakes for the regulation of gene expression remain conserved from yeast to humans.

mRNP biogenesis consists of key coordinated steps of mRNA maturation comprising mRNA transcription, polyadenylation, splicing, and folding. Along this process in the nucleus, the pre-mRNP acquires the export competency granted by specific mRNP maturation factors and RNA binding proteins (RBPs). Maturation steps adjust how efficiently transcripts find and interact with NPCs to be exported, establishing by this way, what is termed: "the mRNA export pathway". mRNA maturation steps are highly dependent on specific transcripts features such as length, intron content, or regulatory motifs and can also vary with cellular contexts. Consequently, routes to achieve export competency can be extremely diverse. While canonical complexes and factors required for mRNA maturation are known, the way they organize cooperatively with NPCs the export of mature mRNPs remains to be unraveled.

### 1.2.1 Pairing mRNA maturation with export

mRNPs have to transit through the NPC, which serves as the central gateway of nucleocytoplasmic transport to reach the cytoplasm. NPCs are large macromolecular assemblies embedded into the nuclear membrane (Fig.2). They are composed of around thirty proteins that assemble into an eight-fold symmetrical structure of different modules[43,44]. The central transport channel is lined with intrinsically disordered domains (IDDs) of central Nup proteins called as FG-Nups (phenylalanine-glycine). They are responsible for creating a diffusion barrier to facilitate nucleocytoplasmic exchange mediated by specific transport receptors. This diffusion barrier limits the passage for cargos above 40kDa unless they are associated with specific transporters called karyopherins[35,36,45].

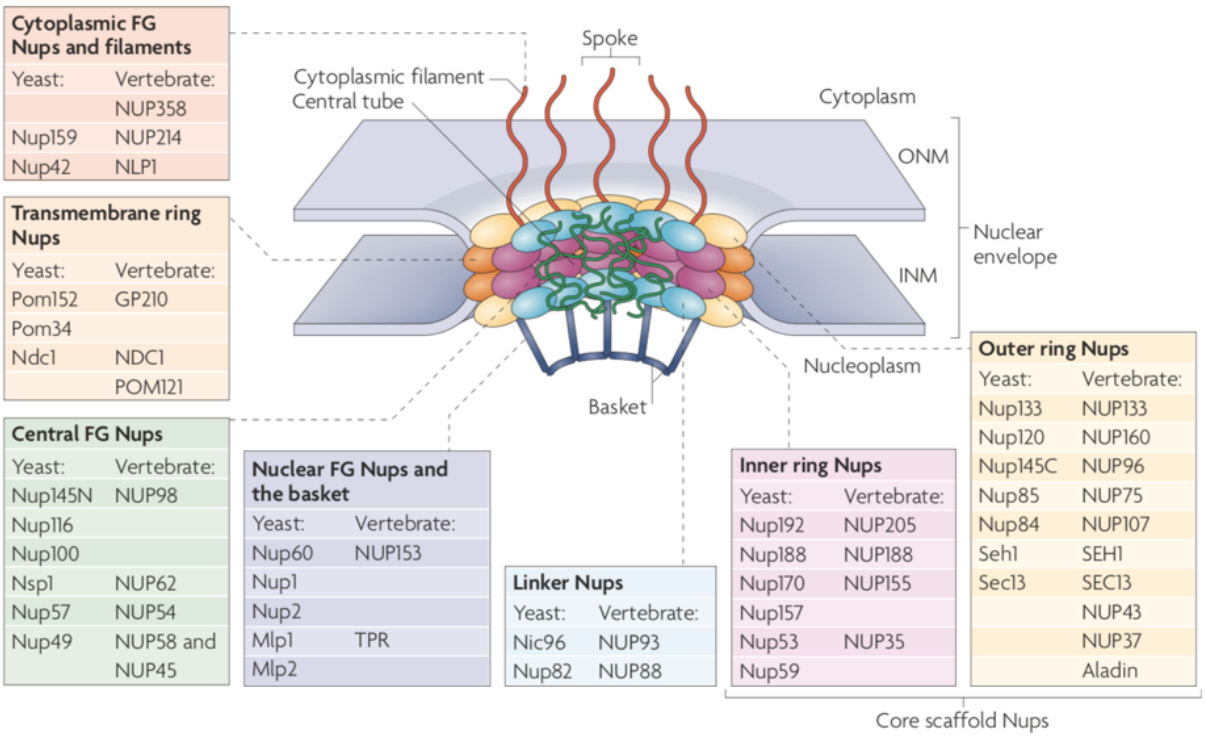


*Figure 2 Nuclear pore complex structure*

*Each nuclear pore complex (NPC) is a cylindrical structure comprised of eight spokes surrounding a central tube that connects the nucleoplasm and cytoplasm. The outer and inner nuclear NPC is anchored to the nuclear envelope by a transmembrane ring structure that connects to the core scaffold and comprises inner-ring and outer-ring elements. Linker nucleoporins (Nups) help anchor the Phe-Gly (FG) Nups such that they line and fill the central tube. NPC-associated peripheral structures consist of cytoplasmic filaments, the basket, and a distal ring. The Nups that are known to constitute each NPC substructure are listed, with yeast and vertebrate homologs indicated. Both inner and outer ring Nups are known to form biochemically stable NPC subcomplexes, which are thought to have a role in NPC biogenesis and nuclear envelope assembly. GP210, glycoprotein 210; Mlp, myosin-like protein; Ndc1, nuclear division cycle protein 1; Nic96, Nup-interacting component of 76 kDa; NLP1, Nup-like protein 1; Pom, pore membrane protein; Seh1, SEC13 homologue 1; TPR, translocated promoter region. This figure has been published in*[43].

Thus, export competent mRNAs are defined by their ability to interact with NPCs and diffuse through the central channel by interacting with FG repeats. This aptitude is essentially mediated

by the recruitment of the conserved heterodimeric, nuclear export receptor NXF1-p15 in human Mex67-Mtr2 in yeast [46]. However, some mRNPs can alternatively use the major receptor for the export of proteins and ribosomal subunits, CRM1[47]. It is believed that mRNPs reaching the pore are associated with cap and poly(A) binding proteins Pab1 and/or Nab2, the TREX and TREX-2 complexes, SR proteins, in addition to proteins marking the splicing events as completed [48,49]. Ultimately, those RBPs serve as adaptors for mRNA export receptors ensuring that properly matured mRNP are selected for export[50,51]. Hence, the mRNA export pathway is highly dependent on pre-mRNPs processing. Pairing the two pathways represents a robust strategy ensuring that only correctly spliced and packed mRNPs reach the cytoplasm (Fig.3). Analyses of the pre-mRNP maturation pathway have shown that, despite a common pattern, the steps and factors involved could vary between transcripts families. Hence, different pre-mRNP specific maturation pathways coexist in the cell suggesting that the export competency can be acquired by different manners[52,53]. This challenges the view of one canonical export route toward the cytoplasm, but rather suggests several mRNA export pathways that may overlap by involving common partners. Genetic screens, knock-down as well as affinity purification (AP) and mass spectrometry (MS) approaches have probably identified most factors involved in mRNP maturation pathways[22,23,54]. However, their stoichiometry within mRNPs and a clear spatio-temporal picture of when they intervene remains incomplete. Furthermore, it is not known whether each of them associates with the bulk of mRNAs or if some mediate the processing and the export of specific transcript subsets. Nevertheless, the diversity of RBPs their respective ability to recruits export receptors indicate that there are multiples routes to reach and interact with NPCs[22], allowing cells to establish a large variety of export selection mechanisms.

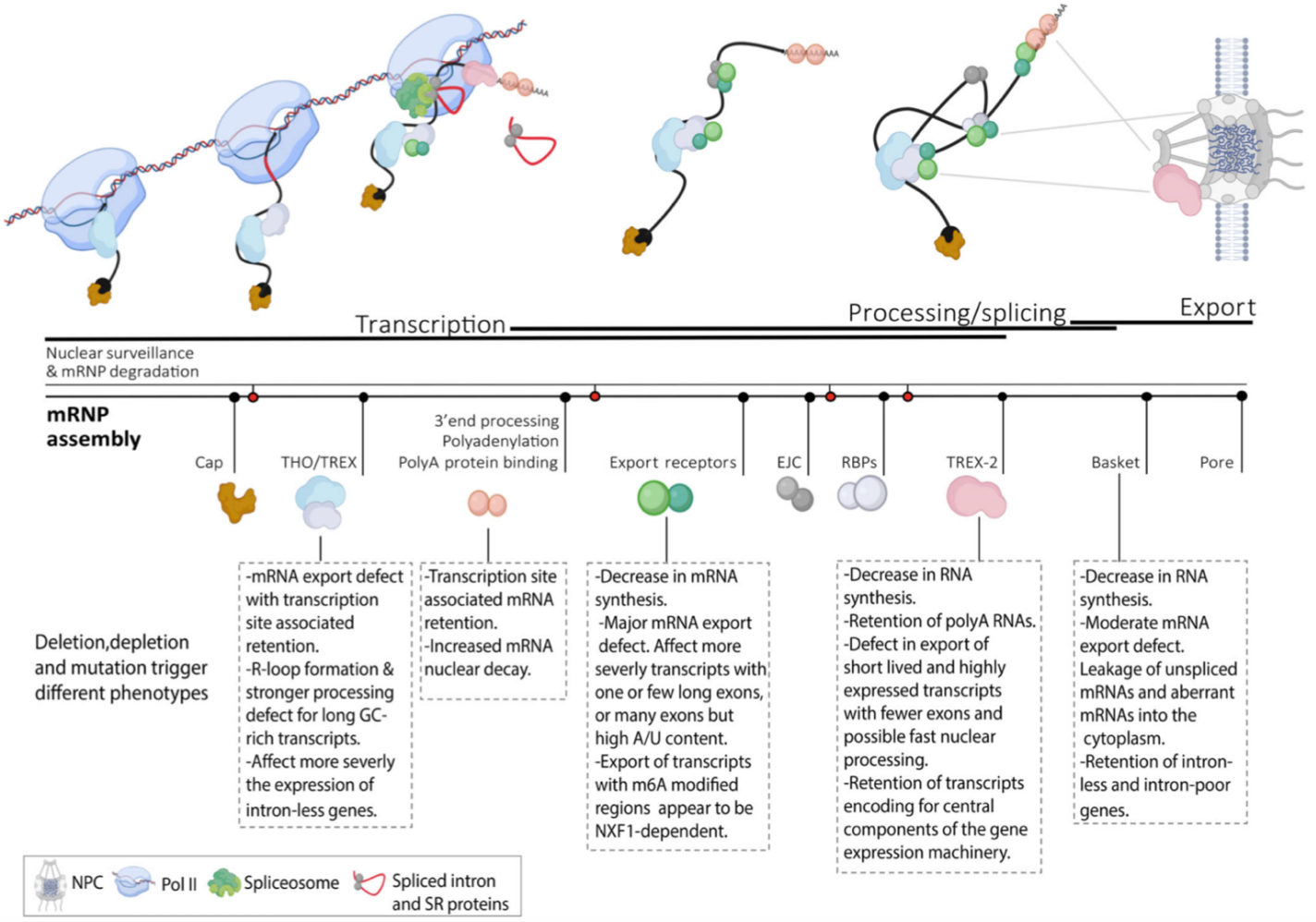


*Figure 3 Stages of the mRNP maturation,quality,and export pathway*

*Nascent mRNAs are capped and assembled with THO and TREX components that serve as adaptors for mRNA export receptors. Transcripts are generally spliced co-transcriptionally and associate with the exon junction complex (EJC), serine-rich proteins (SR) as well as various RNA-binding proteins (RBPs), which enhance export kinetics by recruiting additional export receptors. Cleaved and polyadenylated transcripts associate with nuclear poly(A)-binding proteins and are released from the transcription sites. Export competent mRNPs can either associate with a pore through direct interactions between export receptors and the NPC, or TREX-2 mediated interactions between transcripts, the nuclear baskets, and export receptors. It is assumed that cooperative interactions between the pore, the basket, and RBPs ensure that only correctly processed transcripts have access to and translocate through the pore. Defects in capping, abortive transcription as well as inefficient*

*splicing and/or polyadenylation can trigger mRNA degradation by the nuclear surveillance machinery, and several mRNP processing defects provide entry sites for 3′–5′ exosome decay (indicated by red dots). THO/TREX, TREX-2, export receptor, and basket deficiencies do not affect transcripts or their export in the same manner, with pronounced transcription/export defects observed for specific subsets of transcripts. This figure has been published in*[42].

### 1.2.2 Maturation starts co-transcriptionally: the roles of THO TREX & TREX-2

Different mRNP maturation and export steps are coordinated by the highly conserved THO, Transcription Export complexes TREX, and TREX-2[50,55,56]. So far, THO and TREX complex assembly with mRNAs is described as a two-phase process where the first complex loaded on the nascent transcript is THO recruited by the C-terminal domain (CTD) of the large RNA polymerase II subunit [57]. In a second step, THO recruits the export factors Yra1 and the RNA helicase Sub2 to assemble TREX, to serve as an adaptor for export receptor recruitment.

Run-on assays showed that THO mutants exhibit a 3'end processing defect with a premature transcription termination associated with a decrease in polyadenylation[58,59]. In addition, the yeast TREX subunits Yra1 and Sub2 show an apparent localization bias toward the 3′-ends of genes, suggesting that loading of TREX complex is coupled or enhanced during 3′-end processing[56,60]. Accordingly, components of the yeast TREX complex exhibit both physical and genetic interactions with mRNA cleavage/polyadenylation factors responsible for 3′-end processing[61,60]. Interestingly, THO and TREX mutants display a hyper recombination phenotype provoked by R-loop formation with unusual hybridization between nascent transcripts and adjacent DNA segments [62,63] and THO/TREX are, therefore, considered complexes involved in mRNP packaging. Chromatin immunoprecipitation (ChIP) analysis carried out with THO/TREX components has shown that the two complexes may virtually associate with all actively transcribed genes, which would argue for a canonical and ubiquitous role in transcription/export of all transcript[62]. Accordingly, transcriptomic in human studies demonstrated that depletion of the export factor NXF1 and TREX affected the nuclear/cytoplasmic distribution of the vast majority of mRNAs leading to the conclusion that the export receptors THO and TREX act in the same pathway to promote the export of all transcripts[64]. However, mutations in THO/TREX do not affect transcripts in the same manner suggesting that

those complexes can be involved in the regulation transcription/export of specific transcripts. In yeast, it has been shown that long GC-rich transcripts are particularly sensitive to the mutation of THO subunits. This possibly suggests that GC-rich and long transcripts are more susceptible to hybridize with the non-template DNA and form R-loops[65,66]. Furthermore, it has been shown that altered THO complex activity affects more severely the expression of intron-less as compared to intron-containing genes[67,68,69]. While the role of splicing in nuclear export remains to be fully elucidated, different groups reported that intron-less mRNAs are exported in a TREX-dependent manner reinforcing the idea that THO and TREX participate in the same pathway[70]. Taken together, those data suggest that mRNA export-dynamic disparities might exist between transcripts and are based on transcripts specific features such as their length, the GC content, or the presence of introns.

TREX-2 association with transcripts seems independent of THO/TREX[71]. It is not clear whether THO/TREX and TREX-2 represent parallel and specific export pathways or whether the complexes collaborate to export the same transcripts[72,73]. Initially identified in yeast, TREX-2 is an essential complex that stably interacts with the inner face of NCPs. TREX-2 shares one of its subunits with the transcriptional co-activator complex SAGA[74]. Therefore, it has been suggested that the interaction between SAGA and TREX-2 facilitates the association of actively transcribing genes with nuclear pores[75,76,77]. Similar to THO/TREX, TREX-2 plays a role in mRNA export as depletion of its components results in retention of poly(A)RNA in the nucleus[74,76,78]. It has been shown that export receptors interact directly with TREX-2 main scaffolds Sac3 and GANP in yeast and humans, respectively demonstrating that TREX-2 is used as an adaptor for export receptor[78,79]. In humans, however, mRNA export defects following depletion of the TREX-2 subunits are strikingly milder than what is observed after mRNA export receptors NXF1-p15 knockdowns indicating that its function is not essential for all transcripts. Moreover, genome-wide gene expression profiling upon GANP depletion has highlighted that GANP typically promotes the export of short-lived and highly expressed transcripts, with enrichment for those encoding for central components of the gene expression machinery such as RNA synthesis and processing factors[80]. In addition, those transcripts tend to contain fewer exons indicating that they may require less time to be fully processed into a mature transcript. Therefore, the authors of this study proposed that GANP, and hence TREX-2,

accelerate the nuclear export of specific classes of mRNAs possibly that have to undergo fewer splicing reactions and may facilitate rapid changes in gene expression[80].

Unraveling the functions of THO/TREX and TREX-2 complexes in mRNP biogenesis has, therefore, additional provided evidence for possible selective export pathways within cells, depending on the specific features of the transcripts. Interestingly, it has been speculated that those parallel and yet overlapping maturation/export pathways evolved to limit and control the infection by viruses. Indeed, numerous studies reported that viral RNAs can use the export canonical export pathway. Furthermore, some viral RNAs hack the host machinery to bypass the mRNA quality control (QC) steps and fast-track toward the cytoplasm[45]. While the decision of export is ultimately determined by mRNP ability to interact with the NPC and cross its channel, one other important aspect of mRNA export regulation is nuclear decay.

### 1.2.3 Getting out or decay: "the export of the fittest"

In addition to the need of assembling export competent mRNPs, a second facet of export regulation is to ensure that only correctly processed transcripts escape nuclear decay[81]. Pre-mRNPs are potential targets for the versatile RNA-degradation machine: the RNA exosome complex. The nuclear exosome and its cofactors can recognize the transcripts at the various step of the mRNA biogenesis pathway[81–83]. Furthermore, it has been shown that mRNP processing events can compete with nuclear exosome-mediated degradation[84,69]. Consequently, the exosome exerts constant pressure on sub-optimally processed mRNPs from transcription until export. Rapid processing and export might explain how normal nascent mRNPs avoid degradation by the exosome. Those observations have led to a "kinetic proofreading" model for export where mRNPs can spend a limited amount of time in the nucleoplasm to avoid nuclear decay[85,86]. Thus, transcripts would undergo a simple selection where only correctly packed and timely processed mRNPs reach the cytoplasm. Furthermore, enzymes responsible for RNA nuclear degradation also participate in the 5' and 3' processing of numerous RNA species. Those factors are, therefore, able to impose efficient RNA quality control due to their dual role in processing and trimming as well as in the decay of transcripts[82]. Accordingly, mRNP export rates rise from the kinetic competition between maturation and decay. Consequently, cells can fine-tune their gene expression by

favoring the export rate of some transcripts in a cell-type-specific or condition-dependent manner by two non-mutually exclusive strategies consisting of (i) accelerating the export of some transcripts or (ii) protecting them from nuclear degradation. Hence, mRNP export is an adjusted transcript export rate arising from the balance between maturation and decay. However, in higher eukaryotes, mRNAs and ncRNAs can have long residency times in the nucleus without being necessarily degraded, and some mRNAs take up to two hours to be exported[87,88,89]. What exactly mediates selective retention is still not clear and the role of RBPs in this process is still poorly characterized. However, several studies identified nuclear retention motifs and potential nucleotide modifications such as adenosine to inosine may delay the RNA export. To be protected from degradation, those transcripts can be retained in specific nuclear sub-compartments such as nuclear speckles and paraspeckles. The biological relevance of this specific nuclear retention is unclear but it has been shown that nuclear retention could effectively be a strategy for regulating cytoplasmic levels of transcripts by buffering the temporal fluctuations of transcription of genes expressed in bursts[90].

## 1.3 The nuclear pore and export

To be exported, mRNPs leave the transcription site and need to find their way towards the nuclear periphery. It is believed that they move around the nucleus, simply diffusing by Brownian motion to stochastically find a pore[91,92,93,16]. Single-particle tracking approaches have shown that mRNA velocity varies quite significantly and decreases drastically when the particles enter crowded domains of the nucleus such as chromatin-dense regions,[94,95] slowing down their export. In yeast and to a lesser extent in flies, it has been observed, that some actively transcribed genes are tethered to NPCs[96,97]. Accordingly, genome-wide chromatin immunoprecipitation experiments using nucleoporins as bait have shown that actives genes associate with NPCs. This phenomenon has been particularly well described in *S. cerevisiae*, where activation of genes such as *INO1, GAL1, HXK1* or *HSP104*, induce the re-localization of the loci at the nuclear periphery[98,99,100]. The mechanism for gene tethering at the pore is not fully understood but it has been proposed that the gating of active genes at the periphery is a mechanism that favors encounters between NPCs and mRNPs by bringing the nascent transcripts directly to a pore and ensuring rapid export of the

mRNP. Because RBPs and export receptors can associate to a nascent transcript and have the capacity to bind NPCs, some studies suggested that the transcription site might simply be dragged at the periphery[101]. However, export receptors are associating with all transcripts which raises the question of how gene gating can be specific to some genes instead of being a trend for all transcription sites. Another possibility then is that gene gating might involve TREX-2 which can also bind both NPCs and transcription sites by interacting with SAGA. Interestingly, TREX-2/SAGA-regulated genes represent only a small fraction of the genome (~10%) and many of those genes are involved in adaptative responses to different stresses and changing environmental conditions[102]. Thus, gene gating in yeast might concern only a gene subset and may be used for enhancing specifically the export of a minority of mRNAs to rapidly fine-tune gene expression. Contrary to yeast and flies, in higher mammals, the majority of actively transcribed genes are commonly localized in the nuclei interior, and genes tend to re-localize towards the center of the nucleus upon transcriptional activation while the nuclear periphery is generally associated with heterochromatin[103]. However, gene gating has been described in humans as a means to establish differential mRNA export-dynamic cancer cells[104]. The *MYC* oncogene locus has been shown to relocate to the nuclear periphery through an oncogenic super-enhancer mediated gene tethering at the pore. The cancer-cell-specific gating of MYC leads to differential export kinetics of the *MYC* transcripts[104,105] suggesting that nuclear mRNA export facilitated by the gating principle exist and its role may be underestimated in higher eukaryotes.

It is interesting to note that genes undergoing this type of regulation seem to share the common feature to be involved in phenotypic plasticity. Indeed, in yeast, genes such as GAL and INO are activated upon metabolic transitions, and in humans, MYC participates in oncogenic transformation. Yet regulation of gene expression by gene gating at the pore might be an exception rather than a rule because of the limited number of pores available per cell compared to active alleles (~ 150 pores in yeast for ~ 1000 in human[106,107]). In addition, we can question how it represents a real advantage for export as we are lacking formal evidence that mRNPs are exported through the same pore the gene is tethered to, rather than being released back into the nucleoplasm to be exported through neighboring pores. We can also ask whether finding a pore is a significant rate-limiting step within the gene expression pathway. In yeast, nuclei are very small

and mRNPs reach the periphery in a couple of seconds[108]. This time interval appears negligible when considering that translation or transcription happen usually within a range of few minutes. Alternatively, we can propose that gene gating mediates a selective export not by reducing the time an mRNP needs to find a pore *per se* but instead by allowing mRNPs to escape nuclear exosome-mediated degradation.

## 1.4 Basket, Mlp proteins, and mRNP export

### 1.4.1 Nuclear basket organization

Once at the nuclear periphery mRNPs first encounter a ~60- to 80-nm-long structure on the nuclear face of pores, protruding into the nucleoplasm called the nuclear basket[43].The basket is assembled by the Nup1, Nup2, Nup60, Mlp1, and its paralogue Mlp2 in yeast, whereas the metazoan basket harbors only three components, NUP153, NUP50, and TPR[109,110]. The main basket structural backbone is formed by Mlp1/2 and TPR which are long filamentous coiled-coil proteins with large intrinsically disordered domains in their C-terminal regions[110,111,112]. The coiled-coil regions are believed to form the basket spokes whereas the C-terminal region is thought to shape the top of baskets, called the distal ring. The basket structure is described as an eight-fold symmetry complex and its eight spokes together with the distal ring are particularly visible on the nuclear envelopes (NE) in amphibian oocyte extracts in EM[113] (Fig.7a,b). Conversely, in yeast, the exact shape of the basket is inferred from other model organisms and no EM images are currently available. While the entire structure of the NPC has been solved to the amino acid residue level using an integrative modeling approach including a combination of EM, cross-linking, and AP with mass spectrometry readout, basket morphology remains puzzling[114]. EM approaches however used isolation native of NPCs and the basket may be unstable and fall apart during the preliminary isolation of complexes. Nevertheless, the orientation and position of the Mlp1/Mlp2 have been monitored by immunogold labeling showing the orientation of the two proteins[115] (Fig.4), and quantitative fluorescent microscopy experiments estimated that Mlp1 and Mlp2 are both present in 8 to 16 copies per NPC[116,114].

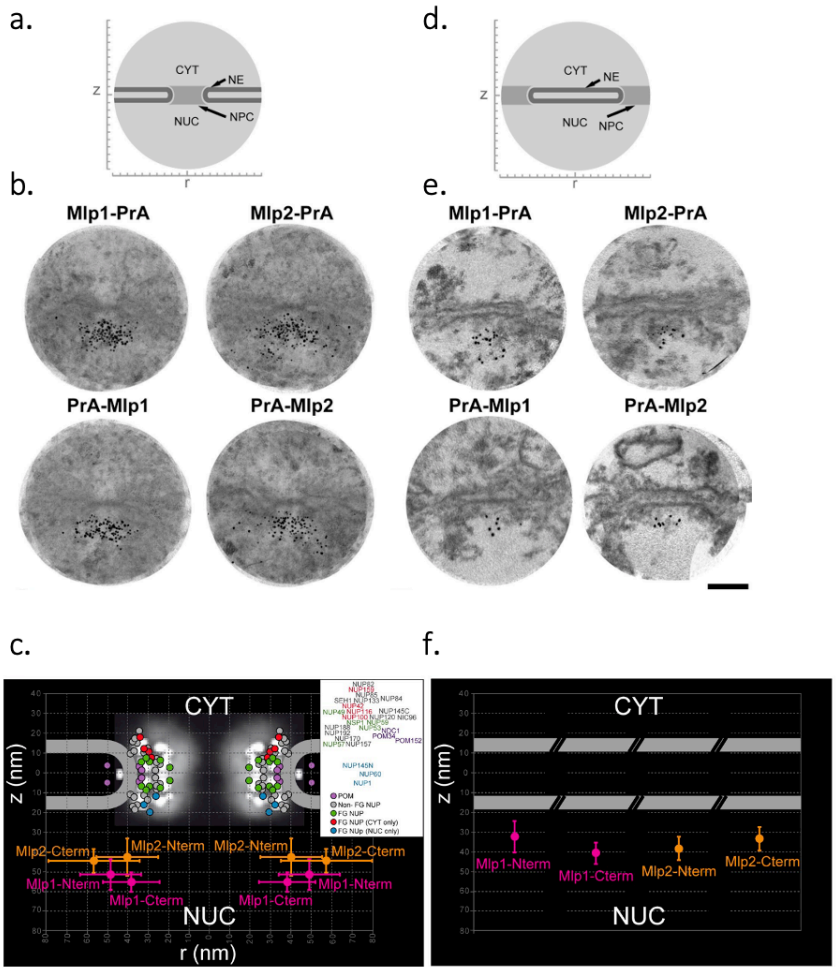


*Figure 4 Mlp proteins localize to the nuclear basket.*

*Schematic depiction of (a) the NPC and (d) the area between NPCs. (b, e) Overlays of multiple IEM images with gold-labeled antibodies bound to the C- (top) and N-termini (bottom) of either Mlp1p (left) or Mlp2p (right), showing circular zones (diameter, 400 nm) around (b) visible NPCs or (e) regions between NPCs. (c, f) Extracted z- and r-positions of the N- and C-termini of Mlp1p and Mlp2p in relation to the (c) NPC or (f) NE in inter-NPC regions. (c) Mlp1p-PrA, n = 210; Mlp2p-PrA, n = 210; PrA-Mlp1, n =122; PrA-Mlp2, n = 121. (f) Mlp1p-PrA, n = 244; Mlp2p-PrA, n = 152; PrA-Mlp1, n =127; PrA-Mlp2, n = 153. Bar, 100 nm (b, e).These data have been published in* [115].

Mlp1 is believed to be the main structural component of the nuclear basket as it has been shown that Mlp1 deletion affects Mlp2 docking at the pore, while Mlp2 does not completely impair

Mlp1 binding at the periphery[117]. Furthermore, the precise manner Mlp1 interacts with the pore and with the rest of the basket Nups, including Mlp2, is not fully understood. Mlp1 docking at the pore is very likely to be a cooperative process as deletions and mutation of basket Nups disrupt Mlp1 association with the periphery[115]. Interestingly, FRAP experiments revealed that basket nucleoporins display a relatively fast turnover at the pore with a recovery rate varying from 30 sec to few minutes, depending on the study[115,118]. Those experiments indicate that basket proteins exchange faster than the Nups that assemble the central framework of the pore. This dynamic of basket Nups at the pore is regulated by the deSUMOylating enzyme Ulp1 which plays an important role in the cycle of ubiquitylation and SUMOylation of these proteins and stimulates their turnover[111,119]. In addition, their post-translational modification profiles differ substantially upon genotoxic and osmotic stress, indicating that adaptation to changing cellular environment may require certain plasticity of this specific region of the NPC[120]. Furthermore in humans, NUP50 and to a lesser extent NUP153, seem to have also a rapid turnover at the pore, possibly indicating that in higher eukaryotes, the nuclear pore platform plasticity also involves basket protein [121,122].

### 1.4.2 Baskets are believed to maintain mRNPs at the nuclear periphery and possibly act as a gatekeepers

#### 1.4.2.1 Mlp-mediated mRNA surveillance in yeast

The nuclear basket seems to be a multifunctional platform involved in gene gating regulation, through its ability to bind transcription sites possibly by interacting with THO/TREX and TREX-2[76,123] (Fig.5). This interaction may require the Mlp proteins and the rest of the basket proteins but remains poorly characterized. However, it has been shown that the C-terminal region of Mlp1 and the N-terminal domain of Nab2 interact directly[124,123,125]. Consequently, the distal ring of the basket is believed to assemble the region where mRNPs dock before they access the pore central channel[112,123]. It has been shown that the over-expressions of Mlp1 or its C-terminal region were sufficient to block Nab2 export and trap poly(A)RNAs in the nucleus. The authors proposed that this phenotype could be caused by the titration of RBPs such as Nab2 and, consequently, mRNA by

Mlp1 within the nucleus through interactions with its C-terminal domain, supporting the hypothesis that Mlp1 contributes to export through interaction with various RBPs.

I participated in a study published in the Journal of Cell Biology, (presented in the annex 2 of this thesis), in which we carried out single-mRNP tracking approaches in yeast to analyze their path in the nucleus toward the cytoplasm. Similar to what was reported in humans, we observed that mRNPs scan the nuclear periphery prior to their export[108,16,89]. The purpose of such behavior as well as the elements at the periphery allowing the scanning are far from clear. Mutation of Nab2, deletion of Mlp1, and the truncation of its C-terminal region affect the scanning behavior and result in the frequent release of mRNPs back into the nucleoplasm, suggesting that baskets participate in increasing mRNP's residency time at the periphery. Possible interpretations of these phenotypes are developed in the discussion of this thesis. The scanning phenomenon has been interpreted as a potential waiting phenomenon, where mRNPs seek a nuclear pore that would allow export[16]. However, baskets may not simply be docking sites facilitating mRNP export, and it is believed that the basket plays a role in mRNA surveillance.

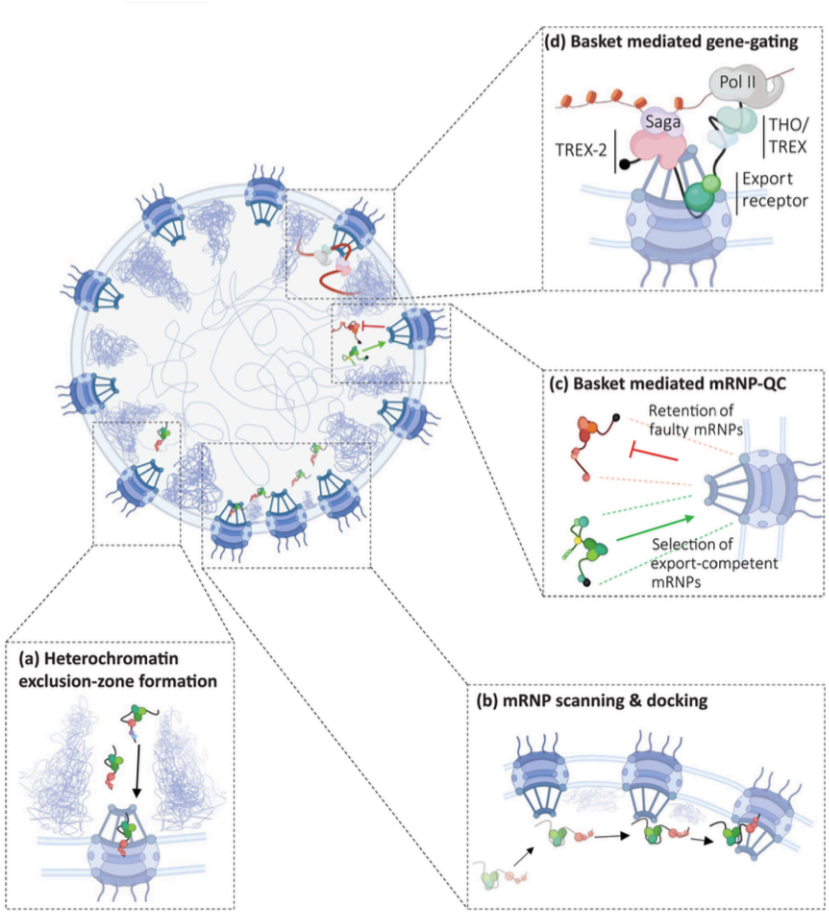


*Figure 5 The nuclear basket may participate in different steps of selective mRNP export.*

*(a) In metazoans, the basket has been linked to the formation of chromatin exclusion zones believed to be used as channels by mRNPs to access the nuclear pore. (b) mRNPs scan the nuclear periphery prior to export, and in yeast, this scanning behavior has been linked to the presence of the basket core component Mlp1 and its interaction with poly(A)-binding proteins, which are suggested to increase the residence time of mRNPs at the periphery and to facilitate binding/docking to the pore (c). The nuclear basket is believed to act as a gatekeeper for aberrant mRNAs. However, at this point, it is unclear whether the basket interacts with RBPs to recognize mature and export competent mRNPs or if aberrant transcripts are retained at the basket either to be matured or targeted for exosome-mediated decay. (d) The basket proteins Mlp1 and TPR were shown to be important for gene gating, or tethering, of actively transcribed genes at the nuclear periphery; in this model, transcription at the periphery is suggested to provide an advantage for mRNA export that may be based on selectivity and/or efficiency. Tethering genes at the NPC were shown to*

*involve TREX-2/SAGA and/or export receptors associating with nascent transcripts. This figure has been published in*[42]

It has been shown that Nab2 can bind poly-adenosines rich regions and dimerizes to participate in mRNP compaction [126]. Therefore, direct interaction of Nab2 with the distal ring would favor the access to properly packed and polyadenylated mRNPs to the cytoplasm. Interestingly, it has been shown that Yra1 and Nab2 depletions cause an mRNA nuclear export defect which was alleviated upon *mlp1/2* deletion[127]. This phenotype indicates that Mlp proteins downregulate mRNA export when the mRNP export/processing pathway is impaired, suggesting that the basket could act as a gatekeeper when the mRNP maturation pathway is compromised. Poly(A) RNA FISH experiments showed that *TPR* and *MLP1* deletions cause only a moderate mRNA export defect and hence that baskets are not essential for export. Instead, *mlp1/TPR* deletion results in the leakage of unspliced mRNAs into the cytoplasm[123,128,129,117]. Yet depletion of basket proteins does not affect splicing *per se* but results in increased levels of an intron-bearing reporter in the cytoplasm[129]. Therefore, it has been proposed that the basket's main function is to act as a gatekeeper for the export of intron-containing mRNAs. Pml39 is another factor anchored to NPCs by Mlp proteins and seems also involved in the retention of unspliced mRNAs. Like Mlp1, Pml39 is not essential for splicing, and its depletion triggers intron-containing mRNA leakage[68]. However, those studies were carried out in the context of highly overexpressed intron-containing reporters, which may escape from the nucleus more easily than endogenous intron-containing mRNAs in a context where gatekeepers such as Mlp1 and Pml39 are depleted. Nevertheless, further evidence links Mlp1 to the retention of unspliced mRNA. As mentioned above, over-expressions of Mlp1 full-length, or of the C-terminal region trigger an accumulation of poly(A) transcripts in the nucleus, however, the nature of the retained mRNAs and whether these are mostly intron-containing transcripts has not been investigated. Interestingly, overexpression of both Pml39 and Mlp1 trap preferentially intron-containing reporters in discrete nuclear foci (Fig.6). The reason for such a preference and potential RBPs involved is not known but this suggests a propensity of Mlp1/Pml39 to efficiently recruit intron-containing pre-mRNPs[68,117,129]. Finally, Mlp1 becomes essential in absence of the splicing factor Prp18 and double mutants show a strong synergistic leakage phenotype to a point where it becomes lethal, suggesting basket gatekeeping functions are crucial in a context where pre-mRNP

processing is defective[129]. However, in yeast, determinants such as specific RNA motifs or RBPs for potential basket-facilitated export and possible specific features corresponding to Mlp1/Pml39 pre-mRNA retention have not been identified.

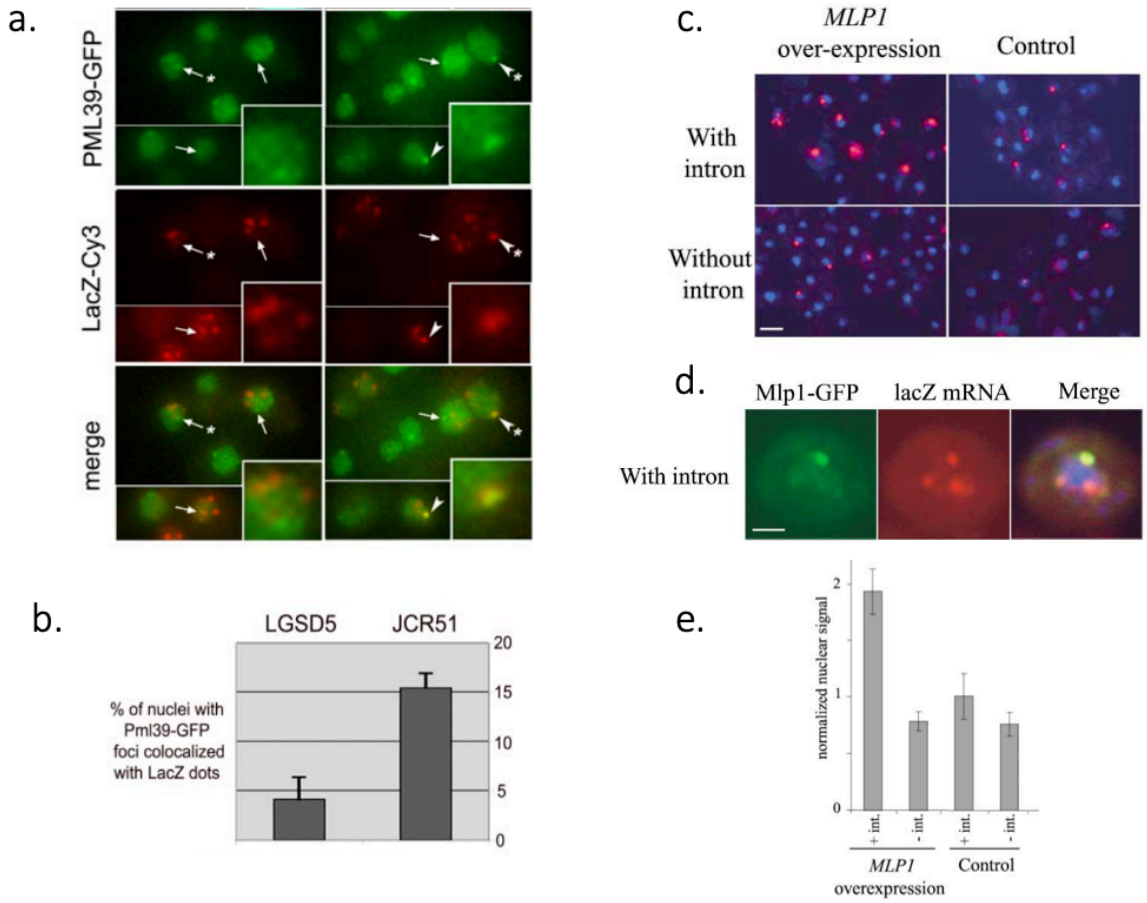


*Figure 6 Pml39 and Mlp1 overexpression foci retain intron-containing mRNAs.*

*(a) RNA FISH analysis of LacZ transcripts in Pml39-GFP-overexpressing cells. Cells transformed with pYX214-PML39-GFP and either pLGSD5 (intron-less LacZ reporter) or pJCR51 (intron-containing LacZ reporter) were induced for 2h in galactose and analyzed for localization of LacZ transcripts by FISH using Cy3-conjugated probes specific to the LacZ sequences. GFP and Cy3 images are two-dimensional projections from z-stacks. DNA staining of the nuclei (4,6-diamidino-2-phenylindole), as well as overlay images of GFP and Cy3 signals (merge), are shown. Arrowheads and arrows respectively point to Pml39-GFP foci containing or not LacZ transcripts. Insets (bottom right corners) show a threefold magnification of nuclei exhibiting typical Pml39-GFP and LacZ transcripts*

*localizations (indicated by a star on the original image). (b) Quantification of the colocalization events from a. The number of nuclei displaying a Pml39-GFP dot merged with one of the LacZ foci was counted among nuclei exhibiting detectable signals for both species. The values represent the means and standard deviations obtained from two independent experiments; the total numbers of counted cells were 285 (pLGSD5) and 363 (pJCR51). (c) Mlp1 overexpression led to the nuclear accumulation of intron-containing mRNAs. Strain BMA64-1a was transformed with either pRS324-GAL-Mlp1 or empty plasmid and with either pLGSD5 (without intron) or pJCR51 (with intron). Overexpression of both Mlp1 and lacZ mRNA was induced for 2hr by the addition of galactose to a final concentration of 2%. LacZ mRNA was detected. Scale bar is equal to 5μm. (b) Mlp1 and RNA derived from intron-containing construct colocalize. Strain BMA64-1a was transformed with pRS324-GAL-GFP- MLP1 and pJCR51. Mlp1-GFP (green), lacZ mRNA expressed from the intron-containing gene (red), and DNA (blue) are shown. Scale bar is equal to 2μm. (c) Quantification was performed for pLGSD5 (- int.) or pJCR51 (+ int.) derived signal. The measured values were normalized using wild- type level of the intron-containing construct. These figures have been published in* [129,130].

#### 1.4.2.2 The basket as a gatekeeper in higher eukaryotes

In human cells, nuclear baskets may facilitate nucleocytoplasmic export by creating heterochromatin-free zones initially described as "nucleoplasmic-channel pathways" for the diffusion of cargos toward a pore[131]. However, the role of the basket as gatekeeper remains uncertain in higher eukaryotes as well. As mentioned above, previous studies highlighted the leakage of unspliced and aberrant mRNAs into the cytoplasm upon TPR deletion [109,128]. However, more recent works questioning the function of the basket in export selectivity and retention have not found a function for it in regulating the retention of unspliced mRNAs in the nucleus[132,133]. Indeed, genome-wide studies investigating the effect of TPR depletion using either a siRNA knock-down approach or an auxin-inducible degron system combined with cell fractionation and RNA-seq suggested a role for the nuclear basket in facilitating mRNA export rather than retention. TPR depletion resulted in the nuclear accumulation of mRNAs primarily expressed from short, intron-less, and intron-poor genes such as those encoding for ribosomal protein genes and histones;

export of longer mRNAs, however, appeared to be less dependent on TPR[133]. An mRNA retention phenotype upon TPR depletion was confirmed using RNA FISH. Additionally, retained transcripts preferentially localized to nuclear speckles, a phenotype previously observed upon deletion of other factors implicated in mRNA export, including those of the basket-associated TREX-2 complex. Moreover, genome-wide gene expression profiling upon depletion of the TREX-2 main subunit GANP, suggests a functional overlap between TREX-2 and the nuclear basket, specifically TPR[76,132]. Similar to the depletion of TPR, loss of GANP resulted only in a partial defect of mRNA export, leading to the retention of a selective subset of transcripts that showed significant overlap to mRNAs retained upon TPR depletion. While the number of mRNAs retained upon depletion of TREX-2 components varied between different studies, which may be due to different experimental set-ups, there was an overall trend correlating specific transcript features with retention in cells depleted of GANP and/or TPR: short length and low intron/exon numbers (0–3). These observations raise once again questions about the role of the basket as well as of Mlp/TPR as a central basket component in mRNA export. If, as these data indicate, the nuclear basket is required for the export of a sub-set of transcripts that contain specific features, is its role driven by providing selectivity, or contributing to transport efficiency? Transcripts whose export depends on TPR—and TREX-2—appear to contain common features, which would point towards a role of the basket in selective transport. However, it is important to note that while one of these features is a low number of introns, it is not—as previously thought—the mere presence or absence of introns, suggesting the basket may not be primarily a designated gatekeeper for unspliced pre-mRNAs. While mediating selective transport could still be one of its roles, nevertheless, features such as short transcript length could also indicate that some mRNAs require the nuclear basket to be efficiently exported; short mRNAs and those that have undergone only one to two splicing events may represent less complex RNPs lacking components to facilitate efficient binding to and transport through the pore. If we consider mRNP scanning of the nuclear periphery as part of a probabilistic process towards successful binding to the pore through specific RBP-pore interactions, shorter transcripts may require the basket to facilitate such a binding event. Consistent with such a notion, recent APEX2 data found short mRNAs enriched with NPCs, which

was suggested to be due to a lower number of NPC-interacting factors on these transcripts that would mediate efficient translocation[134].

Besides length, specific motifs have recently been implicated in the basket-mediated retention and quality control of a selected subset of transcripts in metazoans. The protein TARBP2 was shown to bind a subset of pre-mRNAs, the TARBP2 regulon, via GC-rich structural cis-regulatory RNA elements resulting in *N6*-methyladenosine (m6A)-mediated intron retention and exosome-mediated decay[135]. Transcriptomic and proteomic data link this surveillance process to TPR and, possibly, the nuclear basket, which would be in line with the proposed function of the nuclear basket as a surveillance platform[128,129,109]. The decision of mRNA export is ultimately determined by the ability of mRNPs to efficiently access and get translocated through a nuclear pore, and several works have shown that the nuclear basket is likely to play an important role in this process. Overall, however, the data so far does not provide a clear picture of whether there is a single central function for the basket mediating pore access. Instead, it rather suggests a multitude of functions that may include transcript surveillance as well as facilitating efficient access to the pore. The mechanistic aspects of any of these processes remain unknown. Furthermore, the complete picture - if there is only one- for typical transcripts selected or rejected for export by the basket is still missing both in both yeast and humans.

#### 1.4.2.3 Basket-mediated quality control: A model of modulated export affinities

mRNP QC could be defined as the sum of the processes ensuring that faulty mRNPs do not reach the cytoplasm. A discussed above, the selection exerted by nuclear decay plays important role in this mechanism and RBPs mediating mRNA-pore interaction can act as a checkpoint to assess the maturity of mRNPs. Nevertheless, how the collective interaction of basket proteins with RBPs selects correctly assembled mRNP and filters out faulty or non-mature particles is not clear. Numerous research groups have used biochemistry and biophysics combined with computational simulations to provide a precise picture of how the NPC central channel functions as a selective yet permeable barrier. Generally, those studies apply reductionist approaches with a minimal number of key physical variables to understand biophysical principles driving complex mechanisms

such as the collective behaviors of FG-NUP intrinsically disordered domains during the translocation of cargos[37,45].

In their work "Regulation of RNA-binding proteins, affinity to export receptors enables the nuclear basket proteins to distinguish and retain aberrant mRNAs", M. Soheilypour & M.R.K Mofrab use a modeling approach for complex systems, to develop a minimal model for mRNA QC mechanism[136]. The authors based their simulations on the current model for QC in which RNA-binding proteins serve as adaptors for recruitment of export receptors (NXF1/NXT1 or Mex67/Mtr2), and nuclear basket protein TPR/Mlp1 interacts with RBPs to act as a checkpoint verifying the maturity of the mRNPs. It has been shown that splicing is not an absolute requirement for interaction between export receptors and mRNAs; however, export receptors have a higher affinity for RBPs bound to spliced mRNAs[49,137,138,139]. Therefore, RBPs bound to unspliced mRNAs could still recruit export receptors, yet with lower affinities. First, the authors considered typical mRNAs, spliced or unspliced (designated here as "normal" and "aberrant" respectively), of 2.2 kb length which are expected to have an average of nine RBP binding sites. Their first simulation tested export specificity based only on RPB and export receptors without including TPR/Mlp. By varying the affinity between RBP and export receptors (high for "normal" and low for "aberrant" mRNAs) they showed a percentage of simulated successful export events of "normal" mRNAs three times higher than aberrant mRNAs. Hence, they demonstrate that interactions between RBPs and the export receptor can be sufficient to retain "aberrant" mRNAs. However, "aberrant" mRNAs are not retained when the number of RBP binding sites was increased to tweleve[136].

In a second round, they developed their minimal model by including the interaction between TPR/Mlp and RBPs and tested different RBP-TPR/Mlp affinities. Hence, they calculated that the interactions between TPR/Mlp and RBPs efficiently distinguish aberrant mRNAs and prevent their export even for twelve RBP binding sites. In addition, they observed that the export selectivity in this model was conserved for a low range of RBPs-TPR/Mlp affinities. Lastly, they conducted a set of simulations with 'shorter' mRNAs with a length of 500 bases (conserving the same density of RBPs). Interestingly, while short normal mRNAs were exported efficiently, the QC mechanism was not as efficient in the case of longer mRNAs. They concluded that mRNA QC achieved by the basket could be a length-dependent mechanism.

By no means, the authors claim that their predictive approach is a comprehensive representation of mRNA QC and acknowledge the numerous unknowns that are not implemented in their minimalistic model. However, their data suggest that the basket should not be as efficient to retain short aberrant mRNAs compared to longer ones. This modeling supports the idea that mRNA quality control involving the nuclear basket could be a length-dependent mechanism that could be consistent with the different export/retention phenotypes observed upon TPR depletion. Furthermore, their analysis argues for a very interesting picture for basket-mediated selective export based on relatively low RBPs- TPR/Mlp1 affinities. Hence, they proposed a model for QC at the basket where "*mRNA QC is achieved by cooperation of regulated weak stochastic interactions between the involved proteins rather than deterministic switch-like properties*[136]*."*

## 1.5 The role of the baskets in nuclear architecture

### 1.5.1 Do Mlps assemble a lamin-like network?

The interconnection between NPCs, baskets and a nuclear lattice has been described in metazoan and notably, in the amphibians Xenopus and Triturus based on early cryoEM images although the exact nature of the fibrils observed is not clear[140] (Fig.7 a,b). Nuclei in yeast and higher eukaryotes are different in many ways, likely due to an increased nucleus and genome size as well as greater complexity of the gene expression pathway. A bigger nucleus might require the presence of a lamin network to provide rigidity and maintain nuclear morphology. Structural analysis of human and fly nuclei revealed that lamins frequently interact with NPCs and NPCs tend to be concentrated at the nuclear periphery in areas with a dense lamin network[141,142,143]. Furthermore, recent Bio-ID data of lamin-interacting proteins showed that the A-type lamin variant, lamin C, specifically binds to TPR[143]. *S. cerevisiae* lacks lamins but possesses a lamin-like protein, Esc1, that may interconnect NPCs through its association with the basket[111]. Esc1 is required for correct localization of basket proteins at the periphery as upon Esc1 deletion, basket proteins aggregate in few distinct foci at the periphery[111 & this work]. Different groups reported, based on EM images that Mlp proteins could be found in areas between neighboring nuclear pores in yeast[112,144,145]. Because some Mlp double-deletion strains exhibit blebbing and formation of irregular bulges in

the nuclear envelope, similar to phenotypes observed Esc1 mutants, it has been proposed that Mlps filaments might interconnect neighboring NPCs in a lamin-like manner[112]. The existence of those Mlp filaments is debatable as they have not been observed in fluorescent microscopy and nano-gold immunostaining show only a discrete localization of Mlp1/2 at the pore (Fig.4). Nevertheless, Mlp1/2 and basket Nups may serve as an anchor for a lamin-like Esc1 network[112] (Fig7c).

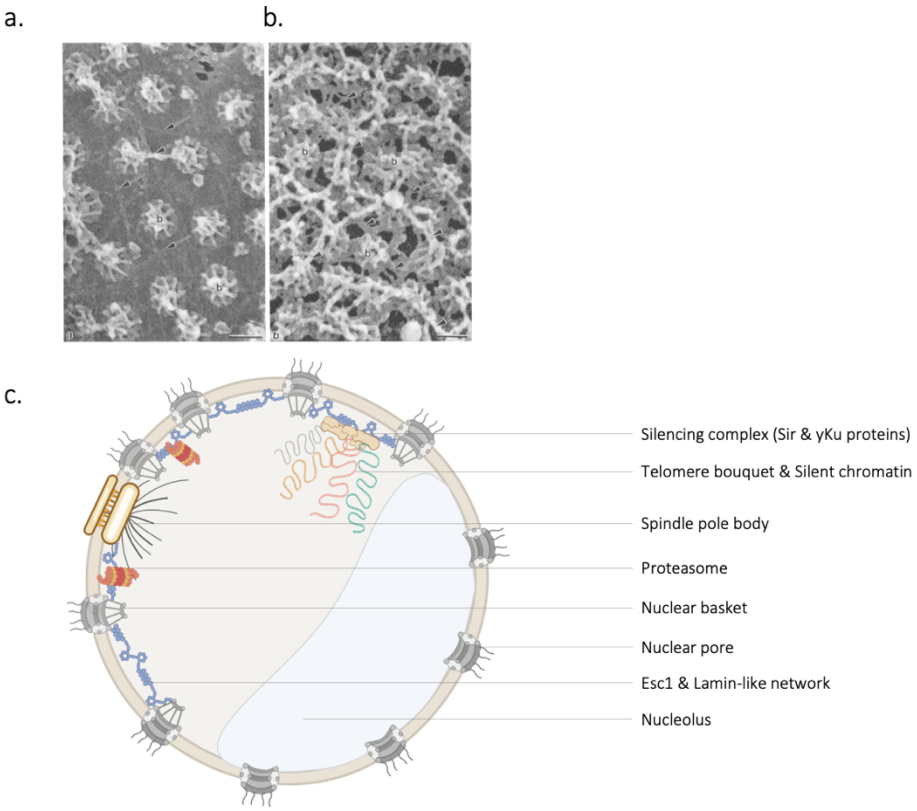


*Figure 7 Basket roles in nuclear architecture.*

*(a) The nucleoplasmic face of "clean" NE. NPCs are well spaced due to the stretching of NE. Possible NE lattice remnants join some basket rings (arrowheads). Arrows indicate fibers attached to INM. (b) NE treated with 0.5% Triton X-100 for 5 min in 5:1 medium to remove membranes. NPC baskets remain intact, but NE lattice is only observed as remnants joined to basket rings (arrowheads). Other fibers, possibly lamina, join NPCs apparently at the level of the nucleoplasmic coaxial rings (arrows). Bars = 100 nm. These images have been published in[113] (c) Mlp proteins connect NPCs and different elements of the NE. Mlp2 interact with the spindle pole body and favor its formation*

*as well as its correct positioning during the mitosis. The proteasome is also part of the basket interactome and participates in the control of cell cycle progression by degrading specific targets allowing anaphase onset. Esc1 is anchored in the nuclear periphery and associates with Mlp proteins to form a lattice between NPCs in a lamin-like manner. Esc1 this network also anchors at the NE the repression machinery involved in telomer bouquet formation and silencing. This basket extended interactome is lacking at the nuclear periphery neighboring the nucleolus, correlating with an absence of Mlp proteins in this specific compartment.*

### 1.5.2 A role for the basket in cell-cycle regulation and spindle pole body assembly

In yeast, the microtubule organizing center, essential for the formation of the mitotic spindle and correct chromosome segregation is called the spindle pole body (SPB). Biochemical analysis revealed that NPCs and specifically basket and TREX-2 are involved in assembly and positioning[146,112,147,106] and demonstrated that Mlp2 but not Mlp1 binds directly to the main components of the SPB core. In the absence of Mlp2 but not Mlp1, errors in cell division have been observed. Indeed, Mlp2 deleted cells display significant delays in proceeding past the late S phase or metaphase. While Mlp2 is not required for proper spindle pole body positioning during the late S to early M phase, cells lacking Mlp2 display SPB-"doublets" (i.e., cells with two SPBs per cell body)[147]. In addition, these cells have a defect in incorporating newly made components into their SPBs, which correlates with smaller SPBs. Therefore, it is believed that Mlp2 specifically helps to incorporate new SPB components into both the mother and daughter SPBs by recruiting them for exchange, or by facilitating their integration. Because budding yeast undergoes closed mitosis (the NE remaining intact along the cell cycle), it is conceivable that this kind of direct communication between the NE and spindle organizer may facilitate the process. However, spindle assembly checkpoint by basket proteins seems to be evolutionarily conserved as it has been found in *S. cerevisiae, Aspergillus nidulans, Caenorhabditis elegans, Drosophila melanogaster*, as well as in human cells[148,149,150,151]. This suggests that anchoring SPB to the NE is common for organisms undergoing open and closed mitosis. Affinity purification experiments have shown that the proteasome is also a complex interacting with the basket although its exact role at the nuclear basket remains an open question[112]. Studies carried out in fission yeast have found that the

proteasome also has a basket-dependent localization at the NE and is required for kinetochore homeostasis placing proteasomal regulation and cell cycle regulation as a new function at the network of the nuclear basket[152,153,154].

### 1.5.3 The basket functions as a telomere and damaged chromatin anchoring platform

In interphase, NE components organize the chromosomes in the nucleus: while centromeres are clustered around the SPB, telomeres are embedded and typically grouped in 3-6 bouquets at the periphery in haploid yeast[155,156]. Specific chromosome regions such as telomers or mating-type (HM) loci display a correlation between perinuclear positioning and silencing in yeast [157,158,159,160,161]. These observations seem in contradiction with the transcription-mediated gene gating at the pore. However, those loci are spatially confined in specific domains where they remain repressed by the cooperative function of Sir silencing factors[161,162]. Their tethering and silencing to the periphery also require numerous factors including the heterodimer yKu70/ yKu80 as well as Esc1[163,164] which may form a parallel and redundant pathway with Sir factors. It has been shown that Mlp2 interacts directly with yKu proteins. In addition, MLP1/2 deletion disrupts the clustering of perinuclear telomeres and releases telomeric gene repression[157,158]. The exact pathway(s) by which the basket and NE favor telomere anchoring, as well as telomere and Hm loci silencing, are still unclear and several studies suggested that Mlp proteins may rather be involved in telomere length control[165,166]. Nonetheless, those results indicate that association with pores is not always correlated with active transcription and underline a role for Mlp proteins in epigenetic silencing.

Telomere regions and associated proteins are also central to genome stability as they differentiate the natural chromosomal ends - which should not be repaired - from accidental double-stranded DNA breaks (DSBs)[167]. It has recently been shown that DSBs as well as eroded telomeres, re-localize to the nuclear periphery at NPCs[168,169] and several functional interplays between the DNA repair machinery and basket extended interactome has been shown[120,170]. Furthermore, in yeast and humans the proteasome, as well as mediators of the DNA damage response are recruited by the basket allowing DNA DSB repair of genes both by homologous

recombination (HR) and non-homologous end-joining (NHEJ) pathways[171,172]. Accordingly, Mlp2 deletion results in a severe deficiency in the repair of DSB, and Mlp1/2 mutants are particularly sensitive to DNA-damaging agents[173]. Notably, Mlp1/2 in yeast and TPR in humans are believed to stabilize and concentrate the SUMO protease Ulp1/ SENP1/2 which are key regulators of the DNA damage response by NHEJ[120,119,111,174] at the periphery, suggesting that basket is also central to genome integrity[175].

Interestingly, similarly to the THO complex, Mlp1/2 are also required to prevent harmful R-loop accumulation[62,176]. While this protection against R-loops seems to necessitate Mlp-mediated gene gating at the pore, the exact mechanism by which the basket prevents hyperrecombination is not clear. Data showed that MLP1/2 deleted cells accumulate replication defects possibly due to stabilized and unresolved R-loops interfering with the progression of replication forks. The authors hypothesized that in presence of a basket and associated factors, mRNPs are produced and exported more efficiently, reducing the probability of back-hybridization with the DNA[106,177]. However, if this model is valid the protection conferred by the basket against R-loops would concern only NPC-gated genes. Nevertheless, taken together those results highlight the function of Mlp proteins and the basket in chromatin organization and genome stability in addition to telomere and DSBs tethering or repair.

### 1.5.4 Coupling nuclear organization and epigenetic: A role for the basket in transcriptional memory?

Multiple organisms can develop a tolerance to severe stress. This acquired stress resistance has been observed in yeasts which can adapt to external conditions variation to maintain their hemostasis by establishing a transcriptional memory. This process involves the genes relocated at the pore upon induction which conserve their position following repression. Therefore, transcriptional memory refers to a gene “remembering” its previous transcriptionally active state and involves the NPC[99]. Such memory confers the ability of a faster rate of transcription initiation and thus faster gene expression when re-induced following a short intervening period of repression. The mechanism of how NPC localization enhances gene expression by conferring rapid reinduction memory is still debated but has been characterized in yeast for the highly expressed

inducible genes *GAL1*, *GAL7*, and *INO1*[178,179,180]. As described in the gene gating section, those genes relocate to the periphery upon activation due to a possible interaction with Mlp1, the SAGA complex, and the nascent mRNP. Interestingly, chromosome conformation capture (3C) analysis and ChIP experiments showed that a subset of genes experiencing the transcriptional memory phenomenon adopts a loop structure characterized by interactions between their promoter and the 3′ end. These memory gene loops (MGLs) are essential for rapid reinduction of the genes possibly by stimulating transcription[181]. It has been suggested that gene looping could facilitate the transfer of polymerases from the terminator to the promoter, therefore, enhancing the re-initiation of transcription. Although still unclear, and possibly more complex than the simple Pol II recycling effect, gene loops may be a common feature of gene activation promoting efficient transcriptional elongation. It has been shown that Mlp1 is needed for the maintenance of MGLs during the repression period, and Mlp1 memory looping can stimulate faster reinduction of Gal1 genes after a 1h period[182]. Furthermore, a DNA zip code called memory recruitment sequence (MRS) has been identified in promoters of genes showing facilitated transcriptional reactivation[183]. Here the transcriptional memory relies on the recruitment of the histone variant H2A.Z mediated by the zip codes. It has been suggested that incorporation of H2A.Z enhances the targeting of the genes to the pore possibly through an association with basket nucleoporins[184]. Therefore, the two different models, gene looping and MRS, describing gene targeting and transcriptional memory propose that basket proteins contribute to genome architecture and epigenetic maintenance of expression programs.

## 1.6 NPC heterogeneity

### 1.6.1 Different pore ‘flavors’ in higher eukaryotes

NPC components are conserved across eukaryotes, however, different studies examining nuclear pore composition showed differential expression of peripheral and inner ring Nups in distinct cell types and during development[185,186,187,188,180]. Additional observations that cells may be differentially affected by mutations in different Nups suggests that NPC composition, as well as nucleoporin function, may not be universal across cell types but that, instead, fine-tuning of gene

regulation could be mediated through selective coupling of transcription and export via subsets of nucleoporins, or selective export is driven by changes in NPC composition and post-translational modifications of specific NPC subunits[185,187,186,189,180]. In CD4+T lymphocytes, lack of NUP210 impaired T cell receptor signaling and negatively affected T cell homeostasis[190], while depletion of NUP153 in mouse embryonic stem cells led to derepression of developmental genes and loss of pluripotency[191]. Mutation of NUP155 in human and mouse models was shown to negatively affect the export of HSP70 mRNA in cardiomyocytes[192]. In Drosophila, NUP96-98 levels were observed to affect mRNA export selectivity during oocyte and germline differentiation[193]; and in mice, cell-cycle dependent variations in NUP96 levels were linked to regulation of cell cycle progression in mitosis through modulation of nuclear export of certain mRNAs, among which are key cell cycle regulators [194,192]. All these studies illustrate a context-dependent role for nucleoporins in selective gene regulation through export. This suggests the stoichiometry of certain nucleoporins in the NPC itself may vary in a cell type- or cell cycle-specific manner to regulate the function of the nuclear pore. Moreover, many nucleoporins have acquired nucleoplasmic functions including transcription regulation and genome organization providing another functional link between transcription, export, and gene regulation in general[195,189,116,196,180,197]. While the mechanistic details are still lacking, overall the data challenge the paradigm that the NPC is a structure of ubiquitous composition but rather show that NPC heterogeneity, i.e., nuclear pores with different compositions and distinct functions in mRNA export, genome organization, and/or transcriptional memory, can modulate gene expression and cell fate in a cell-type-specific manner, providing an additional layer of regulation[187]. As such, an image of the NPC as a plastic structure emerges where different types of pores might co-exist within the same nucleus and exhibit different properties and specialized functions to either mediate efficient and/or selective access to the pore or to stimulate selective transcription in a topology-dependent manner (Fig.8c).

### 1.6.2 Yeast nucleolar & nucleoplasmic pores: A unique case of NPC heterogeneity within the same cell

The nucleolus is a membrane-less organelle known as the site of ribosome biogenesis. In yeast cells, nucleoli have a typical crescent shape and are adjacent to the nuclear periphery. The

nucleolar compartment occupies approximately one-third of the total nuclear volume and is consequently in close vicinity with a third of the NPCs in yeast cells[198]. Curiously, NPCs adjacent to nucleoli are lacking the main basket scaffold proteins Mlp1 and Mlp2 whereas other basket-Nups, Nup1, Nup2, Nup60 are present along the entire nuclear periphery[129,173] (Fig.8a). The mechanistic reasons for why those two proteins are absent from pores in this compartment are currently elusive. Moreover, this nuclear organization begs the obvious question of why yeast cells need to establish two sets of nuclear pores, with and without baskets. Because baskets-less and basket-containing pores occupied distinct nuclear functional domains, the nucleolus, and nucleoplasm, respectively, we can postulate that the two types of pores are involved in different functions by participating in a topology dependent genome organization or a differential nucleocytoplasmic transport. For instance, the nucleolar basket-less pores could organize the nucleolar chromatin bearing the ribosomal DNA repeats whereas the basket-containing pores may rather associate with protein-coding genes. Alternatively, it is also possible that the two types of pores are involved in differential and selective export: nucleolar pores could be involved in ribosomal subunit export, and basket-containing pores could be specialized in mRNPs export. While very appealing, those models have some significant weaknesses. Indeed, the nucleolar chromatin does not seem to interact directly with nucleolar NPCs and rDNA repeats interact with the periphery in an NPC-independent manner[199,168]. Moreover, it has recently been shown that pre-ribosomal subunits can also be exported through pores in the nucleoplasm[200]. For those reasons, the asymmetrical distribution of Mlps in the yeast nucleus may be based on a slightly more complex model than the binary picture with specialized roles for nucleolar pores in organizing rDNA or pre-ribosomal subunits export, and nucleoplasmic pores specialized in mRNA export. However, it suggests a specific role for the basket that is limited to aspects of RNA metabolism that occurs in the nucleoplasm.

The rapid turnover of the proteins assembling the basket, as mentioned above, indicates that baskets are dynamic structures in yeast. In addition, it has been observed that upon heat shock Mlp proteins disassemble from pores and form intranuclear granules[201]. Those granules contain poly(A) RNAs and some RBPs such as Nab2 and Yra1, suggesting that they serve as storage structures and sequester some mRNPs waiting for the heat stress to be resolved (Fig.8b).

Alternatively, Mlp granules formation could be an efficient way to remove the basket from the pore and allow the rapid export of mRNAs encoding for heat shock proteins without any delay caused by QC steps. It has been shown that heat shock induces the dissociation of Mex67 and its adaptor proteins from regular mRNAs to prevent general mRNA export. At the same time, heat-shock mRNAs are rapidly exported in association with Mex67, without the need for adapters known to interact with the basket[48]. Those results indicate that the export of bulk mRNA is stalled during cellular stress and mRNA QC is bypassed for immediate export of stress-responsive transcripts. This illustrates the highly dynamic and plastic nature of the pore in response to cellular changes to adapt mRNA exports. It also strengthens the idea that baskets are formed on pores in yeast to take on the function of gatekeeper for mRNAs. Taken together those data could suggest a model where basket-containing pores in the nucleoplasm, but not basket-less pores in nucleoli, are specialized in mRNP export regulation and specific QC steps. While the basket is not crucial for the export of the bulk of mRNP, it is not clear whether it represents a pore specialization for only a yet-to-be-identified subset of mRNPs.

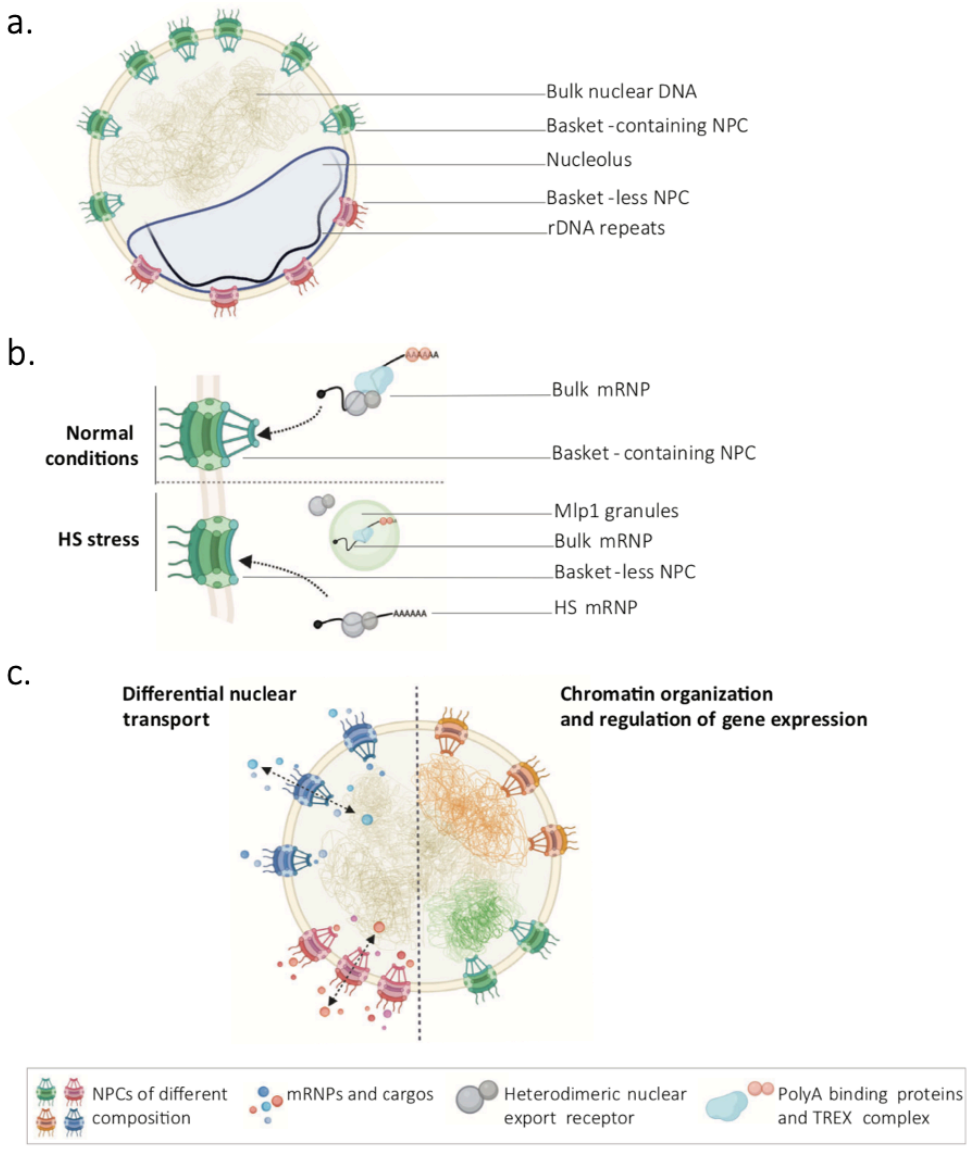


*Figure 8 Nuclear pore heterogeneity.*

*(a) In the yeast S. cerevisiae, basket-containing pores occupy the nucleoplasmic periphery, while nuclear pores along the nuclear membrane adjacent to the nucleolus lack basket structures; in particular, the basket core components Mlp1 and Mlp2. (b) Upon heat-shock of yeast cells, Mlp1 detaches from nuclear pores and assembles into nucleoplasmic granules. These granules also contain the bulk of sequestered mRNAs as well as TREX components and poly(A)-binding proteins such as Nab2. While export receptors dissociate from bulk mRNPs upon heat shock, they facilitate the export of heat-shock transcripts in a basket-independent manner. (c) Potential models for NPC*

*heterogeneity have been proposed in higher eukaryotes, which could be required to establish nuclear sub-domains with specific chromatin organization, regulate the transport of specific cargos in a topological dependent manner or, similar to yeast, occupy specific regions along the nuclear periphery. This figure has been published in* [42].

## 1.7 Research objectives of this work

This thesis presents my research projects aiming to understand mRNA export-dynamic once they reach the nuclear periphery. My main focus has been to determine how a nuclear pore complex structure protruding into the nucleoplasm called the nuclear basket regulates mRNA export. Therefore, I analyzed the modalities of mRNP export from two different perspectives: (i) the direct study of mRNAs at the periphery of nuclei, and (ii) the nuclear basket dynamics in yeast *S. cerevisiae*.

The first part is a pure RNA-centric approach where we study single mRNA molecules and their path toward the cytoplasm using live-cell microscopy strategies. We dissected their behavior at the vicinity of the nuclear periphery and aimed to understand the modalities of mRNP scanning.

The second and main part of my Ph.D. has been devoted to understanding basket function and asymmetric distribution in yeast nuclei. Because most of the basket roles have been so far related to the regulation of Pol II transcribed genes/transcripts, our main working hypothesis has been that basket formation is contingent on events occurring in the nucleoplasm (*i.e.* excluded from the nucleolar region). Therefore, in this study, we explore the possibility that Mlp1 association with NPCs, resulting in the formation of a basket, relies on mRNAs transcription adjacent to the pore and/or subsequent mRNA processing events preceding mRNP export. Accordingly, we also hypothesized that the lack of those events in nucleoli results in the absence of baskets on pores adjacent to nucleoli.

# 2. Article 1: Imaging single mRNAs to study dynamics of mRNA export in the yeast *Saccharomyces cerevisiae*

Pierre Bensidoun[1,2], Pascal Raymond[1], Marlene Oeffinger [1,2,3], Daniel Zenklusen [1]

[1]Département de Biochimie et médecine moléculaire, Faculté de médecine, Université de Montréal, Montréal, Québec H3C 3J7, Canada

[2]Institut de recherches cliniques de Montréal, 110 Avenue des Pins Ouest, Montréal, Québec H2W 1R7, Canada c Faculty of Medicine,

[3]Division of Experimental Medicine, McGill University, Montréal, Québec H3A 1A3, Canada

Published in Methods, vol 98 pp104 114 (2016). doi: 10.1016/j.ymeth.2016.01.006

## 2.1 Context of the article

In this section published in 2016 in Methods, we describe a detailed protocol to fluorescently tag mRNAs enabling to image mRNP transport with high spatial and temporal resolution in yeast *S. cerevisiae*. This strategy has been applied in different contexts, in yeast and higher eukaryotes, allowing to monitor mRNA localization, translation, and the life cycle of highly regulated mRNAs and ncRNAs. Here, we detail a strategy for the PP7 mRNA labeling strategy, combined with fast image acquisition and image registration to study mRNP export in real-time. We published in 2015 in the Journal of Cell Biology an article entitled "*The nuclear basket mediates perinuclear mRNA scanning in budding yeast"* present in the annex 2 of this thesis[108]. In this article, the RNA tagging method has been used to examine the mRNP-NPC interaction in living cells and characterize different scanning parameters such as the scanning time and distance and the residency time of static transcripts at the periphery. I have been involved in the experimental part, and I am the second author of the article reporting these results. We also published the method in a collaborative work with D.Grunwald and B.Montpetit groups in Methods Molecular Biology in 2019[202] which is present in the annex 3.

### 2.3 Author contributions

The experimental design of the approach published in the 2015 JCB paper, mentioned above and reported in this method, has been done by Daniel Zenklusen and Marlene Oeffinger. I have been involved in the imaging part and the complementary biochemistry approach consisting of NPC affinity purifications. Pascal Raymond and I carried out some optimizations of the approach, notably of the imaging conditions, for the method detailed below. In addition, I have been involved in the production of the manuscript.

## 2.2 Text of the article

### 2.2.1 Abstract

Regulation of mRNA and protein expression occurs at many levels, initiated at transcription and followed by mRNA processing, export, localization, translation and mRNA degradation. The ability to study mRNAs in living cells has become a critical tool to study and analyze how the various steps of the gene expression pathway are carried out. Here we describe a detailed protocol for real time fluorescent RNA imaging using the PP7 bacteriophage coat protein, which allows mRNA detection with high spatial and temporal resolution in the yeast S. cerevisiae and can be applied to study various stages of mRNA metabolism. We describe the different parameters required for quantitative single molecule imaging in yeast, including strategies for genomic integration, expression of a PP7 coat protein GFP fusion protein, microscope setup and analysis strategies. We illustrate the method's use by analyzing the behavior of nuclear mRNA in yeast and the role of the nuclear basket in mRNA export.

### 2.2.2 Introduction

Translating the genetic information from DNA to proteins requires the synthesis of a messenger RNA molecule, the mRNA. Eukaryotic cells have separated the site of protein production and transcription by storing DNA in a separate cellular organelle, the nucleus, requiring mRNAs to transit to the cytoplasm to meet with ribosomes for translation. Nucleocytoplasmic exchange is mediated by nuclear pore complex (NPC), a large multiprotein complex embedded in the nuclear

membrane[203]. To pass through nuclear pores, mRNA interacts with specific transport receptors through association with adaptor proteins that mediate the interaction and translocation through the NPC[50].

After transcription by RNA polymerase II and assembly into RNA–protein complexes (mRNPs), mRNPs are released from the DNA template into the nucleoplasm. Various studies have shown that mRNAs show diffusional behavior within the nucleoplasm and no directed transport towards the periphery has been documented[16,89,93,95]. mRNP movement is, however, influenced by the chromatin environment and restricted movement of mRNAs in chromatin dense regions have been observed in higher eukaryotes. Thus, the time required for mRNAs to reach the nuclear periphery is influenced by the size of the nucleus, chromatin environment as well as by the position of the gene it is transcribed from. In yeast, a number of genes are transcribed at the nuclear periphery, however, whether gene targeting to the nuclear periphery stimulates mRNA export, serves other regulatory processes such as transcription regulation, or both, is not yet fully understood (reviewed in[96,204]).

To ensure rapid and efficient protein expression, it seems reasonable for cells to optimize the kinetics of the different steps leading the nucleocytoplasmic export. This includes facilitating mRNA association with NPCs upon reaching the periphery and ensuring that such association leads to translocation to the cytoplasm. In higher eukaryotes, the release of mRNPs from the nuclear periphery back into the nucleoplasm is likely to significantly prolong the time it takes for an mRNA to reach the cytoplasm, as the diffusive behavior of mRNAs in the nucleoplasm will result in a delay for the mRNA to re-associate with the periphery and thus the potential for subsequent export. Stabilizing interactions with the periphery therefore facilitates export and studies in yeast as well as in higher eukaryotes have shown that mRNPs frequently show a scanning behavior a the nuclear periphery prior to export[16,108]. In budding yeast, components of the NPC and factors associated with mRNAs are required for this process[108]. In particular, the myosin like protein Mlp1, a structural component of the nuclear basket that extents from the central scaffold of the NPC into the nucleoplasm, is required for perinuclear mRNA scanning in budding yeast. In this book chapter, we describe the experimental setup and image analysis methods used to show that the nuclear basket

is implicated in maintaining mRNPs at the periphery by providing an interaction platform for mRNPs at the NPC, possibly allowing mRNP arrangement required for export to occur before mRNA enter the NPC for translocation. These examples illustrate how single molecule resolution imaging using the PP7 system in combination with sub diffraction resolution particle tracking is used to study mRNA export in budding yeast. Budding yeast has been used extensively to study mRNA export. Genetic, biochemical and microscopy based approaches have identified many factors involved in the different steps of the mRNA export pathway, including components of the NPC, RNA binding proteins and the export receptor Mex67[203]. With most players identified, a next step towards a better mechanistic understanding of mRNA export is to study how the different factors affect specific steps, such as the docking of mRNPs to the NPC or the translocation process. These processes reflect dynamic interactions and are difficult to study using biochemical and genetic approaches. Studying such dynamic processes therefore requires the ability to visualize individual mRNA in high spatial and temporal resolution in living cells. Such approaches can further be combined with yeast genetic approaches, such as the use of a large number of mutant yeast strains affecting mRNA export, making yeast a powerful system to study this complex process. Different methods have been developed allowing mRNA detection in cells, including fluorescent in situ hybridization (FISH), molecular beacons, labeling of RNA binding proteins and various aptamer based techniques (reviewed in[205,206]). A subset of these techniques has the sensitivity to detect single RNA molecules, and only a few allow single mRNA detection in real time in living cells. Some of these approaches require the injection of labeled proteins into cells or use plasmid-based expression systems to introduce reporter constructs for single molecules studies. Quantitative single molecule studies, however, are ideally performed studying mRNA and proteins expressed at endogenous levels, reducing the risk of altered mRNA behavior due to overexpression or altered expression patterns caused by exogenous expression. The yeast *S. cerevisiae* provides a powerful experimental system to study gene expression from a single molecule perspective. Targeted genomic integration using homologous recombination allows expression of tagged versions of endogenous RNAs and proteins in their proper genomic context[206,207]. Furthermore, many mRNAs in yeast are expressed at levels of only a few copies per cell, facilitating the study of individual molecules[208]. However, from a microscopy perspective, yeast does also have disadvantages. The

presence of a thick cell wall in yeast introduces significant light scattering affecting signal-to-noise ratio. Single molecule resolution imaging in yeast therefore requires microscope setups optimized for visualizing low intensity mRNA signals. Aptamer-based mRNA labeling, where RNA-stem loop sequences recognized by fluorescent protein fused RNA binding proteins are introduced into an mRNA of interest, is one of the most frequently used techniques for in vivo RNA detection[209]. In this chapter, we describe the use of an RNA labeling strategy that uses the addition of binding sites for the bacteriophage PP7 coat protein to a selected RNA in order to visualize single mRNA molecules in high spatial and temporal resolution in yeast. We will illustrate the use of the approach by studying the behavior of nuclear mRNAs prior to their export to the cytoplasm.

### 2.2.3 Overview of the method

The use of bacteriophage coat proteins to label mRNAs was initially developed in the Singer laboratory showing that insertion of binding sites for the MS2 coat-protein in the 3′ untranslated region (UTR) of the ASH1 mRNA allowed visualization of the targeting of the ASH1 mRNA to the bud tip in dividing yeast cells[13]. Different RNA binding proteins have since been used to label mRNAs, including lambda N, U1A, PP7 coat protein and others, which enabled the study of RNA dynamics in different organisms[207,210–212,213]. The PP7 coat protein (PCP) has recently been introduced as an RNA imaging tool to study the dynamics and complexity of different molecular mechanism of mRNA metabolism. Becoming established as a widely used tool to study RNA dynamics, it is often used in combination with the MS2 system, allowing for multiplex mRNA visualization in livings cells, as demonstrated in budding yeast, Drosophila and mammalian cells [108,12,17,214 215–218]. The PCP, like the MS2 coat protein (MCP), is derived from a single-stranded (ss) RNA bacteriophage. Although sharing only 15% sequence identity with MCP, PCP has a very similar structure than MCP, and both proteins bind to an RNA stem-loop as a homodimer, thus doubling the number of labels that are added per binding site introduced to an RNA of interest [219]. Comparing MCP and PCP ability to bind to RNAs in mammalian cells in vivo showed that MCP forms a weaker dimer than PCP. Furthermore, these in vivo studies showed that not all MS2 stem-loop get bound by MCP–GFP in cells, however, all binding sites for PP7–GFP were occupied on a PP7 stem-loop containing RNA, concluding that the PP7 system performs better for RNA labeling than

the MS2 system[220]. Comparing the stability of 24 MS2 and PP7 stem-loops integrated into the yeast genome showed that PP7 stem-loops are less frequently lost through recombination than MS2 stem-loops, further suggesting that the PP7 system is easier to use than the MS2 system[207]. However, it should be noted that loss of stem-loops through recombination can be minimized by modifying the nucleotide sequences to make the stem-loops nonrepetitive[221]. Wu and co-workers further showed that dimer formation and consequently signal-to-noise ratio can be increased by expression of MCP or PCP as single chain tandem dimers [220]. Furthermore, an almost background free variation of the MS2 and PP7 system has been described where a chimeric RNA containing alternating MCP and PCP binding sites and split versions of GFPs fused to MCP and PCP were constructed[222]. However, complement fluorescent protein formation is slow and it needs to be seen if this system is useful in yeast where most RNAs have short half-lives. Furthermore, all direct comparisons of the MS2 and PP7 RNA labeling system that tested the ability to detect RNA have been performed in mammalian cells. Therefore, it has yet to be shown whether there is a significant difference between MS2 and PP7 for their ability to detect RNAs in yeast. To visualize RNA in vivo, insertion of a single binding site for PCP does not allow detection of individual RNAs, and binding sites for PCP have to be multimerized to enable visualization. Early studies have used 24 stem-loops to allow single molecule detection, however, more recent studies showed that fewer copies are sufficient[108,215,218]. The number of stem loops will determine the fluorescent intensity of RNA signals, and insertion of fewer loops decreases the signal-to-noise ratio. This requires either more sensitive detection tools or longer exposure times during image acquisition, which in turn can limit the ability to detect fast diffusing RNA molecules. Furthermore, adding multiple RNA stem-loops, each bound to a dimer of PCP–GFP, adds significant size and mass to an mRNP, but it has not yet been systematically determined whether increasing the number of stem-loops affects RNA metabolism. Many studies have shown that RNAs labeled with MS2 or PP7 stem-loops are properly transcribed, localized, translated and degraded. In yeast, tagging of the essential genes MDN1 and CLB2 mRNAs with 12 or 24 PP7 stem-loops does not alter mRNA and protein levels or affects cell growth, and a transgenic mouse where both alleles of the beta-actin contain 24 MS2 stem- loops in its 3′ UTR is viable[108,207,223]. This suggests that in most cases repeat insertion is well tolerated. However, a recent report showed that the stem-loop containing fragment of

mRNAs labeled with MS2 stem-loops can accumulate in cells due to the difficulty of the 5-3′ degradation machinery to degrade such RNAs, and that accumulation is more pronounced with higher number of stem-loops[224]. Insertion of stem-loops increases the length of the UTR and could also induce 'faux 3′ UTR NMD'[225]. We have not observed destabilization of mRNAs due to the insertion of PP7 stem-loops, however, faux 3′ UTR NMD might occur for specific RNAs (unpublished observations). Therefore, to ensure that the insertion of PP7 stem-loops does not affect RNA metabolism (transcription, translation or degradation) and that signals observed using PCP–GFP are corresponding to a full length RNA and not just degradation intermediates of PP7 stem-loops, expression of PP7 stem-loop-labeled RNAs should always be compared to endogenous RNA levels using either single molecule resolution FISH and/or RT-PCR or northern blot analysis with probes specific to the mRNA as well as the PP7-stem loops; in addition, protein levels should be determined by Western blotting. The position of where PP7 stem-loops are inserted within an mRNA has to be carefully chosen and is influenced by the biological question that is investigated. Most often stem-loops are inserted into the 3′ UTR of an mRNA. Stem-loops can also be placed into the 5′ UTR or within an open reading frame, however, this requires a specific design of the stem-loop and linker sequence to ensure that mRNAs metabolism is not affected. The initially described 24 PP7 cassette contains multiple translation initiation codons and stop codons, and mRNAs tagged with this cassette in the 5′ UTR will therefore not be translated [17,207]. Recently, a modified version of the PP7 stem-loop cassette has been described containing 6 PP7 stem-loops and no stop codons, and was shown to allow translation of an mRNA when the cassette was inserted as part of an open reading frame in mammalian cells [218]. It has not yet been demonstrated whether insertion of this new version of PP7 stem-loops into the 5′ UTR or within an open reading frame will allow translation of an mRNA in yeast. The insertion of an unrelated stem-loop in the 5′ UTR of the MFA2 mRNA was shown to inhibit translation, which could indicate that the insertion of multiple PP7 stem-loops bound by PCP could similarly limit the ability of the ribosome to initiate translation when PP7 stem-loops are present in a 5′ UTR[226]; however, this still needs to be experimentally determined. Independent of the translational defect of the PP7 stem-loops in the 5′ UTR, 5′ UTR insertions have been used to study nuclear processes, in particular transcription

dynamics. 5′ tagging results in fluorescent labeling of nascent RNAs, and measuring fluctuations of nascent mRNA signals allows the investigation of transcription kinetics and mRNA export[17,108,207,215].

In the following sections, we describe in detail the different steps for labeling and imaging of 5′ and 3′ labeled mRNA in *S. cerevisiae*, (i) using the CLB2 mRNA as an example for an RNA labeled with 12 PP7 stem-loops in its 3′ UTR, and (ii) an inducible reporter strain in which the promoter of the GLT1 gene is replaced by a galactose-inducible GAL1 promoter and contains 24 PP7 stem-loops placed in the 5′ UTR of the gene. These genes were chosen to reflect two types of genes frequently used to mRNA export and gene expression regulation in general: an RNA expressed from an endogenous gene transcribed at low levels (CLB2), and a reporter gene whose expression is modulated by an inducible promoter such as the GAL1 promoter.

## 2.2.4 Detailed protocol

### 2.2.4.1 Endogenous labeling of genes using PP7 stem-loops

In yeast, integration of exogenous DNA within any position in the genome can be achieved using homologous recombination with sequence homologies as short as 40nt. Therefore, PP7 stem-loops can be inserted using PCR amplifying cassettes that contain PP7 stem-loops as well as selectable markers (Fig. 9B)[108,207]. Cassettes are amplified using PCR primers that contain homology sequences to the targeted integration sites. Alternatively, DNA fragments cloned into plasmids can be similarly integrated using homologous recombination. Here, we describe two tagging strategies that target either the 3′ or the 5′ UTR, illustrated by the endogenous tagging of the CLB2 mRNA, or the integration of promoter and an RNA tagging cassette into the 5′ UTR of the GLT1 gene. CLB2 mRNA is labeled by inserting 12 PP7 RNA step-loops into the 3′ UTR. To this end, a tagging cassette is amplified using primers that contains 50 nt homology to the insertion site that is directly adjacent to the stop coding of the CLB2 gene (Fig. 9B). The integration cassette contains 12 PP7 stem-loops followed by a loxP recombination site, an ADH1 terminator, a kanamycin (KAN) resistance gene containing its own promoter and terminator, and a second loxP site[108]. The loxP sites allow removal

of the KAN selection marker and ADH1 terminator after the insertion of the cassette into the yeast genome and places the endogenous 3′ UTR directly after the PP7 stem-loops. The 12 PP7 cassette adds 576 nt to the endogenous 3′ UTR. The ADH1 terminator allows transcription termination of the CLB2-PP7 RNA before the selection marker is excised.

The cassette is amplified from plasmid pDZ617 (available from addgene.org) and transformed into a diploid wild-type W303 yeast strain using standard procedures [108]. Positive clones are selected by plating cells on G418-containing media (200ug/ml) and will appear after 2 days. In case of high background, cells are replica- plated onto fresh G418 plates after two days and grown for 1–2 additional days. Single colonies are then isolated, and positive clones verified by PCR with primers flanking the insertion site. To reconstitute the CLB2 3′ UTR, cells are transformed with a centromeric plasmid carrying a URA selectable marker and expressing CRE recombinase under the control of a galactose inducible promoter (pSH47) [227]. CRE recombinase recognizes a 34 bp DNA sequence termed loxP and allows the excision of DNA located between two loxP sites oriented in the same direction. CRE expression is induced by growing cells in synthetic media lacking uracil and containing 3% galactose overnight. Approximately 100 cells are plated the following day onto YPD media ($OD_{600} \sim 10^7$ cells). Colonies are then replica plated onto YPD and YPD G418 plates to test for loss of the selection marker and reconstitution of the CLB2 3′ UTR, leaving only the 12 PP7 stem loops and a single loxP (Fig. 9B). Correct size and sequence of the inserted stem-loops is then tested by PCR and sequencing. To remove the CRE expressing plasmid, which contains a URA3 selectable marker, cells are plated on media containing 5-Fluoroorotic acid (5-FOA) at a concentration of 0.1% (SD complete plus 5-FOA). 5-FOA is converted to the toxic form in strains expressing the functional URA3 gene coding for orotine-5-monophosphate decarboxylase that is involved in the synthesis of uracil. Cells will grow after 1–2days on 5-FOA containing media.

Finally, to evaluate that insertion of the PP7 stem loops does not affect general mRNA metabolism, cell growth is measured by establishing growth rates compared to a wild-type strain, and mRNA and proteins expression levels are determined by northern and western blotting, or

similar techniques. Single molecule resolution RNA FISH is a good control to ensure that expression and localization of mRNAs is not affected by the insertions of PP7 stem-loops [208]. To create an inducible reporter, a plasmid containing a selection gene followed by a GAL1 promoter and 24 PP7 stem-loops was used (pDZ305). Marker, promoter and stem-loops are flanked by 500 base pairs of homology defining the insertion sites within the GLT1 promoter, replacing the GLT1 promoter with the integration cassette (Fig. 9A) [108]. The cassette is then excised from the plasmid pDZ305 by enzymatic digestion with PacI and NotI and transformed into yeast cells; positive clones are selected and tested for integration by PCR and sequencing.

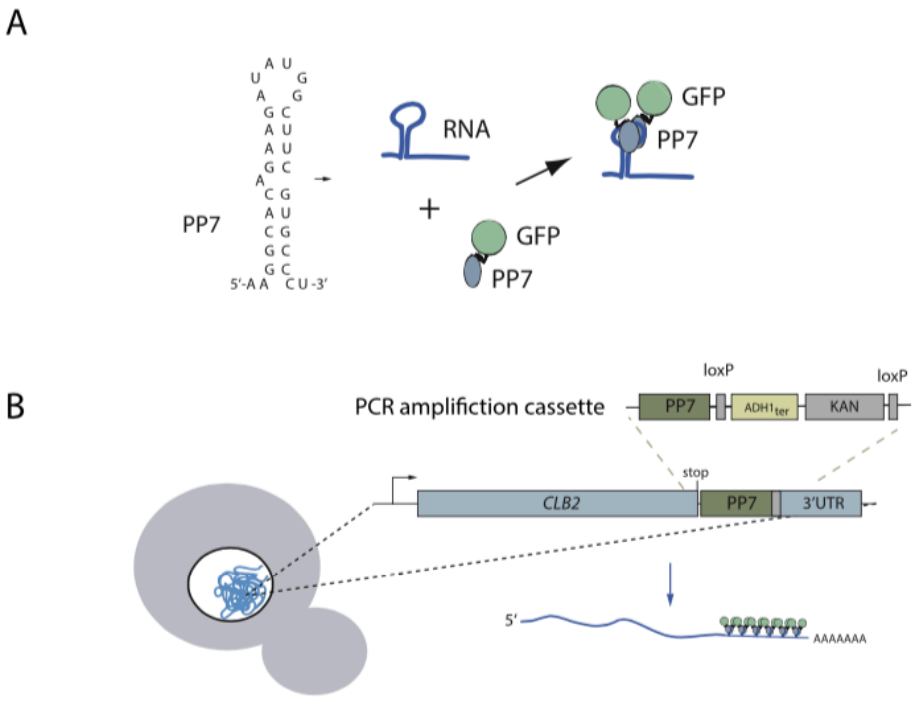

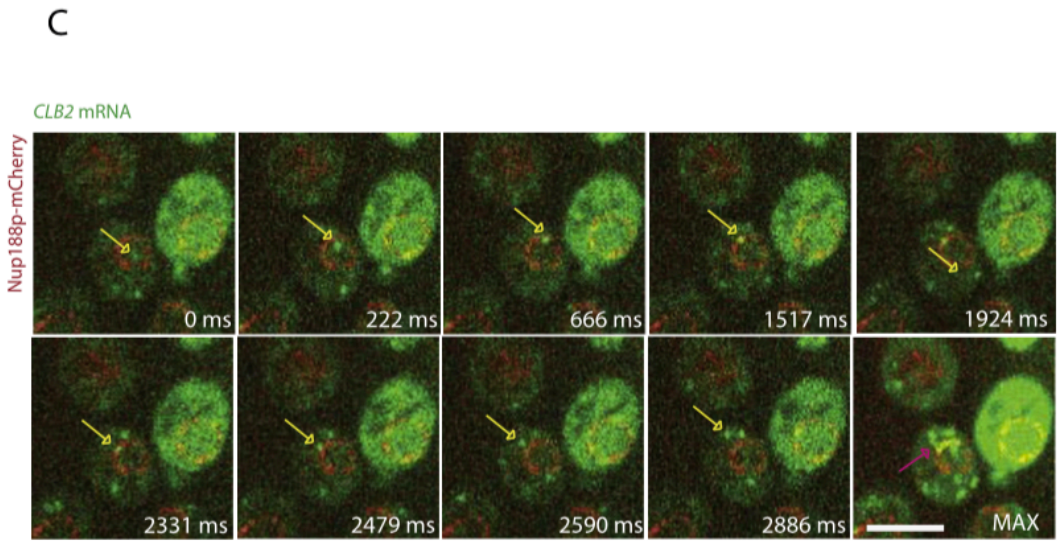


*Figure 9 Visualization of single mRNAs in living cells using the PP7 system.*

*A) Cartoon illustrating the PP7 RNA labeling approach. Binding of a GFP tagged PP7 coat proteins to a PP7 stem-loop structure results in a fluorescently labeled RNA. (B) Labeling strategy for the insertion of PP7 stem-loops to the 3′ UTR of endogenous yeast genes. A PCR product containing flanking sequences to the insertion sites in the 3′ UTR of a target gene is transformed into yeast cells. Two loxP sites allow the removal of the ADH1 terminator and the kanamycin resistance marker after insertion of the tagging cassette into the genome, reconstituting the endogenous 3′ UTR. (C) Live cell imaging of CLB2 mRNA. Individual frames from a movie acquired in 37 ms intervals. MAX shows maximum intensity projection of all frames of the movie. mRNA is shown in green, nuclear pores in red. Scale bar is 5um. Adapted from Saroufim et al.*[108].

#### 2.2.4.2 Expression of PP7-GFP fusion protein

The number of stem-loops is only one parameter that influences signal-to-noise ratio for single mRNA detection. Of equal importance is the expression level of the PCP–GFP fusion protein. At any given time, only a fraction of the free PCP–GFP is bound to RNAs contain PCP–GFP binding sites, and the free fraction of PCP–GFP is the main factor influencing the ability to detect single RNAs above background GFP-levels. To ensure that PP7 binding sites are occupied by PCP–GFP quickly after the RNAs is synthetized, the protein has to be expressed at sufficient levels. However, if the

PCP–GFP protein expression is too high, the high number of PCP–GFP molecules not associated with the tagged mRNA leads to elevated fluorescence background unfavorable for single mRNAs detection. Therefore, the expression level has to be carefully titrated. We have constructed an expression plasmid where PCP–GFP is expressed from an ADE3 promoter resulting in a low expression level of PCP–GFP protein and allowing single mRNA detection of low abundant RNAs [108]. Moreover, two copies of a yeast optimized GFP are fused to the PP7 coat protein. The NPC creates a diffusion barrier resulting in proteins larger than ~40 k Da to only inefficiently diffuse to the nucleus in the absence of specific nuclear localization signals (NLS) [228,229]. Although larger than 40 kDa, expression of a non-NLS containing PCP–GFP fusion in yeast results in equal distribution PCP–GFP in the nucleus and the cytoplasm (Fig. 10A left panel). However, when inducing strong transcription of genes containing PP7 binding sites, such as induction from a galactose-inducible promoter as shown in Fig. 10B, nuclear levels of PCP–GFP deplete over time, suggesting that PCP–GFP nuclear import is slow. When studying nuclear RNAs of strongly induced genes, the presumably slow nuclear import of a non-NLS containing PCP–GFP protein should be taken into consideration as it could result in not all nuclear PP7-tagged RNAs being bound by PCP–GFP. However, to study gene regulation of low abundant genes, expression of PCP–GFP using an ADE3 promoter without an NLS works well for the detection of low abundant nuclear and cytoplasmic single RNAs, such as MDN1 and CLB2 mRNA. In all yeast studies to date, PCP is expressed as a fusion protein with a fluorescent protein fused on its C-terminus (Fig. 9A)[17,108,207,214]. If only cytoplasmic RNAs are studied, signal-to-noise of cytoplasmic mRNAs can be enhanced by targeting PCP–GFP to the nucleus using an NLS added to the N-terminus of the fusion protein. However, expressing NLS-PCP–GFP from an ADE3 promoter leads to very high levels of PCP–GFP in the nucleus and does not allow visualization of single nuclear mRNAs due to high fluorescent background (unpublished observations).

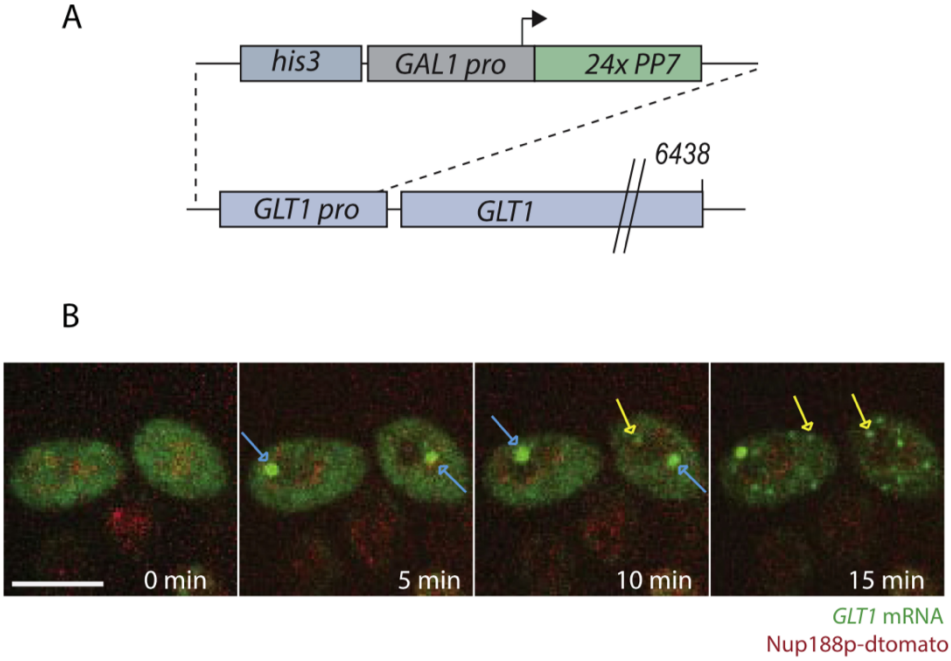


*Figure 10 Labeling strategy for inserting PP7 stem-loops to the 5' UTR of genes*

*(A) Cartoon illustrating a targeting construct containing a histidine selectable marker, a galactose inducible promoter and a 24 PP7 stem-loops flanked by homology regions that result in replacing the endogenous promoter and 5′ UTR with the reporter construct. (B) Kinetics of 24PP7-GLT1 mRNA expression upon induction by galactose. Single images of 24PP7-GLT1 mRNA (green) and nuclear pores (red) for indicated time points after addition of galactose (right). Blue arrows show sites of transcription where multiple nascent mRNAs are associated with the GAL1pro-24PP7-GLT1 locus. Yellow arrows show single mRNAs. Scale bar is 5µm. Adapted from Saroufim et al.,*[108].

### 2.2.4.3 Labeling a reference structure

Different aspects of single molecule behavior can be studied using fast live cell imaging such as the diffusion characteristic of molecules in different environmental conditions, or the movement of individual molecules relative to a reference structure. This can include studying the association/dissociation behavior from subcellular structures or the translocation from one cellular compartment to another. In any case, such studies require the labeling of a reference structure with a fluorescent protein with different spectral characteristics. Fluorescent proteins emitting light in green/yellow and red spectra are most frequently used for live cell imaging due to their

brightness, photostability and the availability of laser lines (488/514 nm and 641 nm). For single mRNA imaging, most commonly green or yellow fluorescent proteins are used to label RNAs, while reference structures are often labeled with red fluorescent proteins[17,108,207,214–217]. However, red fluorescent proteins can also be used for RNA tracking, in particular as red fluorescent spectra show less auto fluorescence than the green spectra, and recently various bright and photostable red fluorescent proteins have become available[205,230]. mKate2 and mCherry have been used for single mRNA imaging in yeast[207,215,217]. However, in our hands, we have been more successful in using green fluorescent proteins for RNA tracking[17,108,216]. A website at Nikon Imaging Center at University of California San Francisco QB3 summarizes the properties of most available fluorescent proteins and is a good reference to select fluorescent protein pairs (http://nic.ucsf.edu/FPvisualization/). In yeast, reference structures are usually labeled using a similar PCR based homologous recombination strategy as described for RNA tagging (Fig. 9A). To investigate nuclear mRNA movements and mRNA export, tagging components of the nuclear pore complex serve as a reference structure to analyze and interpret the behavior of single mRNAs. Nup188 is an inner ring component of the nuclear pore complex and its labeling with 2 mCherry or dTomato does not affect mRNA export, different to the labeling of some other commonly used NPC components such as Nup49 (unpublished observations). As shown in Fig. 9C, to follow the path of CLB2 mRNA towards the cytoplasm, nuclear pores were labeled with two copies of a mCherry C-terminal inframe fusion on Nup188. Adding two copies of mCherry or dTomato expressed as a tandem dimer allows enhancing the NPC signal (Figs. 10 and 12).

#### 2.2.4.4 Growing and attaching cells to coverslips

An important parameter of live cell imaging is to ensure that cells are kept in physiological conditions and remain in the imaging plane during image acquisition. Unlike most mammalian cells that can be grown on coated glass coverslips, yeast cells are grown in liquid cultures and are only attached to cover glass shortly prior to imaging. When grown in liquid culture, yeast cells will cycle through different metabolic states depending on cell density and availability of nutrients. Prior to transferring to the microscope, cells should be grown in conditions that reflect the growth conditions suitable to the process that is studied. For most studies in *S. cerevisiae*, cells are grown

in exponential phase (rule of thumb: $OD_{600} < 0.6$) over the course of a few hours before being transferred to microscope coverslips. For imaging, yeast cells are best grown in synthetic complete media as rich media (YPD) results in strong background autofluorescence and cannot be used for imaging. Yeast cells do not naturally attach to glass coverslips. However, for imaging cells over time, cells should stay immobilized on the glass surface to limit cell movement during image acquisition. Moreover, cells continue to grow and divide and cell density will increase, introducing cell movement when cells are close to each other. Different methods have been tested to restrict cell movement during image acquisition. A frequently used method is to use depression microscope slides that allow the deposition of a media/agar patch on the slide where cells can be placed before a coverslip is added on top and sealed. Recently, microfluidics systems that trap cells in small chambers and limit cell growth to the surface of the coverslip have been used successfully, in particular for long time-laps imaging (such as CellASIC). When cells are imaged for short times as in the experiments described here, a simple and cost-efficient way is to immobilize cells using glass bottom plates/dishes (such as 96-well plates) coated with Concanavalin A, a lectin that binds to sugars in the yeast cell wall. Cells adhere tightly to the Concanavalin A treated glass surface and can be imaged for many minutes. However, when growing on Concanavalin A treated glass, new buds often appear distant to the glass surface and will not adhere to the Concanavalin A treated glass surface. This method is therefore best suited for short-term experiments. Cells grown in liquid culture often clump together, making spreading of cells in a single layer on glass slides difficult. To avoid cells clumps in 96-well plates, cells are vortexed prior to disposition on the glass. 200ul of cell culture at $OD_{600}$ = ~0.5 are transferred to an Eppendorf tube and vortex for 10 s. Then 100ul of the vortexed culture are added to a well of the 96-well plate and cells collected at the bottom of the well by centrifugation for 10 s at 900xg using a swing-out rotor. This will result in a single layer of yeast cells in each well ready for imaging. Alternatively, let cells settle by gravity for ~2–5 min. Coating of glass bottom 96-well plates (Matriplate MGB096-1- 2-LG-L) by Concanavalin A.

1. Make 1 mg/ml stock of Concanavalin A (Sigma L7647) in 1 PBS pH 5.5, filter sterilize and aliquot and store at 20 C.
2. Add 100 ll of Concanavalin A to the bottom of the wells and incubate for 5 min at room temperature.

3. Remove Concanavalin A solution. Concanavalin A can be reused many times when stored frozen.
4. Activate Concanavalin A by adding a solution containing 20 mM $CaCl_2$ + 20 mM $MnSO_4$ (filter sterilized) for 5 min at room temperature.
5. Rinse twice with $H_2O$. Prevent well from drying by adding 200 ll of sterile $H_2O$ until use.
6. NOTE: It is best to freshly coat wells. However, Concanavalin A coated wells can be rinsed with $H_2O$, air dried and used later (days), but efficiency of cell attachment will be decreased and can vary significantly.

#### 2.2.4.5 Microscope setup

Single mRNA molecule imaging requires sensitive imaging equipment. Various imaging setups will be able to detect single mRNAs, however, by far not all imaging systems are suited for this kind of studies and the choice of the right microscope system is essential for successful single molecule detection. High signal-to-noise RNA detection is achieved by the use of microscope components selected for highest sensitivity. For the microscope setup described here, critical components are high power lasers for illumination, a high numerical aperture objective, and a sensitive imaging sensor that ensures the collection of as much light as possible. Furthermore, combining a spinning disk confocal ability to reject out-of-focus light with an EMCCM camera allows high signal-to-noise at fast frame rates. EMCCD detectors have a very high quantum efficiency (>90%) and are particularly suited for light limited applications such as single molecule detection. Furthermore, EMCCDs allow continuous image acquisition at high frame rates because signal read out of the chip and exposure occur simultaneously. Furthermore, the use of laser illumination ensures efficient excitation of the fluorophores. The images shown in Figs. 9–12 were acquired using a Zeiss Observer Z1 microscope equipped with a 488 nm (100 mW) and 561 nm/40 mW excitation lasers, a Zeiss 100/1.46 N/A oil alpha Plan Apochromat objective, a Yokogawa CSU-X1 spinning disk head with an automated emission filter wheel containing Semrock single bandpass emission filters for GFP (525 nm/50 nm) and the red fluorescent proteins (617 nm/73 nm), and an Evolve 512 EMCCD camera (Photometrics) mounted on the spinning disk head.

#### 2.2.4.6 Image acquisition

Imaging mRNA requires fast image acquisition. One main difficulty of imaging mRNAs in living cells is that mRNAs move in three dimensions and that the speed of mRNA movement makes it difficult to follow mRNAs through the entire cell volume in real time[16,93,95]. Although microscope setups able to simultaneously image multiple planes have been developed recently, these are not available to most researchers[231,232].Similarly, a microscope setup allowing fast 3D acquisition by continually moving the stage while acquiring multiple images (z-sweep) has been used, but is not commercially available[207].Therefore, single RNA tracking is most often done by imaging mRNAs in a single imaging plane. The observation volume of a single imaging plane using the confocal setup used here allows mRNA detection of ~750 nm in z. mRNAs moving within this imaging plane can therefore often only be observed for a short time frame before they move out of the imaging plane. However, RNAs can reenter the imaging plane multiple times within an acquisition period leading to multiple observations of the same RNA.

To best describe RNA behavior, images should be acquired as fast as possible as too slow image acquisition might result in missed events, such as short stops along a path, and can result in misinterpretation of the biological events that are studied. However, it is difficult to estimate whether all possible events have been captured with a set imaging acquisition speed, as the data collected often represents the best possible dataset that can be obtained with the available technology. The use of mutant strains that perturb mRNA export is one way to interrogate whether mRNA behavior changes in mutant backgrounds, as was shown in[108,216]. However, often only technical advances leading to a further increase in acquisition rates will show if previous observations represented the full complexity of biological events.

Understanding the potential as well as limitations of an imaging system is important in order to obtain the best possible data. Two main factors dictate the maximal image acquisition rate: (i) signal intensity, and (ii) read out speed of the camera. Signal intensity can be modulated by increasing laser power; however, this will affect the bleaching behavior and can lead to phototoxic effects. When observing mRNA behavior over very short time periods (few seconds), as was done in the experiments shown in Figs. 9–12, high laser power can be used to optimize signal intensities.

The maximum frame rate for continuous image acquisition is defined by the camera and most EMCCD cameras can further increase their frame rate by using only a subset of the chip. The photometrics Evolve 512 allows 33.7 frames per second when using the full chip (512x512 pixels), but 124 frames per second at 128 x128 pixels.

For imaging of a reference structure, images can either be acquired simultaneously in two colors, or sequentially. Simultaneous two-color image acquisition requires either a two-camera setup or a beam splitter that allows the collection of two channels onto a single image sensor. Simultaneous imaging will allow more precise comparison of the spatial relationship between an mRNA and reference structure. However, even if such a system is available, continuous two-color imaging is not always possible due to differences in photostability of the fluorescent proteins, and the fluorescent label of the reference structure might have bleached halfway through the movie. Therefore, it is often preferred to image reference structure and RNA signal sequentially; usually the reference structure is imaged first, followed by the acquisition of the RNA signal. Depending on the length of the acquisition, cells/reference structures can shift, resulting in an offset of the RNA signal and the reference structure. To control for movement of the reference structure, it should be imaged before and after acquisition of the RNA signal. The two images can be overlaid to test for movement of the reference structure during image acquisition. In addition, the alignment of the two channels should be determined. Depending on the microscope setup, optical filters in the emission light path of a fluorescence microscope are specifically designed to eliminate or minimize pixel shift. However, this is not true for all microscope setups and aberrations associated with pixel shift can lead to erroneous interpretation on co-localization. Pixel shifts can be measured using sub-diffraction beads that emit in different colors, such as TetraSpeck Microspheres (Invitrogen #T-7279), and images can be corrected using software such as 'Transfrom J Translate' plugin in ImageJ/Fiji.

In the images shown in Figs. 9, 10 and 12, cells were first imaged by acquiring a single plane of a red fluorescent signal, followed by the acquisition of 500 frames in the GFP channel to image the RNA movements. Images were acquired at 37 ms exposure per frame using a camera gain of 500 and 50% laser power. As shown in Fig. 9, single mRNAs can be observed with high signal-to-noise

ratio for the entire length of the movie. However, after 500 frames at such high laser power, signals bleach and do not allow further single molecule observations.

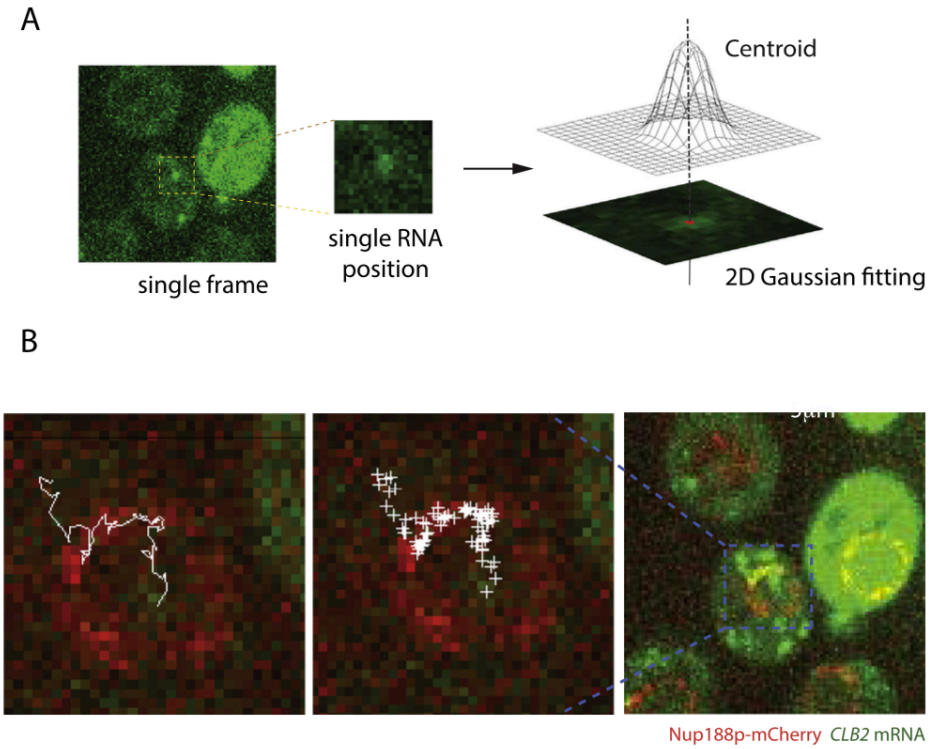


*Figure 11 mRNA detection and tracking using Gaussian fitting*

*(A) The position of an RNA in each frame is determined using 2D–Gaussian fitting, allowing subdiffraction localization precision. (B) Tracking software uses the positions determined by the spot detection software (middle panel) to create the path of an mRNA on its way to the cytoplasm (left panel). Adapted from Saroufim et al.*[108].

### 2.3.4.7 Image analysis

Different parameters can be measured when analyzing mRNA movement. mRNAs travel within the nucleoplasm by diffusion[16,93,95]. However, because of the small size of a yeast nucleus, mRNAs quickly reach the nuclear periphery where they either collide with the lipid bilayer of the nuclear envelope or components of the nuclear pore complex[108]. Nuclear pores are densely

distributed within the nuclear membrane and mRNAs will frequently interact with NPCs and, in particular, the nuclear basket[106]. Therefore, at the periphery, the diffusion characteristics change and this behavior can be measured. Furthermore, binding of mRNP components to the NPC results in prolonged residency times at the NPC, presumably to induce mRNP rearrangements prior to translocation and to allow quality control processes required prior to export to occur (Fig. 12C)[51]. Analysis of mRNA movement occurs in two steps, (i) determining the position of an mRNA in each frame of a movie, followed by (ii) connecting the individual coordinates to reveal its track.

Various methods for spot detection are available and have been used for mRNA detection/visualization and tracking[233]. Spot-detection using 2D Gaussian fitting is one of the most commonly used methods[234]. Although computationally more demanding than other methods, Gaussian fitting is frequently used due to its high sensitivity and reliability even at low signal-to-noise ratios. Furthermore, Gaussian fitting allows the precise localization of mRNAs by determining the center of the Gaussian fitted to the signal that is distributed over multiple pixels, resulting in a localization precision that is much higher than the ~200 nm usually obtained in conventional light microscopy. Due it is ability to precisely determine the position of a single molecule Gaussian fitting is used in localization-based super resolution techniques, such as PALM or STORM. The accuracy with which an mRNA signal can be localized relies in the use of high NA objectives, the wavelength of the fluorophore, as well as the signal intensity and therefore varies between samples and imaging setup; however, localization precision as low as 8 nm has been reported [16,235]. Furthermore, when detecting moving mRNAs, the signal of an mRNA is distorted due to the image exposure of each frame, and mRNA spots will not appear as perfect 2D-Guassians but as ellipses. Therefore, depending on the speed of the movement, fitting using elliptical Gaussians will detect the position of an mRNA more accurately[235]. In the tracking of mRNAs scanning the nuclear periphery performed in Saroufim et al.[108] and shown in Figs. 11 and 12, a fitting algorithm based on Thompson et al.[234] using a spherical 2D-Gaussian was applied (Fig. 11A)[234].

Tracking algorithms use the coordinates from spot detection performed on individual frames and connect them to produce trajectories of individual mRNAs. What is trivial for the human eye is not necessarily trivial from a computational point of view. Conceptually, spot detection algorithms use the coordinates of signals in one frame and search for signals in the

vicinity of the next frame. These programs then connect the two signals and create a track. This process is then repeated for all frames in the movie. The distance between the signals of particles in two consecutive frames permits to connect two particles in a track that is set in the tracking program. Choosing this parameter is influenced by particle speed as well as the acquisition rate of the movie and has to be chosen carefully to ensure that the tracking software does not induce a bias in the analysis by including or excluding mRNAs showing unusual behaviors. Furthermore, fast single molecule imaging often results in low signal-to-noise ratio that is close to the detection limit of the spot detection algorithm. Thus, spot detection is sometimes unable to detect RNAs in individual frames even when the visual tracking of an RNA through consecutive frames suggests mRNAs are present in every frame. Hence, to facilitate automatic tracking, spot detection algorithms usually allow tracks to miss one or two frames before abolishing a track. The spot detection and tracking programs used for the analysis in Figs. 11 and 12 were developed by Dan Larson, described in[17,215,234,236] and are available at www.larsonlab.net.

Analyzing mRNA tracks allows measuring different parameters of mRNA behavior in the nucleus and the nuclear periphery. First, the scanning behavior of mRNAs when reaching the nuclear periphery can be quantified by measuring time of continuous mRNA movement at the periphery. Therefore, mRNA tracks are analyzed for the time a single mRNA spends at the nuclear periphery before being either exported to the cytoplasm, lost from the imaging plane or released back to the nucleoplasm. Perinuclear localization is scored by overlap of the mRNA signal with the nuclear pore signal. As shown in Fig. 12C (left panel), mRNAs scan the periphery for up to a second, however, most mRNAs show shorter scanning. Deletion of the nuclear basket proteins Mlp1/2 significantly reduces the time mRNAs scan the periphery and leads to frequent release of mRNAs back into the nucleoplasm, demonstrating that the nuclear basket is required for mRNA scanning at the periphery. mRNA behavior at the periphery can further be quantified by measuring the distance mRNAs move between frames (jump distances). Jump distances can be compared to the movement of a gene locus tethered to the nuclear periphery. In yeast, various genes were shown to associate with the nuclear periphery through interactions with the NPC[96,204]. When studying genes with high initiation frequencies, such as transcription from the GAL1 promoter driven GLT1 reporter, nascent mRNAs appear as bright perinuclear spots where multiple nascent mRNAs are in

the process of being synthesized. Nascent mRNAs transcribed from a loci bound to the NPC are expected to move very little during the time intervals used for single mRNA tracking (37 ms per frame for mRNA tracks shown in Fig. 12). Measuring jump distances of the transcription site shows movement of ~50 nm between frames, longer than what one would intuitively expect from a nascent mRNA of an NPC tethered gene. However, the measured distances are a combination of gene/nascent mRNA movement and the limitations in the ability to accurately localize a fluorescent signal in cells (localization precision). As the localization precision depends on multiple factors, including signal intensity (see above), determining the localization precision that corresponds to tracked mRNAs requires acquiring and tracking of a fixed, diffraction limited signal emitting with the same intensity of the mRNA signals measured for mRNAs tracked in cells. The 'jump distances' measured of a fixed sample will reveal the accuracy with which a signal can be localized[233]. Here, we do not measure the localization precision, but use the jump distances of nascent transcripts to determine the movement of an mRNA when bound to an NPC (nascent mRNA) and compare it to the jump distances of nucleoplasmic or perinuclear mRNAs during scanning. As shown in the middle panel of Fig. 12C, scanning mRNAs move larger distances between frames than nascent mRNAs, and distances further increase in the absence of Mlp1/2, illustrating a role for the basket in restricting mRNA movement at the periphery. An additional parameter that can be measured is whether mRNAs associate with individual NPCs for an extended amount of time during the scanning process. NPCs are unevenly distributed within the nuclear envelope, with a peak density in the distance distribution between the center of two pores of ~240 nm[106]. NPCs have a diameter of ~100 nm, therefore, the distance between two pores is greater than the pore diameter. To measure if mRNAs bind to individual pores for multiple frames, tracks were analyzed for the presence of multiple continual frames where mRNAs move less than 100nm per frame. This analysis showed that deletion of the nuclear basket reduces prolonged binding of mRNAs at individual pores. Such quantitative description of mRNA movement in wild-type and mutant backgrounds shows that the presence of the nuclear basket changes the scanning behavior of mRNAs at the nuclear periphery, suggesting a role of the nuclear basket in providing an interaction platform that keep RNAs at the periphery, possibly to allow mRNA rearrangement prior to mRNA export. As demonstrated, this kind of analysis can be used to study behavior of different mRNAs

and in different mutant backgrounds and will be a useful tool to study mRNA export at the single molecule level.

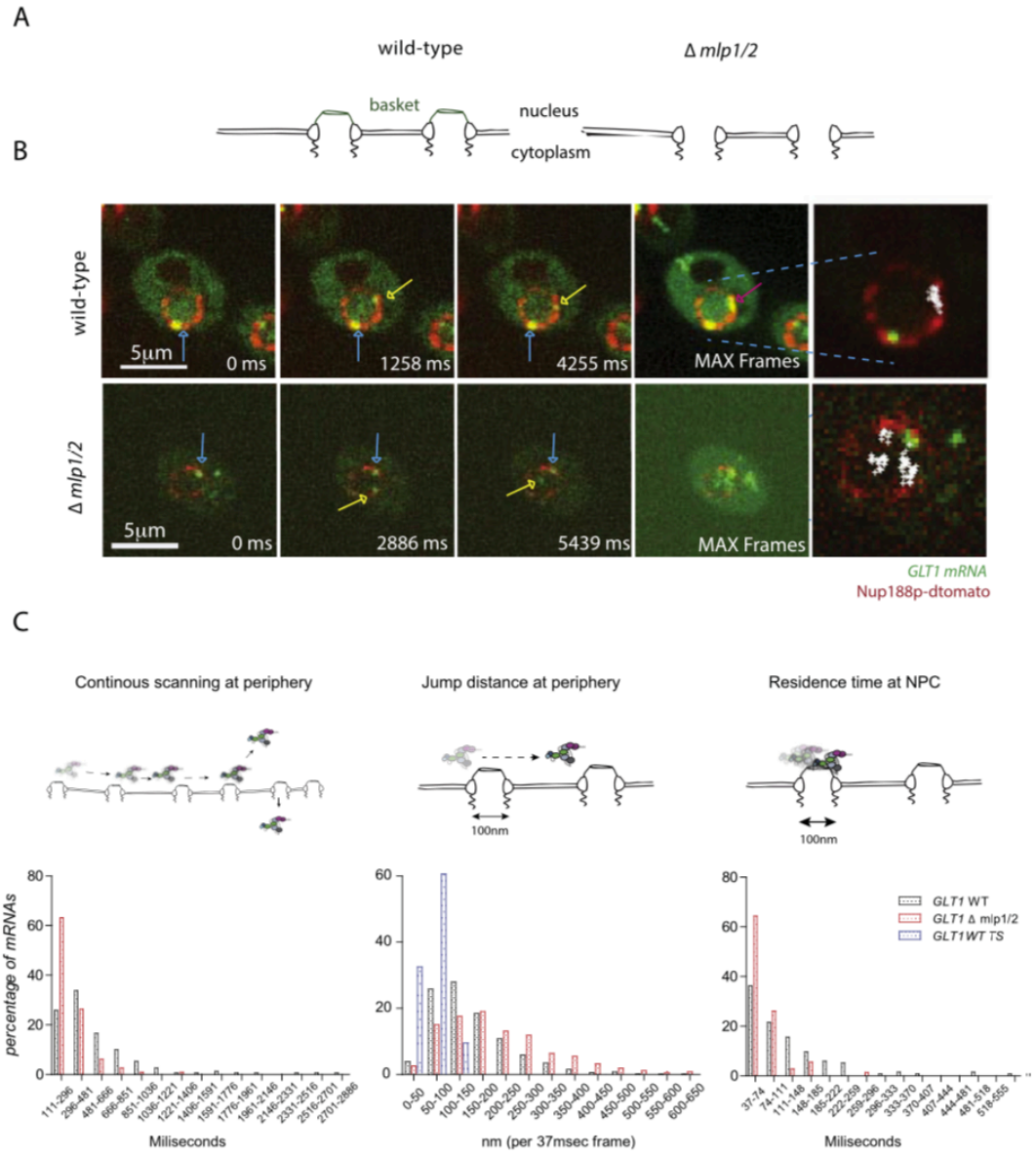


*Figure 12 Single mRNA tracking allows determining different parameters for nuclear mRNA behavior*

*(A) Cartoon illustrating the phenotype of mlp1/2 deletion resulting in basketless pores. (B) The behavior of nuclear mRNAs at the nuclear periphery depends on the presence of the nuclear basket. Live cell RNA imaging of GAL1pro-24PP7-GLT1 mRNA shows that in wild-type cells, mRNAs scan the*

*periphery for prolonged times after reaching the periphery and are infrequently released back into the nucleoplasm. In cells where the basket components mlp1/2 are deleted, mRNAs are frequently released back into the nucleoplasm. Individual frames from a movie acquired in 37 ms intervals are shown. Lower right panel shows all nuclear positions of a single RNA superimposed onto a single frame. (C) Characterization of perinuclear mRNA scanning for GAL1pro-24PP7-GLT1 site of active transcription and nuclear mRNAs in wild-type (WT) and delta mlp1/2 strain. Timescales of continuous mRNP scanning at the periphery (left), the distance mRNAs move within 37 ms when at the periphery (middle) and timescales where mRNAs move for less than 100 nm between frames (right) are shown. GLT1 WT TS shows jump distances of the site of transcription in a wild-type background, illustrating the difference of mRNA movement compared to the movement of the active gene locus. Adapted from Saroufim et al.*[108].

#### 2.3.4.8 Concluding remarks

The ability to combine endogenous RNA labeling with genetics makes yeast a powerful experimental system to study gene expression processes using single molecule resolution microscopy. The PP7 labeling system provides a simple, high signal-to-noise RNA visualization tool allowing mRNA tracking in real time and at high frame rates. However, mRNA tracking is still mostly limited to 2D tracking and future technical developments allowing simultaneous imaging of mRNAs in multiple planes and in single molecule resolution will be required to make these labeling and imaging methods even more powerful, and to make them standard assays used to dissect the molecular mechanisms that control the different aspects of gene expression regulation.

### 2.2.5 Acknowledgments

We thank Srivathsan Adivarahan for help with Fig.11A. This work is supported by a discovery grant from the Natural Sciences and Engineering Research Council, the Canadian Institute for health research (MOP-232642), the Canadian Foundation for Innovation (D.Z). D.Z. holds a FRSQ Chercheur Boursier Junior I. M.O. holds a CIHR New Investigator Award and a FRSQ Chercheur Boursier Junior I and is supported by a grant from the Natural Sciences and Engineering Research Council (RGPIN 386315).

# 3. Article 2: Mlp1 assembles basket scaffold as part of the mRNP nuclear export pathway on a subset of NPCs

Pierre Bensidoun[1,2],Taylor Reiter[4], Ben Montpetit[4], Daniel Zenklusen[2,*], and Marlene Oeffinger[1,2,3,*]

1- Institut de recherches cliniques de Montréal, 110 Avenue des Pins Ouest, Montréal, Québec, Canada, H2W 1R7

2- Département de biochimie et médecine moléculaire, Faculté de médecine, Université de Montréal, Montréal, Québec, Canada H3T 1J4

3- Faculty of Medicine, Division of Experimental Medicine, McGill University, Montréal, Québec, Canada H3A 1A3

4- Department of Viticulture & Enology, University of California at Davis, 3128 RMI North Davis, California, United states of America 95616

* Corresponding authors:

daniel.r.zenklusen@umontreal.ca, marlene.oeffinger@ircm.qc.ca;

Keywords

mRNA export, nuclear pore complex, nuclear basket, nuclear compartmentalization, Mlp1, Nucleolus, NPC heterogeneity, basket accessory interactome, poly(A) transcripts.

## 3.1 Context of the article

The absence of basket scaffold onto pore in the nucleolus is a yeast-specific feature and has been a subject of curiosity for the past two decades. We still do not have a satisfactory answer explaining why yeasts assemble different types of pores. Dr Oeffinger's lab has a long-lasting

interest in the architecture, composition, and maturation pathways of ribosomes. Hence, we initiated this project to study the nucleolar basket-less pores and test whether they specialized in pre-ribosomal subunits export. Additionally, we also wanted to determine whether these NPCs were associated with a specific interactome preventing basket formation. At the time, we assumed that the absence of baskets represented the sign of a possible pore specialization. However, some aspects of basket dynamic, such as their disassembly/re-assembling upon heat shock, suggested that the basket is a mobile accessory platform that can assemble onto basket-less pores depending on the conditions. At the beginning of my project, one aspect of baskets and pores distribution was also very puzzling to me: pores can move around nuclei. Indeed, NPCs are mobile and are believed to diffuse on the nuclear membrane at ~1µm/s in yeast *S. cerevisiae*. They move through relatively long distances without any reported bias for nucleolar or nucleoplasmic periphery[237]. This motion begs the simple question of whether baskets disassemble when pores enter the nucleolar area to reform once they exist.

Therefore, the analysis of the basket's dynamic nature and the plasticity of the nucleoplasmic pore platform became more central, and we decided to ask a slightly different question: Do baskets represent the specialization for a pore, and do they need events happening only in nucleoplasm to assemble?

## 3.2 Author contributions

The following chapters represent the majority of my work in Dr Zenklusen and Dr Oeffinger's labs. All approaches and experimental designs have been chosen and discussed by Dr Zenklusen and Dr Oeffinger, and me. I carried out the experimental parts, including the image and data analysis. The production of the manuscript has been done with equal contributions of the authors. Complementary RNA seq analyses were carried out with the help of Taylor Reiter and Ben Montpetit, who were also involved in central discussions for the development of our article.

## 3.3 Text of the article

### 3.3.1 Abstract

To determine which transcripts should reach the cytoplasm for translation, eukaryotic cells have established mechanisms to regulate selective mRNA export through the nuclear pore complex (NPC). The nuclear basket, a substructure of the NPC protruding into the nucleoplasm, is thought to function as a platform where mRNAs are rearranged and undergo quality control (QC) prior to export, ensuring that only mature mRNAs reach the cytoplasm. Here, we use proteomics, genetic, live-cell, and single-molecule resolution microscopy approaches in budding yeast cells, to demonstrate that baskets assemble only on a subset of NPCs and that their presence is dependent on RNA polymerase II (Pol II) transcription and subsequent mRNP assembly. Specifically, we observe that the polyadenylation machinery, Pab1, and some factors of the introns containing mRNA surveillance are required for proper basket localization and assembly. Thus, our observations suggest that, in yeast, baskets are not a default structure of the NPC. We propose a model where Mlp1, the main basket scaffold, associates on pores as part of the mRNP export pathway only on a subset of pores, within a process possibly linked to the selective export or quality control steps of specific classes of mRNAs.

### 3.3.2 Introduction

Exchange of macromolecules between nucleus and cytoplasm occurs through the NPC, a large multi-protein complex assembled by 30 different proteins (called nucleoporins (Nups)), embedded in the lipid bilayer of the nuclear membrane[114,238]. Transport through the NPC is mediated by transport receptors that bind their cargos and facilitate movement across the NPC by interacting with phenylalanine-glycine (FG) repeats containing proteins (FG Nups) that line the inside of the NPCs central transport channel. Access to and release from the NPC, however, is modulated by asymmetrically distributed subcomplexes of the NPC. On the nuclear site, this is accomplished by a large basket-like structure protruding ~80nm into the nucleoplasm, termed the nuclear basket.

Various asymmetric nuclear Nups, generally termed basket nucleoporins, have been identified; however, the basket's main scaffolds are assembled by the filamentous protein TPR (Translocated Promoter Region protein) in humans and the two paralogues Mlp1 and Mlp2

(myosin-like protein) in budding yeast[110,129,173]. Electron microscopy studies have shown that deletion of TPR and Mlp1/2 results in the loss of basket-like structures at NPCs as well as the loss of a chromatin exclusion zone that is established by the physical presence of the nuclear basket, pointing towards a structural role of these proteins. Mlp1/Mlp2/TPR are large proteins with predicted coiled-coil regions spanning approximately the first 2/3 of the proteins and a large intrinsically disordered domain (IDD). The coiled-cold regions are thought to form the spokes of the basket anchoring the basket at the NPC, whereas the C-terminus forms the top of the basket; however, unlike for the central framework of the NPC, high-resolution structures of the nuclear basket have not yet been solved, nor has the exact stoichiometry of these proteins at individual NPCs been determined[114,116,238,239].

The nuclear basket has been shown to contribute to a range of nuclear activities, including modulation of DNA topology, DNA repair, epigenetic regulation, and anchoring genes at the nuclear periphery, however, its main role is believed to facilitate the access of mRNPs to the NPC [99,100,187,197]. Early studies investigating the long Balbiani Ring mRNPs in salivary glands of *Chironomus tentans* showed that mRNPs associate with the top of the basket before rearranging and entering the NPC, leading to a model where the basket acts as a rate-limiting step of RNA transport and a site of RNP reorganization[240]. Various studies have since demonstrated mRNP reorganization involving basket-associated proteins, and single-molecule studies further established the basket as a rate-limiting step of mRNP export. Surprisingly, Mlp1/2/TPR are not required for mRNA export per se, as their deletion/depletions only lead to a partial/mild export defect, indicating that the basket might either facilitate the export of some transcripts or have alternative or additional function[48,69,108,123].

One of these functions is to provide a quantity control platform that ensures that only mature messenger ribonucleoproteins (mRNPs) are exported to the cytoplasm. Deletion of MLP1 leads to the leakage of intron-containing RNAs to the cytoplasm suggesting that the basket can selectively grant NPC access to spliced but not pre-mRNAs[68,129]. The mechanisms driving this process are not fully understood but might involve RNA binding proteins (RBPs) associating with mRNPs and serving as signals for export or retention, possibly modulating the ability of mRNPs to interact with baskets[49]. Consistent with such a model, various RBPs showing pre-mRNA leakage

phenotypes and either associating with pre-mRNPs or Mlp1/basket have been identified, including the RBPs Gbp1, Hrb1, the Pre-mRNA Leakage proteins Pml1 and Pml39, as well as the nuclear envelope protein Esc1 and the basket protein Nup60. Moreover, different RBPs required for mRNA export interact with Mlp1, including the nuclear poly(A) binding protein Nab2, which directly interacts with the C-terminus of Mlp1, further pointing towards the basket as a site of pre-mRNP retention and/or a late step of nuclear mRNP metabolism[48,69,108,123].

While one might expect from such a platform to be stability anchored at the NPC, fluorescence recovery after photobleaching (FRAP) experiments have shown that Mlp1 at the pore is faster than that of other core Nups[118,147]. Moreover, Mlp1 and Mlp2 dissociate from NPCs during heat-shock at 42$^{o}$C and assemble into intra-nuclear granules sequestering mRNAs and mRNA export factors[48,201]. Why Mlp1/2 display such dynamic interaction with the pore and the mechanisms leading to the formation of these granules as well as their role are poorly understood. Moreover, in *S. cerevisiae*, not all NPCs contain baskets. *S. cerevisiae* possesses one unique crescent-shaped nucleolus adjacent to the nuclear rim occupying about a third of the nuclear volume[161]. Interestingly, NPCs contiguous to nucleoli are devoid of baskets[112,129]. Yet how cells establish these basket-less pores and whether they represent specialized NPCs with functions differing from pores with baskets is not known.

Here, we show that, unlike previously thought, basket-less pores are not a specialized state of NPCs, but instead can also be observed along nucleoplasmic pores as baskets and are not a default component of nucleoplasmic NPCs. Instead, our data demonstrates that baskets assemble dynamically onto only a subset of nucleoplasmic pores in an mRNA-dependent manner. Inhibition of RNA polymerase II transcription results in the abrogation of basket assembly at nucleoplasmic NPCs, and interference with 3' end processing and polyadenylation leads to the loss of nuclear baskets, linking specific steps of mRNA maturation to basket assembly. Proteomic, microscopy and RNA sequencing experiments furthermore suggests that both types of pores can be involved in mRNP export, but some mRNA export factors, such as TREX-2, associate preferentially with basket-containing pores. Thus, we propose that Mlp1 assemble an NPC accessory platform as part of the mRNP export pathway, excluding specifically basket-associated proteins from nucleoli.

### 3.3.3 Results

#### Mlp1 can access and bind pores in the nucleolus

While nuclear pores are evenly distributed along the nuclear periphery, not all parts of the NPC follow this pattern of distribution. In *S. cerevisiae*, the nuclear basket proteins Mlp1 and Mlp2 are excluded from nuclear pores next to the nucleolus, a large crescent-shaped membrane-less compartment that is positioned adjacent to the nuclear membrane and is the site of ribosome biogenesis. Nucleoli, however, change with stress, cellular aging, cell cycle stage as well as overall metabolic activity, which can cause significant variability in nucleolar size and shape between cells in non-synchronous cultures[198,241], suggesting that the number of nuclear pores that are bound by Mlp1/2 may also vary. Measuring the distribution of Mlp1-GFP to the nucleolar marker Gar1-dTomato along the circumference of the nuclear envelope, we observed a negative correlation between the nucleolar and Mlp1-occupied territories (Fig.13a, b). This suggests that variations in nucleolar size negatively affect the number of pores available to bind Mlp1 and, moreover, that the number of basket-containing pores is not fixed but instead may vary from cell to cell and over time.

Although Mlp1 is generally excluded from the nucleolus, in rare cases (~1 out of 100 cells), we observed an Mlp1-GFP focus along the nucleolar-occupied territory, here referred to as an ectopic basket (Fig.13c). The presence of an ectopic basket correlated with an invagination in the nucleolar signal surrounding the Mlp1 focus indicating that baskets can assemble along the nucleolar periphery but that these territories are mutually exclusive and cannot co-occur. Whether ectopic basket formation represents the infrequent assembly of Mlp1 onto nucleolar NPCs, or a basket-containing nuclear pore that formed prior to nucleolar expansion and the inability of nucleolar pores to assemble baskets is unclear.

To determine the possibility of Mlp1/basket association onto nucleolar NPCs, we investigated whether an N-terminal fragment of Mlp1 (N-terminal fragment 2) previously shown to be sufficient to associate with NPCs was able to bind nuclear pore along the nucleolar periphery[112]. Mlp1 N-terminal 2 region fused to GFP was expressed in an *Δmlp1/2* background to avoid competition with endogenous Mlp1 (Fig.13d, e). The N-terminal 2 region of Mlp1 was able to bind NPCs both in the

nucleoplasm as well as in the nucleolus (Fig.13e) suggesting that nuclear pores along the nucleolar periphery are, in principle, able to bind Mlp1.

A hallmark of liquid-phase separated compartments, such as nucleoli, is their ability to concentrate or exclude specific factors depending on their biochemical properties[24,26,198]. Hence, the nucleolus could represent a diffusion barrier for full-length Mlp1. FRAP experiments have shown that Mlp1 associates dynamically with the NPC and exists in two pools within the nucleus: an NPC-bound fraction and a free pool that could also assemble baskets on NPCs in the nucleolus [112,118]. We therefore analyzed the diffusion pattern of the free Mlp1 using single-protein tracking of Halo-tagged Mlp1, compared to Halo-tagged Nup188 and Halo-NLS bound by the organic dye JF-549 in cells expressing Gar1-GFP. To observe single proteins, cells were imaged until most fluorophores were bleached and single molecules were detected for tracking (Supplementary movies S1-3). While most single molecules were bound to the periphery and static, a nuclear diffusing fraction could also be observed for all three proteins. Free diffusing Mlp1-Halo was able to enter the nucleolus, similar to the Nup188-Halo and Halo-NLS controls, with about 30% of the tracks overlapping with the nucleolar area (Fig.13f, g; Supplementary Fig.21a).

Taken together, our data suggest that NPCs along the nucleolar periphery can bind Mlp1 and thus should be able to form baskets at nucleolar pores; however, the formation of baskets at nucleolar pores is rare and results in an invagination of the nucleolus.

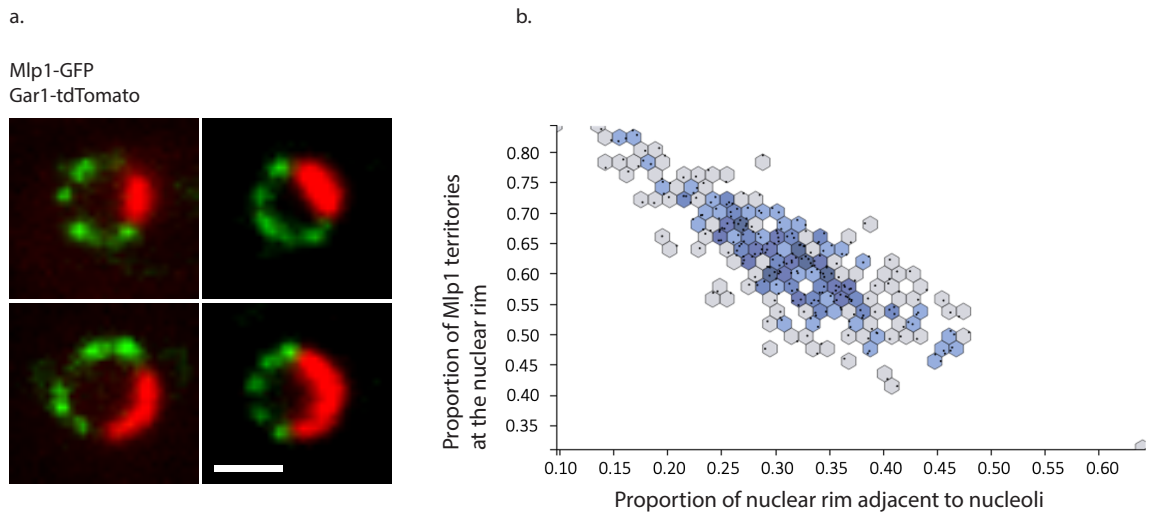

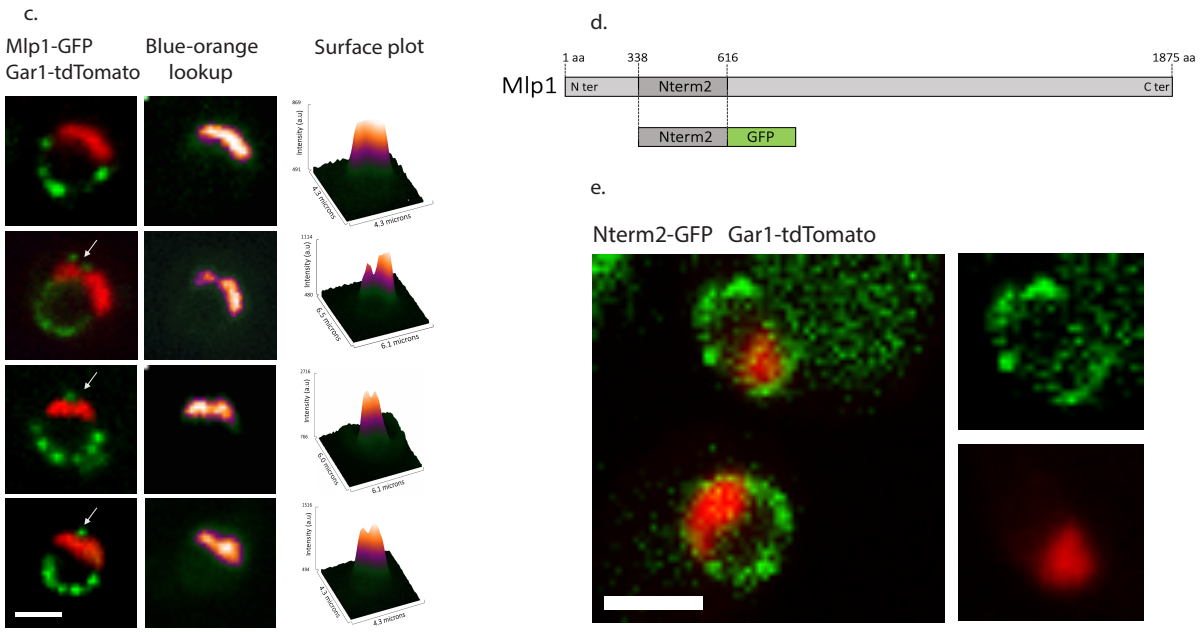


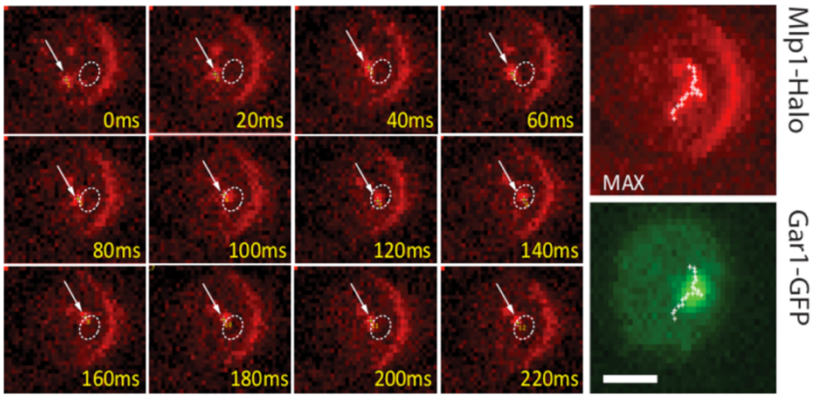


g.

| | Tracks nucleoplasm | Tracks nucleolus |
|---|---|---|
| Mlp1-Halo | 72% | 28% |
| Nup188-Halo | 79% | 21% |
| NLS-Halo | 75% | 25% |

*Figure 13 Pores in the nucleolus are competent to assemble baskets.*

*(a) Fluorescent microscopy analysis shows that Mlp1-GFP and Gar1-tdTomato distribution can vary from cell to cell in non-synchronized cultures. (b) Representation of the percentage of nuclear*

*periphery occupied by Mlp1-GFP versus percentage occupied by the nucleolar are for n=200 cells (c) Mlp1-GFP can assemble an ectopic basket at the periphery adjacent to nucleoli (white arrows). This ectopic basket colocalizes with a loss of Gar1-tdTomato signal characteristic of a density-loss (blue-orange lookup) and defining an invagination in the nucleolar phase (Surface plots). (d) The Mlp1 pore binding domain N-terminal 2 spawns on 278 amino acids in the Mlp1 N-terminal region (e). This N-terminal 2-GFP fragment can bind the periphery including the nucleolar area in Mlp1/2-Δ, Gar1-tdTomato strain. (f) Live cell imaging of Mlp1-Halo in HILO microscopy. Individual frames from video acquired in 20-ms intervals. White arrows show Mlp1-Halo in each frame and the dashed circle represents the nucleolar area. MAX shows the maximum intensity projection of all frames with the path of Mlp1-Halo highlighted with white dots. Mlp1-Halo is shown in red, nucleolus in green. (g) The table summarizes for Mlp1-Halo, Nup188-Halo, Halo-NLS tracking experiments the proportion of frames showing individual diffusing particles in the nucleoplasm and in the nucleolus (n=50 for each construct). (Scales bars =2µm).*

## mRNA metabolism drives basket formation: asymmetrical basket distribution is based on the functional asymmetry between nucleoplasm and nucleolus

The main differentiating feature between the nucleoplasmic and nucleolar region is the synthesis of two distinct types of RNA: RNA Polymerase I (Pol I) synthesizing ribosomal RNA (rRNA) in the nucleolus by, and RNA Polymerase II (Pol II) producing messenger RNA (mRNA) in the nucleoplasm, initiating the assembly of two distinct types of RNPs. We therefore considered the possibility that basket assembly is linked to events solely occurring in the nucleoplasm and tested whether this requires processes linked to mRNA metabolism. To that end, we constructed strains in which the large subunit of either Pol I (RpbA135) or Pol II (Rpb2) were tagged with an Auxin Inducible Degron cassette (AID-HA), to enable their depletion upon addition of auxin (Fig.14a). We observed that depletion of Pol II, but not Pol I, resulted in the loss of Mlp1-GFP at the nuclear periphery and its redistribution into the nucleoplasm after 120 min (Fig.14b). Mlp1-GFP re-localization from the periphery to the nuclear interior was also observed in *rpb1-1* at non-permissive temperature (37C) after 10 minutes (Fig.14d). Moreover, in both strains, a large fraction of cells (~80%) exhibited the formation of a singular nuclear Mlp1 granule that was excluded from

the nucleolus (Fig.14c, e; Fig.16c, d). Similar granule formation has previously been observed upon heat-shock at 42C, where Mlp1 dissociates from pores and forms granules that also contain several mRNA maturation factors, as well as upon deletion of NUP60, which is required for the anchoring of Mlp1 at the NPC[48,201]. These observations link basket formation, which is restricted to the nucleoplasm, to Pol II activity and hence nuclear mRNA metabolism. However, these experiments do not discriminate whether loss of transcriptional activity per se or the consequential absence of mRNA maturation and/or mRNA export is required for NPCs to assemble baskets.

To discriminate between these possibilities, we next blocked mRNA export using a temperature-sensitive mutant of the main mRNA export receptor Mex67, *mex67-5*[48]. Upon shift to non-permissive temperature (37C), we did not observe redistribution of Mlp1 from the nuclear periphery (Fig.14d), suggesting that blocking Pol II transcript production, and possibly downstream events, but not mRNP export affects basket formation.

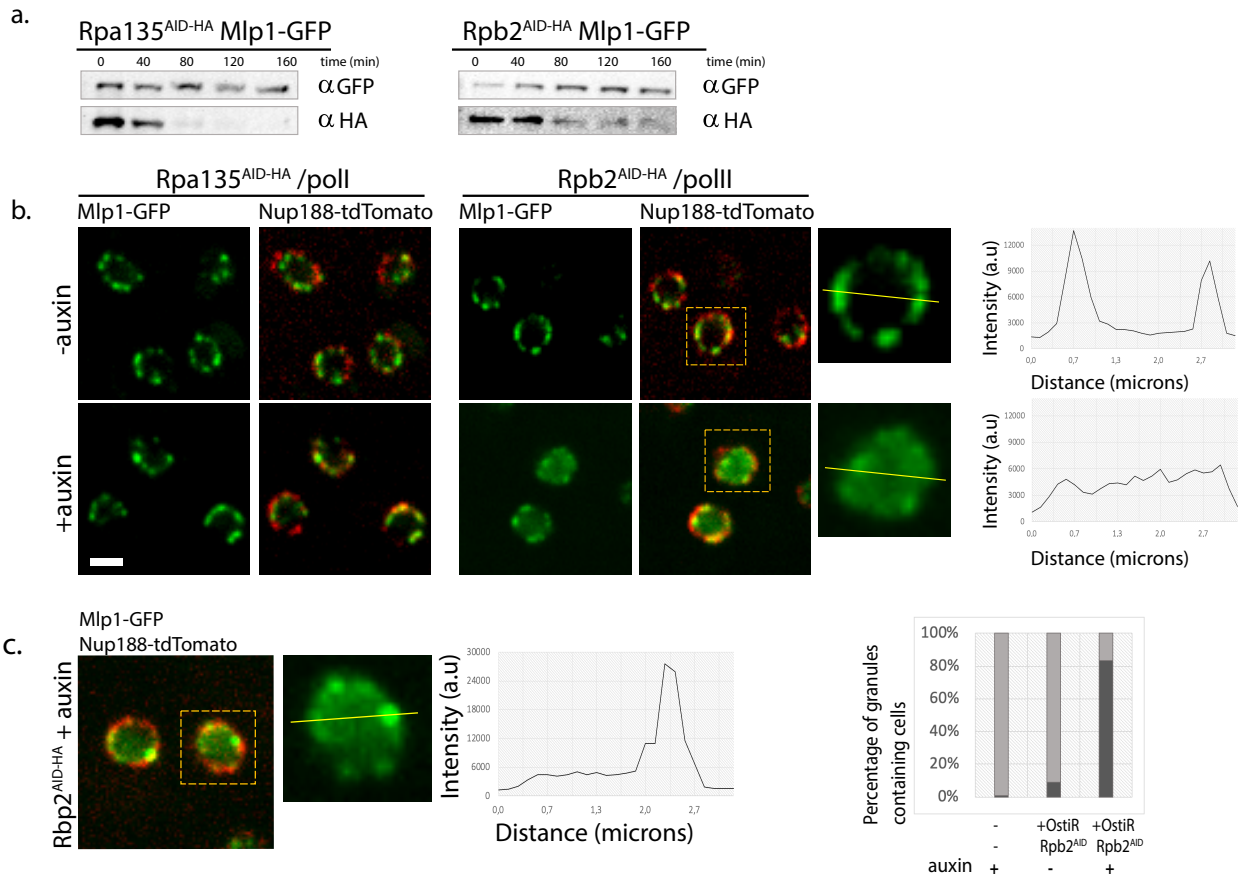

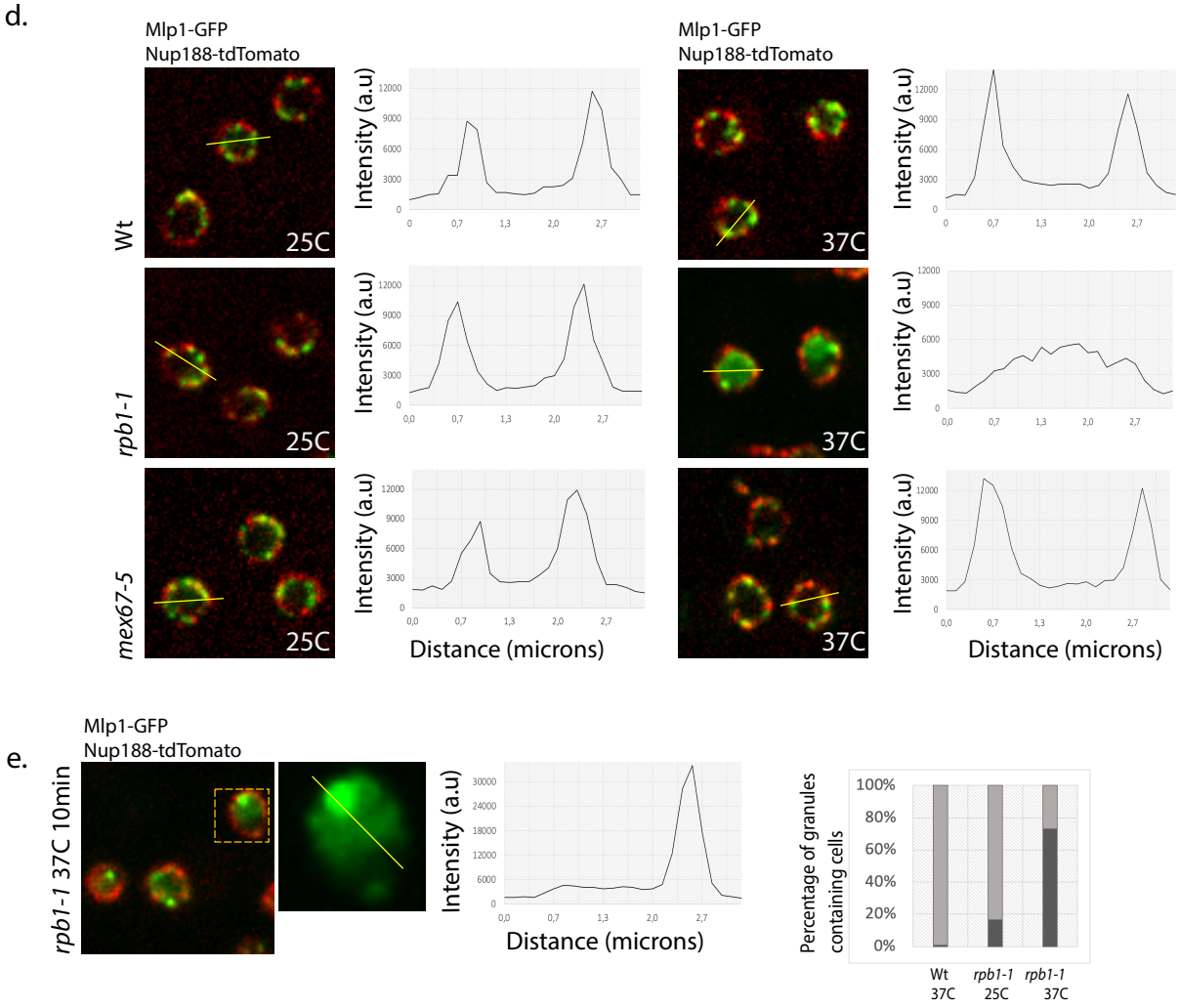


*Figure 14 RNA polymerase II shutdown results in the redistribution of Mlp1 in the nuclear interior.*

*(a) Western blotting on total cell lysates showing the levels of Rpb2$^{AID-HA}$, Rpa135$^{AID-HA}$, and Mlp1-GFP upon addition of auxin. (b) Fluorescent microscopy reveals that the Mlp1-GFP signal decrease at the nuclear periphery upon addition of 500 µm auxin after 120 min in Rpb2$^{AID-HA}$ while the Nup188-tdTomato remains unchanged at the periphery. In Rpb2$^{AID-HA}$ strain but not in Rpa135$^{AID-HA}$ the signal increases in the nucleoplasm (right panel). (c) Mlp1-GFP signal redistribution in Rpb2$^{AID-HA}$ strains is also associated with a single bright Mlp1-GFP granule formation present in ~80% of cells. (d) In normal cells or the temperature-sensitive mutant mex67-5, Mlp1-GFP and Nup188-tdTomato signal localization remain unchanged after a shift at 37C for 10min. The temperature-sensitive mutant rpb1-1 displays a redistribution of Mlp1-GFP in the nucleoplasm at restrictive*

*temperature. (e) ~80% of rpb1-1 mutant cells display single Mlp1-GFP granules at 37C. (Scales bars =2µm).*

In another scenario, mRNPs reaching the periphery could be a requirement for basket formation. It has previously been shown that mutations in some RNA maturation and surveillance factors, such as Dis3, Csl4 and the ribosome biogenesis factor Enp1, share a common phenotype which includes the accumulation of different polyadenylated (poly(A)) mRNAs and mRNA-associated proteins in the nucleolus[242,243]. In this context, we asked how such re-localization of the mRNA maturation machinery to the nucleolus would affect basket formation. Enp1 was depleted using a Enp1$^{AID\text{-}HA}$ strain and basket formation monitored using Mlp1-GFP (Fig.15a; Supplementary Fig.23a). 120 min after addition of auxin, Mlp1-GFP signal was mostly lost from nucleoplasmic pores and re-distributed to the nucleolar periphery, suggesting that pores adjacent to nucleoli are able to assemble baskets upon nucleolar mRNP accumulation (Fig.15a). A similar redistribution of Mlp1-GFP was seen in Csl4 $^{AID\text{-}HA}$ cells upon addition of auxin (Supplementary Fig.22b).

To determine that Mlp1 assembles onto NPCs along the nucleolar periphery upon Enp1 depletion, we performed affinity purification (AP) of Mlp1-PrA and analyzed its interactome by semi-quantitative mass spectrometry (MS) with and without the addition of auxin. Under both conditions, Mlp1-associated interactomes were similar in terms of NPC components isolated, suggesting that the proteins assemble with pores in both compartments (Fig.15b). Furthermore, consistent with the accumulation of mRNPs in the nucleolus, we identified RNA maturation and export factors associated with nucleolar Mlp1-PrA upon Enp1 depletion (Fig. 15b). While the overall levels of those factors were comparable in both conditions, we observed that Pab1 was significantly enriched in Mlp1-PrA APs upon the addition of auxin. We also identified a low level of nucleolar proteins copurifying with Mlp1-PrA indicating a relative proximity between baskets and nucleoli upon Enp1 depletion. Taken together, those results suggest that upon mRNP accumulation in the nucleolus, Mlp1 assembles *bona fide* baskets at pores along the nucleolar periphery.

a.

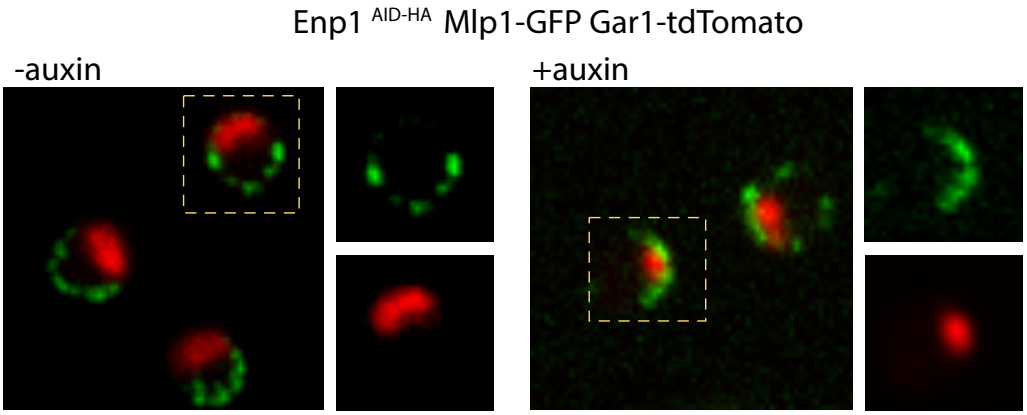


b.

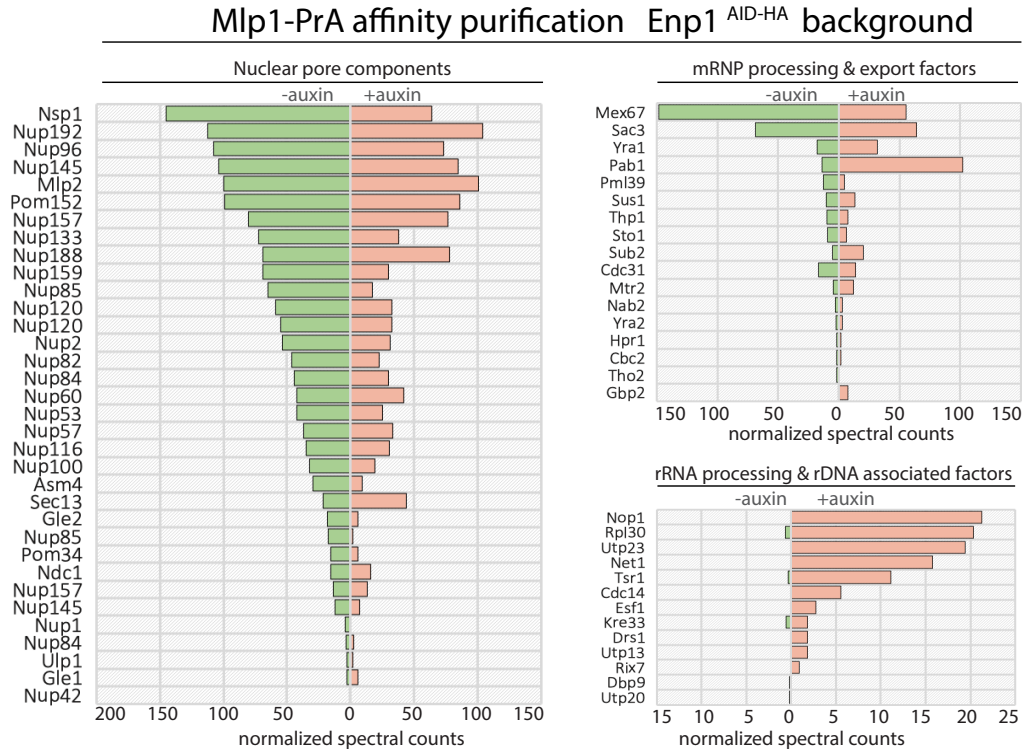


*Figure 15 Accumulation of poly(A)RNA in the nucleolus results in the relocalization of baskets at the periphery adjacent to the nucleolus.*

*(a) Mlp1-GFP signal is redistributed in Enp1$^{AID-HA}$ cells at the periphery adjacent to the nucleolus labeled by Gar1-tdTomato after the addition of 500 µm auxin for 120 min. (b) Normalized spectral counts detected by mass spectrometry of proteins co-purified with Mlp1-GFP before and after the addition of 500 µm auxin for 120 min.*

Under these conditions, nucleoli were often spherical, fragmented and internalized with little or no overlap between Mlp1-GFP and Gar1-tdTomato signals (Supplementary Fig.22a). Such basket–nucleoli incompatibility resembles the invagination in the nucleolus caused by ectopic baskets (Fig.13c). Overall, our data suggest that basket assembly requires elements or events of the mRNA maturation pathway that under normal conditions only occur in the nucleoplasm, but upon the rerouting to the nucleolus, can lead to basket assembly along the nucleolar periphery. However, basket assembly along the nucleolar periphery appears to be incompatible with the cooccurrence of a nucleolus.

## Polyadenylation, Pab1, and some elements of the Pre-mRNA retention machinery are required for basket assembly

To further dissect the processes along the mRNA maturation pathway required for basket assembly, we carried out a targeted AID screen, depleting selected mRNA maturation factors and monitoring Mlp1-GFP distribution upon auxin treatment. This included factors related to co-transcriptional mRNP assembly such as components of the THO/TREX/TREX-2 complex (Yra1, Tho2, Sus1, Sac3); 5' cap-binding (Cbc2); splicing (Prp18, Prp5, Snu17, Luc7); proteins involved in 3' end cleavage, polyadenylation and poly(A)-binding (Rna14, Rna15, Pap1, Nab2, Pab1); as well as proteins linked to nuclear retention of intron-containing mRNAs and quality control (Hrb1, Npl3, Gbp2, Pml1, Pml39) (Supplementary Table 2). Depletion phenotypes were compared to $Nup60^{AID\text{-}HA}$ cells, previously shown to interfere with Mlp1 binding to the NPC and resulting in the formation of intranuclear Mlp1 granules, as well as $Rpb2^{AID\text{-}HA}$ and $Enp1^{AID\text{-}HA}$ (Fig.14-15)[111,244].

Phenotypes observed were not common across various stages of the pathway but distinct for specific subsets of proteins. Overall, depletion of early factors did not affect basket formation, as neither depletion of Cbc2 nor of components of the THO/TREX complex (Yra1, Tho2) changed the Mlp1-GFP localization pattern at different time points after the addition of auxin (Fig.16; Supplementary Fig.23a, b). Interfering with different stages of splicing did also not induce Mlp1 relocalization as neither depletion of U1 (Luc7), U2 (Snu17) nor U5 (Prp18) snRNP-associated factors changed Mlp1-GFP localization at the nuclear periphery, with the exception of Prp5, an ATPase required for pre-spliceosome assembly (Fig.16; Supplementary Fig.23b)[245]. Prp5 depletion

resulted in an increase in nucleoplasmic Mlp1-GFP signal (Fig.16), similar to that observed in Rbp2 $^{AID\text{-}HA}$ after auxin treatment (Fig.14), as well as redistribution of Mlp1 along the nuclear periphery. In addition to its role in splicing, *prp5* mutants were shown to affect Pol II transcription suggesting that this phenotype might be linked to transcription rather than splicing[246].

Depletion of factors involved in 3' processing and polyadenylation, however, displayed strong Mlp1 relocalization phenotypes. Specifically, depletion of factors involved in 3' end cleavage (Rna14, Rna15), the RNA poly(A) polymerase Pap1 as well as the poly(A) binding protein Pab1 showed altered Mlp1-GFP distribution suggesting that these steps are significant for basket formation at NPCs, while phenotypes observed varied between strains. Upon depletion of Rna14$^{AID\text{-}HA}$ and Rna15 $^{AID\text{-}HA}$, Mlp1 was redistributed to the nucleolar periphery (Fig.16a, b), similar to what was observed upon loss of Enp1$^{AID\text{-}HA}$ (Fig.15). In addition, these strains frequently exhibited fragmented nucleoli, a phenotype that has previously been described for *rna14-1* and *ran15-2* at non-permissive temperature (37C)[247]. An accumulation of polyadenylated RNA in the nucleolus has also been observed in *rna14* and *rna15* mutants as a consequence of disrupting 3' end cleavage, polyadenylation and export[212]. Similar to *csl4* and *enp1* mutants, where nucleolar accumulation of poly(A) RNA results in nucleolar sequestration of mRNPs[242], redistribution of the mRNA maturation machinery to nucleoli may responsible for basket formation along the nucleolar periphery in Rna14$^{AID\text{-}HA}$ and Rna15 $^{AID\text{-}HA}$ cells. While Pap1$^{AID\text{-}HA}$ depletion also led to a redistribution of Mlp1, an increase in nucleoplasmic Mlp1 levels and decrease of Mlp1 signal along the nuclear periphery with the concomitant formation of larger Mlp1 foci in ~ 50% of the cells was observed (Fig.16), which was reminiscent of a Rbp2$^{AID\text{-}HA}$ depletion phenotype (Fig.14). A similar phenotype was seen upon loss of Pab1$^{AID\text{-}HA}$ (Fig.16), which also resembled that of a Nup60 $^{AID\text{-}HA}$ depletion strain (Fig.16). No change in Mlp1 pattern was observed upon Nab2 depletion (Fig.16), however, nor upon that of Gbp2 or Hrb1, two poly(A)-binding proteins linked to the maturation of intron-containing mRNAs, or Npl3 (Supplementary Fig.23)[49].

We also tested proteins that have previously been linked to nuclear basket function for their role in Mlp1 localization[248]. Of the two pre-mRNA surveillance factors (Pml1, Pml39), only Pml39 displayed a phenotype upon auxin treatment, where Mlp1 signal was decreased along the nuclear periphery with an increase in nucleoplasmic Mlp1, away from NPCs, while TREX-2 components

(Sac3, Sus1) showed no phenotype (Fig.16). We, furthermore, determined Mlp1-GFP localization upon depletion of NPC- and nuclear basket-associated factors Esc1, Ulp1, and the Mlp1 paralog Mlp2. Upon addition of auxin, Esc1 $^{AID-HA}$ exhibited formation of larger Mlp1 granules along the nuclear rim with a simultaneous loss of evenly distributed Mlp1 rim staining, while Ulp1 $^{AID-HA}$ and Mlp2 $^{AID-HA}$ showed no phenotype (Fig.16).

Overall, we did not observe a common phenotype but rather various ones across different stages of mRNA maturation suggesting that basket assembly is not a consequence of nuclear mRNA metabolism *per se* but rather the completion of specific steps. Mlp1-GFP granules that were observed upon depletion of Rpb2 $^{AID-HA}$, Pab1 $^{AID-HA}$, Pap1 $^{AID-HA}$, Nup60 $^{AID-HA}$, and Esc1 $^{AID-HA}$ were similar to those previously described in this work insofar as they were systematically excluded from nucleolar areas (Fig.13c; Fig.15a, c; Fig.16c,d). On the other hand, when nucleoplasmic Mlp1 levels were significantly increased upon auxin treatment and baskets disassembled (i.e., Rpb2$^{AID-HA}$, Prp5$^{AID-HA}$ Pab1$^{AID-HA}$, Pml39$^{AID-HA}$ Nup60$^{AID-HA}$), nuclear Mlp1-GFP signal overlapped with the nucleolar region corroborating our previous observation that the nucleolus does not present a diffusion barrier for free-diffusing Mlp1 (Fig.13f, g; Fig.16c). These observations suggest that Mlp1 exclusion from the nucleolar phase occurs upon Mlp1 multimerization during nuclear basket or granules assembly (Fig. 16d). Moreover, in Prp5$^{AID-HA}$, Pml39$^{AID-HA}$, and to a lesser extend in Pab1$^{AID-HA}$, Pap1$^{AID-HA}$, and Rpb2$^{AID-HA}$ depleted cells, we observed a weak Mlp1-GFP signal at the nuclear periphery, as well as along the nucleolus/nuclear envelope interface in Prp5$^{AID-HA}$, Pab1$^{AID-HA}$, and Pml39 $^{AID-HA}$ cells (Fig.16c, white arrows). This Mlp1-GFP signal along the nucleolar periphery was not associated with any nucleolar fragmentation or invagination as was observed upon nucleolar poly(A) transcript sequestration (Fig.15), or ectopic basket formation (Fig.13c). This may indicate that depletion of Pap1$^{AID-HA}$, Pab1$^{AID-HA}$, Pml39$^{AID-HA}$ or Prp5$^{AID-HA}$ does not affect the ability of Mlp1 to bind an NPC *per se*, unlike in Nup60-depleted cells, but rather their capacity to form fully assembled baskets.

Taken together, our results suggest that basket formation on NPCs is a consequence of completing specific steps of nuclear mRNA maturation and requires the presence of poly(A) transcripts as we observed a significant loss of Mlp1-GFP along the nuclear periphery and its redistribution into the nucleoplasm upon depletion of Rbp2$^{AID-HA}$, Prp5$^{AID-HA}$ Pap1$^{AID-HA}$, Pab1$^{AID-HA}$,

and Pml39$^{AID\text{-}HA}$. Moreover, mRNA poly(A) tail polymerization by Pap1 and Poly(A)-tail binding protein Pab1. Yet not all Poly(A)-tail binding proteins seem to be required for basket formation as neither depletion of Gbp2, Hrb1 nor Nab2, which has been linked to Mlp1 in the context of mRNA export and shown to directly interact with the Mlp1 C-terminal region[124], affected nuclear basket formation.

a.

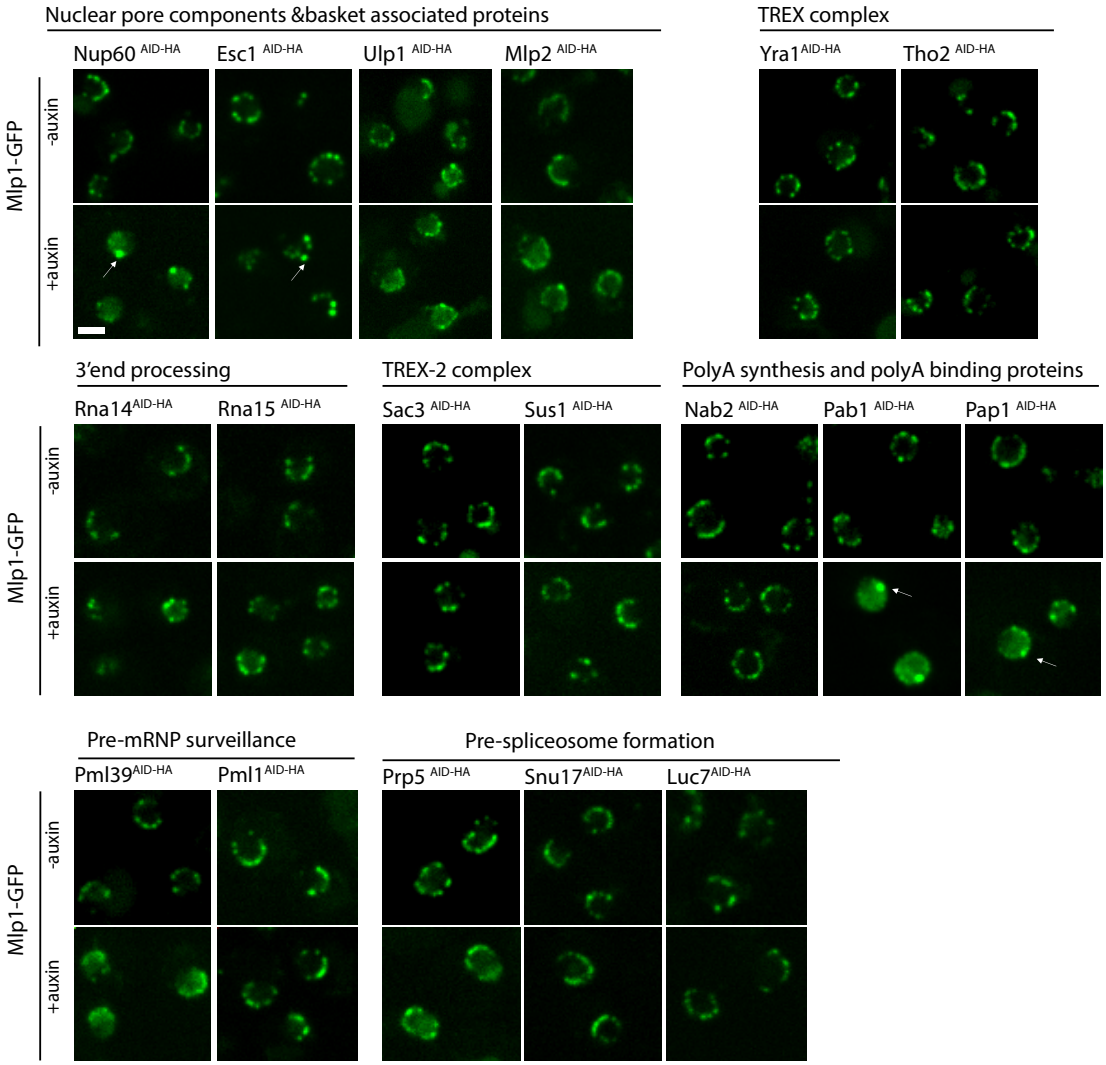

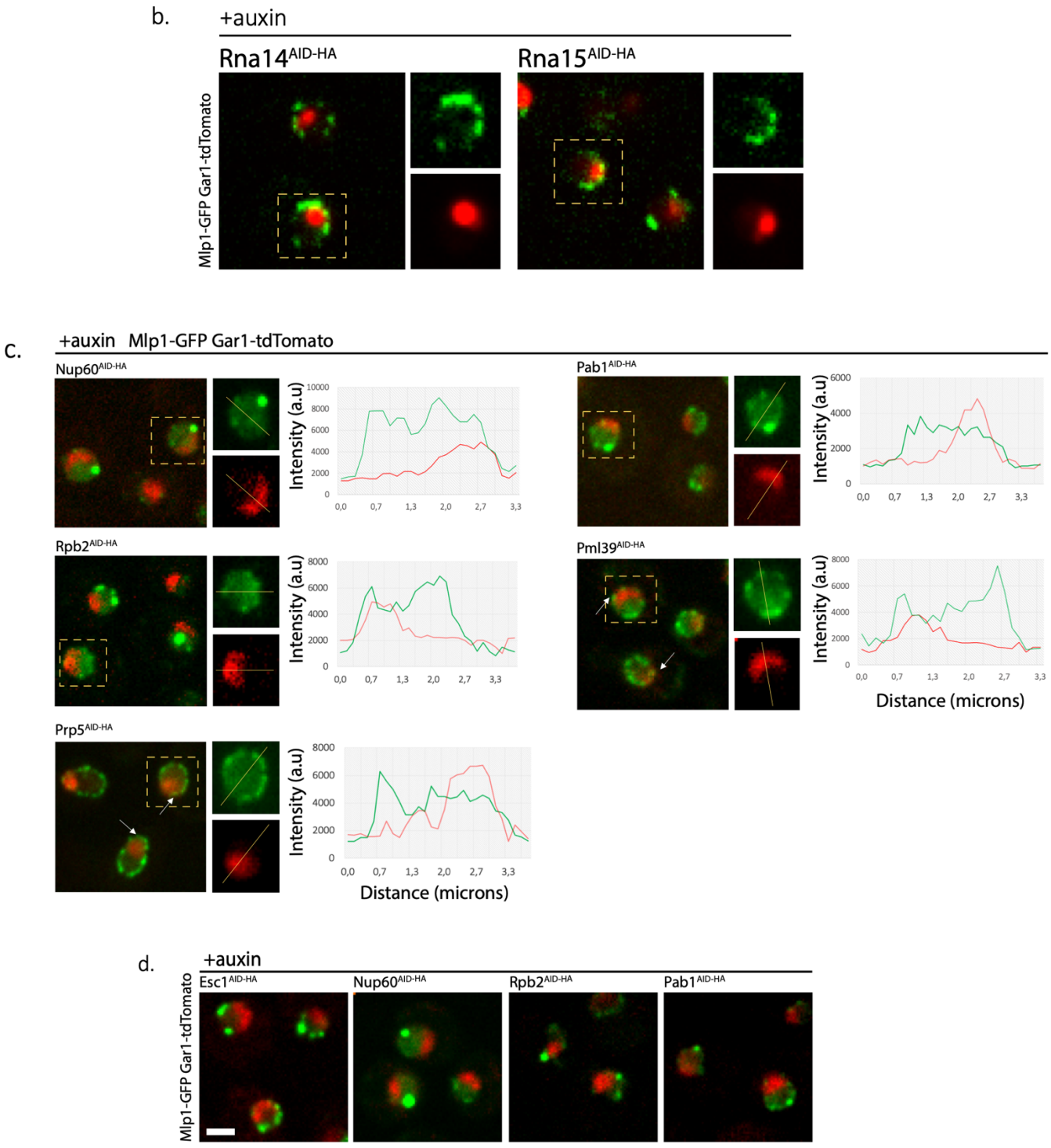


*Figure 16 Polyadenylation, Pab1, and some elements of the Pre-mRNA retention machinery are required for basket assembly.*

*(a) Auxin depletion screen for Mlp-GFP tagged strain where components of different complex related to NPCs or mRNA processing and export pathway have been depleted with the addition of 500 µm auxin for 120 min. Mlp1-GFP granules observed in upon Nup60$^{AID-HA}$, Esc1$^{AID-HA}$, Pab1$^{AID-HA}$, Pap1$^{AID-HA}$ depletion are shown with white arrows. (b) Mlp1-GFP signal is redistributed in RNA14$^{AID-HA}$ and RNA15$^{AID-HA}$ cells at the periphery adjacent to the nucleolus labeled by Gar1-tdTomato after addition of 500 µm auxin for 120 min. (c-d) The position of the free fraction of Mlp1-GFP and of Mlp1 granules were monitored with respect to the nucleolus within cells where baskets are destabilized upon the addition of auxin. Graphs represent the overlaps of Mlp1-GFP and Gar1-tdTomato signals (green and red curve respectively). White arrows show Mlp1-GFP signals remaining at the periphery including in the nucleolar area after basket destabilization. (Scales bars =2µm)*

## Not all nucleoplasmic NPCs contain baskets

The requirement for an active mRNP maturation pathway for basket assembly might suggest that baskets assemble randomly at individual NPCs and that not all pores assemble baskets at all times or with the same frequency at all NPCs; this in turn might result in a functional heterogeneity at nucleoplasmic NPCs. Consistent with such a model, Mlp1-GFP distribution at the nuclear periphery, when imaged using spinning disk microscopy, often shows a discontinuous staining pattern (Fig.13a). To investigate possible NPC heterogeneity at nucleoplasmic NPCs, we analyzed distribution and co-localization of different NPC components using Structured Illumination microscopy (SIM) (Fig.17). Signal distribution of two components of the central framework Y-complex, Nup84-GFP and Nup188-tdTomato, along the nuclear periphery showed an overall continuous staining and co-localization pattern, and quantification of normalized intensities around the nuclear periphery do not reach a background value, consistent with a homogeneous distribution of NPCs all around the nuclear periphery (Fig.17a)[106,237]. Mlp1-GFP staining however, showed a discontinuous distribution with regions where GFP signal was interspaced by segments devoid of GFP signal, suggesting that several regions of basket-less pore segments occupy the nuclear periphery.

To better define the position of basket less-areas in relation to the basket devoid nucleolar area, we imaged double-tagged strains Mlp1-GFP / Gar1-tdTomato and observed that several

regions at the nuclear periphery in addition to the nucleolar area are devoid of Mlp1-GFP, further indicating that not all nucleoplasmic NPCs contain baskets (Fig.17b).

Previous works have shown that basket proteins Nup60, Nup1, Nup2 are present on pores adjacent to nucleoli, and co-staining of Nup-188-tdTomato with Nup60-GFP confirmed the association of Nup60 with all NPCs (Fig.17c)[129]. However, Mlp2-GFP showed a localization pattern similar to Mlp1, and colocalized with Mlp1-Halo (Fig.17d), consistent with the requirement of Mlp1 NPC association for Mlp2 perinuclear localization, and indicating that NPC heterogeneity implicates Mlp1/2, but not the other asymmetric nuclear NPC proteins Nup60, Nup1, Nup2 (Fig.17c)[112]. Together, our data show that NPC heterogeneity extends beyond the nucleolus and implies that basket formation is not a default state of nucleoplasmic NPCs.

## Nucleoplasmic basket NPCs contain an accessory interactome

Various proteins generally not considered *bona fide* nucleoporins associate with NPCs have been linked to the nuclear basket, including components of the TREX-2 complex, Pml39 and ubiquitin-like modifier Ulp1[68,173]. These proteins have previously been shown to be excluded from the nucleolar periphery, indicating that these proteins might be part of the specialized, basket-containing NPCs in the nucleoplasm[119,130,249,250]. Thus, we analyzed the distribution of TREX-2 main scaffold protein Sac3-GFP, Ulp1-GFP and Pml39-GFP relative to Nup188-tdTomato. All three proteins display a patchy pattern along the periphery similar to Mlp1-GFP (Fig.17c). Moreover, Ulp1-GFP, Sac3-GFP and Pml39-GFP colocalize with Mlp1-Halo signal in double-tagged cells, indicating that these proteins associate preferentially with baskets-containing nucleoplasmic NPCs (Fig.17d and supplementary Fig.24a). These proteins also colocalize in Mlp1 granules that form upon heat-shock at 42$^{o}$C (Fig.17e) or upon Pol II shutdown (Fig.17f), and Sac3 co-isolates with Mlp1 when basket-containing pores assemble along the nucleolar periphery upon Enp1 depletion (Fig.15a, b), further linking these proteins to basket-containing NPCs.

The localization of these proteins is different to Mex67-GFP which shows a distribution pattern that occupies the entire nuclear periphery, overlapping with Nup188-tdTomato signal (Fig. 17c). This is consistent with recent models that suggest that Mex67 is a *bona fide* nuclear pore component associating with pore independent of its association with RNA [251]. Moreover, it might

also indicate that all NPCs might, in principle, be able to export mRNAs using the Mex67-dependent RNA export pathway, however, that only some nucleoplasmic NPCs contain an additional platform that contains various factors implicated in mRNA metabolism, including the TREX-2 complex, Ulp1 and Pml39, assembled in a Mlp1-dependent manner.

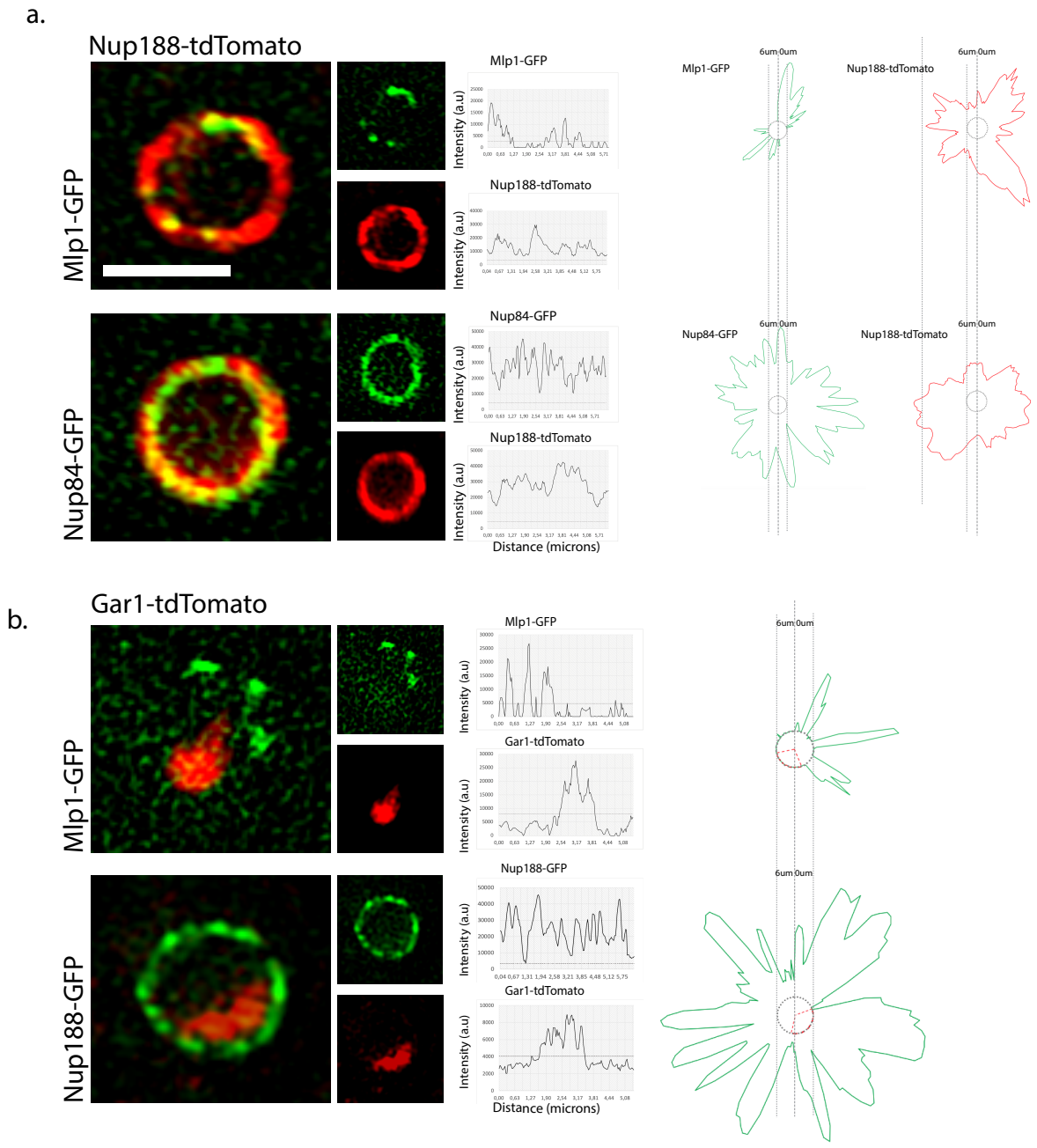

c.

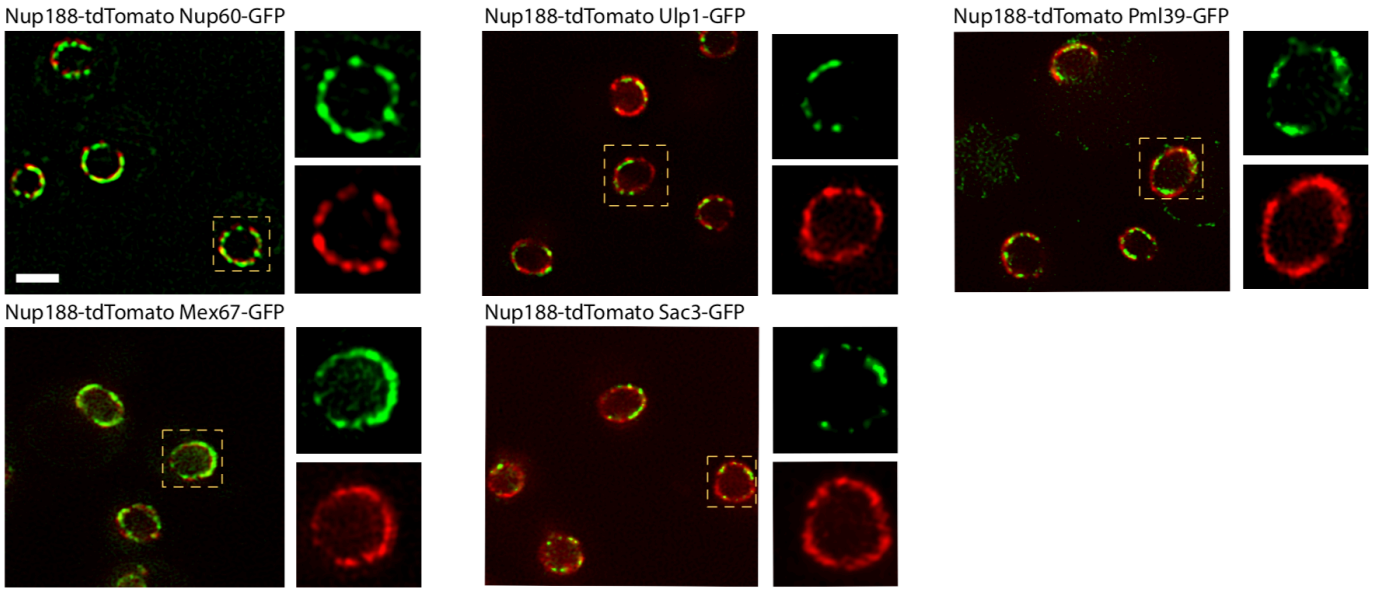
Nup188-tdTomato Nup60-GFP
Nup188-tdTomato Ulp1-GFP
Nup188-tdTomato Pml39-GFP
Nup188-tdTomato Mex67-GFP
Nup188-tdTomato Sac3-GFP

d.

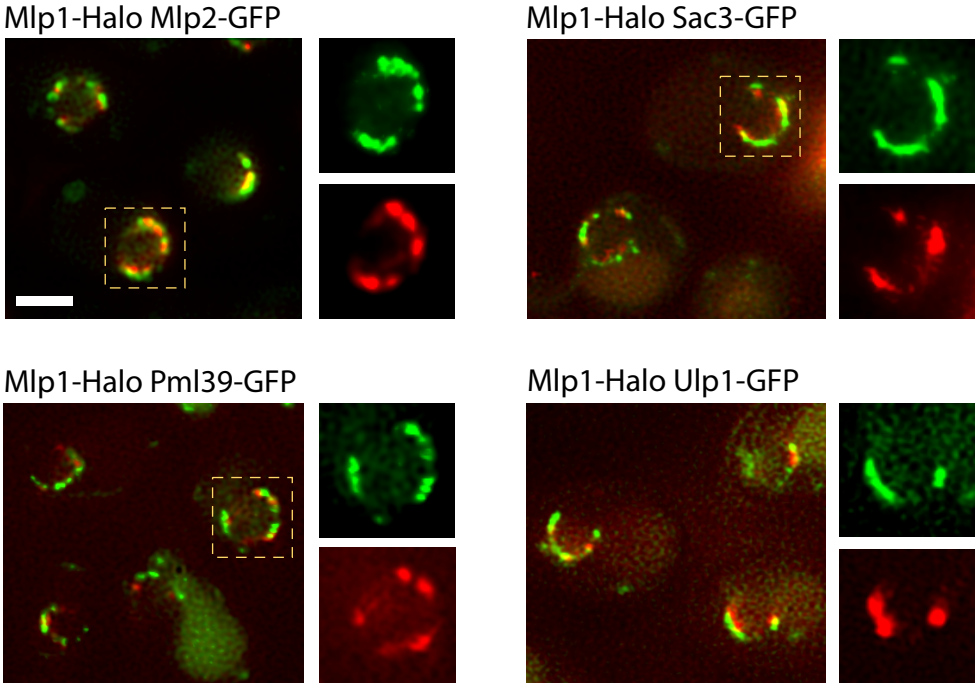
Mlp1-Halo Mlp2-GFP
Mlp1-Halo Sac3-GFP
Mlp1-Halo Pml39-GFP
Mlp1-Halo Ulp1-GFP

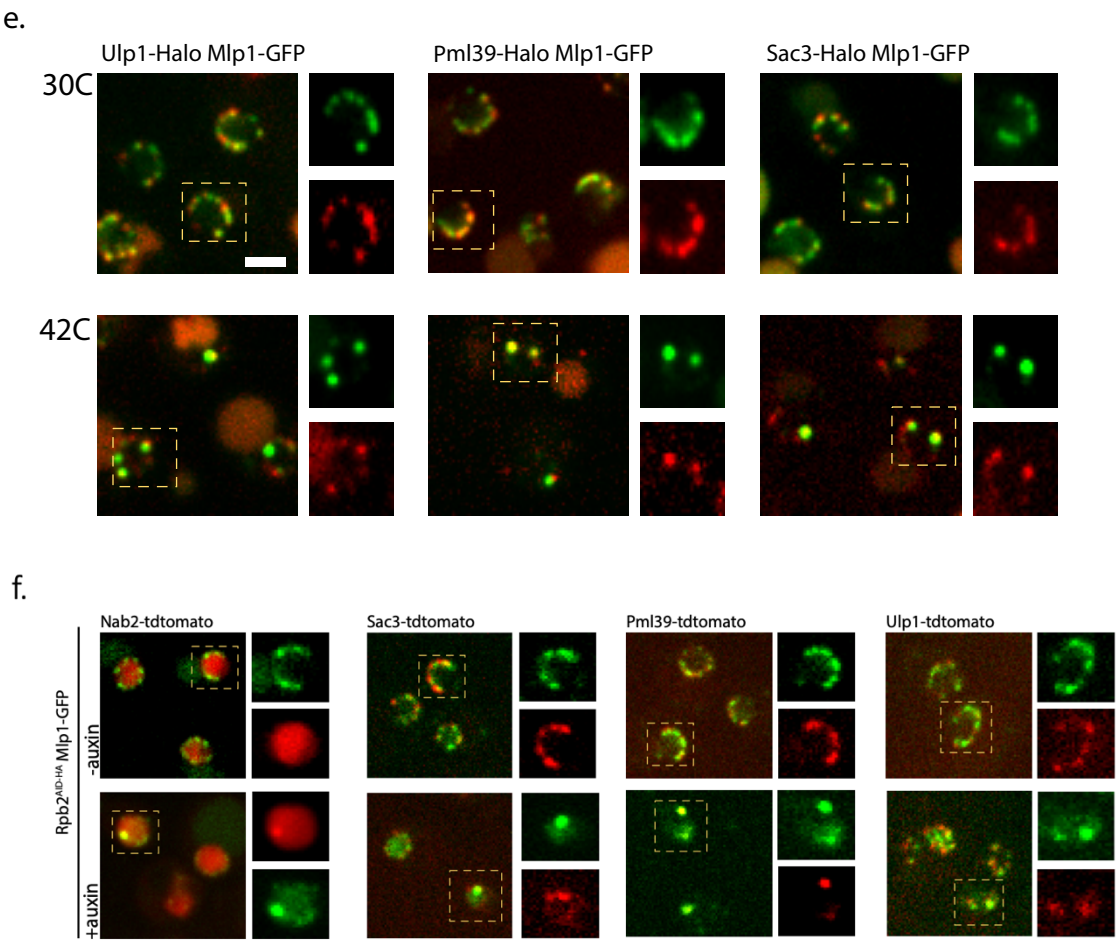


*Figure 17 Basket assemble on a subset of NPCs in the nucleoplasm and capture an NPC accessory interactome.*

*(a) Structured illumination microscopy (SIM) images of Nup188-tdTomato Mlp1GFP and Nup188-tdTomato Nup84-GFP tagged cells and the respective intensities of each signal around the nuclear periphery on right panels. The grey circles represent the average background value for each signal. (b) SIM images of Gar1-tdTomato Mlp1GFP and Gar1-tdTomato Nup188-GFP tagged cells and the respective intensities of each signal around the nuclear periphery on the right panels. The grey circles represent the average background value for each signal red dashed area represents the*

*nucleolar periphery adjacent to the nuclear rim. (c) SIM distribution analysis of the basket protein Nup60-GFP and NPCs accessory proteins Mex67-GFP, Ulp1-GFP, Sac3-GFP, Pml39-GFP relative Nup188-tdTomato distribution. (d) SIM distribution analysis of Mlp1-halo relative to Mlp2-GFP, Pml39-GFP, Sac3-GFP, Ulp1-GFP. (e) Colocalization analysis of Pml39-Halo, Sac3-Halo, Ulp1-Halo in Mlp1-GFP granules upon heat shock 1h at 42C. (f) Colocalization analysis of Pml39-Halo, Sac3-Halo, Ulp1-Halo and Nab2 in Mlp1-GFP granules upon Rpb2$^{AID\text{-}HA}$ depletion (Scales bars =2µm).*

## Specific nuclear mRNA maturation factors are enriched at basket-containing NPCs

To determine whether the presence of baskets on nuclear pores correlates with the presence a specific interactome, including mRNPs associating with NPCs, we characterized the interactomes of pores with and without nuclear basket. First, to analyze the general nuclear pore interactome ('all NPCs'), we carried out single-step affinity purifications (ssAP) of nuclear pores followed by mass spectrometry from an Mlp1-PrA/Nup133-GFP double-tagged yeast strain, using Nup133-GFP as bait protein (Supplementary Fig.25a (i))[252]. To ensure the capture of dynamic interactors, we stabilized NPCs and associated proteins using a short in-lysate glutaraldehyde fixation prior to incubation with antibody-conjugated magnetic resin. To compare the interactomes of pores with and without nuclear baskets, we applied a differential affinity purification approach (dAP) that enabled us to separate and isolate the two types of pores from the same lysate via two consecutive APs. In a first step, incubation with IgG-conjugated resin allows for the isolation of Mlp1-PrA and its associated complexes including basket-containing nuclear pores ('Basket$^{plus}$') (Supplementary Fig.25a (ii)); on the flow-through, a second affinity purification is carried out using Nup133-GFP to isolate the remaining basket-less pores ('Basket$^{minus}$') (Supplementary Fig.25a (iii)). Moreover, to identify proteins associated with nuclear pores in an Mlp1- and/or nuclear poly(A) mRNA-dependent manner, we also affinity purified NPCs and their interactome from a *Δmlp1/2*/Nup133-GFP strain and Enp1$^{AID\text{-}HA}$ cells upon auxin treatment using Nup133-GFP and Mlp1-PrA, respectively. AP-MS and dAP-MS experiments were carried out in triplicate and normalized across samples. AP-MS data for 'all NPCs' (Nup133-GFP) revealed an enrichment for nucleoporins, which constituted the majority of the isolated NPC interactome, proteins involved in mRNA export and processing, proteasome components, ribosome biogenesis factors, karyopherins, transcription

and chromatin-associated proteins as well as spindle pole body (SPB) proteins, spliceosome components, surveillance factors and other nucleolar proteins (Supplementary Fig.25b). Efficient separation of basket-containing ('Basket$^{plus}$', Mlp1-PrA) and basket-less pores ('Basket$^{minus}$', Nup133-GFP) was confirmed by a good depletion of Mlp1 and Mlp2 levels in 'Basket$^{minus}$' samples compared to 'all NPCs' (Fig.18a).

We then analyzed the relative abundance of RBPs as well as factors required for mRNA maturation, RNA export and surveillance by comparing their normalized spectral counts across the different samples (Fig.18b). The mRNA export receptor heterodimer Mex67 and Mtr2 was identified with both basket-containing ('Basket$^{plus}$') and basket-less ('Basket$^{minus}$') pores as well as with NPCs in *Δmlp1/2* cells, consistent with Mex67 localization (Fig.17c) and supporting the notion that Mex67 may be systematically present at NPCs[251] and, moreover, that RNP export can occur through both types of pores. Yra1, other THO/TREX complex components as well as the poly(A)-binding protein Pab1 were also purified with both basket-containing ('Basket$^{plus}$') and basket-less ('Basket$^{minus}$') pores and with NPCs in *Δmlp1/2* cells (Fig.18b), suggesting that mRNPs containing these factors can interact with NPCs independent of a basket or Mlp1 and consistent with previous observations that deletion of MLP1/2 causes only a moderate mRNA export defect[123,129]. These proteins, however, were all enriched with Mlp1-PrA in Enp1$^{AID-HA}$ cells upon auxin treatment (Fig.15b) indicating that while, unlike Pab1, THO/TREX components are not required for basket formation, they are tightly linked to nuclear poly(A) mRNA metabolism. Similar behavior was also observed for the poly(A)-binding proteins Nab2 and Gbp2, yet their overall spectral counts were too low to compare their distribution across samples (Supplementary Fig.25c).

Unlike THO/TREX, TREX-2 components (Sac3, Sus1, Thp1, Cdc31) were enriched with basket-containing ('Basket$^{plus}$') over 'all NPCs' and absent in basket-less ('Basket$^{minus}$') pores, while present at low levels in *Δ mlp1/2* cells (Fig.18b; Supplementary Fig.25c). Those results are consistent with our previous observation that Sac3-GFP colocalized with Mlp1-Halo along the nuclear periphery (Fig.17d) and the suggestion that TREX-2 associates preferentially with baskets-containing nucleoplasmic NPCs. While Ulp1 levels were too low to compare its distribution across samples, similar to TREX-2, the pre-mRNA surveillance factor Pml39 was significantly enriched with basket-containing ('Basket$^{plus}$') pores (Fig.18b, Supplementary Fig.25c), again in agreement with our

observation that Pml39 localizes only with Mlp1-Halo and basket-containing pores (Fig.17d). Pml39 was absent in *Δmlp1/2* cells (Fig.18b, Supplementary Fig.25c) while it was enriched with Mlp1-PrA at nucleolar pores in Enp1$^{AID-HA}$ cells (Fig.15b, Supplementary Fig.25c), both consistent with previous data that its association with the NPC is dependent on the presence of nuclear baskets, i.e., Mlp1[117].

To further analyse the differences between basket-containing and basket-less pore interactomes, we organized identified proteins based on their sub-localization within the nucleus. To that end, co-purified proteins were divided into four groups: (i) nucleoporins and NPC-associated proteins present in both nucleus and nucleolus (Fig.18c); (ii) nuclear non-periphery-associated proteins (Fig.18d); (iii) complexes associated with nucleoplasmic pores (Fig.18e); and (iv) nucleolar proteins (Fig. 18f). Proteins from groups i and ii were identified across all samples (Fig.18c, d), consistent with their relative abundance across samples compared to 'all NPCs' (Fig. 18a,b, Supplementary Fig.25c). Again, while mRNA maturation and export factors (group ii) were found enriched with Mlp1-PrA and 'Basket$^{plus}$' pores, their presence with 'Basket$^{minus}$' pores and NPCs in *Δmlp1/2* cells indicates that mRNA export is not basket-dependent; moreover, the significantly lower number of mRNA maturation and export factors found with NPCs in the *Δmlp1/2* background also suggests that while for our analysis Mlp1-PrA complexes were considered NPC-associated, we cannot rule out that some proteins identified with Mlp1-PrA interact only transiently with the periphery or with free nucleoplasmic Mlp1. Within group iii, complexes known to interact with nucleoplasmic pores, possibly in a basket-dependent manner (e.g., TREX-2, SPB proteins)[147,250] were significantly enriched with basket-containing ('Basket$^{plus}$') in wild-type and Enp1$^{AID-HA}$ cells and mostly absent from basket-less pores ('Basket$^{minus}$') (Fig.18e). Conversely, group iv nucleolar proteins were found significantly under-represented with nucleoplasmic basket-containing pores ('Basket$^{plus}$') compared to basket-less pores ('Basket$^{minus}$') and 'all NPCs' (Fig.18f). This category was also increased with nucleolar basket-containing NPCs upon re-localization of Mlp1 to the nucleolar periphery in Enp1$^{AID-HA}$ cells auxin treatment (Fig.15b) suggesting overall that while pre-ribosomes and tRNPs may preferentially interact with basket-less ('Basket$^{minus}$') pores, they are equally able to interact with basket-containing pores ('Basket$^{plus}$'). However, as no ribosome export factors were identified in our AP-MS samples and depletion of Enp1$^{AID-HA}$ is a

terminal phenotype it is unlikely that these pores are actively exporting pre-ribosomes, or mRNPs [242]

Taken together, our AP-MS results show that, overall, basket-less and basket-containing pores associate with a common pool of mRNA maturation and export factors suggesting that mRNPs can bind, and most likely export, through both types of pores. This is also in accordance with the observation that mRNA export does not require Mlp1/2, or a nuclear basket. However, despite that, a number of specific factors, namely TREX-2 components and the pre-mRNA surveillance factors Pml39 were significantly enriched with basket-containing pores suggesting that these pores may represent a preferential export route for at least a subset of mRNPs, and that basket formation is linked to poly(A) mRNA metabolism, as not only Mlp1 but also a large number of mRNA maturation factors associate with nucleolar Mlp1 and basket-containing NPCs upon sequestration of poly(A) transcripts into the nucleolus.

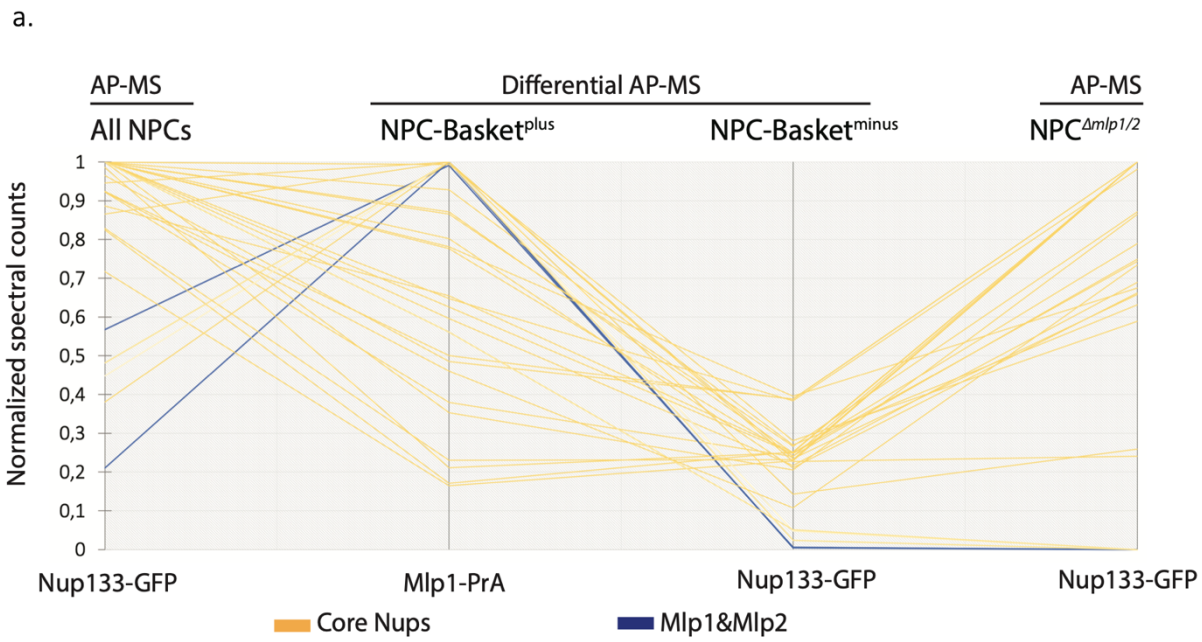

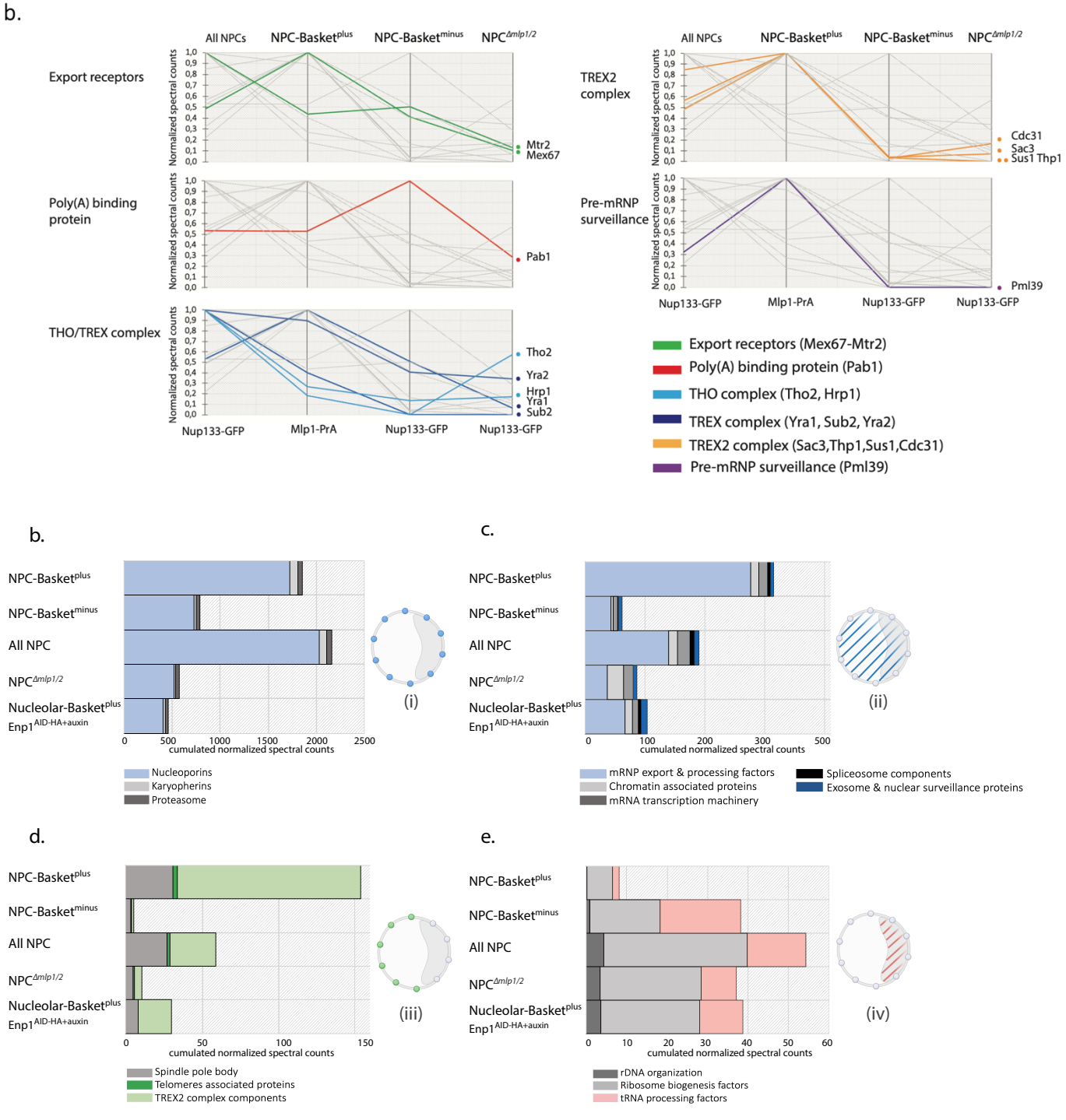


*Figure 18 NPC interactome dissection.*

*(a-b) Normalized spectral counts values of individual proteins in each NPC purification are represented scaled from 0 to 1. Each line represents the relative abundancies for one protein*

*through the series of APs: All NPC, NPC-Basket$^{plus}$, NPC-Basket$^{minus}$, NPC$^{\Delta Mlp1/2}$ background. (c-d-e-f) Histograms represent the sum of normalized spectral counts of proteins co-purified with the different pore APs known to localize: at the nuclear periphery (group (i), c); inside the nucleus (group (ii), d); at the nuclear periphery excluded from nucleoli (group (iii), e); in the nucleolus (group (iv), f). Histogram-associated cartons represent a yeast nucleus with the nucleolus represented by a grey crescent. Spheres represent proteins associating with the nuclear periphery without bias in blue or preferentially out of nucleoli in green. Dashed blue lines represent the localization of nuclear proteins with no reported bias nucleolus/nucleoplasm. Dashed pink lines represent the localization of nucleolar proteins.*

## Analysis of the transcriptomes purified with NPCs suggests different export dynamics for transcripts at basket-less and basket-containing pores

Interactome dissection of NPCs with and without a basket (i.e., Mlp1) showed that while mRBPs associate with both types of pores, there was a distinct subset of mRNP export and processing factors found enriched with basket-containing pores, suggesting that some mRNAs may be exported preferentially via basket-containing pores. To determine if subsets of nuclear mRNAs are differentially associated with basket-containing pores ('Basket$^{plus}$') compared to basket-less pores ('Basket$^{minus}$') and 'all NPCs', AP-RNA-seq was performed on oligo-dT-purified RNA samples isolated with either 'all NPCs' (Nup133-GFP) or 'Basket$^{plus}$' (Mlp1-PrA) and 'Basket$^{minus}$' (Nup133-GFP) using differential APs. Control experiments for background binding were carried out using strains expressing PrA or GFP alone and RNAs identified in these samples were filtered from those identified with Mlp1-PrA and Nup133-GFP, respectively. Furthermore, we compared each sample to a poly(A) library generated from a total RNA extraction representative of all transcripts detected in cells. We postulated that, if all mRNAs interact with a pore identically, they would be identified in our APs in a ratio reflective of the total poly(A) library. Therefore, transcripts would not be designated differentially enriched as the relative compositions of the APs will be identical to the total poly(A) library. However, transcripts enriched in the APs compared to the poly(A) library will represent transcripts displaying a higher probability to be purified in one of the APs relatively to their abundance in the overall transcriptome. Here, we used a log2 fold change (FC) cut-off of

greater than (>) 1 to determine which transcripts are enriched over the total poly(A) library. With this specific thresholding, we found 701 poly(A) transcripts enriched with 'all NPCs', 545 with 'Basket$^{minus}$', and 1411 with 'Basket$^{plus}$' pores APs compared to the total poly(A) library (Fig.19a left). Out of these, 439 transcripts were enriched across all three APs (Fig.19a, left), which may represent mRNAs with longer residence times and/or stronger/more robust/less dynamic interactions with both types of pores. In differential APs, 755 transcripts were found exclusively enriched with 'Basket$^{plus}$' AP, while only 9 were exclusively enriched with 'Basket$^{minus}$' AP.

We next used this thresholding strategy to calculate the FC of transcripts designated as enriched with 'Basket$^{plus}$' and across the three APs in a direct comparison of 'all NPCs' versus 'Basket$^{minus}$' pore AP. The vast majority of the 755 transcripts enriched with 'Basket$^{plus}$' and the 439 mRNAs enriched across the three APs were found to be significantly under-represented with 'Basket$^{minus}$' AP (Fig.19b, left). Taken together, those results suggest that mRNPs can associate with both types of pores, however,–that there is a specific subset of mRNAs that are preferentially associated with basket-containing NPC, that mRNPs may reside longer at the nuclear face of Mlp1/basket-containing NPCs compared to basket-less pores.

We further considered transcripts underrepresented in all three APs compared to the poly(A) library. Here, we used a log2 fold change (FC) cut-off of inferior to (<) 1, with p values < 0.05. We identified 497 transcripts underrepresented in all three APs, while 725 transcripts were specifically under-represented among RNAs co-purified with 'Basket$^{plus}$' AP (Fig.19a, right). By once again comparing these under-represented transcripts in "all NPCs" versus 'Basket$^{minus}$' APs, we observed that the majority of transcripts underrepresented with 'Basket$^{plus}$' were enriched with 'Basket$^{minus}$' AP (Fig.19b, right); the same was also observed for RNAs under-represented across all three APs (Fig.19b, right). Overall, this suggests that these transcripts may either form unstable interactions with basket-containing pores or have shorter residence times at the basket-containing NPC and are exported more rapidly. This could also suggest that these transcripts are preferentially exported through basket-less pores.

We next looked at specific features and found that longer transcripts were enriched across all APs (Fig.19c, blue curve) compared to controls, while short transcripts represented a significant fraction of RNAs underrepresented over poly(A) library (Fig.19c pink curve). This distinction was

not observed in control samples, indicating that this is not an experimental bias (Fig.19c). This suggests that short transcripts may have more labile interactions with the NPC and/or are exported more rapidly. In yeast, the nuclear basket has previously been linked to the export of intron-containing mRNAs, many of which are short in length (>1000nt). FC comparisons of intron-containing mRNAs across the different samples showed that, overall, intron-containing mRNAs, in particular short ones (>1000nt), were generally underrepresented across all three APs; the highest level of under-representation was observed with basket-containing 'Basket$^{plus}$' APs, the least with basket-less 'Basket$^{minus}$'APs (Fig.19d). Taken together, this suggests that a short transcript, regardless of the presence of an intron, preferentially associate with basket-less pores and longer mRNAs with basket-containing NPCs.

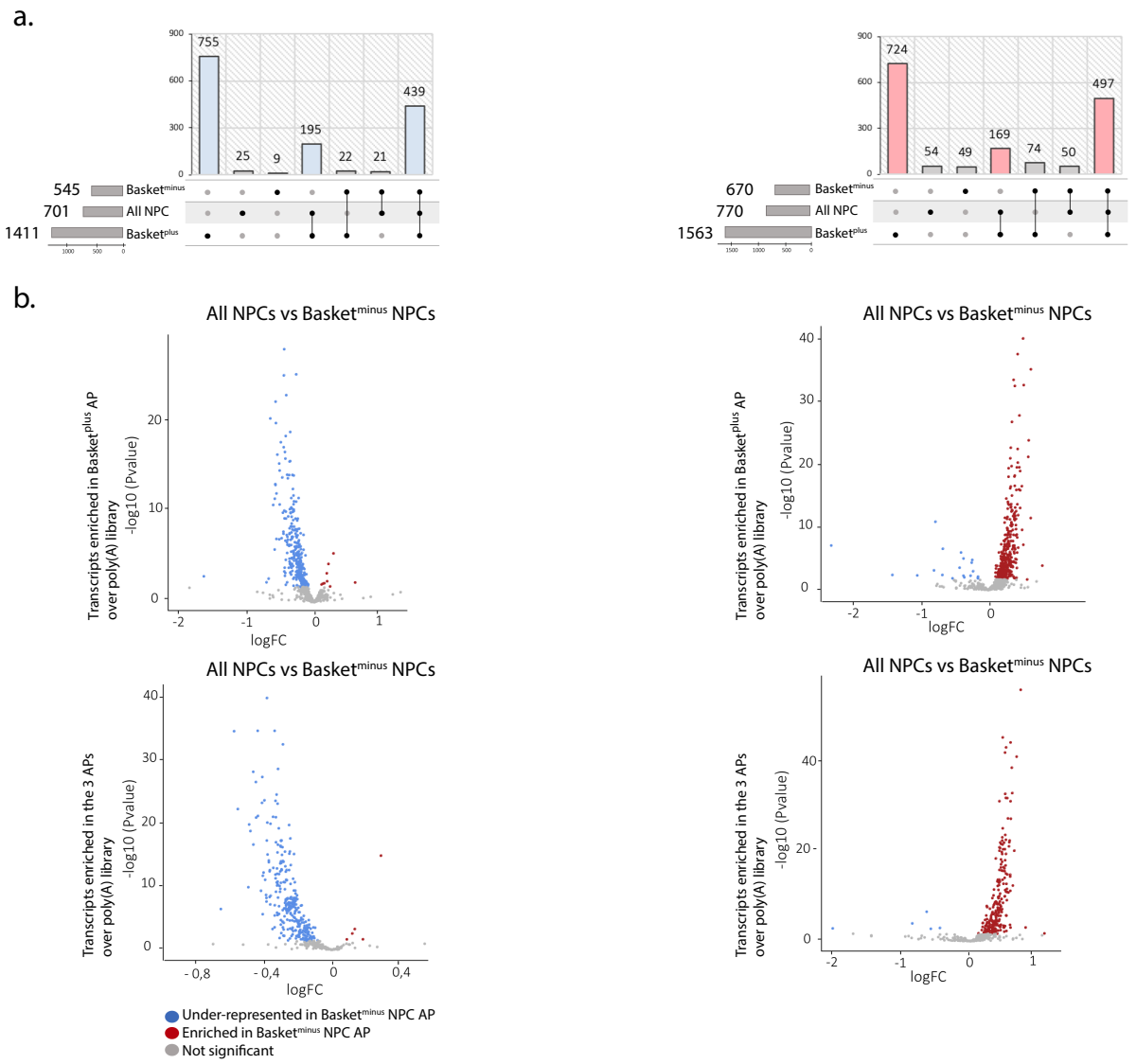

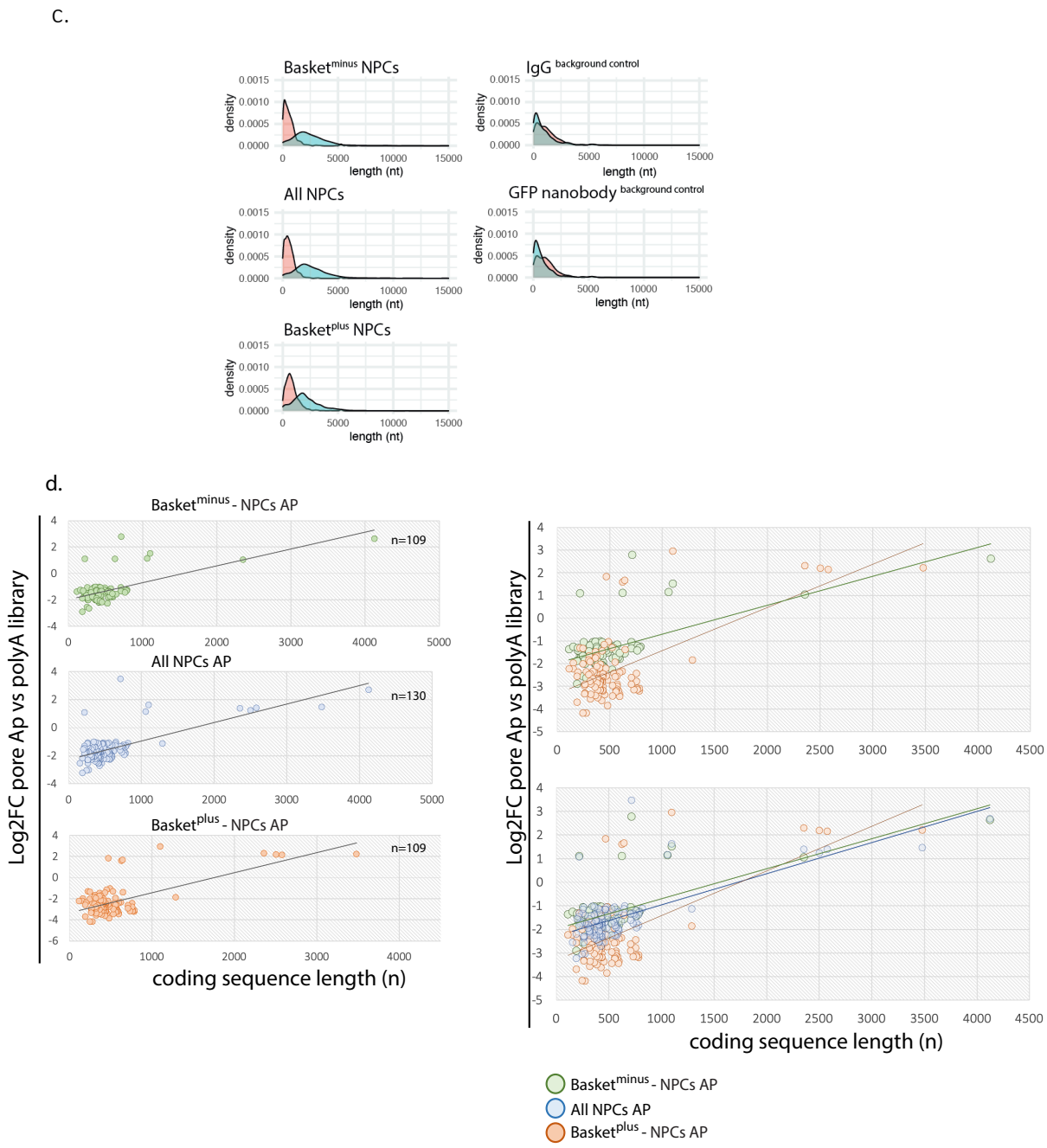


*Figure 19 Transcripts associate with both types of pores*

*(a)The blue upset plot on the left represents the genes identified with 'All NPCs', 'Basket$^{plus}$' and 'Basket$^{minus}$' NPC APs as significantly enriched with a Log2fc > 1 compared to the poly(A) library. On the other hand, the pink upset plot on the right represents the genes significantly underrepresented with a Log2fc < 1 compared to the poly(A) library. The grey bars represent the number of transcripts identified with this specific threshold in each APs. The histograms show the distribution of the*

*transcript populations: each bar represents the number of transcripts identified only in one AP or common to two or all APs. (b) The volcano plots represent the fold changes calculated from a direct comparison 'Basket$^{minus}$' vs 'All NPCs'. These fold changes have been calculated for transcripts enriched with 'Basket$^{plus}$' over the poly(A) library (top left), enriched with the three APs over the poly(A) library (bottom left), underrepresented with 'Basket$^{plus}$' compared to the poly(A) library (top right) and underrepresented with three APs compared the poly(A) library (bottom right). (c) The density plots represent the distributions of transcript length across the 3 APs and in the AP $^{background\ control}$ for IgG and GBP beads. The length distribution of the transcripts enriched with a Log2fc > 1 above the poly(A) library are shown in blue and the length distribution of the transcripts underrepresented with a Log2fc < 1 in pink. (d) Each graph represents the length of individual transcript encoded from intron-containing genes (x-axis) and its Log2FC compared to the poly(A) library (y-axis). The correlations between length and enrichment compared poly(A) library are shown for the three APs individually on the left. They have been plotted together on the right with 'Basket$^{minus}$' and 'All NPCs' (on top) or with the 3 APs (bottom).*

### 3.3.4 Discussion

Starting our path investigating basket localization, dynamics and function, we first show that nucleolar pores are competent to bind Mlp1 and that on rare occasions, a basket is present on nucleolar pores. Moreover, we demonstrate that the free fraction of Mlp1 can enter the nucleolus and does not have a restricted access to nucleolar pores. Collectively those results reinforced the idea that the absence of baskets in nucleoli is not due to the exclusion of its main scaffold Mlp1, but rather that the presence of baskets on pore is dependent on events happening mainly out of nucleoli.

#### mRNPs and specific RBPs trigger the formation of baskets

By inhibiting Pol II transcription and poly(A) polymerization, we demonstrate that mRNP production and downstream processing are essential for basket stability. To distinguish whether this phenotype is caused by interfering with transcription *per se*, or rather with downstream mRNP maturation/ export events, we used specific mutants in which Pol II transcription is still active but accumulate mRNA, newly poly(A) RNA transcripts, as well as RBPs into the nucleolus. Interestingly,

in these cells, we inverted basket localization and Mlp1 assembles *bona fide* baskets at nuclear periphery adjacent to nucleoli indicating that mRNPs themselves trigger baskets formation. Taken together, those results suggest a model where baskets are dynamic structures with a relatively short lifespan and do not persist after transcription shutdown. In this model, baskets would require contacts with mRNPs to be constantly re-assembled and/or remain stable. Hence, because the bulk of mRNPs transiting toward the cytoplasm is more abundant at the nucleoplasmic periphery compared to the nucleolar periphery, baskets would be more likely to form at the nucleoplasmic periphery (Fig.20a left panel). Therefore, when poly(A) transcripts accumulate into the nucleolus, baskets would gradually decay at the nucleoplasmic periphery, and Mlp1 protein would reassemble baskets at the rim adjacent to nucleoli, stabilized at the pore by contact with mRNPs (Fig.20a right panel).

We screened within mRNA maturation and export pathway which factors were essential for basket formation. We specifically demonstrate that the essential poly(A)-binding protein Pab1, as well as Prp5 and Pml39 involved in spliceosome formation and intron-containing mRNA, surveillance respectively, are necessary for basket stability. At first glance, those results were surprising as we would have expected a defect in basket formation upon depletion for keys RBPs known to interact directly with Mlp1/2 such as Yra1, Nab2, or Sac3[123,250,253]. Although we cannot rule out the possibility that they also participate in basket stability and re-assembling, their depletions did not affect Mlp1 localization in our experimental conditions. Overall, mRNA export defect is associated with a global reduction in poly(A) transcripts level due to an increase in transcript degradation caused by several nuclear decay factors such as the nuclear exosome, and other exonucleases[81,85,86]. Both poly(A)-binding proteins Nab2 and Pab1 are believed to promote mRNA export by interacting with different nuclear export factors, besides protecting the transcripts from nuclear decay[254].

Therefore, why baskets formation requires specifically Pab1 while Nab2 and other proteins included in our depletion screen cause an export defect and a global decay of poly(A) transcripts as well? One straightforward hypothesis could be that Pab1 promotes the export of a subset of mRNPs composed of a different RBP content from Nab2-associated mRNPs. Thus, in this scenario, only Pab1-associated mRNPs would trigger basket formation. However, it has been reported that

Pab1 and Nab2 can bind similar substrates *in vivo,* and it has been shown that Pab1 overexpression can partially alleviate export defects caused by Nab2 depletion[242,255]. It is believed that Pab1, recruits the poly(A)-dependent nuclease PAN to adjust the tail length and complete the 3'end processing preceding the cleavage and release of transcripts from the transcription sites[225,256–258]. Hence, Pab1, together with Pap1, could participate in the final steps of mRNA biogenesis and couple 3'end processing to mRNA export.

We can propose an alternative, but not incompatible hypothesis, where contrariwise to Nab2 depletion, upon Pab1 depletion part of the transcripts are retained and degraded before they are released from the transcription site and never reach the nuclear periphery. Consequently, Pab1 depletion would affect more drastically the quantity of mRNPs reaching the periphery, causing defects in basket formation.

Among the various spliceosomal factors depleted in our study, only Prp5 depletion affected basket formation. In addition to its function in the splicing process, Prp5p was shown to regulate transcription initiation/elongation as well as pre-spliceosome assembly in cooperation with transcriptional coactivator complex SAGA, and the mutant allele *prp5–1* induces a decrease in the recruitment of Pol II to intron-containing genes[246]. This suggests that impairment of basket formation upon Prp5 depletion is likely caused by a decrease in mRNPs production, possibly mainly from intron-containing genes, but not by splicing inhibition *per se*. Together, this suggests that splicing itself is not required for basket formation.

Because Mlp1 and Pml39 depletions lead to a leak of unspliced mRNAs in the cytoplasm, several studies proposed that baskets are involved intron-containing mRNA surveillance. In this study, we show that basket formation is affected by Pml39 depletion. Curiously, it has been reported that Mlp1 is also required for Pml39 to associates with pores suggesting that Mlp1 and Pml39 stabilize each other at the periphery[130]. Here, we are also showing that mRNPs reaching the periphery favor the recruitments of Mlp1 onto pores to assemble baskets. Interestingly, overexpression of Mlp1 or Pml39 leads to mRNPs retention in intra-nuclear foci with a stronger accumulation of intron-containing mRNAs[117,129]. It is not known whether retained mRNAs are pre-or fully spliced mRNP in Mlp1/Pml39 foci, however, taken together, those results advocate for a model where Mlp1, Pml39, and mRNPs, can recruit each other. Therefore, we can propose that mRNPs trigger the association

of Mlp1/Pml39 at the periphery to assemble a fully stabilized basket which would capture in a second time mRNPs on their way toward the cytoplasm (Fig.20b).

### Mlp1 nucleate a nucleolar-excluded compartment able to recruit an NPC accessory interactome

In addition, upon Pml39, Prp5, Pap1, and Pab1 depletion and to a lesser extent upon Pol II shutdown, we observed an Mlp1-GFP signal remaining at the nuclear periphery. This signal is significantly weaker than basket signal in wild type strains and, conversely to baskets signal, continuous on the nuclear rim, including the nucleolar periphery. This signal is possibly generated by the Mlp1 that binds to NPCs without being able to reach the proper stoichiometry of normal and stabilized baskets. Furthermore, we observed that Mlp1 binding pores in low abundance, as well as free diffusing once, are not excluded from the nucleolar phase. Pol II transcription inhibition as well as Pap1 and Pab1 depletion cause granules formation similar to granules observed when Mlp1-pore association is impaired upon Nup60 depletions. Mlp1 likely needs to reach a critical concentration in the nucleoplasm to aggregates, as granules formation seems to scale with the severity of the loss of Mlp1 at the periphery (Fig.20a middle panel). Our observations show that Mlp1 is an aggregation-prone protein and suggest that Mlp1 granule formations are prevented by contact with mRNPs. This aggregation capacity could have been retained by cells either to rapidly assemble granules for sequestration of specific mRNPs and/or as a manner to remove baskets and basket mediated QC from the pore upon heat shock. Conversely, to the free-diffusing Mlp1 fraction, we observed that Mlp1 was excluded from the nucleolus when the protein multimerizes to form a basket or a granule. Indeed, the nucleolar invagination caused by ectopic baskets and the internalized nucleoli when nucleolar basket assembles may indicate that Mlp1, basket-associated proteins, and possibly mRNPs form a micro-environment acquiring a set of biophysical properties repelling the nucleolar phase (Fig.20a right panel).

Therefore, by triggering the assembly of a basket, mRNP flow primes the formation of a compartment non-miscible with the nucleolar phase, mediating by this way its own exclusion from the nucleolus. Consequently, one role of baskets proteins could be to provide another level of nuclear compartmentalization segregating mRNPs export from the nucleolar compartment in yeast cells.

We have shown that baskets do not assemble on every pore at the nucleoplasmic periphery, suggesting that having a basket is not the default state for a pore but rather depends on nuclear events occurring in their vicinity. While their distribution seems to follow a stochastic pattern, we have shown that baskets can capture a specific interactome such as the TREX-2 complex or Ulp1. However, interactome dissection of pores indicates that both types of pores can be competent for export consistently with the fact that Mlp1/2 are not required for export *per se.*

## Long and short transcripts may have different export kinetics on basket-containing and basket-less pores

Overall, our results NPC-RNA-AP-sequencing showed that mRNPs could interact with both types of pores. However, the vast majority of mRNPs are enriched with basket-containing pores. While long transcripts are enriched with NPCs, shorter mRNA are underrepresented in NPCs APs. Therefore, we propose that interactions of long transcripts with NPCs, mainly at basket-containing pores, are more frequent, longer, and/or more stable. Longer residency time at the pore could correlate with structural rearmament and adjustment in the composition of large mRNPs before they access the central channel of the pore. Accordingly, our results could reflect a fast or labile interaction of short mRNAs with pores. However, short RNAs are enriched with basket-less pores, this could suggest a delayed and less efficient export on basket-less NPCs or a preferential export with basket-less NPCs.

a.

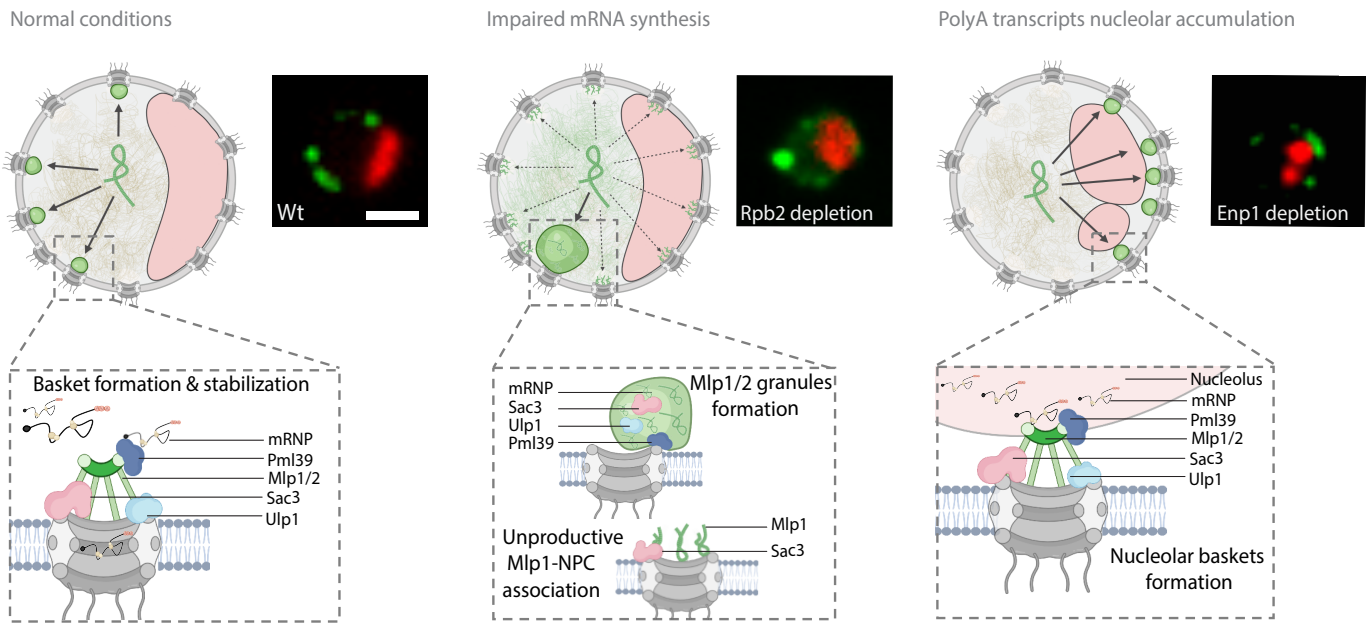


b.

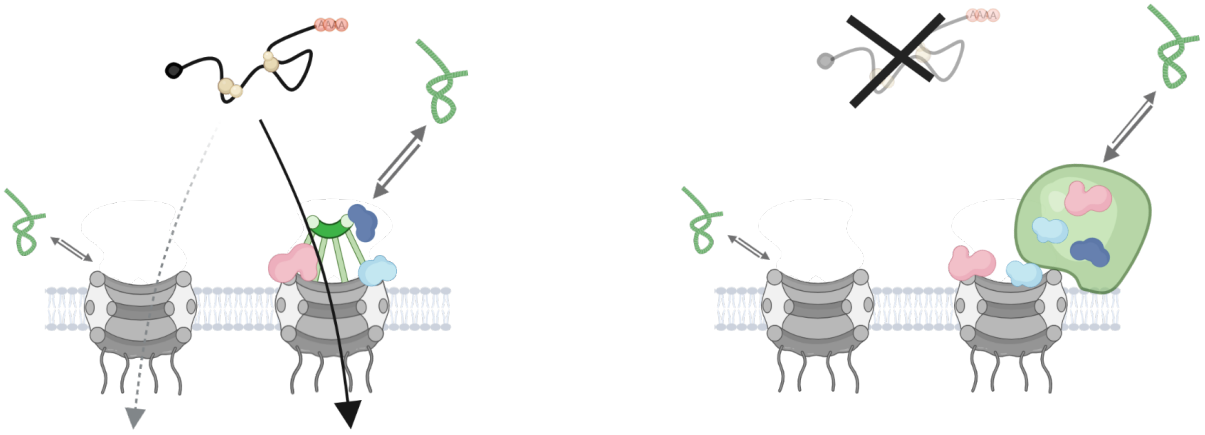

*Figure 20 A model for a cooperative basket assembly between Mlp1/2 and mRNPs.*

*Yeast nuclei are illustrated here with a nucleolus shown as a red crescent. Mlp1, represented with a green ampersand, associates with a subset of pores in the nucleoplasm. Mlp1/2 proteins reach their maximal stoichiometry at the pore and are stabilized with Pml39 to assemble a basket. Baskets recruit accessory proteins such as Ulp1 and the main TREX-2 scaffold Sac3 (left panel). mRNPs play*

*an essential role in basket nucleation as well: When mRNP production is impaired, baskets disassemble, and Mlp1 concentration increases into the nucleoplasm. In those cells, Mlp1-NPCs interactions are unproductive: Mlp1 does not reach the proper stoichiometry of fully stabilized baskets and binds the entire nuclear periphery including the nucleolar area. Furthermore, Mlp1/2 form granules containing Sac3, Pml39, and Ulp1, suggesting that mRNPs interacting with Mlp1 at the pore prevents their aggregation (middle panel). When poly(A) transcripts accumulate into the nucleolus, Mlp1 assembles fully stabilized baskets at the nucleolar periphery. Baskets relocalization correlates with the internalization of fragmented and spherical pseudo-nucleolar domains suggesting a biophysical incompatibility between basket compartments and nucleolus (right panel). (b) Guided by RBPs interacting with Mlp1/2, mRNPs associate preferentially with basket-containing pores. Mlp1 turnover represented with a grey double arrow is established between Mlp1 "free fraction" and basket-assembling Mlp1. When mRNP production/maturation are impaired and in absence of specific RBPs (Pab1), baskets are destabilized and Mlp1 forms intranuclear granules.*

### 3.3.5 Materials and methods

**Yeast tagging and growth.** Yeast strains and plasmids used in this study are listed in Supplementary Tables 1 and 2. Yeast strains are all derived from W303 and epitope-tagged proteins have been C-terminally tagged. Yeast strains were constructed by homologous recombination using a recombination cassette generated by PCR (for primers, see Supplementary Table 3) with 50 bp homology arms as described in[259]. Cells were grown in YPD or synthetic complete media lacking the appropriate amino acid to maintain plasmids when appropriate.

**Mlp1 N-terminal fragments expression.** All expression plasmids encoding yEGFP3-NLS-Mlp1 truncations have been generously provided by C. Strambio-De-Castillia [147]. Cells transformed with these expression plasmids were grown in the presence of 150 mg/l methionine for live-cell microscopy to reduce the expression level of the GFP-NLS–tagged Mlp1p fragments.

**Auxin depletion.** Yeast cells were grown at 30°C in YPD to an $OD_{600}$ ~0.3. Indole-3-acetic acid (auxin; Sigma-Aldrich) was added to a final concentration of 500 µM[260]. After 120 min, cells were prepared for live-cell imaging in SD with 2% glucose supplemented with 500 µM of auxin. For western

blotting, 20 ml of culture were harvested at an $OD_{600}$ of ~0.6 with or without 500 µm auxin, and protein extraction and western blotting carried out as described below.

**Protein extraction and western blot analysis.** For western blotting analysis, proteins were extracted from yeast cells was performed as previously described in [252] and separated on 10% or 4–12% Tris/Glycine SDS-PAGE gels. Proteins were transferred to PVDF membranes and detected using either monoclonal anti-GFP (1:1000; Sigma, 11814460001), anti-HA 12CA5 (1:1000; Sigma, 11583816001), or anti-mouse HRP (1:5000; Abcam, ab6728) antibodies. Images were acquired using a ChemiDoc MP Imaging System (Biorad).

**Preparing cells for live-cell imaging.** Yeast cells were grown at 30°C in SD with 2% glucose to an $OD_{600}$ ~ 0.4–0.6. For imaging, 100-µl cell suspension was added to a 96-well glass-bottom plate (MGB096-1-2-LG-L; Brooks Life Science Systems) previously coated with concanavalin A (Con A) and concentrated on the bottom of the well by centrifugation. Wells were coated by adding 100 µl of 1 mg/ml Con A (Sigma-Aldrich) for 10 min before unbound Con A is removed and the Con A activated by adding 100 µl of 50 mM $CaCl_2$/50 mM $MnSO_4$ for 10 min. The solution was then removed, washed once with 100 µl ddH2O, and air-dried. To minimize motions of the nucleus, for SIM images cells were briefly fixed for 5 min with 70% EtOH chilled at -20C then wash with cold PBS before been added to glass-bottom plates coated with ConA.

**Halo labeling.** For Halo labeling, cells were grown in YPD to an $OD_{600}$ ~0.15 in log phase. We added 100 nM of Halo ligand JF-549 (generously provided by Lavis Lab) [261] and available with Promega (Janelia Fluor® 549, cat number GA1110). Cells were incubated for 90 min with the Halo-ligands, then washed 3 times quickly followed by a long wash in YPD, agitating for 30 min. Finally, cells were washed 3 times in SD with 2% glucose for live-cell imaging. For SIM experiments, cells were fixed after the last wash as described above.

**Image acquisition.** Unless mentioned otherwise in the text, images were acquired on a spinning disk confocal microscope (Observer SD; Carl Zeiss) using a 100×/1.43 NA objective (Carl Zeiss), 488-nm (100 mW), and 561-nm (40 mW) excitation laser lines, and Semrock single bandpass filters for GFP (525 nm/50 nm) and RFPs (617 nm/73 nm). Images were captured using an electron-multiplying charge-coupled device camera (Evolve 512; Photometrics) using Zen blue software.

Images were captured using an electron-multiplying charge-coupled device camera (Evolve 512; Photometrics) using Zen blue software.

***Structured illumination microscopy*.** SIM images were acquired with a 63x NA 1.46 oil objective on a Zeiss Elyra PS.1 system equipped with an Andor EMCCD iXon3 DU-885CSO VP461 camera (1004x1002 pixels), and with the following lasers: 50 mW405 nm HR diode, 100 mW 488 nm HR diode, 100 mW 561 nm HR DPSS, 150 mW 642 nm HR diode. Each image was acquired using 3 rotations and a grid size of 42mm for all channels.

***HILO microscopy***. Cells were concentrated and mounted for imaging as described above. Image acquisition has been done with a 63x NA 1.46 oil objective on a Zeiss Elyra PS.1 system equipped with an Andor EMCCD iXon3 DU-885CSO VP461 camera (1004x1002 pixels), and with the following lasers: 50 mW405 nm HR diode, 100 mW 488 nm HR diode, 100 mW 561 nm HR DPSS, 150 mW 642 nm HR diode. To minimize the out-of-focus light, time-lapse movies were acquired with a Highly Inclined Laminated Optical (HILO) sheet, imaging system. Images were acquired as fast as possible with constant laser exposure. Image size was cropped to 512x512 pixels, which resulted in a frame interval of 20 ms, corresponding to a frame rate of 50 Hz (frames per second).

## Affinity purification and mass spectrometry

***Cell grinding.*** Unless noted otherwise, cells for RNA-based or protein-based analyses were isolated, rapidly frozen in liquid nitrogen, and cryo-lysis was performed by solid phase milling in a planetary ball mill (Retsch) producing a fine cell grindate[252]. All grindate was stored at -80°C until processed either for affinity purification or RNA extractions.

***Affinity purification.*** Affinity purifications (AP) were performed in triplicate per conditions as previously described[54]. In brief, cells were grown to late log phase, frozen by immersion in liquid nitrogen, and mechanically ground using a planetary ball mill (Retsch). For each AP, 1 g of cell powder was thawed in 9 ml of extraction buffer (1X tributyltin, 50 mM NaCl, 1 mM DTT, 0.5 % Triton X-100, 1X protease inhibitor cocktail [4 mg/mL pepstatin A (Sigma), 180 mg/mL PMSF (Sigma)], antifoam B (Sigma, 1:5000), and 40U/mL RNAsin (Promega), homogenized with a Polytron for 25 s, and cleared by centrifugation at 4,000 g for 5 min. 10mM glutaraldehyde was added for 5 min and samples were gently agitated on ice before the reaction was quenched with Tris-HCl pH8

to a final concentration of 100mM. Lysates were incubated with either IgG (anti-rabbit IgG, Sigma) or GFP-nanobody (expressed from pDZ580-pET28a-GBP and purified as described in [262])-conjugated magnetic beads (Dynabeads M-280) for 30 min. After removal of the super-natant, beads were extensively washed in extraction buffer, then detergents removed by washing the bead-bound complexes in 0.1 M $NH_4OAc$/0.1 mM $MgCl_2$ before a final was and resuspension in 50μl of 20-mM Tris-HCl, pH 8.0. Isolated proteins were digested on-bead at 37°C with 1 μg trypsin (Pierce Trypsin Protease, MS Grade) for 16 h[252]). The digestion was stopped by adding formic acid to a final concentration of 2%. For differential APs, the flow-through was incubated with GFP-nanobody-conjugated magnetic beads for 30 min and the beads then treated as described above.

*Peptide preparation for injection in mass spectrometer.* Tryptic peptides were cleaned using C18 ZipTips as per supplier recommendations (Milli-pore). Samples were injected to near saturation of the signal, while an equivalent volume of their respective negative controls were injected. Liquid chromatography was performed using a PicoFrit fused silica capillary column (15 cm × 75 μm i.d; New Objective, Woburn, MA, USA), self-packed with C-18 reverse-phase resin (Jupiter 5 μm particles, 300 Å pore size; Phenomenex, Torrance, CA, USA) using a high-pressure packing cell on the Easy-nLC II system (Proxeon Biosystems, Odense, Denmark) and coupled to Orbitrap Fusion™ Tribrid™ Mass Spectrometer equipped with a Proxeon nanoelectrospray Flex ion source. 0.2% formic acid (Solvent A) and 100% acetonitrile/0.2% formic acid (Solvent B) were used for chromatography and peptides were loaded on-column at a flowrate of 600 nl/min and eluted with a three-slope gradient at a flowrate of 250 nl/min. Solvent B was first increased from 2 to 25% over 20 min, then from 25 to 45% over 40 min, and finally from 45 to 80% B over 10 min.

***Protein identification.*** The peak list files were generated with Proteome Discoverer the following as described in. Protein database searching was performed with Mascot 2.5 (Matrix Science) against the NCBI - *S. cerevisiae* protein database (20160802). The mass tolerances for precursor and fragment ions were set to 10 ppm and 0.6 Da, respectively. Trypsin was used as the enzyme allowing for up to 1 missed cleavage. Cysteine carbamidomethylation was specified as a fixed modification, and methionine oxidation as variable modifications. Data analysis was performed using Scaffold (version 4.8.4).

***Mass spectrometry data analysis.*** Protein and peptide identification thresholds in Scaffold™ was set to 95% which resulted in decoy false discovery rate of 6%. Exclusive spectrum counts (ESC) were used for semi-quantification of protein preys, and mass spectrometry results were analyzed as previously described in [263]. Briefly, only Exclusive Spectral Counts (ESCs) above background detected in controls were retained. In silico digestion using MS digest (http://prospector.ucsf.edu) was performed for each protein to take protein size and predicted cleavage sites into accounts. Values were normalized against the average values of the proteins associated with the bait proteins in the different APs: Mlp2 for Mlp1-PrA and Y complex nucleoporins (Nup84, Nup85, Nup120 Nup145C) for Nup133-GFP. This allowed normalization of the data sets against proteins with a similar size, stoichiometry, and segregation.

## Affinity purification RNA-seq

***PolyA-RNA preparation and sequencing.*** RNA Affinity purification was performed using 1 g of cell powder per triplicate as described above but without crosslinking. Lysates were incubated with either IgG- or GFP-nanobody-conjugated magnetic beads for 30 min. Beads were washed extensively (8 times) in extraction buffer before being resuspended in 1 ml of Trizol (Invitrogen, 15596026) and vortexed vigorously. The total poly(A) library was generated by RNA extraction using 100 mg of cryo-ground cell powder thawed into Trizol in triplicates. RNA was then extracted using the Direct-zol Miniprep Kit (Zymo research, R2050) and Dnase treatment was performed on-column according to manufacturer's instructions. Samples were resuspended in 30 μl ultra-pure water (Invitrogen, 10977023), and the quality of RNA was assessed by Qbit and Bioanalyzer chip. RNA extracts were Poly(A)-RNA enriched via a Poly(A) mRNA magnetic Isolation Module oligo-dT (NEBNext), and cDNA libraries were prepared using the Kapa RNA HyperPrep Kit (96 rxns, Roche) and TruSeq DNA UDI 96 indexes (Illumina). RNA-sequencing was performed using Nocaseq6000 flowcell S2 PE50.

## RNA sequencing analysis

Part of the analysis has been carried out on Galaxy platform. RNA-seq reaction quality was assessed using FastQC and Paired- end reads were trimmed using Trimmomatic (version 0.38.0) to quality

trim and remove adapters. Trimmed reads were aligned on Ensemble Yeast Genome (R64-1-1 https://fungi.ensembl.org/Saccharomyces_cerevisiae/Info/Index?db=core). Differential enrichment analysis was performed using DESeq2 (Galaxy version 2.11.40.6). All five APs (Basket$^{plus}$, Basket$^{minus}$, 'all NPCs', IgG, and GFP alone) were compared against the total poly(A) library representative of the total transcriptome to generate log2(FC) values for each transcript. Log2(FC) values were then used to generate Upset- and volcano plots as well as density maps for transcript length comparisons. DESeq2 for a direct comparison between APs samples was carried out using the entire libraries for 'Basket$^{plus'}$, 'Basket$^{minus'}$, 'all NPCs'; however, only transcripts enriched or under-represented in these samples over the total poly(A) library with a Log2fc > or < 1 (pvalue <0.05) were considered.

### 3.3.4 Acknowledgments

We thank Srivathsan Adivarahan, Pascal Raymond, Carolina Aguilar and Christian Trahan for discussions and help in the optimization of different experimental approaches. This work was supported by Natural Sciences and Engineering Research Council Discovery Grants to D.Z. (RGPIN-2015-05922) and M.O. (RGPIN-2015-06568), a joint Canadian Institute for Health Research Project grant to D.Z. and M.O. (PJT-425798), and the Canadian Foundation for Innovation (D.Z. and M.O.). D.Z. holds a FRSQ Chercheur Boursier Senior. Figures have been created with Biorender.com (License #DD20C0D9-0001).

### 3.3.5 Supplementary figures and tables

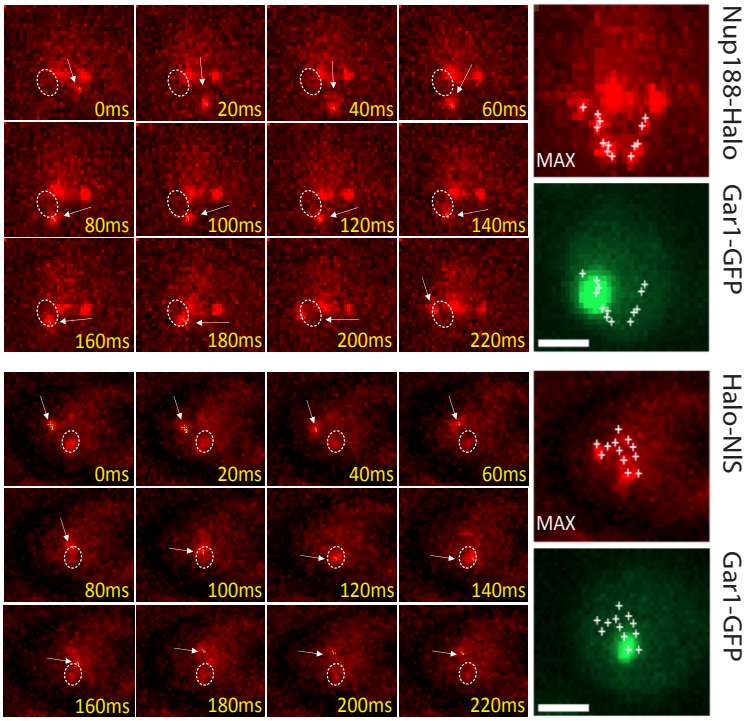


*Supplementary Figure 21 Nup188-Halo and Halo-NLS tracking*

*Individual frames from video from live-cell tracking of Nup188-Halo and Halo-NLS. White arrows show Nup188-Halo and Halo-NLS in each frame and the dashed circle represents the nucleolar area. MAX shows the maximum intensity projection of all frames with the path of Nup188-Halo and Halo-NLS highlighted with white crosses. Single particles are shown in red, nucleolus in green. (Scales bars =2µm).*

*Supplementary movies S1-3*

*Movies from live-cell imaging of Mlp1-Halo, Nup188-Halo, and Halo-NLS acquired in 20-ms intervals. For Mlp1 and Nup188 images show, in the early steps of the acquisition, the steady-state of the proteins at the nuclear periphery.*

a.

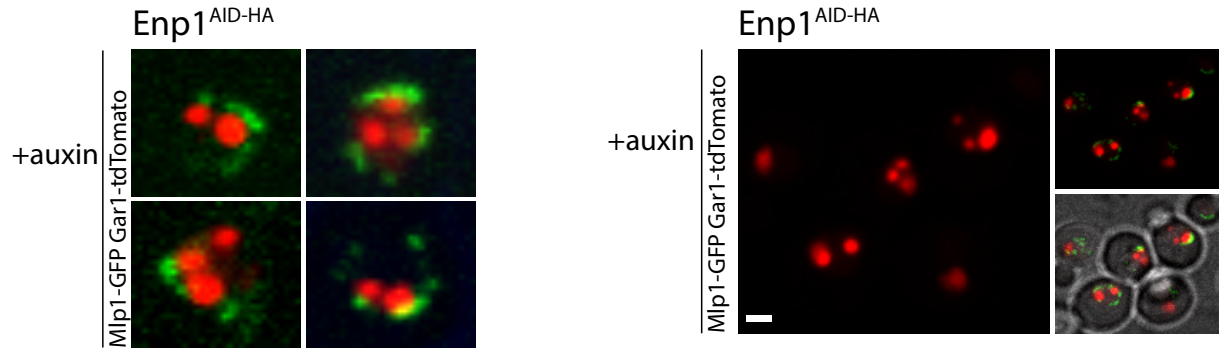


b.

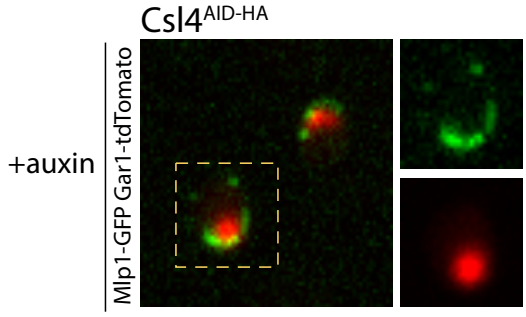


.

*Supplementary Figure 22 The shape of the nucleolus is affected upon Enp1$^{AID-HA}$ and Csl4 $^{AID-HA}$ depletion*

*(a) Most Enp1$^{AID-HA}$ cells display fragmented and internalized spherical nucleolar compartments when Mlp1-GFP relocalizes at the periphery of nucleolus upon addition of 500 µm auxin for 120 min.(b) Csl4 $^{AID-HA}$ depletion leads to the relocation of baskets at the periphery of the nucleolus.*

a.

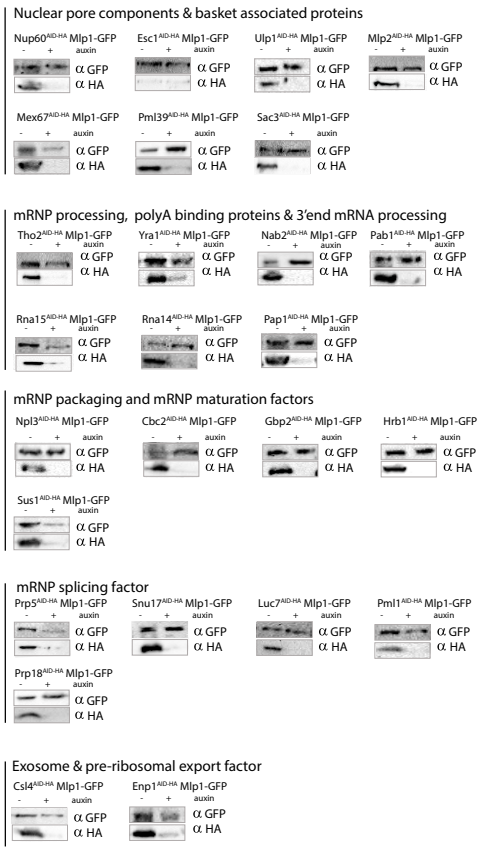


b.

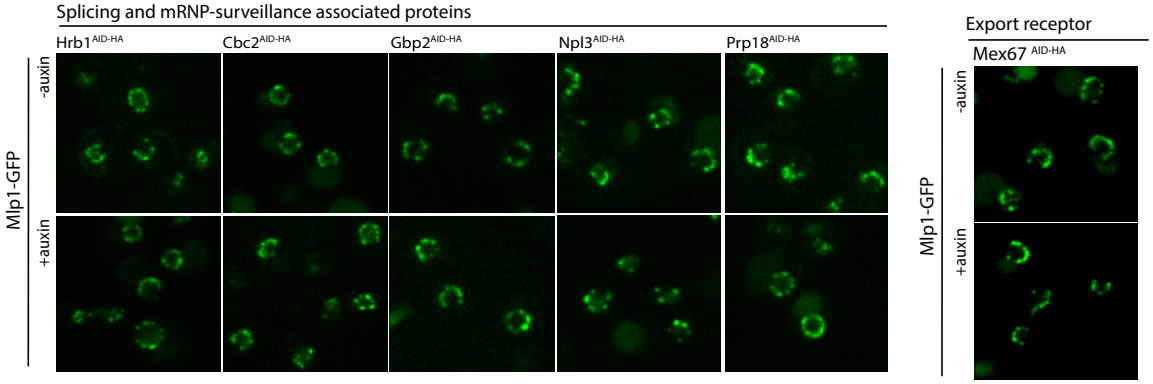


*Supplementary Figure 23 Auxin depletion screen*

*(a) Western blotting on total cell lysates showing levels of Mlp1-GFP tagged strains where spliceosomal components and Mex67 have been depleted with 500 µm auxin for 120 min. (b) Fluorescent microscopy showing Mlp1-GFP localization upon depletion of spliceosomal components and Mex67.*

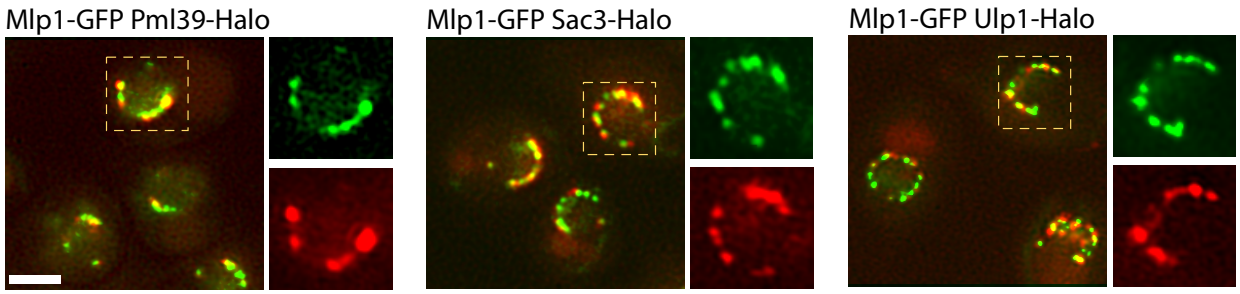


*Supplementary Figure 24 basket capture an NPC accessory interactome SIM distribution analysis of Mlp1-GFP relative to Pml39-Halo, Sac3-Halo, Ulp1-Halo*

a.

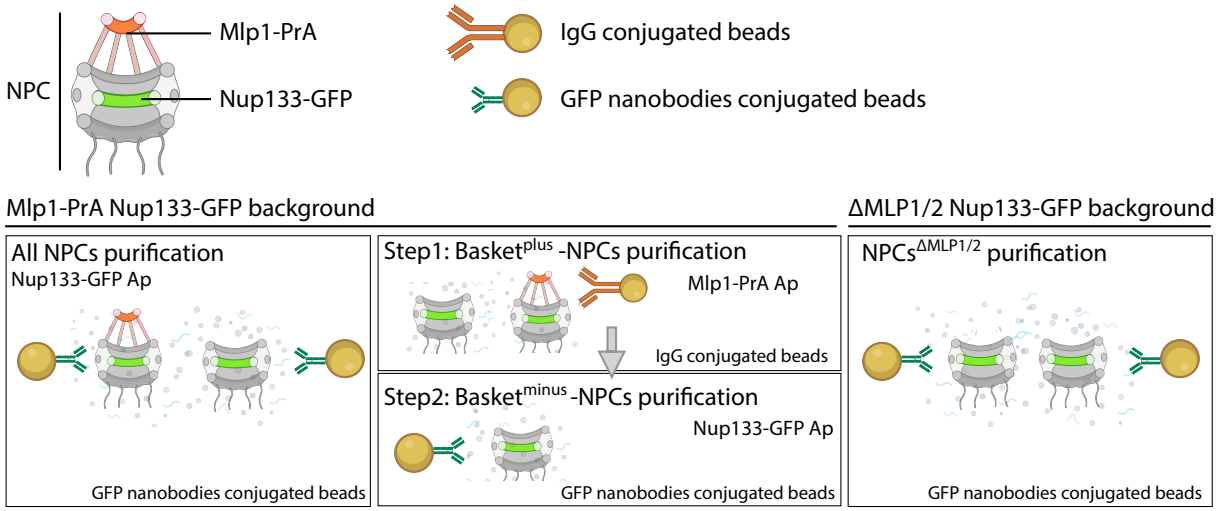


b.

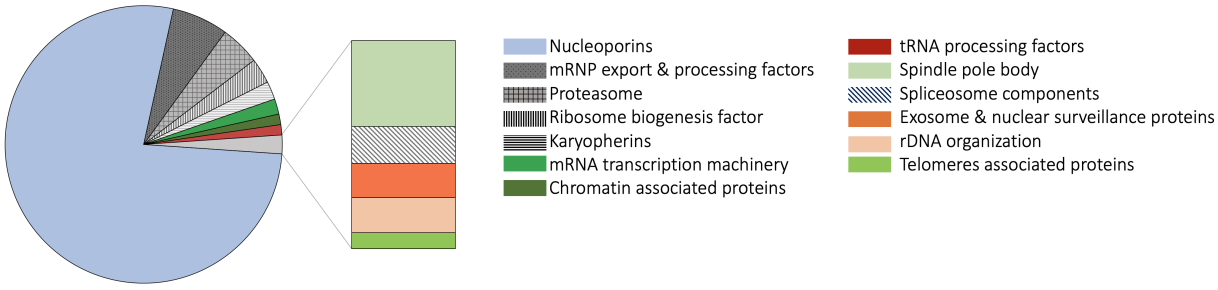


Basket^plus vs all NPCs
Basket^minus vs all NPCs
NPC^Δmlp1/2 vs all NPCs
Nucleolar-Basket^plus vs all NPCs
0%
50%
100%
Nuclear pore complex
Karyopherins
Basket associated proteins
mRNP export and processing factors
Spliceosomal complex
Spindle pole body
Chromatin associated proteins
Telomere associated proteins
Pol II and Pol II transcription associated proteins
Proteasome components
RNA surveillance and decay
Pol I and rDNA organzation
Ribosomal subunit biogenesis
Large and small Ribosomal subunit components
PolIII and tRNA processing

C.

*Supplementary Figure 25 NPCs APs strategy and proteome analysis.*

*(a) Illustration of the NPCs APs. All NPCs have been purified with GFP-nanobodies conjugated beads using cell extract from an Mlp1-PrA, Nup133-GFP tagged strain. The separation of basket-containing and basket-less pores has been carried out on cell extract from an Mlp1-PrA, Nup133-GFP strain using a sequential affinity purification using IgG-conjugated beads followed by GFP-nanobodies conjugated beads respectively. Basket-less pores have been also isolated with GFP-nanobodies conjugated beads using cell extract from an Mlp1/2-Δ, Nup133-GFP strain. (b) Overview NPC interactome from the "All NPC AP". Each protein categories represent the sum of the normalized spectral counts of proteins purified with NPCs. (c) Histograms represent normalized spectral counts of all proteins co-purified with the different pore APs localized relative to the "All NPCs" AP.*

Tableau 1. – Yeast strains used for this study.

All strains generated in this study are constructed in W303 background *MATa/MATα (leu2-3,112 trp1-1 can1-100 ura3-1 ade2-1 his3-11,15)*

| Description | Strain | Reference |
|---|---|---|
| Mlp1-GFP, Gar1-tdTomato | 6772 | This study |
| Delta Mlp1/Mlp2, Gar1-tdTomato, Nterm2-GFP | 6773 | This study.<br>Nterm2 expression Plasmid generated in Niepel et al., 2005 |
| Nup188-tdTomato, Nterm1-GFP | 6774 | This study<br>Nterm1 expression Plasmid generated in Niepel et al., 2005 |
| Nup188-tdTomato, Nterm2-GFP | 6775 | This study<br>Nterm2 expression Plasmid generated in Niepel et al., 2005 |
| Nup188-tdTomato, Nterm3-GFP | 6776 | This study<br>Nterm3 expression Plasmid generated in Niepel et al., 2005 |
| Nup188-tdTomato, Nterm4-GFP | 6777 | This study<br>Nterm4 expression Plasmid generated in Niepel et al., 2005 |
| Nup188-tdTomato, Nterm5-GFP | 6778 | This study<br>Nterm5 expression Plasmid generated in Niepel et al., 2005 |
| Nup188-tdTomato, Nterm6-GFP | 6779 | This study<br>Nterm6 expression Plasmid generated in Niepel et al., 2005 |
| Nup188-tdTomato, Cterm7-GFP | 6780 | This study<br>Cterm7 expression Plasmid generated in Niepel et al., 2005 |
| Nup188-tdTomato, GFP-NLS | 6781 | This study<br>GFP-NLS expression Plasmid generated in Niepel et al., 2005 |
| Mlp1-Halo, Gar1-GFP, Pdr5 delta | 6711 | This study |

| | | |
|---|---|---|
| Nup188-Halo Gar1-GFP Pdr5 delta | 6714 | This study |
| Halo-NLS ,Gar-GFP, Pdr5 delta | 6782 | This study<br>Halo-NLS, PDR5 delta generated by R.Reyes lab. |
| ATTIR1-9myc, MLP1-GFP, Nup188-tdTomato, Rpb2-AID-HA | 6754 | This study,<br>URA::ADH1-ATTIR1-9myc background generated in Morawska et al, 2013 |
| ATTIR1-9myc, MLP1-GFP , Nup188-tdTomato, Rpa135-AID-HA | 6757 | This study,<br>URA::ADH1-ATTIR1-9myc background generated in Morawska et al, 2013 |
| *mex67-5*, Nup188-tdTomato Mlp1-GFP | 6758 | This study |
| *rpb1-1*, Nup188-tdTomato Mlp1-GFP | 6755 | This study |
| Nup188-tdTomato, Mlp1-GFP | 6426 | This study |
| ATTIR1-9myc, Mlp1GFP, Gar1-tdTomato, Enp1-AID-HA | 6699 | This study,<br>URA::ADH1-ATTIR1-9myc background generated in Morawska et al, 2013 |
| ATTIR1-9myc, Mlp1GFP, Gar1-tdTomato, Csl4-AID-HA | 6700 | This study,<br>URA::ADH1-ATTIR1-9myc background generated in Morawska et al, 2013 |
| ATTIR1-9myc, Mlp1GFP, Gar1-tdTomato, RNA14-AID-HA | 6720 | This study,<br>URA::ADH1-ATTIR1-9myc background generated in Morawska et al, 2013 |
| ATTIR1-9myc, Mlp1GFP, Gar1-tdTomato, RNA15-AID-HA | 6729 | This study,<br>URA::ADH1-ATTIR1-9myc background generated in Morawska et al, 2013 |
| ATTIR1-9myc, Mlp1-prA, Gar1-tdTomato, Enp1-AID-HA | 6783 | This study, URA::ADH1-ATTIR1-9myc background generated in Morawska et al, 2013 |
| ATTIR1-9myc, Mlp1-GFP, Nup60-AID-HA, Gar1-tdTomato | 6721 | This study, URA::ADH1-ATTIR1-9myc background generated in Morawska et al, 2013 |
| ATTIR1-9myc, Mlp1-GFP, Esc1-AID-HA Gar1-tdTomato | 6748 | This study, URA::ADH1-ATTIR1-9myc background generated in Morawska et al, 2013 |
| ATTIR1-9myc, Mlp1-GFP, Ulp1-AID-HA Gar1-tdTomato | 6766 | This study, URA::ADH1-ATTIR1-9myc background generated in Morawska et al, 2013 |
| ATTIR1-9myc, Mlp1-GFP, Mlp2-AID-HA | 6765 | This study, URA::ADH1-ATTIR1-9myc background generated in Morawska et al, 2013 |
| ATTIR1-9myc, Mlp1-GFP, Yra1-AID-HA | 6731 | This study, URA::ADH1-ATTIR1-9myc background generated in Morawska et al, 2013 |
| ATTIR1-9myc, Mlp1-GFP, Tho2-AID-HA | 6737 | This study, URA::ADH1-ATTIR1-9myc background generated in Morawska et al, 2013 |
| ATTIR1-9myc, Mlp1-GFP, Sac3-AID-HA | 6740 | This study, URA::ADH1-ATTIR1-9myc background generated in Morawska et al, 2013 |
| ATTIR1-9myc, Mlp1-GFP, Sus1-AID-HA | 6742 | This study, URA::ADH1-ATTIR1-9myc background generated in Morawska et al, 2013 |

| | | |
|---|---|---|
| ATTIR1-9myc, Mlp1-GFP, Nab2-AID-HA | 6727 | This study, URA::ADH1-ATTIR1-9myc background generated in Morawska et al, 2013 |
| ATTIR1-9myc, Mlp1-GFP, Pab1-AID-HA Gar1-tdTomato | 6701 | This study, URA::ADH1-ATTIR1-9myc background generated in Morawska et al, 2013 |
| ATTIR1-9myc, Mlp1-GFP, Pap1-AID-HA | 6726 | This study, URA::ADH1-ATTIR1-9myc background generated in Morawska et al, 2013 |
| ATTIR1-9myc, Mlp1-GFP, Pml39-AID-HA Gar1-tdTomato | 6722 | This study, URA::ADH1-ATTIR1-9myc background generated in Morawska et al, 2013 |
| ATTIR1-9myc, Mlp1-GFP, Pml1-AID-HA | 6724 | This study, URA::ADH1-ATTIR1-9myc background generated in Morawska et al, 2013 |
| ATTIR1-9myc, Mlp1-GFP, Prp5-AID-HA Gar1-tdTomato | 6747 | This study, URA::ADH1-ATTIR1-9myc background generated in Morawska et al, 2013 |
| ATTIR1-9myc, Mlp1-GFP, Snu17-AID-HA | 6752 | This study, URA::ADH1-ATTIR1-9myc background generated in Morawska et al, 2013 |
| ATTIR1-9myc, Mlp1-GFP, Luc7-AID-HA | 6753 | This study, URA::ADH1-ATTIR1-9myc background generated in Morawska et al, 2013 |
| ATTIR1-9myc, Mlp1-GFP, Mex67-AID-HA | 6784 | This study, URA::ADH1-ATTIR1-9myc background generated in Morawska et al, 2013 |
| ATTIR1-9myc, Mlp1-GFP, Hrb1-AID-HA | 6735 | This study, URA::ADH1-ATTIR1-9myc background generated in Morawska et al, 2013 |
| ATTIR1-9myc, Mlp1-GFP, Cbc2-AID-HA | 6728 | This study, URA::ADH1-ATTIR1-9myc background generated in Morawska et al, 2013 |
| ATTIR1-9myc, Mlp1-GFP, Gbp2-AID-HA | 6741 | This study, URA::ADH1-ATTIR1-9myc background generated in Morawska et al, 2013 |
| ATTIR1-9myc, Mlp1-GFP,Npl3-AID-HA | 6738 | This study, URA::ADH1-ATTIR1-9myc background generated in Morawska et al, 2013 |
| ATTIR1-9myc, Mlp1-GFP,Prp18-AID-HA | 6732 | This study, URA::ADH1-ATTIR1-9myc background generated in Morawska et al, 2013 |
| ATTIR1-9myc, MLP1-GFP, Gar1-tdTomato, Rpb2-AID-HA | 6746 | This study, URA::ADH1-ATTIR1-9myc background generated in Morawska et al, 2013 |
| Nup188-tdTomato, Nup84-GFP | 6683 | This study |
| Nup188-GFP, Gar1-tdTomato | 6785 | This study |
| Nup188-tdTomato, Nup133-GFP | 6881 | This study |
| Nup188-tdTomato, Nup49-GFP | 6682 | This study |
| Nup188-tdTomato, Nup60-GFP | 6687 | This study |
| Nup188-tdTomato, Sac3-GFP | 6685 | This study |
| Nup188-tdTomato, Pml39-GFP | 6688 | This study |
| Nup188-tdTomato, Ulp1-GFP | 6686 | This study |
| Nup188-tdTomato, Mex67-GFP | 6689 | This study |
| Mlp1-Halo, Mlp2-GFP | 6786 | This study |
| Mlp1-Halo, Sac3-GFP | 6696 | This study |
| Mlp1-Halo, Pml39-GFP | 6698 | This study |

| | | |
|---|---|---|
| Mlp1-Halo, Mex67-GFP | 6697 | This study |
| Mlp1-Halo, Ulp1-GFP | 6643 | This study |
| Mlp1-GFP, Sac3-Halo | 6717 | This study |
| Mlp1-GFP, Pml39-Halo | 6787 | This study |
| Mlp1-GFP, Ulp1-Halo | 6716 | This study |
| ATTIR1-9myc, MLP1-GFP, Rpb2-AID-HA, Pml39-tdTomato | 6769 | This study |
| ATTIR1-9myc, MLP1-GFP, Rpb2-AID-HA, Ulp1-tdTomato | 6768 | This study |
| ATTIR1-9myc, MLP1-GFP, Rpb2-AID-HA, Sac3-tdTomato | 6770 | This study |
| ATTIR1-9myc, MLP1-GFP, Rpb2-AID-HA, Nab2-tdTomato | 6767 | This study |
| Nup133-GFP Mlp1-prA | 6668 | This study |
| DeltaMlp1/Mlp2 Nup133 GFP | 6688 | This study |
| | | |

Tableau 2. – Auxin depletion screen summary

| Protein | Function | Phenotypes upon depletion |
|---|---|---|
| Rpb2 | Pol II subunit | Basket destabilization and Mlp1 granule formation |
| Rpa135 | Pol I subunit | - |
| Enp1 | Small ribosomal subunit export | Basket re-localization at the nucleolar periphery |
| Csl4 | Exosome-non catalytic core component | Basket re-localization at the nucleolar periphery |
| Ulp1 | Ubiquitin-like modifier, Basket associated protein | Basket destabilization |
| Mlp2 | Basket scaffold Mlp1 homologue | Basket destabilization |
| Nup60 | Basket nucleoporin | Basket destabilization and Mlp1 granule formation |
| Esc1 | Lamin-like protein | Basket destabilization and Mlp1 granule formation |
| Pml39 | Unspliced pre-mRNA surveillance, basket associated protein | Basket destabilization |
| Mex67 | Export receptor | - |
| Tho2 | Co-transcriptional mRNP packaging | - |
| Yra1 | TREX subunit ; mRNA export factor | - |
| Sus1 | SAGA and TREX-2 subunit | - |
| Sac3 | TREX-2 scaffold ; mRNA export factor | - |
| Pap1 | Poly(A) polymerase | Basket destabilization and Mlp1 granule formation |
| Nab2 | Poly(A) binding protein | - |

| | | |
|---|---|---|
| Pab1 | Poly(A) binding protein | Basket destabilization and Mlp1 granule formation |
| Rna14 | Cleavage and mRNA polyadenylation | Basket re-localization at the nucleolar periphery |
| Rna15 | Cleavage and mRNA polyadenylation | Basket re-localization at the nucleolar periphery |
| Cbc2 | Cap binding complex subunit | - |
| Prp5 | Pre-spliceosome formation; RNA helicase | Basket destabilization |
| Snu17 | Splicing factor;U2 snRNP complex | - |
| Luc7 | Splicing factor; U1 snRNP complex | - |
| Pml1 | Unspliced pre-mRNA surveillance | - |
| Npl3 | Nuclear mRNA surveillance | - |
| Gbp2 | Nuclear mRNA surveillance | - |
| Prp18 | Splicing factor; component of snRNP U5 | - |
| Hrb1 | Nuclear mRNA surveillance | - |

Tableau 3. – Primers used in this study for C-terminal tagging

| C-terminal tagging (5'-3') | Sequence |
|---|---|
| Mlp1-GFP (Fwd) | AAGATGAGGAAGAAAAAGAAACCGATAAGGTGAATGACGAGAACAGTATACGTACGCTGCAGGTCGAC |
| Mlp1-GFP (Rev) | ACATTGAAAAAGGTTTAGTTTGTATTGATCCCTTGTTTTTACTATCTCCTATCGATGAATTCGAGCTCG |
| Gar1-tdTomato (Fwd) | GGATCTCGTGGCGGATCTCGTGGTGGTTTCAGAGGAGGTAGAAGAGCTCTAGAACTAGTGGATCC |
| Gar1-tdTomato (Rev) | CAGATATAGTAAGTTGGAAGAAATGAAGAATTGTGAAAGATAAAGGGCATAGGCCACTAGTGGATCTG |
| Nup188-tdTomato (Fwd) | CAAGGGTATCAGCAGAGACATTAAAGCATTACAAGATTCACTATTTAAGGACGTTGCTCTAGAACTAGTGGATCC |
| Nup188-tdTomato (Rev) | GCACTTGCACTGTTCATTATTATATTATGTAGCTTTACATAACCTGCAAAATAAGGCATAGGCCACTAGTGGATCTG |
| Mlp1-Halo (Fwd) | GAGGAAGAAAAAGAAACCGATAAGGTGAATGACGAGAACAGTATAGGTGACGGTGCTGGTTTA |
| Mlp1-Halo (Rev) | GCAGAATGAAGCTCCTCCACATTGAAAAAGGTTTAGTTTGTATTGACACAGGAAACAGCTATGACC |
| Nup188-Halo (Fwd) | CAAGGGTATCAGCAGAGACATTAAAGCATTACAAGATTCACTATTTAAGGACGTTGGTGACGGTGCTGGTTTA |
| Nup188-Halo (Rev) | GCACTTGCACTGTTCATTATTATATTATGTAGCTTTACATAACCTGCAAAATAAGACACAGGAAACAGCTATGACC |
| Rpa135-AID-HA (Fwd) | CTATCCGCAATGGGTATAAGATTGCGTTATAATGTAGAGCCCAAACGTACGCTGCAGGTCGAC |
| Rpa135-AID-HA (Rev) | CCTTCATTTACCATTCTATATCAATTTGGAAAGAAGGGTATTTCTATCGATGAATTCGAGCTCG |
| Rpb2-AID-HA (Fwd) | ATGAACATTACACCACGTTTATATACCGATCGTTCGAGAGATTTTCGTACGCTGCAGGTCGAC |
| Rpb2-AID-HA (Rev) | AATGTTTTTTATTATTTTACTTTCTTAGAGTTACAACATTATTTCATCGATGAATTCGAGCTCG |
| Enp1-AID-HA (Fwd) | CAGGGAGTTTGTTGATCCACAGGAAGCTAATGATGATTTAATGATTGATGTCAATCGTACGCTGCAGGTCGAC |
| Enp1-AID-HA (Rev) | TGAAAGGGGGAAAGACCGAGCGATATAAAATTGATGAAAAATTGATATTACAGCAATCGATGAATTCGAGCTCG |
| Csl4-AID-HA (Fwd) | GATGACTTCACCGGTTACAGGCGCTACAGAAAAGCGCAAATGTGCCAAACCTTTTCGTACGCTGCAGGTCGAC |
| Csl4-AID-HA (Rev) | TACCCTCTTTTAAATATATACGCGTCTATATGCACTGTAGATAAGCTGTTACATAATCGATGAATTCGAGCTCG |
| Rna14-AID-HA (Fwd) | GAATTTTTTAAATGATCAAGTAGAGATTCCAACAGTTGAGAGCACCAAGTCAGGTCGTACGCTGCAGGTCGAC |
| Rna14-AID-HA (Rev) | TTATAATAGATGTGTTGGTATAAATATTCATATATACCTATTTATTAACGTAATGATCGATGAATTCGAGCTCG |
| Rna15-AID-HA (Fwd) | GATGGCTATTTGGGACTTAAAACAAAAAGCATTAAGGGGAGAATTTGGTGCATTTCGTACGCTGCAGGTCGAC |
| Rna15-AID-HA (Rev) | GTTGCCTCATCATTGCGGAACCGCATTTTTTTTTTGTATTTTTGCCTCCCTAGTTATCGATGAATTCGAGCTCG |
| Nup60-AID-HA (Fwd) | AAATGGCTTGGTTGATGAAAATAAAGTTGAGGCTTTCAAGTCCCTATATACCTTTCGTACGCTGCAGGTCGAC |
| Nup60-AID-HA (Rev) | CTTACGTATTGAGTTGGGCTATACGGTAATTATGTCACGGCTAAAATTTTCATTAATCGATGAATTCGAGCTCG |

| | |
|---|---|
| Esc1-AID-HA (Fwd) | TAGGGGGCACGAGCCAAAAAGCCGTGGACAGAATACGCATCCAAGTGTTGACAAACGTACGCTGCAGGTCGAC |
| Esc1-AID-HA (Rev) | AGAAAAACGCATCGCAATAATTATTACTATCTACATATTCCTGTATACAATTTGAATCGATGAATTCGAGCTCG |
| Ulp1-AID-HA (Fwd) | TGCGATTAGGATGAGAAGATTTATTGCCCATTTGATTTTAACCGACGCTTTAAAACGTACGCTGCAGGTCGAC |
| Ulp1-AID-HA (Rev) | CAATGATCTGAATATTTCTACTTATGTATAATAATTGTATATTATAAAAGAATAAATCGATGAATTCGAGCTCG |
| Mlp2-AID-HA (Fwd) | ACACCAAAAAGGTTAAAGAGAGTCCAGCAAATGATCAAGCTTCCAACGAGCGTACGCTGCAGGTCGAC |
| Mlp2-AID-HA (Rev) | AAAATATGTAGATGTTTCATATTTATATAATTACATTGTTTAATATTACAATCGATGAATTCGAGCTCG |
| Yra1-AID-HA (Fwd) | TAAGAAAAGTCTTGAAGATCTGGACAAGGAAATGGCGGACTATTTCGAAAAGAAACGTACGCTGCAGGTCGAC |
| Yra1-AID-HA (Rev) | GGaaaaattaaatttaataaaaccaaattaaatcaaacaaaaaaTTGACAATTAAATCGATGAATTCGAGCTCG |
| Tho2-AID-HA (Fwd) | TCAGGCGCTTCCGCAAGGTCCCAAGGGTGGGAATTACGTCAGTAGGTACCAGAGGCGTACGCTGCAGGTCGAC |
| Tho2-AID-HA (Rev) | GGGAACTATCAAAGTACACGTTAAAATTCAGCTCGGGTATGTTAAGTACTAGTAAATCGATGAATTCGAGCTCG |
| Sac3-AID-HA (Fwd) | TATATTAGAGCTGAAGATCTTGATCGATTCTGTCAAGAAGAAAGTAAATAATGATCGTACGCTGCAGGTCGAC |
| Sac3-AID-HA (Rev) | TTCCTAAAGCTATAGAAAAAATGCACATTTCTTTTGTTTATATATTACAAATGCTATCGATGAATTCGAGCTCG |
| Sus1-AID-HA (Fwd) | GTTTTAAAGCAAATAAGGGAATTTCTTGAAGAGATTGTAGATACACAACGTACGCTGCAGGTCGAC |
| Sus1-AID-HA (Rev) | TTTCCCGATGAGCATATGTAATAATATTGGGAATTAAGGTGCATTTTCGTATCCTATCGATGAATTCGAGCTCG |
| Nab2-AID-HA (Fwd) | AAATGCTCCTCCGCAAACCAGTTTTACGCACCAAGAACAAGATACGGAAATGAACCGTACGCTGCAGGTCGAC |
| Nab2-AID-HA (Rev) | CTTCCATCAAAAGGGTCACAGGAACATGAATTTCGTTCCGTGATTTTAATAGTAAATCGATGAATTCGAGCTCG |
| Pab1-AID-HA (Fwd) | TTCTGCTGCCTATGAGTCTTTCAAAAAGGAGCAAGAACAACAAACTGAGCAAGCTCGTACGCTGCAGGTCGAC |
| Pab1-AID-HA (Rev) | AGAAAAAAAAGATGATAAGTTTGTTGAGTAGGGAAGTAGGTGATTACATAGAGCAATCGATGAATTCGAGCTCG |
| Pap1-AID-HA (Fwd) | AGATGCTGCTTCAGGTGACAACATCAATGGCACAACCGCAGCTGTTGACGTAAACCGTACGCTGCAGGTCGAC |
| Pap1-AID-HA (Rev) | GTTTATGACTGATTAACCTATATTAATAAACTATTCAACTATAAATAGGAATGTCATCGATGAATTCGAGCTCG |
| Pml39-AID-HA (Fwd) | GAAATTGGGCGTGGGAGAAAGACTAAATAAATTAGAGGCTGTTCTACAAACTTTACGTACGCTGCAGGTCGAC |
| Pml39-AID-HA (Rev) | CAGCATGGGGGCATATACAAGCATATGAGAATTTGGATAATGTATTACATCTAATATCGATGAATTCGAGCTCG |
| Pml1-AID-HA (Fwd) | TACACTTTCAGAATTTGAAGAAGATACCGATTACGAACTCATCTTCATGAATGTACGTACGCTGCAGGTCGAC |
| Pml1-AID-HA (Rev) | CAGCATTCAAAGAAGAATAATTAAAACACACTGAAAGTGTGTTTCTTATATATGGATCGATGAATTCGAGCTCG |
| Prp5-AID-HA (Fwd) | GGGGTCGTAAAGGCTGCAAGCTTGTCTTTGAAGAGTACTAAATACCGTACGCTGCAGGTCGAC |
| Prp5-AID-HA (Rev) | AACTACGAAAGTATATAGCACCACGAGTGAGTTAAATTCTAAAAAATCGATGAATTCGAGCTCG |
| Snu17-AID-HA (Fwd) | ATAGCTGATAGACTGTGGAGTCGTAAAGAATTTCGCTTGGGGACCCGTACGCTGCAGGTCGAC |
| Snu17-AID-HA (Rev) | GAGCGAGCCTTTCCCTTTTGGGACGCGCGCCAAGGCCCTTCTGTTATCGATGAATTCGAGCTCG |
| Luc7-AID-HA (Fwd) | AACGCCAGCAAGACAGCTACTACACTACCCGGAAGACGCTTTGTGCGTACGCTGCAGGTCGAC |
| Luc7-AID-HA (Rev) | TCCTTCGAACAAAATTTTTCTAGCATCATTTTTTTATGTATGGCCATCGATGAATTCGAGCTCG |
| Mex67-AID-HA (Fwd) | AAAGGGTTTTCAGAGTAGCATGAATGGCATCCCTAGAGAAGCATTTGTGCAGTTCCGTACGCTGCAGGTCGAC |
| Mex67-AID-HA (Rev) | GCTTAAACTGTATATTTTTTGTGATACTGTGCGGCTGAAACAGGGAACAATATCAATCGATGAATTCGAGCTCG |
| Hrb1-AID-HA (Fwd) | GAATAATTATAACTATGGGGGTTGTGATTTGGATATATCGTACGCTAAACGCCTCCGTACGCTGCAGGTCGAC |
| Hrb1-AID-HA (Rev) | ATAAATACTTGTCGCAGATCCAATAGGTGAGAAAGTATATAGATCGAGAGTAGTTATCGATGAATTCGAGCTCG |
| Cbc2-AID-HA (Fwd) | TACTTTCAGACCAGGTTTCGATGAAGAAAGAGAAGATGATAACTACGTACCTCAGCGTACGCTGCAGGTCGAC |
| Cbc2-AID-HA (Rev) | atatatatatatatatCTGTGTGTAGAATCTTTCTCAGATATAAATTGATTGATTATCGATGAATTCGAGCTCG |
| Gbp2-AID-HA (Fwd) | AAATAATTATAATTATGGTGGTTGTAGTTTACAGATCTCTTATGCTAGACGTGATCGTACGCTGCAGGTCGAC |
| Gbp2-AID-HA (Rev) | TTATTTATACGTTATCATAAAGTACACAGGTCATGGTTCGGTTGGTGCTTAGGAAATCGATGAATTCGAGCTCG |
| Npl3-AID-HA (Fwd) | TCCAAGAGATGCATACAGAACCAGAGATGCTCCACGTGAAAGATCACCAACCAGGCGTACGCTGCAGGTCGAC |
| Npl3-AID-HA (Rev) | ACAATTCATATCTTTTGTTAATTTCTCCTTTTTTTTTCTCAACTATATAAATGGCATCGATGAATTCGAGCTCG |
| Prp18-AID-HA (Fwd) | TAAAAGATTAATAACTTTTGAAGAATGGTATACCAGCAACCACGATAGCTTAGCCCGTACGCTGCAGGTCGAC |
| Prp18-AID-HA (Rev) | TTATTTTGGCCGCATGATATCGTGCCACGCGATAACGAAAACAATAGTTCAACAAATCGATGAATTCGAGCTCG |

| | |
|---|---|
| Nup84-GFP (Fwd) | TGGAAAGTTAAAAGAGTATCTGGATCTCGTTGCTCGCACAGCAACCCTTTCGAACCGTACGCTGCAGGTCGAC |
| Nup84-GFP (Rev) | TAAAATTATTGCTGTTTACTTAAAATATAAACTTATTCTGCAATACATTAATTGAATCGATGAATTCGAGCTCG |
| Nup60-GFP (Fwd) | AAATGGCTTGGTTGATGAAAATAAAGTTGAGGCTTTCAAGTCCCTATATACCTTTCGTACGCTGCAGGTCGAC |
| Nup60-GFP (Rev) | CTTACGTATTGAGTTGGGCTATACGGTAATTATGTCACGGCTAAAATTTTCATTAATCGATGAATTCGAGCTCG |
| Nup49-GFP (Fwd) | GCCGTGTTACATCAAAAAACGAAAACACTGGCATCATTGAGCATAGCTCTAGAACTAGTGGATCC |
| Nup49-GFP (Rev) | TGTACAAGACATTTGTACTTGTTATACGCACTATATAAACTTTCAGCATAGGCCACTAGTGGATCTG |
| Nup133-GFP (Fwd) | TGTAGCGAAAGAAAAAAACTATACCATCAACTATGAAACCAACACTGTAGAATACCGTACGCTGCAGGTCGAC |
| Nup133-GFP (Rev) | TATTATCATTCCCCAGTAAAGTTTATTATATATATGTAAAATTGTATTATAGATAATCGATGAATTCGAGCTCG |
| Ulp1-GFP (Fwd) | TGCGATTAGGATGAGAAGATTTATTGCCCATTTGATTTTAACCGACGCTTTAAAACGTACGCTGCAGGTCGAC |
| Ulp1-GFP (Rev) | CAATGATCTGAATATTTCTACTTATGTATAATAATTGTATATTATAAAAGAATAAATCGATGAATTCGAGCTCG |
| Pml39-GFP (Fwd) | AGGAGAAATAAAACATTATTCCCCAGGAATTGAGAGGAAAGTAGGGCAGTTACTACGTACGCTGCAGGTCGAC |
| Pml39-GFP (Rev) | CAGCATGGGGGCATATACAAGCATATGAGAATTTGGATAATGTATTACATCTAATATCGATGAATTCGAGCTCG |
| Mex67-GFP (Fwd) | AAAGGGTTTTCAGAGTAGCATGAATGGCATCCCTAGAGAAGCATTTGTGCAGTTCCGTACGCTGCAGGTCGAC |
| Mex67-GFP (Rev) | GCTTAAACTGTATATTTTTTGTGATACTGTGCGGCTGAAACAGGGAACAATATCAATCGATGAATTCGAGCTCG |
| Sac3-GFP (Fwd) | TATATTAGAGCTGAAGATCTTGATCGATTCTGTCAAGAAGAAAGTAAATAATGATCGTACGCTGCAGGTCGAC |
| Sac3-GFP (Rev) | TTCCTAAAGCTATAGAAAAAATGCACATTTCTTTTGTTTATATATTACAAATGCTATCGATGAATTCGAGCTCG |
| Mlp2-GFP (Fwd) | ACACCAAAAAGGTTAAAGAGAGTCCAGCAAATGATCAAGCTTCCAACGAGCGTACGCTGCAGGTCGAC |
| Mlp2-GFP (Rev) | AAAATATGTAGATGTTTCATATTTATATAATTACATTGTTTAATATTACAATCGATGAATTCGAGCTCG |
| Ulp1-Halo (Fwd) | TGCGATTAGGATGAGAAGATTTATTGCCCATTTGATTTTAACCGACGCTTTAAAAGGTGACGGTGCTGGTTTA |
| Ulp1-Halo (Rev) | CAATGATCTGAATATTTCTACTTATGTATAATAATTGTATATTATAAAAGAATAAACACAGGAAACAGCTATGACC |
| Pml39-Halo (Fwd) | GAAATTGGGCGTGGGAGAAAGACTAAATAAATTAGAGGCTGTTCTACAAACTTTAGGTGACGGTGCTGGTTTA |
| Pml39 Halo (Rev) | CAGCATGGGGGCATATACAAGCATATGAGAATTTGGATAATGTATTACATCTAATACACAGGAAACAGCTATGACC |
| Sac3-Halo (Fwd) | TATATTAGAGCTGAAGATCTTGATCGATTCTGTCAAGAAGAAAGTAAATAATGATGGTGACGGTGCTGGTTTA |
| Sac3-Halo (Rev) | TTCCTAAAGCTATAGAAAAAATGCACATTTCTTTTGTTTATATATTACAAATGCTACACAGGAAACAGCTATGACC |
| Nab2-tdTomato (Fwd) | AAATGCTCCTCCGCAAACCAGTTTTACGCACCAAGAACAAGATACGGAAATGAACGCTCTAGAACTAGTGGATCC |
| Nab2-tdTomato (Rev) | TTGAATAGGTGTCTTCCATCAAAAGGGTCACAGGAACATGAATTTCGTTCCGTGAGCATAGGCCACTAGTGGATCTG |
| Sac3-tdTomato (Fwd) | TATATTAGAGCTGAAGATCTTGATCGATTCTGTCAAGAAGAAAGTAAATAATGATGCTCTAGAACTAGTGGATCC |
| Sac3-tdTomato (Rev) | TTCCTAAAGCTATAGAAAAAATGCACATTTCTTTTGTTTATATATTACAAATGCTGCATAGGCCACTAGTGGATCTG |
| Pml39-tdTomato (Fwd) | GAAATTGGGCGTGGGAGAAAGACTAAATAAATTAGAGGCTGTTCTACAAACTTTAGCTCTAGAACTAGTGGATCC |
| Pml39-tdTomato (Rev) | CAGCATGGGGGCATATACAAGCATATGAGAATTTGGATAATGTATTACATCTAATGCATAGGCCACTAGTGGATCTG |
| Ulp1-tdTomato (Fwd) | TGCGATTAGGATGAGAAGATTTATTGCCCATTTGATTTTAACCGACGCTTTAAAAGCTCTAGAACTAGTGGATCC |
| Ulp1-tdTomato (Rev) | CAATGATCTGAATATTTCTACTTATGTATAATAATTGTATATTATAAAAGAATAAGCATAGGCCACTAGTGGATCTG |
| Mlp1-PrA(Fwd) | GACTGAAGATGAGGAAGAAAAAGAAACCGATAAGGTGAATGACGAGAACAGTATAGGTGAAGCTCAAAAACTTAAT |
| Mlp1-PrA(Rev) | CCTCCACATTGAAAAAGGTTTAGTTTGTATTGATCCCTTGTTTTTACTATCTCCTATCGATGAATTCGAGCTCG |

Tableau 4. – **Plasmids used in this study** (Chapter 3)

| | |
|---|---|
| pZUT3 centromeric plasmid carrying GAR1-GFP, URA3 | Niepel et al.[112] |
| centromeric plasmid pEXPGFPNLS_M2NT2 for Nterm2 Mlp1 fragment expression, HIS3 | |
| centromeric plasmid pUG34_GFPNLS HIS3 | |

# 4. Complementary results: Mlp1 multivalency may be central in its dynamics and localization

This Chapter presents unpublished experiments aiming to better understand how Mlp1 could multimerize to assemble baskets and determine Mlp1 vicinity interactomes. This short section may highlight certain aspects of Mlp1 assemblies, such as the baskets and granules, which could be informative for possible models of basket formation. This Chapter contains three preliminary independent experiments suggesting that Mlp1 is a highly multivalent protein. Indeed, the following results may indicate that Mlp1 has a high combining capacity and can create multiple bonds with itself and with Mlp2. In addition, I showed that this valency and the ability to multimerize might be modulated by post-translational modifications (PTMs).

## 4.1 Mlp1 fragments can aggregate spontaneously

I expressed the Mlp1 N-terminal region 2, previously described as the Mlp1 pore binding domain from plasmids, to analyze its distribution at the nuclear periphery. In addition, we expressed additional GFP-fused Mlp1 fragments and observed that three out of seven Mlp1 fragments spontaneously form intranuclear granules (Fig.26a, b). This observation is consistent with the frequent Mlp1 aggregation observed when Mlp1 concentration increases into the nucleoplasm as observed in the section 3.3.3 of this work. The ability of Mlp1 fragments to interact together to form large granules suggests that Mlp1 is an aggregation-prone protein possibly due to its high ability to multimerize. Interestingly, as discussed in the introduction, this propensity to assemble granules seems to have a biological relevance during specific stresses such as heat shock when Mlp1 foci assemble into the nucleoplasm sequestering some poly(A) transcripts and specific RBPs[201]. Therefore, I carried out heat shock experiments using cells expressing the different Mlp1 fragments and observed that N-terminal 2 region assembles granules upon heat stress. While this specific region aggregates within few minutes, the fragments N-terminal 4,6 and C-terminal 7 did

not form granules even upon 2h heat shock (Fig.26b). This may suggest that Mlp1 heat shock foci formation is triggered by this region.

To further characterize the nucleolar-basket exclusion, I analyzed the distribution of the specific Mlp1 fragments in cells where the nucleolus position was determined by tagging the endogenous Gar1 with tdTomato. While Mlp1 N-terminal fragments 2 and 4 did not show any exclusion from the nucleolus, the signals of the N-terminal 1,3,5,6 and C-terminal fragments did not overlap with the nucleolar compartment (Fig.26c). Furthermore, we observed the internalization and the fragmentation in one or several pseudo-nucleolar domains in cells expressing the N-terminal 1,5,6 and C-terminal fragments (Fig.26c). Nucleoli are believed to be highly acidic compartments, and I hypothesized that a higher content in negatively charged, acidic amino acids may be present in the fragments excluded from the nucleolus. Mlp1 sequence analysis showed that Mlp1 is a highly charged protein, both negatively and positively, with an even distribution of charged residues within its sequence (Fig.26d). We have not been able to highlight the molecular signature of the nucleolar exclusion. However, this could suggest that the high abundance of these specific peptides, which appear to display a strong non-miscibility with the nucleolus, can induce the deformation of the nucleolar phase.

Interestingly, it has been shown that overexpression of the C-terminal domain of Mlp1 induced retention of poly(A) transcripts in the nucleus[123]. Therefore, I hypothesized that the accumulation of other elements such as transcripts and associated RBPs also participates in the nucleolar deformation upon expression of Mlp1 fragments. Overall, my results suggest that the ability to aggregate and the non-miscibility with the nucleolar phase is encoded within the Mlp1 sequence.

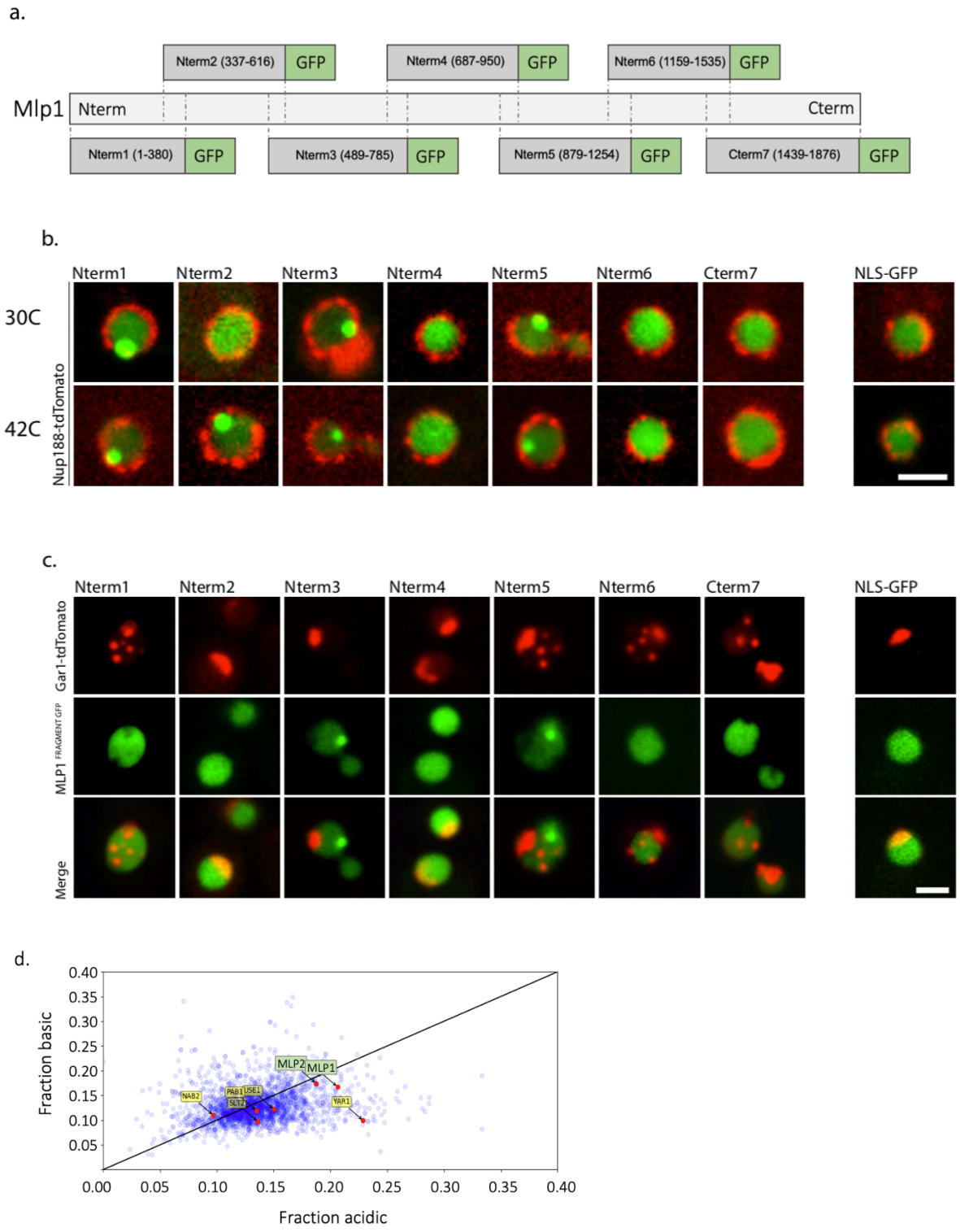


*Figure 26 The ability to aggregate and nucleolar exclusion may be intrinsic properties of Mlp1.*

*(a) Seven overlapping Mlp1 fragments have been fused to a GFP and expressed from a plasmid in Nup188-tdTomato tagged cells. (b) N-terminal fragments -1, -3, and -5 form spontaneous*

*aggregates in strains grown at 30C. The Mlp1 pore binding domain N-terminal 2-GFP forms aggregates upon heat shock at 42C. (c) N-terminal -1, -5, -6, and C-terminal Mlp1 regions are excluded from the nucleolar phase and induce the fragmentation in spherical domains (scale bars=2µm). (d) The entire yeast proteome is plotted according to their content in acidic and basic amino acids, respectively negatively and positively charged. Mlp1 and Mlp2 are slightly acidic proteins with higher charged residues content than the rest of the proteome. This representation has been generated for this project by Shelly Deforte (University of South Florida).*

## 4.2 Mlp1 granule formation may be mediated by phosphorylation upon heat shock

It is now well established that PTMs can adjust the ability of specific proteins to associate with different proteins and control their aggregation, mainly when the PTMs occurs on IDD[264]. This has been well characterized for phosphorylation and, to some extent, for other PTMs such as ubiquitination, methylation, and SUMOylation[265]. In addition, it has been shown that Mlp1 phospho-mutants display defects in the NPCs-tethering of transcribed genes[177]. I hypothesized that the Mlp1 phosphorylation profile would vary between basket-assembling Mlp1 and granule-assembling Mlp1 upon heat shock. Therefore, I analyzed the phosphorylation marks of Mlp1-PrA APs from cells grown under normal and heat shock conditions. In short, starting with peptides generated from the tryptic digestions of Mlp1-PrA APs, I enriched for phosphorylated peptides using TiO2 phosphopeptide pipette tips to carry out tandem-mass spectrometry analysis and identify phosphorylated peptides (see the following method section for details). With this experimental set-up, we enriched mainly for phosphorylated Mlp1 peptides. The maps of the enriched peptides and the phosphor-marks are shown in (Fig.27) aligned with the distribution of predicted Mlp1 IDDs. I observed 63 phosphorylation sites common to heat shock and standard conditions, with 40 of them located in the predicted IDDs.

Many phosphorylation sites were found flanking or within the N-terminal 2 fragments only upon heat shock condition. This fragment which goes from residue 337 to 616, is believed to be the Mlp1 pore-binding domain and aggregates upon heat shock. Therefore, one could hypothesize that the phosphorylation of these specific regions regulates Mlp1-aggregation. The turnover of

basket proteins is regulated by the deSUMOylating enzyme Ulp1[118,120] indicating that cells control the plasticity of the nuclear face of the pore through PTMs. Therefore, it would be interesting to test whether Mlp1 turnover is also adjusted by the phosphorylation of the residues identified in the vicinity of the Mlp1 pore binding domain.

Interestingly, numerous phosphorylation sites, common to both conditions, were also found in the Mlp1 C-terminal domain believed to form the docking site for mRNPs. It has been suggested that Mlp1 is a target for intra-S checkpoint kinase Rad53 and that Mlp1 C-terminal domain phosphorylation on the residue 1710 could result in the release of DNA gated at the NPC[176,177]. While still debated, these data could indicate that Mlp1 functioning may also be regulated by phosphorylation. Therefore, we can propose that the numerous phosphorylation sites identified here could also regulate the association of baskets with transcription sites or with RBPs. Overall, these data provide an interesting groundwork to dissect the role of phosphorylation in Mlp1 interactions, mRNP maturation, and basket formation and could indicate that phosphorylation in specific IDD influences the Mlp1 dynamic behavior.

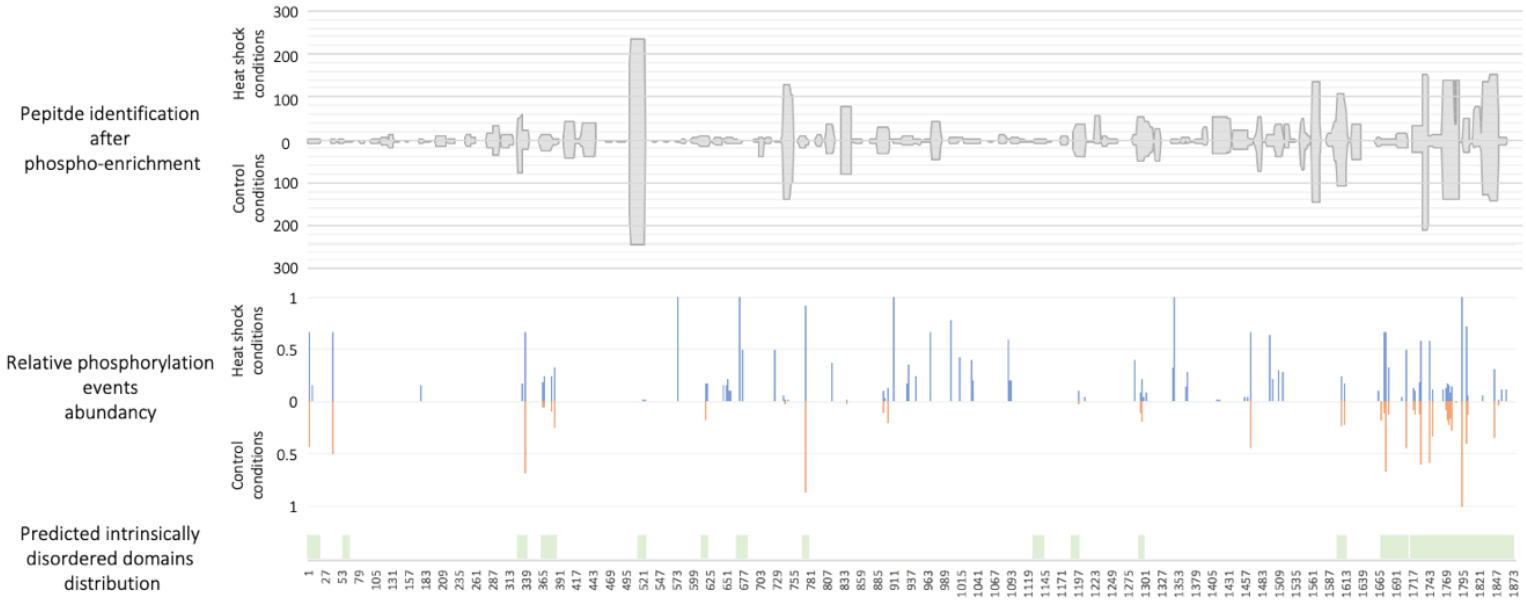


*Figure 27 Mlp1 displays numerous phosphorylation sites correlating with putative IDDs.*

*The grey map (on top) represents the number of peptides purified after phospho-enrichment identified by MS aligned onto the Mlp1 sequence from N-terminal to C-terminal regions for heat*

*shock and control conditions. The blue and orange lines for heat shock and control conditions, respectively, represent the frequency of phosphorylation for specific Serines and Tyrosines identified by tandem mass spectrometry. IDDs, mapped in green, have been determined using DisEMBle prediction software.*

## 4.3 Multiple regions of Mlp1 and Mlp2 can interact together

Finally, I tried to determine the Mlp1 vicinity interactomes using crosslinking coupled to AP-MS. Here, I hypothesized that the position of crosslinked peptides pinpointing the exact interacting domains between Mlp1, Mlp2, basket nucleoporins, and basket accessory interactome would help to unravel basket architecture. In addition, this approach was supposed to help identify the domains of Mlp1 interacting with mRNPs and RBPs.

To do so, I carried out Mlp1-PrA APs and crosslinked the complexes on beads using DSS. The Crosslinked peptides were enriched post-trypsin digest and analyzed by MS. Our data set identified predominantly Mlp1- Mlp1 and Mlp1-Mlp2 crosslinked peptides. This suggests that the conditions only allowed detecting the most abundant interactions: Mlp1 with itself and with Mlp2. I identified multiple segments of Mlp1 crosslinked together (Fig.28). While the very short-distance crosslinks separated by few amino acids are consistent with the Mlp1 coiled-coil structures, I also found long-distance crosslinks. It is difficult to determine whether these represent intra-molecular contacts generated from one protein folding on itself or inter-molecular contacts between two proteins interacting with different domains. In addition, I observed numerous contacts between Mlp1 and Mlp2, mostly localized in the Mlp1 C-terminal region. I verified that Mlp2 crosslinked peptides do not display sequences homologies or similarities with Mlp1 to confirm that they represent actual intermolecular bonds between the two proteins. This last result may be consistent with the fact that Mlp1 docks Mlp2 at the pore, as suggested by a previous attempt to dissect the structure of NPC submodules. Furthermore, the crosslink positions have a low correlation with the strongest phospho-sites. Therefore, it is hard to determine the architecture of the basket based on our data and how phosphorylation may modulate interactions within and between Mlp proteins. Furthermore, nothing in my data set indicates that Mlp1 and Mlp2 have only one defined mode to interact, and it is possible that the interaction map obtained here is an average of multiple

conformations adopted by Mlp proteins. However, our data indicate that Mlp1 is a highly multivalent protein able to interact with itself and with Mlp2.

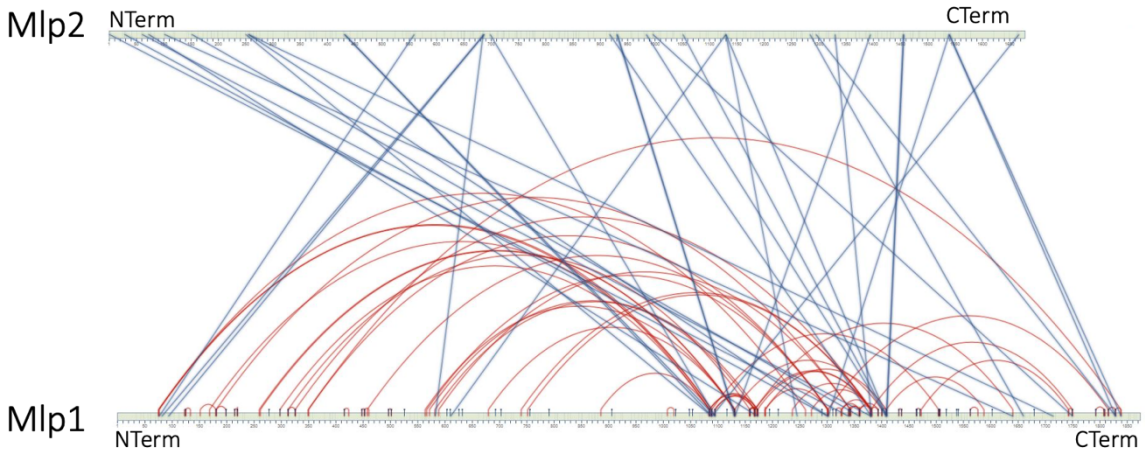


*Figure 28 Schematic visualization of crosslinked regions identified between Mlp1 and Mlp2.*

*Blue and red lines link the crosslinked peptides. Red lines represent crosslinks between peptides on Mlp1. These crosslinks can be intra-molecular crosslinks, as represented here suggesting a folding of Mlp1 bringing the N-terminal region closer to the C-terminal region but could also indicate intermolecular crosslink between two Mlp1 proteins (as represented with Mlp2). Blue lines represent inter-molecular crosslinks between Mlp1 and Mlp2. This visualization represents only two proteins as a matter of simplification. It is equally possible that this crosslink pattern is generated by multiple copies interacting with one another or represents different Mlp1/2 complexes conformations coexisting within cells.*

## 4.5 Materials and methods

**Mlp1 fragments expression.** All expression plasmids encoding yEGFP3-NLS-Mlp1 truncations have been generously provided by C. Strambio-De-Castillia [147]. Cells transformed with these expression plasmids were grown in the presence of 150 mg/l methionine for live-cell microscopy to reduce the expression level of the GFP-NLS–tagged Mlp1p fragments.

**Image acquisition.** Images were acquired on a spinning disk confocal microscope (Observer SD; Carl Zeiss) using a 100×/1.43 NA objective (Carl Zeiss), 488-nm (100 mW), and 561-nm (40 mW)

excitation laser lines, and Semrock single bandpass filters for GFP (525 nm/50 nm) and RFPs (617 nm/73 nm). Images were captured using an electron-multiplying charge-coupled device camera (Evolve 512; Photometrics) using Zen blue software. Images were captured using an electron-multiplying charge-coupled device camera (Evolve 512; Photometrics) using Zen blue software.

**Heat shock induction.** For heat shock experiments, the stage of the spinning disk confocal microscope was preheated to 42°C using a Zeiss incubation chamber controlled by TempModul S. Cells have been incubated for few minutes up to 1h in the chamber to monitor different heat shock-time points.

## PhosphoProteomic and Crosslinking MS

***Mlp1-PrA AP.*** Affinity purifications were performed without glutaraldehyde crosslink as previously described in section 2.3.5 using cryo-grindates from cells grown in normal conditions or upon heat shock during 1h before harvesting. The cellular lysate was incubated with IgG (anti-rabbit IgG, Sigma)-conjugated magnetic beads (Dynabeads M-280) for 30min in extraction buffer (see section 2.3.5 and method [54]). Isolated proteins were digested on-bead at 37°C with 1 μg trypsin (Pierce Trypsin Protease, MS Grade) for 16 h [252]) in a volume of 50μl MS grade- TRIS-HCl 100mM.

***Phosphopeptide enrichment.*** The sample volume was reduced to 5 µl by speed-vac and afterwards dissolved in 100 µl loading buffer (80% acetonitrile, 5% TFA, and 1M glycolic acid). The samples were submitted to extensive up and down using Uptitip coated titanium pipette tips (Interchim BU3630). Two washing steps were performed (washing buffer 1: 80% acetonitrile, 1% TFA; washing buffer 2: 10% acetonitrile, 0.2% TFA). For elution of the bound phosphopeptides, 50 µl elution buffer (40 µl ammonia solution [28%] in 960 µl $H_2O$) was added, and the samples were incubated on the shaker at room temperature for 10 min. The supernatant containing the phosphopeptides was transferred to a new tube, and the sample volume was reduced to 5 µl using a speed-vac. 30 µl 0.1% formic acid (FA) was added, and the samples were stored at −20°C until measured.

***Liquid Chromatography Coupled to Tandem Mass Spectrometry.*** Samples were injected to near the saturation of the signal. Liquid chromatography was performed using a PicoFrit fused silica capillary column (15 cm × 75 µm i.d; New Objective, Woburn, MA, USA), self-packed with C-18 reverse-

phase resin (Jupiter 5 um particles, 300 Å pore size; Phenomenex, Torrance, CA, USA) using a high-pressure packing cell on the Easy-nLC II system (Proxeon Biosystems, Odense, Denmark) and coupled to Orbitrap Fusion™ Tribrid™ Mass Spectrometer equipped with a Proxeon nanoelectrospray Flex ion source. 0.2% formic acid (Solvent A) and 100% acetonitrile/0.2% formic acid (Solvent B) were used for chromatography and peptides were loaded on-column at a flow rate of 600 ul/min and eluted with a three-slope gradient at a flow rate of 250 nl/min. Solvent B was first increased from 2 to 25% over 20 min, then from 25 to 45% over 40 min, and finally from 45 to 80% B over 10 min. The effluent from the column was directly electrosprayed into a LTQ Orbitrap XL mass spectrometer (Thermo), operated in data-dependent mode to automatically switch between full-scan MS and MS/MS acquisition. Survey full-scan MS spectra (from m/z 300 to 2000) were acquired in the Orbitrap with a resolution of R = 60,000 at m/z 400 (after accumulation to a "target value" of 500,000 in the linear ion trap).

*Mass spectrometry data analysis.* Protein and peptide identification thresholds in Scaffold™ was set to 95%, which resulted in a decoy false discovery rate of 4.5%. MS/MS spectra were searched with the following parameters: three missed tryptic cleavages; static modification of 57.02146 Da (carboxyamidomethylation) on cysteine; and dynamic modifications of 79.96633 Da (phosphorylation) on serine, threonine, and tyrosine, 15.99491 Da (oxidation) on methionine, 10.00827 Da on arginine, and 8.01420 Da on lysine. Exclusive spectrum counts (ESC) were used for semi-quantification of protein preys, and mass spectrometry results were analyzed as previously described in [263]. Briefly, only Exclusive Spectral Counts (ESCs) above background detected in controls were retained. In silico digestion using MS digest (http://prospector.ucsf.edu) was performed for each protein to take protein size and predicted cleavage sites into accounts

*DSS crosslink.* Affinity purifications were performed without glutaraldehyde crosslink, as previously described in section 2.3.5. Mlp1-PrA extracts were incubated in extraction buffer for 30min at 4C and wash three times with the extraction buffer. After the binding step, the beads were resuspended in 500 µl of extraction buffer with DSS at 3mM in Eppendorf tubes (Thermo Scientific 21555). The samples were agitated at room temperature for 30min before the crosslinking reaction was quenched by adding 100mM Tris HCl pH 8.0. Samples were washed three times with the extraction buffer 100mM Tris HCl pH 8.0. The samples were resuspended in 50ul 20mM Tris

HCl pH 8.0 with 5mM DTT +0.02% proteasemax and incubated at 55C for 20min. Alkylation was carried out by addition of 10mM IAA before tryptic digestion. The trypsin digestion was carried out as described previously with 1 μg of trypsin (Pierce Trypsin Protease, MS Grade) for 16 h [252]. Samples were bound on an MCX plate (Oasis MCX 96-well plates 1157F63) according to the instructions of the manufacturer. 0.5%TFA was added to the samples and were washed with 0.3M NaCl/40%methanol/0.5%TFA. The samples were washed a second time with 0.5%TFA/50%acetonitril/50%methanol. Finally, the peptides were eluted with 80% methanol and 5%NH4OAc, then lyophilized and stored at -80.

***Mass spectrometry for crosslinked peptides.*** The method detailed here follows the pipeline published in [266]**.** The lyophilized peptides were resuspended in 10 µl MSB and loaded directly onto a PicoFrit fused silica capillary column (15 cm × 75 µm i.d; New Objective) packed with C-18 reverse-phase material (Jupiter 5 µm particles, 300 Å pore size; Phenomenex) using a high-pressure packing cell. This column was installed on the Easy-nLC II system (Proxeon Biosystems) and coupled to the Q-Exactive (ThermoFisher Scientific) equipped with a Proxeon nanoelectrospray Flex ion source. The chromatographic separation of peptides was carried out in a 0.2% formic acid (buffer A) and 100% acetonitrile/0.2% formic acid (buffer B). Peptides are loaded on-column at a flow rate of 600 nl/min and eluted with a two-slope gradient at a flow rate of 250 nl/min. Solvent B was increased from 10 to 40% B over 42 min, and then from 40 to 85% B over 18 min. LC-MS/MS data were acquired using a data-dependent top 12 method combined with a dynamic exclusion window of 5 s. The mass resolution for the full MS scan was set to 70 000 (at m/z 400), and lock masses were used to improve mass accuracy. The mass range window was set to 330–2000 m/z for MS scanning with a target value at $1 \times 10^6$, the maximum ion fill time (IT) at 100 ms, the intensity threshold at $1.2 \times 10^4$ and the underfill ratio at 0.9%. The data dependent MS2 scan events were acquired at a resolution of 17 500 with the maximum ion fill time at 75 ms and the target value at $1 \times 10^5$. The normalized collision energy used was at 27, and the capillary temperature was 250ºC. Nanospray and S-lens voltages were set to 1.3–1.7 kV and 50 V, respectively.

Data analysis. For data analysis, Thermo Excalibur .raw files were converted into mgf format using MASCOT software. The .mgf files were used as input for data searches with pLink software v1.21

(http://pfind.ict.ac.cn/software/pLink/), set to use higher-energy collisional dissociation (HCD) ion types. The pLink default 20 ppm error window for MS/MS fragment ion mass for HCD dataset in the instrument.ini file was used, and missed cleavages were set to a maximum of 4. The $SM(PEG)_2$ cross-linker mass and the sequence was added to the xlink.ini file for pLink for correct mass addition to peptides linked by the cross-linker. In addition, since the NHS ester group can result in O-acylation of serine, threonine and tyrosines, three more cross-linker masses corresponding to these reactions were added into xlink.ini. The default search window of +/− 5 Da on the precursor mass tolerance for combinatorial mode was used to cover all precursors monoisotopic and isotopic peaks to better assign monoisotopic peaks to MS/MS spectra. A filter of +/− 10 ppm was used for all precursors isotopic mass accuracy. The *E*-value was set to 0.001, which corresponds to a false discovery rate (FDR) of less than 0.05% according to the determined relation between *E*-values and FDR. The pLink analysis of MS data was carried out using simultaneously all four cross-linkers set in xlink.ini for each analysis. Identified peptides were run against a whole proteome of *S. cerevisiae* W303 fasta file in pLink and against custom fasta files from the BioGRID (http://thebiogrid.org/) lists of proteins known to interact with each CH-bait. All peptide spectra were manually validated, including their ion fragmentation patterns, and peptides displaying >5 ppm difference between theoretical and observed masses were eliminated from the compiled results.

Tableau 5. – Plasmids used in this study (Chapter 4)

| | |
|---|---|
| centromeric plasmid pEXPGFPNLS_M2NT1 for Nterm1 Mlp1 fragment expression, HIS3 | Niepel et al.[112] |
| centromeric plasmid pEXPGFPNLS_M2NT2 for Nterm2 Mlp1 fragment expression, HIS3 | |
| centromeric plasmid pEXPGFPNLS_M2NT3 for Nterm3 Mlp1 fragment expression, HIS3 | |
| centromeric plasmid pEXPGFPNLS_M2NT4 for Nterm4 Mlp1 fragment expression, HIS3 | |
| centromeric plasmid pEXPGFPNLS_M2NT5 for Nterm5 Mlp1 fragment expression, HIS3 | |
| centromeric plasmid pEXPGFPNLS_M2NT6 for Nterm6 Mlp1 fragment expression, HIS3 | |
| centromeric plasmid pEXPGFPNLS_M2CT for Cterm Mlp1 fragment expression, HIS3 | |
| centromeric plasmid pUG34_GFPNLS HIS3 | |

# 5. Discussion

## 5.1 Characterizing mRNP scanning: Hypothesis for a scanning scaffold

Using the RNA tagging strategy described in Chapter 2, we have been able to dissect the behavior of 3 different transcripts *MDN1, CLB2*, and *GLT1* mRNA in living cells. Overall nuclear mRNAs were rare, consistent with the fact that once transcripts are released from transcription sites, they are rapidly exported and spend most of their time in the cytoplasm. We have been able to dissect the scanning phenomenon defined as a continuous movement at the periphery. To characterize the scanning, we measured the time scale of scanning characterized by the period for which mRNAs parkour the nuclear periphery and the jumping distance represented by the distance separating the position of mRNA between two frames. We also measured a third parameter: the residency time of static transcripts at the periphery. These parameters highlighted similar export kinetics, with an identical distribution of scanning time and jump distances for the three mRNAs analyzed in this study. In addition, we observed that deletion of basket components Mlp1/2 and Nup60, as well as Mlp1 C-terminal truncation and Nab2 mutation, reduced the mRNA scanning times, jumping distances, and residency times, with a more frequent release of mRNPs into the nucleoplasm. Taken together, those results indicate that basket and Nab2 mediated interactions enhancing mRNP residency time at the periphery. It is possible that specific RBPs, similarly to Nab2, need to be incorporated into mRNPs to assemble particles with a full ability to scan. Therefore, mRNP aptitude to remain at the nuclear periphery and find a basket would require a certain degree of maturation. Consequently, scanning would reflect a facet of export QC where correctly compacted and assembled mRNPs have a higher probability to get exported. It is hard to estimate how saturated NPCs are and whether mRNPs, ribosomes, and other cargos can compete for access to a pore. However, we could propose that scanning represents the path of mRNPs probing the periphery to find pores available for export. If this is true, we can predict that the delays to find available pores defined by scanning times would be reduced in conditions where nucleocytoplasmic transport is less active. It could also be interesting to examine possible differences in RNA export kinetic based on different transcripts features believed to influence the

interaction with the basket, such as the presence of an intron or transcripts length. Once mRNPs detach from a basket, what could direct their motion to scan toward the next one and prevent them from diffusing away in the nucleoplasm? CryoEM images measured that NPCs are evenly spread on NEs and separated by ~240nm[106]. On the other hand, the basket protrudes toward the center of the nucleus and is approximatively 80nm high [147]. Likely, Mlp1/2 do not extend far enough to cover the distance between pores, raising the simple question of what could guide mRNPs scanning?

### 5.1.1 A lamin-like scanning scaffold?

Although mRNA export *per se* was moderately affected, we proposed that basket depletion induces a delay in export kinetic. Surprisingly, scanning was not completely abolished in Mlp1/2 deleted cells. This could suggest that another NE scaffold is used for mRNP scanning. Therefore, one candidate for this function could be the lamin-like protein Esc1. Interestingly, Esc1 occupies only the periphery excluded from the nucleolus. Esc1 could consequently form the scanning trail at the periphery of the nucleoplasm, establishing a zone where mRNPs are preferentially maintained to meet with complexes and factors required for the export or QC, such as baskets and basket accessory factors. While a role for Esc1 in facilitating the export of the bulk mRNA has not been investigated, it has been shown that Esc1 was required for the retention of unspliced pre-mRNAs in the nucleus. However, depletion of Esc1 causes a significant defect in basket assembly, as Mlp1/2, Nup60, and Ulp1 aggregate in two or three large nuclear foci. Therefore, its role in export could be limited in the maintenance of basket integrity, and the consequences of Esc1 depletion on mRNA scanning and subsequent export would be hard to dissociate from its structural role.

Nevertheless, baskets could have a dual role by providing a docking site for mRNPs reaching the pore and connecting the Esc1-network and NPCs. Hence, reduced scanning times and jumping distances upon MLP1 deletion could be caused by a faulty link between Esc1 and the pore. Surprisingly, mRNA export and growth phenotypes caused by Mlp depletion are more pronounced in a diploid cell. Therefore, we could suggest that the role(s) of Mlp1/2 in nuclear architecture and NE organization is more critical in larger nuclei where the probability for mRNPs to find a pore by simple diffusion is slightly lower and/or where a robust NE support is essential.

### 5.1.2 The nuclear periphery as a compartment facilitating mRNP diffusion

Alternatively, we can propose that there is no scanning scaffold *per se,* and the vicinity of the nuclear periphery represents a region of the nucleus where transcripts are retained by a cooperative meshwork of weak interactions with NPCs and yet to be identified proteins concentrated at the nuclear periphery. This picture of a nuclear periphery as a micro-environment by and of itself will be developed in section 5.4, where different models for basket formation are proposed. This proposition could be supported by observations from single-particle tracking experiments and Nab2 localization analysis.

We observed that mRNPs could traverse the nucleolar phase. *MDN1* mRNA was seen more frequently in the nucleolus than *CLB2* or *GAL1* transcripts, possibly because of the gene's close localization to the ribosomal DNA repeats. Hence, we observed that mRNA export could also occur through nucleolar pores (Fig.29a). However, we did not test whether those nucleolar export events were preceded by scanning events. Moreover, we do not know whether nucleolar export events happened more frequently through pores harboring nucleolar ectopic baskets (Fig.13c). This question would be difficult to address directly considering the rarity of nucleolar export events and ectopic baskets as well as the short time frame in which ectopic baskets can be observed due to pore motion and photobleaching. Yet, we can hypothesize that the mRNP capture by a pore with an ectopic basket should be more efficient when compared to basket-less neighboring pores. We have made an interesting observation possibly supporting this view in Nab2-tdTomato Mlp1-GFP cells (images have not been published and are shown Fig.29b). In these cells, the position of the nucleolus can be interfered by the section of the nuclear periphery lacking baskets, which correlates with a crescent-shaped dark area lacking Nab2-tdTomato. Consequently, we could pinpoint ectopic baskets, which appear as isolated and discrete Mlp1-GFP signal, in a Nab2-depleted area. We observed that the presence of an inferred ectopic basket correlates with an accumulation of Nab2-tdTomato Fig.29b. Although the causal link leading to the colocalization of Mlp1 and Nab2 in a confined space of the nucleolus is unclear, it may indicate that Mlp1-GFP and RBPs can concentrate within a specific domain of the periphery and could argue for an efficient capture of mRNPs by an ectopic basket-containing pore.

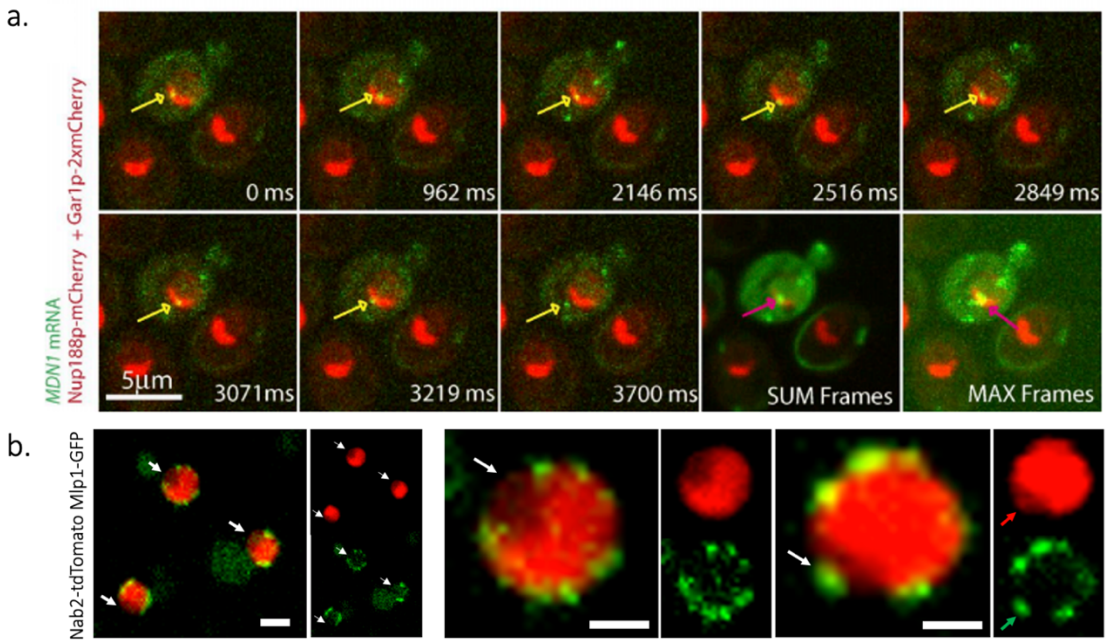


*Figure 29 At the nucleolar periphery, the presence of an ectopic basket may confer similar properties to those of the rest of the nuclear periphery.*

*(a) MDN1 mRNAs can get trapped in the nucleolus and exit through pores at the nucleolus. Individual frames from video acquired in 37-ms intervals. Nucleolus and nuclear pores are marked in red by labelling Gar1 and Nup188 with mCherry. SUM and MAX show summary and maximum intensity projection of all frames. Yellow and purple arrows indicate tracked mRNAs in individual and in SUM and MAX projected images, respectively. (b) The position of nucleoli (white arrows) is designated by areas from which Mlp1-GFP and Nab2-tdTomato are absent or underrepresented. The presence of an ectopic basket (green arrow) correlates with a local increase of Nab2 concentration (red arrow), scale bars=2µm.*

Taken together, we can propose that contiguous basket-containing pores in association with basket accessory factors, Esc1, and RBPs could create an area along the periphery allowing the cooperative recruitment and maintenance of mRNPs at the periphery beyond the simple basket limits. The structure of P granules has inspired this scenario in *C. elegans*, where pore components provide a molecular lattice to assemble a membrane-less compartment on the cytoplasmic side of the nuclear membrane to regulate nucleocytoplasmic transport (Fig.30a,b)[267]. In yeast, such an area could then represent NE sub-domains where mRNPs would diffuse into, preferentially or scan

before interacting stably with a pore to be exported without the requirement of a scanning scaffold *per se.*

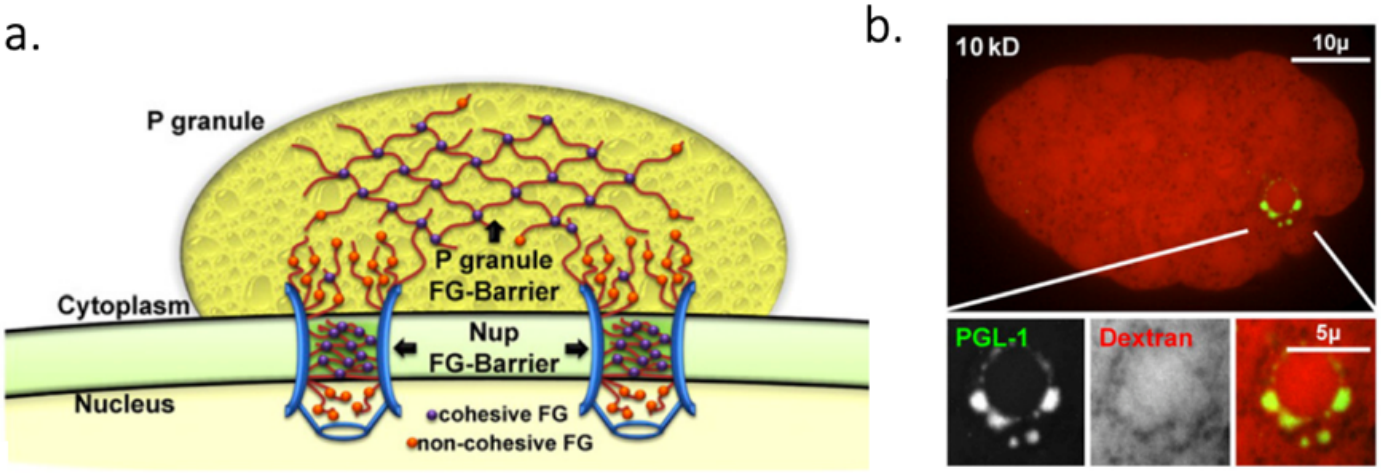


*Figure 30 Model illustrating how P granules could extend the NPC environment through FG interactions.*

*(a) Many nuclear pore proteins have cohesive FG dipeptide repeats (blues) that function to establish a permeability barrier of the NPC. FG repeats are also found in several P granule proteins, extending the exclusion barrier. (b) Small 10-kDa fluorescent dextran molecules (red) can diffuse freely across the NE and into P granules (visualized with GFP:: PGL-1; green) adapted from Updike et al. (2011)*[268]

## 5.2 Prerequisite for basket formation: The NPC's nucleoplasmic platform and intranuclear mRNPs metabolism

We interrogated the role of the basket in mRNP export by asking (i) what are the requirements for the formation of the basket and (ii) does the bulk of mRNPs favor basket formation, or are there specific mRNPs triggering the formation of a basket? Our auxin depletion screen guided us to better characterize how the nuclear platform of the NPC is organized and what steps of mRNA metabolism processes were essential for basket formation. On the other hand, the role of mRNPs in basket formation was instead addressed by the dissection of basket-less and basket-containing interactomes using Proteomic and RNomic approaches.

### 5.2.1 The nuclear face of the pore is a platform of co-stabilizing proteins

Consistent with published data, the auxin depletion screen confirmed that the basket nucleoporin Nup60 is essential for Mlp1 localization at the pore[114,115,244]. Mlp1 covers the entire nucleoplasm, and a fraction of the protein aggregates in one single large granule in these cells. Other studies reported that the other basket Nups, Nup1, and Nup2, were also important for Mlp1 association with the pore[112,244]. We observed that Esc1 depletion results in the aggregation of basket proteins in few foci without any major increase of the intranuclear concentration of Mlp1. Interestingly, we measured in the pore affinity purifications interactome dissection in section 2.3.3 of this work that basket nucleoporins were detected in basket-containing and basket-less NPCs MS-AP. This is consistent with microscopy data showing that Nup1, Nup2 and Nup60, are present on all pores without exclusion from the nucleolar periphery[129]. However, we measured that these Nups were absent from the pores APs in the *Δmlp1/2* background (Fig.31). We did not confirm the loss of Nup1, Nup2, and Nup60 at the periphery in *Δmlp1/2* background by fluorescent microscopy. However, these data could suggest that Mlp proteins also stabilize the basket Nups at the periphery directly or by tethering components required for Nup-dynamics regulation at the pore. Ulp1 protein associates with Mlp1 and is essential to control the PTMs adjusting the turn-over of basket Nup at the periphery[111,120,249]. Therefore, it is possible that Mlp1 indirectly stabilizes Nup1, Nup2, Nup60 by maintaining Ulp1 at the periphery. This proposition seems counterintuitive as basket-less pores also contain Nup60, Nup1, and Nup2. Therefore, we can propose that in wild-type cells, pores switch between states with or without Mlp1, depending on their position along the periphery or the process they are engaged in. In this scenario, transient contacts with Mlps and cofactors such as Ulp1 are sufficient to stabilize basket Nups at the periphery while Mlp1/2 permanent absence is detrimental for their association with the pore. Alternatively, we can propose that Mlp proteins and possibly Ulp1 are required to form a stable pore nuclear platform when new pores are assembled and could, once pore biogenesis is completed, detach without affecting the stability of basket-Nups. A complex interdependency of basket proteins at the NPC has also been observed in higher eukaryotes where a TPR knockdown using siRNAs affects the localization of the basket-Nups NUP50 and NUP153[131]. This has been interpreted as defects of incorporation of basket proteins in the absence of TPR during NPC synthesis. On the other hand, fast depletion of TPR using

auxin degron system did not affect NUP50 and NUP153 positioning at the pore[132]. This would suggest a role for the basket scaffold and possibly for the conserved Ulp1 homolog SENP1 in nuclear pore platform stability in humans as well. Overall, those data suggest a cooperative stabilization of the basket-Nups and basket scaffold at the periphery to assemble the nuclear face of the NPC.

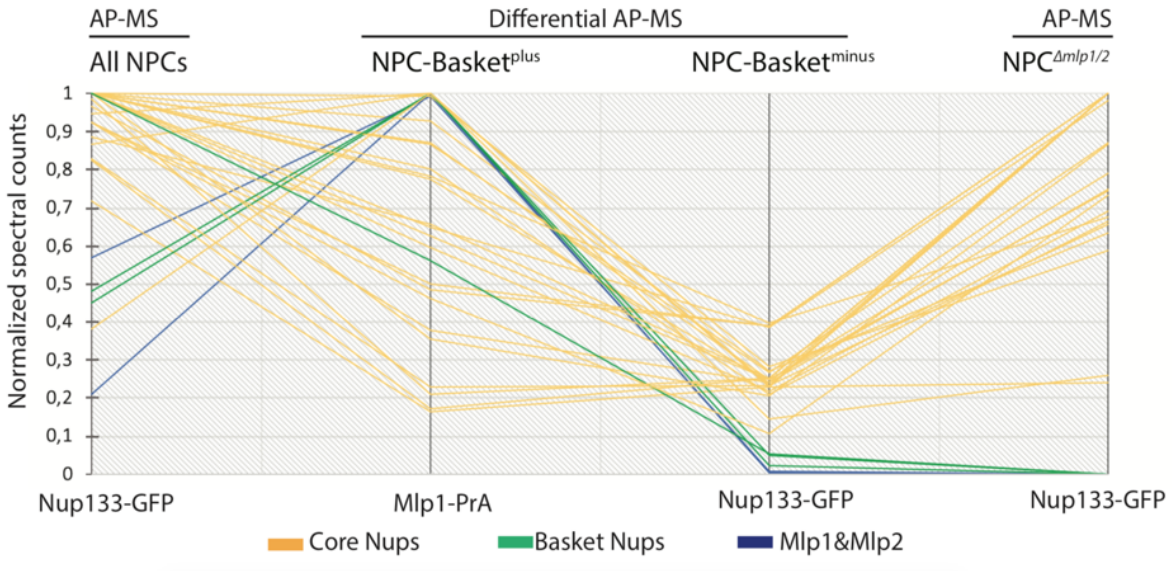


*Figure 31 Basket nucleoporins are present in NPC-Basket$^{minus}$ AP but not detected in NPC$^{\Delta mlp1/2}$*

*Normalized spectral counts values of individual proteins in each NPC purification are represented scaled from 0 to 1. Each line represents the relative abundance for one protein through the series of APs: 'All NPC', 'Basket$^{minus}$NPCs', 'Basket$^{minus}$ NPCs', 'NPC$^{\Delta mlp1/2}$'.*

## 5.2.2 Different key processes of mRNP metabolism trigger basket formation

### 5.2.2.1 mRNP themselves are required for basket formation

We have shown that Pol II transcriptional activity is crucial for basket assembly (Fig.14). In yeast, many genes are transcribed at the nuclear periphery and found to associate with NPCs by ChIP, including Mlp1[96]. Therefore, it could be possible that basket assembly might be connected to gene tethering at NPCs, establishing a direct link between transcription of specific genes and export through specific basket-containing NPCs. This raised the question of whether the mRNPs

themselves or the active transcription sites tethered at the pore that drive basket assembly. By inducing the accumulation of newly poly(A) transcripts and re-routing mRNPs to the nucleolus, we observed the formation of baskets at the nucleolar periphery. Because NPCs are mobile, we ensured that the nucleolar relocation was specific to Mlp1/2 proteins and not associated with a complete nucleolar NPC-clustering phenotype. This strongly suggested that the accumulation of poly(A) transcripts was sufficient to induce basket formation. We interpreted this phenotype as an indication that poly(A) transcripts and associated RBPs, but not the interaction of NPCs with genomic loci and/or active sites for transcription is required to initiate baskets formation.

It is, however, possible that the non-physiological accumulation of transcripts in the nucleolus caused by depletions of Enp1, Csl4, and to some extent Rna14 and Rna15 do not exactly represent the normal levels of mRNPs present at the nucleoplasmic periphery in wild type cells. Indeed, it is likely that the excess of nucleolar poly(A) transcripts titrates Mlp proteins away from the nucleoplasm. Therefore, these experiments do not entirely rule out the eventuality that interactions with genomic loci and/or nascent mRNPs could also participate in basket formation. Such a possibility would imply that transcription sites at the periphery should localize preferentially with domains where baskets are observed. One way to test such a model would be to analyze the localization of genes previously shown to associate with the nuclear periphery (e.g., *INO1, GAL1, GAL10*) genes with respect to the nuclear periphery occupied by basket-containing NPCs. The positioning of those loci upon transcription activation could be monitored using Lac operator (LacO) arrays integrated into the flanking regions of the genes able to recruit GFP-Lac (usually expressed from a plasmid) ), a process that has been extensively studied previously, but not in the context of a putative colocalization with basket-containing or basket-less NPCs[269].

Both Pol II shutdown and nucleolar accumulation of transcripts showed that the production of poly(A) transcripts trigger basket formation. This also suggests that baskets are unstable, and Mlp1 gradually detaches from the NPCs in the absence of mRNPs. We did not carry out any time-course to estimate precisely the half-life of baskets in the absence of transcripts in the nucleus (Pol II shutdown) or in the nucleoplasm (transcript relocation in the nucleolus). However, rapid Pol II shutdown using the *rpb1-1* thermosensitive mutant showed that baskets are destabilized within a

few minutes -if not less- after a shift to restrictive temperatures, suggesting that they are labile structures.

#### 5.2.2.2 Defect(s) in mRNP export do(es) not correlate with basket destabilization

Overall, our experiments showed that proteins involved in export, such as Mex67, or its adaptor Yra1, were not essential for basket formation. Those proteins are believed to mediate the interaction between mRNPs and the FG-Nup meshwork in the central channel of the pore. While these factors possibly help mRNPs associate with the basket, their function seems pivotal, mainly in the central channel. Therefore, their depletion may not drastically affect the ability of mRNPs to dock at the periphery and to stimulate basket formation. As illustrated in this work, the current view of the mRNP export and processing pathway is one of a cooperative process between multiple RBPs and the pore. Therefore, it is likely that some partial redundancy or complementation between factors depleted in our screen exists and prevent basket destabilization. This could be tested by simultaneously inducing depletion of export receptors, SR proteins, TREX and TREX-2 complex components.

Export defects cause a strong nuclear accumulation of transcripts observed by poly(A) FISH[86,270,271]. Because we postulate that mRNPs themselves can trigger basket formation, we can suggest the following: a nuclear excess of mRNPs can increase the number of baskets assembled at the periphery and potentially the number of ectopic baskets. Accordingly, the number of nucleoplasmic basket-less NPCs should decrease.

#### 5.2.2.3 A potential link between basket formation and 3' UTR processing

The single largest group of factors identified in our screen that affect basket assembly are proteins implicated in 3' end processing, polyadenylation and binding to the poly(A) tail. We identified the component of the cleavage and polyadenylation factor Rna14 and Rna15, the poly(A) polymerase Pap1 as well as the poly(A) binding protein Pab1 as factors required for basket stability. Previous studies have shown depletion of Pap1, Rna14 and Rna15, in addition to their role in processing, also result in significantly reduced levels of total poly(A) transcripts[247, 82 83 272]. Because we observe that mRNP production is crucial for basket assembly, our results could suggest that

Rna14, Rna15, and Pap1 depletion upset the balance between polyadenylation/RNA release from the transcription site and mRNA degradation by causing defects in the 3'end termination and polyadenylation affecting basket formation in a similar manner to Pol II shutdown. However, the phenotypes induced by Rna14 and Rna15 depletion were different from that of Pap1. Baskets tend to relocate at the nucleolar border upon Rna14 and Rna15 depletion, similar to what was observed when mRNPs accumulate into the nucleolus (Fig.15a; Supplementary Fig.22). Interestingly, it has been reported that Rna14 and Rna15 depletion induce the accumulation of the nucleolar box C/D and box H/ACA snoRNP components Nop1 and Gar1, respectively, in fragmented pseudo-nucleolar bodies (Fig.32)[247]. The depletion of those factors, combined with depletion of the RNA exosome catalytic subunit Rrp6, leads to the formation of identical pseudo-nucleolar foci containing poly(A)transcripts. Therefore, we interpreted the relocation of baskets at the periphery of fragmented nucleoli (or pseudo nucleolar domains) as driven by a possible accumulation of poly(A) transcripts into those domains. Although we did not carry out Rna14, Rna15 depletion in combination with Rrp6 knockdown, we observed basket repositioning and nucleolar fragmentation 2h after Rna14, Rna15 depletion. This depletion period was twice as long as the depletion reported previously and is potentially sufficient to induce an accumulation of poly(A) transcripts into the pseudo-nucleolar domains. Accordingly, we could expect an accumulation of Poly(A) FISH signal colocalizing with the pseudo-nucleolar domains adjacent to baskets in Rna14 and Rna15 depleted cells. In addition, we can propose that the concomitant deletion of Rrp6 would enhance a basket relocation phenotype.

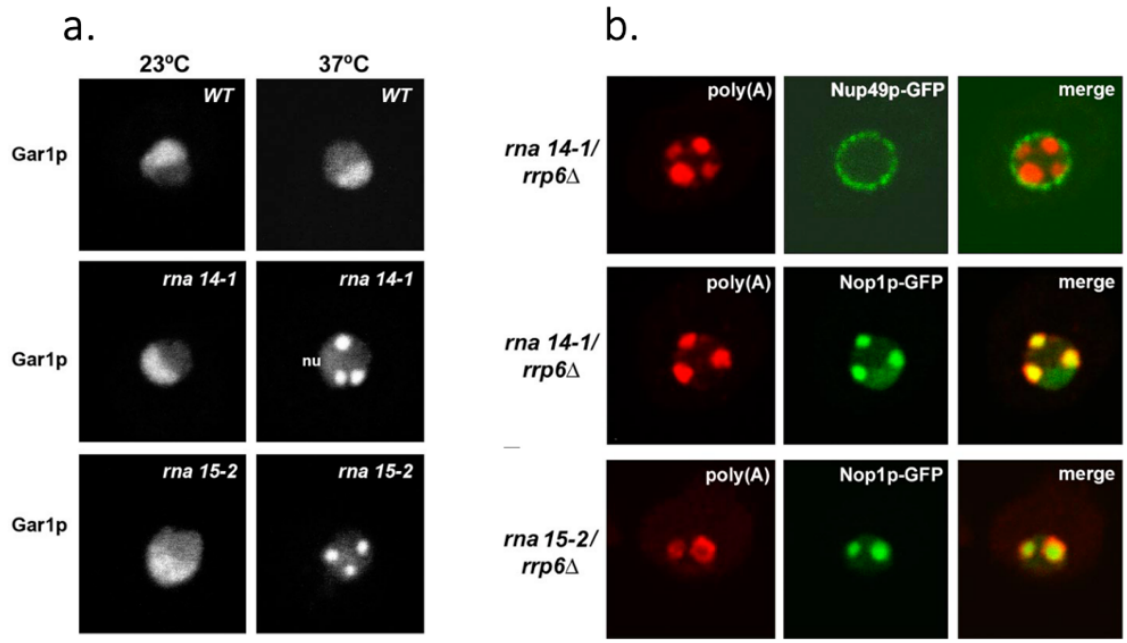


*Figure 32 Subnuclear distribution of Gar1 and polyadenylated RNAs upon Rna15 and Rna15 depletion*

*(a) H/ACA snoRNP proteins Gar1 redistributes from the nucleolus to nucleoplasmic foci in rna14-1 and rna15-2 mutants. The strains indicated were shifted to 37°C for 1h. Wild-type and mutant cells are expressing a Gar1-GFP fusion protein. (b) Poly(A) RNA was detected by FISH using a Cy3-labeled oligo(dT)50 probe. Cells expressing the nucleolar protein Nop1-GFP or the nucleoporin Nup49-GFP. Rna14-1/rrp6Δ and rna15-2/rrp6Δ were shifted to 37°C for 1h. These images have published in*[247].

The phenotype observed upon Pab1 depletion was quite surprising. At this point, it is unclear whether the basket destabilization phenotype seen under these conditions is caused by cytoplasmic stress on poly(A) transcripts triggering a feedback loop to decrease the transcription, or instead by the loss of Pab1 function in the nucleus. However, this could be tested by interfering with Pab1 presence in the nucleus, either using an anchor away strategy or an import deficient Pab1 variant[256].

While Nab2 is believed to be the main nuclear poly(A) binding protein, Nab2 and Pab1 are thought to participate in mRNA 3'processing and possibly poly(A) elongation, as discussed in Chapter 3. It has been shown that Pab1 can be imported into the nucleus and partially alleviate

nuclear homeostasis defects[242,273]. Notably, it has been reported that the essential functions of Nab2 can be met when Pab1 is overexpressed[242]. Therefore, we could suggest that Pab1 compensates for Nab2 depletion, preventing the destabilization of baskets. However, if the function of the two proteins can partially overlap, a possible Pab1-specific nuclear role required for basket formation remains to be determined.

Overall, the stability of the basket is affected upon depletion of the 3'end processing machinery. However, a direct link between basket formation and 3'end processing has not been established. In other words, defects in basket formation and the position may instead be caused by the loss of nuclear mRNP stability upon Pap1and Pab1 depletion and by the relocation of poly(A) transcripts upon Rna14 and Rna15 depletion.

#### 5.2.2.4 Basket formation and intron-containing mRNP processing/export

Because a role for the basket in the control of intron-containing mRNP export has been suggested multiple times in the literature[68,109,128,129], we tested whether basket formation was dependent on splicing events. Our depletion screen indicates that splicing *per se* not an absolute requirement for basket formation as only Prp5 depletion, but not depletion of the other essential splicing factors correlated with Mlp1 relocation into the nucleoplasm. However, Prp5 induced a partial relocation of Mlp1 into the nucleoplasm, possibly due to a defect in the transcription of intron-containing mRNAs[246]. Although intron-containing genes represent only ~4% of the yeast genome, it is estimated that they generate ~40% of the transcriptome as those genes encode for highly expressed proteins, mostly ribosomal proteins[274]. Affecting their transcription would accordingly represent a significant reduction of the total level of nuclear transcripts. In this scenario, Prp5 depletion could disturb basket formation by affecting the expression of a substantial fraction of mRNAs. Therefore, it would be interesting to analyze the magnitude of the transcriptional defect and the decrease nuclear transcripts level by poly(A) northern analysis upon Prp5 depletion compared to other splicing factors.

Although splicing is not an absolute requirement for basket formation, the nuclear surveillance factor Pml39 is also essential for correct Mlp1 association with the pore. It remains plausible that intron-containing mRNPs are more efficiently recruited by Mlp1/Pml39 and are therefore more

likely to participate in basket formation than other mRNP. In the absence of Pml39, this process would be impaired at the basket inducing Mlp1 re-localization into the nucleoplasm and would be consistent with data showing that intron-containing mRNPs, Pml39, and Mlp1 can recruit each other efficiently (Fig6). Those results might further suggest that intron-containing mRNPs, Pml39, and Mlp1 cooperatively associate in foci to enhance intron-containing mRNP capture. However, because Pml39 is found associated exclusively with basket-containing pores, it may also just play a simple structural role, stabilizing Mlp1 at the pore in normal conditions.

It is hard to predict how spliced-mRNPs generated from intron-containing genes differ from other mRNPs once they reach the periphery and why specific mRNPs could facilitate basket formation. No proteins associating exclusively with spliced-mRNPs reaching the pore have been identified yet, and none of the proteins involved in assembling pre-mRNA retention and splicing complex[275,248] were identified in our analysis of NPCs interactomes.

Therefore, to analyze whether the presence of specific mRNPs at the pore correlates with the formation of baskets, we carried out differential APs of NPCs followed by MS and RNA seq.

## 5.3 Do baskets represent a specialization of NPC for export/QC of specific mRNP?

### 5.3.1 From proteomic to RNA-seq: both types of pores can interact with mRNPs

Our proteomic analysis confirmed that we were able to efficiently separate NPC interactomes. Indeed, most of the expected basket-interactome was enriched in basket-containing pore APs in particular telomere-associated proteins, SPB, and proteasome components. On the other hand, nucleolar proteins were enriched in basket-less pore APs.

Surprisingly, Esc1 and Ulp1 were detected only at very low levels in basket-containing pore interactomes. This possibly suggests that specific pore/ nuclear membrane isolation methods would be required for an optimal purification of these proteins, as illustrated by the different conservation states of the nuclear lattice observed in amphibian oocytes (Fig.7a, b). Except for Pml39 and TREX-2 components, mRNP export and processing factors were enriched with basket-containing pores but also detected with basket-less pores. The presence of RBPs and mRNA export

factors in each pore preparation indicated that mRNPs can associate with the pore in an Mlp-independent manner and that baskets are not essential for export. We also identified a pore accessory interactome recruited onto the same pores as Mlp1/2, but none of the splicing factors and components of the complex believed to bridge splicing and export were identified in pore APs. This indicates that mRNPs reaching the periphery are already spliced, very likely co-transcriptionally, and the hypothesis that baskets assemble a platform where splicing events happen prior to mRNP export appears very unlikely. Instead, those results suggest that the functional difference between basket-containing and basket-less pores may not lie in a specialization of the pore for export of specific mRNPs but could simply be a difference in quantities of mRNP contacting each type of pores. Therefore, those results guided us in the design of the NPC-AP RNA-seq experiments, and we set up an approach where differences in quantities of transcripts could be interpreted between 'all NPCs', basket-containing and basket-less pores ('Basket $^{plus}$' and 'Basket $^{minus}$' respectively) pore APs.

### 5.3.2 Basket-less and basket-containing pores are not dedicated to the export of distinct pools of transcripts

NPC-AP RNA-seq approach and analysis strategies, as well as the results, are developed in the results section of the article. In short, we showed that mRNPs associate with both types of pores; however, a stronger enrichment was found with the 'Basket $^{plus}$' APs. This observation remains consistent with the proteomic data suggesting that RBPs can associate with both types of pores but are preferentially found with basket-containing ones. "Basket$^{minus}$" and "Basket$^{plus}$" transcriptomes did not display any apparent differences in the nature of the associated transcripts, and we did not identify distinct pools of transcripts specific to one type of pores. Indeed, different gene ontology (GO) enrichment analyses carried out using PANTHER and ShinyGO did not reveal any significant bias in the functional classification of the different interactomes except for transcripts coding for ribosomal proteins enriched with "Basket$^{minus}$" AP. This bias may not be directly linked to the function of those genes but instead to some characteristic of the transcripts: their length. Indeed, transcripts encoding for ribosomal proteins tend to be expressed from short, intron-containing genes, which appears to be a relevant parameter to fine-tune export-dynamic.

As suggested in Chapter 3, the function of the proteins encoded by transcripts co-purified with our APs may not be a relevant parameter influencing intranuclear mRNPs fate/processing. However, mRNA features such as secondary structures, specific RBP binding motifs, or 3'UTRs are poorly characterized in yeast, which limited our analysis.

### 5.3.3 Different types of pores may correlate different mRNP export kinetic

The read-out of our NPC-AP RNA-seq only indicates the frequencies with which transcripts are found associated with the different pores and does not allow us to draw any conclusions on the export event itself: we do not know whether the particles actually crossed the pore and reached the cytoplasm. Indeed, as illustrated by the scanning phenomenon, contacts between mRNPs and pores do not always result in successful export events. Therefore, we interpreted the relative fold changes between APs as follows: an enrichment can represent a more frequent interaction between pores and mRNPs, a robust interaction, or/and a longer residency time at the pore. Conversely, underrepresentation in the AP could represent unstable and labile or less frequent interactions (Fig.33a, b).

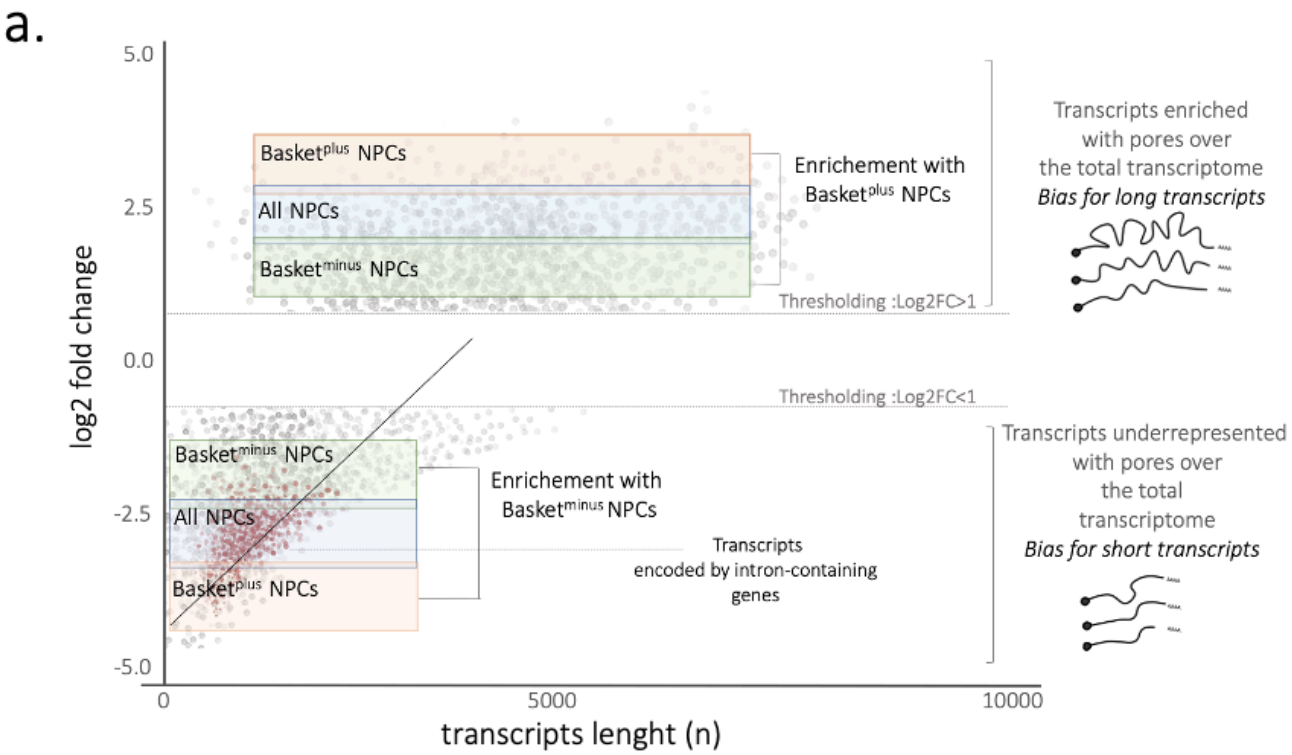

b.

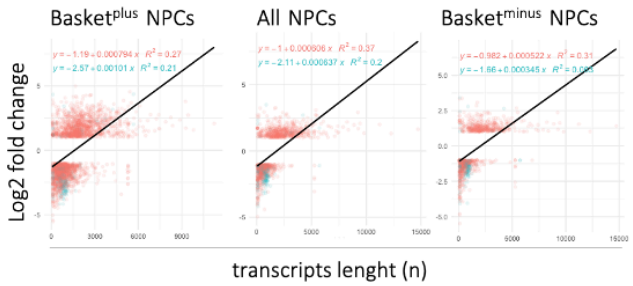


c.

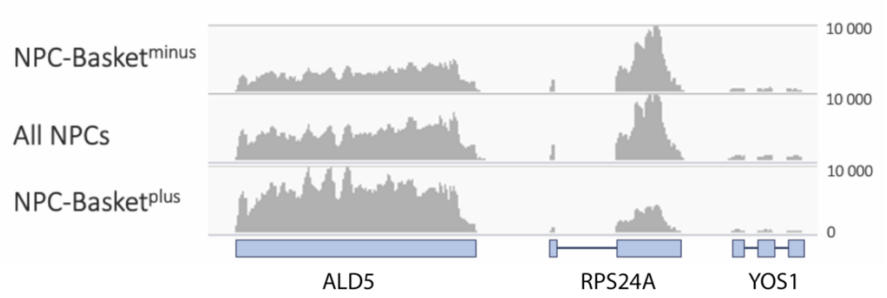


*Figure 33 Short and long transcripts may have different export kinetics on basket-containing and basket-less pores.*

*(a) Schematic representation of the transcripts enrichment in 'Basket$^{plus}$ NPCs', 'All NPCs', and 'Basket$^{minus}$ NPCs' APs overlaid. The thresholding log2fc < 1, >1 allows highlighting transcripts highly enriched or underrepresented in the three APs over the yeast transcriptome. (b) Representation of the actual transcripts enrichment for the three APs separately. (c) Read-seq mapping of a selected genomic region hosting two intron-containing genes RPS24A (390pb) and YOS1 (250pb) with one intron-less gene ALD5 (1560pb). Exons are represented by blue rectangles and intronic regions with a blue line.*

First, we observed a bias in the transcript populations co-purified with all APs when comparing their abundance in the total transcriptome. Longer mRNAs were over-represented in the pore APs compared to the total transcriptome. Furthermore, their enrichment was higher in basket-containing pores. This may indicate that longer transcripts develop a more stable interaction with

pores, possibly facilitated by a higher RBP content, mediating more contacts with the pore, mainly when the latter harbors a basket. Therefore, we can formulate two non-mutually exclusive hypotheses: large mRNPs have higher RBP content and (i) display higher association frequencies with basket-containing pores due to Mlp-RBP interactions and /or (ii) interact more stably with basket-containing pores leading to a possible delay in export. This export delay could be correlated with structural rearrangements of the mRNP to fit the NPC central channel or more elaborated modifications in mRNP compositions required for the export.

On the other hand, shorter transcripts (<1000nt) were underrepresented in pore APs. This could argue for a rapid and/or unstable interaction of smaller mRNPs and NPCs. Furthermore, we observed that short transcripts tend to be less abundant in "Basket$^{plus"}$ compared to "Basket$^{minus"}$ pores AP. This possibly suggests that basket-containing pores are occupied by larger mRNPs and could be less available to export smaller mRNPs, leading to an enrichment of smaller mRNPs with basket-less pores. Alternatively, this may indicate differences in export kinetics for smaller mRNPs depending on the type of pore they associate with. Indeed, we might suggest that access of short transcripts to NPC central channel is slower on basket-less pores. Such a delay could be explained by a relatively low RBP content associated with short mRNAs, which mediates only a minimal number of interactions with the NPC. Therefore, these mRNPs may appear globally underrepresented in NPC APs because their interaction with pores is more labile. However, the basket could function as a structure accelerating the export of short transcripts and thus, these transcripts are underrepresented in "Basket$^{plus"}$ AP. This would be consistent with the conclusion drawn in humans, where the basket has been envisioned as a structure facilitating the export of specific RNAs. Indeed, TPR depletion resulted in the nuclear accumulation of mRNAs primarily expressed from short genes, whereas the export of longer mRNAs appeared to be less dependent on TPR [132,133].

Interestingly, mRNP generated from intron-containing genes are short transcripts (essentially ~500 nt or less), and their enrichment in the APs scaled with their lengths: transcript abundance in APs increased with the length of the coding sequence (Fig.19d). This suggests that the size of the transcript may facilitate its interaction with a pore. However, our results indicate that transcripts generated from intron-containing genes are mainly enriched with basket-less pores compared to

basket-containing pore APs. This observation was surprising as a suggested role for Mlp proteins is believed to establish a gatekeeping structure for unspliced mRNAs. However, our data set show that most of the transcripts associated with the pore do not display intronic reads, suggesting that once they are spliced, these mRNPs may behave like any short mRNAs (Fig.33c). Therefore, in normal conditions, when most splicing events are carried out successfully, the gatekeeping functions of Mlp1 may not be central in the export of mRNP generated from intron-containing genes. Conversely, we could hypothesize that those transcripts, and intronic reads, should be enriched with basket-containing APs when the splicing machinery is impaired. Furthermore, we can propose that the overexpressed splicing reporter used to demonstrate the leakage of unspliced transcripts to the cytoplasm in *MLP1* deleted cells would also be enriched in basket-containing pore APs. However, the reporter used in these studies is long (~3kb) and may not represent how typical intron-containing mRNPs behave.

Taken together, these results could partially address the conundrum of how a basket-mediated gatekeeping mechanism can monitor the export of unspliced mRNA efficiently if it is unevenly dispersed at the periphery. Most of the time, splicing may be correctly completed, and Mlp gatekeeping functions are not required. On the other hand, a basket may facilitate the export of short and spliced transcripts. However, the ability of the basket to associates with most mRNPs and trap intron-containing transcripts suggests that it can delay or block their export to prevent leakage of pre-mRNPs into the cytoplasm when the splicing machinery is deficient.

## 5.4 Possible models for Mlp1 dynamics and basket distribution in yeast nuclei

In yeast, many aspects of the dynamic of Mlp proteins challenge the consensus model of the basket. Indeed, the picture of the basket as a static scaffold as presented in Fig2 may not exactly fit with Mlp turnover measured at the periphery. In addition, baskets do not assemble in the absence of Pol II transcription and can relocate to follow the localization of poly(A) transcripts. Consequently, mRNPs need to be included in any models on basket formation in yeast. Furthermore, it would be pertinent to address the distribution of baskets– excluded from the nucleoli and absent from a subset of pores in the nucleoplasm– based on the roles of those two

nuclear compartments. Therefore, the following sections will discuss different models of basket assembly by Mlp1/2, describing their potential functions and distribution.

### 5.4.1 Possible interaction of Mlp1 and mRNPs into the nucleoplasm: A role for Mlp1 function as a mobile nuclear pore component

We might propose that free diffusing Mlp1 fraction binds mRNPs in the nucleoplasm. Mlp1 would associate with mRNPs until the pore where Mlp1 docks for a limited amount of time after the mRNP has been exported. Therefore, baskets assembly would be impaired in the absence of mRNPs guiding Mlp1 toward a pore. In this model, mRNP/Mlp1 transiting together from the nucleoplasm to the periphery could sustain the Mlp1 turnover observed by FRAP at the pore. In addition, some mRNPs can associate with Mlp1 when it is not assembled into baskets, as indicated by the presence of transcripts in intranuclear Mlp foci reported upon overexpression of Mlp1 and during heat shock [201]. Such a model could also partially explain how mRNPs displace Mlp1 from the nucleoplasmic periphery to trigger the assembly of baskets in the nucleolus when poly(A) transcripts accumulate in nucleolar domains. This scenario would be very close to that of Mex67, which has been described as a mobile nucleoporin, binding mRNPs in the nucleoplasm until the channel of the pore, with a steady-state at the periphery. However, Mex67 is known to possess RNA binding domains allowing for a direct association with transcripts, whereas such domains have not been identified for the Mlp1/2. Furthermore, Mex67 steady-state is not affected when mRNP production is impaired, indicating that the dynamic of the two proteins may not be directly comparable.

While very intuitive, this model displays significant weaknesses and may be challenged by some of our data. First, we showed that Mlp1 could enter the nucleolar phase; therefore, we could expect at least a mild accumulation of an Mlp1-free fraction bound to mRNPs into the nucleolus when poly(A) transcripts accumulate there. However, we do not observe any Mlp1-GFP signal in the nucleolus, suggesting that Mlp1 may not behave as the RBPs found accumulated with mRNPs.

RNomic and proteomic approaches suggest that basket-less pores can also associate with mRNPs. Therefore, we should expect an even distribution of Mlp1 at the periphery, similarly to

what is observed for Mex67. However, we observe that Mlp1 and the basket accessory interactome are concentrated on specific pores. Hence, this model does not explain why Mlp1 is absent from specific pores in the nucleoplasm. The discontinuous distribution of baskets would imply that mRNPs bring Mlp1 to assemble baskets on certain pores, only avoiding a subset of them.

During the design of the different pore APs, we reasoned as follow:

$$\text{All NPCs}^{\text{interactome}} = \text{NPC}^{\text{Basket plus interactome}} + \text{NPC}^{\text{Basket minus interactome}}$$

Here, Mlp1-PrA is used as bait for basket-containing pore APs. Therefore, 'NPC $^{\text{Basket plus interactome}}$' is a mixture of basket-assembling Mlp1 interactome with Mlp1 "free fraction" interactome. Consequently, if Mlp1 binds mRNPs into the nucleoplasm, we expect to find significantly more mRNP components in the 'NPC $^{\text{Basket plus interactome}}$' than in 'All NPCs $^{\text{interactome}}$' APs. Proteomic analysis of the interactomes showed ~9 times higher quantities of Mlp1 purified using Mlp1 as bait in 'NPC$^{\text{Basket plus interactome}}$' (measuring the Mlp1 free fraction + basket-assembling Mlp1) compared to amounts of Mlp1 in 'All NPCs$^{\text{interactome}}$' (measuring basket-assembling Mlp1 only) (Supplementary Fig.25c). On the other hand, the quantities of mRNP export, processing factors, and Mlp2 were overall similar in both APs. Therefore, Proteomics data indicate that Mlp1 binds to mRNPs and Mlp2 mostly at the pore and not as a mobile nuclear pore component.

We carried out some attempts to test this model and tried to isolate the Mlp1 "free fraction" to look at its interactome by MS and RNAseq. The approach chosen was also a differential AP where all pores were first purified, leaving the flow through with the Mlp1 free fraction and its potential interactome. This free fraction was then purified in the second AP. However, our MS analysis showed systematic contamination of the pore components in the supposed Mlp1 "free fraction", showing that our isolation of Mlp1 "free fraction" was inefficient. While this model seems to have some caveats for the reasons mentioned above, it could still be tested. This would require optimizing the NPC-APs to reach a perfect depletion from the flow-through, potentially by testing different tags and baits located at different positions of the pores.

### 5.4.2 Can the basket assemble a phase-like micro-environment?

We observed different types of Mlp1 distribution in the nucleus, from a simple free diffusing population in the nucleoplasm, NPC bound as a basket and large granules assembled under various conditions. These different Mlp1 'states' raise the question of how and why Mlp1 can switch from

one state to another and what are the implications for possible basket structures. The different distributions of Mlp1 were reminiscent of behaviors observed for proteins known to phase separate, switching from a soluble fraction to biomolecular condensates (Fig.34). Therefore, in the next section, I will examine a model in which baskets are described as phase-like organized compartments requiring the spontaneous association of its scaffold Mlp1 and Mlp2 as well as accessory factors and mRNPs. I will also question the modalities for the positioning of this compartment at the pore, excluded from nucleoli.

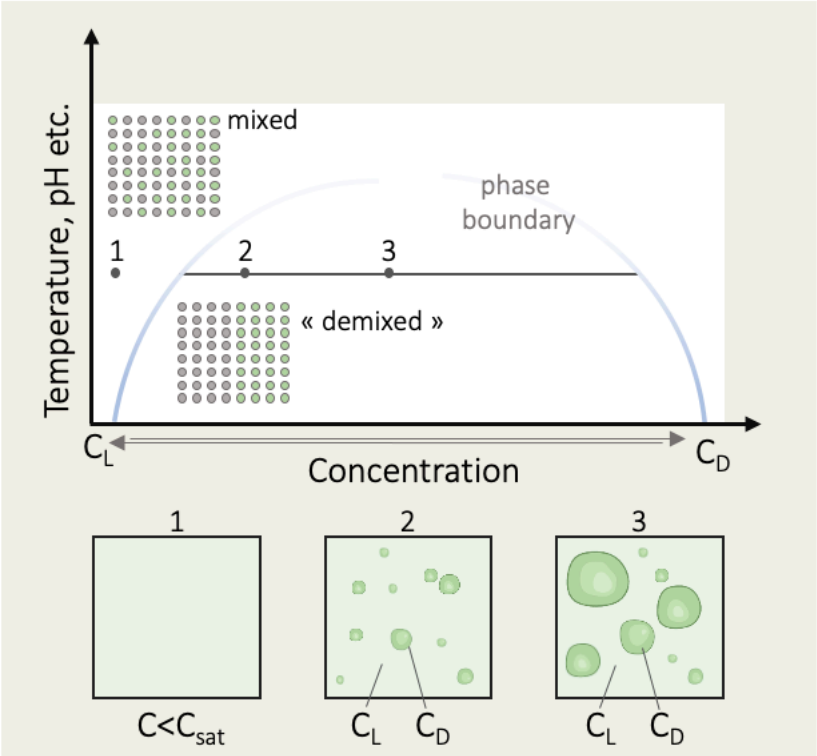


*Figure 34 Schematic Phase Diagram.*

*The coexistence of mixed and 'demixed' regimes is a function of environmental conditions such as temperature, pH, etc. The system does not undergo phase separation beyond a critical point where concentrations and environmental conditions allow the formation of a two-phases regime. At concentrations below the concentration of saturation $C_{sat}$, the system is in the one-phase regime. At any condition within the two-phase regime, the system demixes into a light phase (with $C= C_L$) and a dense phase (with $C = C_D$)*[34,30].

#### 5.4.2.1 Whether the variations of Mlp1 states inform us about the property and the structure of the basket

##### 5.4.2.1.1 Mlp1 can assemble granules in physiological conditions

Proteins assembling membrane-less compartments possess at least two major characteristics driving the phase separation. Protein multivalency allows their oligomerization with multiple partners and with itself to create associative complexes. In addition, the presence of IDDs seems to be a determinant for phase separation [38,276]. These domains display a sequence-intrinsic preference for conformational heterogeneity with a biased amino acid composition and repetitive sequence and can, therefore, be detected in silico using disorder predictors. As mentioned in the section 4.3 of this work, disorder predictors indicated that Mlp1 possesses several IDDs including a ~200 amino acids long low complexity domain in its C-terminal region (Fig.27). Moreover, the expression of Mlp1 fragments showed that some Mlp1 regions could associate to form large granules (Fig.26), consistent with our Mlp1 crosslinking data showing multiple crosslinks with itself (possibly intra- or inter-molecular) and with Mlp2 (Fig.28). These observations indicate that some domains of the Mlp1/2 protein can multimerize and suggest that Mlp1/2 are highly multivalent proteins and, therefore, good candidates to seed biomolecular condensates.

We observed that the frequency and the size of Mlp1 granules were correlated with a high Mlp1 signal in the nucleoplasm, corresponding to the free-protein fraction and, accordingly, with a loss of Mlp1 signal at the periphery. This suggests that increasing the concentration of Mlp1 in the nucleoplasm (the light phase, in the schematic phase diagram) enhances the formation of large Mlp1 aggregates. Mlp1 aggregation was maximum when Mlp1 association with the pore is completely abolished upon Nup60 depletion and almost as strong upon Pol II transcription shutdown or when 3'end processing and polyadenylation are impaired (Fig.14-15). This indicates that an intact nucleoplasmic pore platform and correct intranuclear mRNA metabolism are required to maintain Mlp1 at the periphery and prevent its demixing in large granules. However, we do not know whether Pol ll transcription shutdown and 3'end processing defect can affect the structure of the nucleoplasmic pore platform, preventing correct Mlp1 localization at the periphery. The material properties of these aggregates are not known either but could inform us of the nature of the basket. Indeed, if Mlp1/2 participates in forming liquid or gel-like

compartments upon stress, can they conserve this property at the periphery and organize the basket together with mRNP as a liquid or hydrogel compartment? In other words, is there a continuum of material properties between the different states of Mlp1 going from a completely soluble phase in the nucleoplasm to large granules, and where could we place the basket in this continuum? It is not clear whether Mlp1 granules behave as liquid compartments, gel-like, or solid aggregates. It Is generally accepted in the field that liquid droplets display spherical shapes and can fuse when two of them meet, while gel-like aggregates are typically unable to fuse and coalesce[30]. So far, we did not observe the coalescence of Mlp1 granules when multiple Mlp1 foci were generated simultaneously in cells. However, this could be due to the Mlp1 granule spatial confinement caused by the chromatin and other nuclear elements; hence the granules may never be close enough to fuse. Mlp1 aggregates are systematically spherical, and it remains possible that the large unique granules observed in different conditions are the results of the fusion of multiple smaller ones.

In liquid-liquid phase separation, the molecules are concentrated into the phase but diffuse in and out of the compartment. Therefore, FRAP can be performed on droplets as an assessment of their liquidity. Indeed, rapid recovery of the signal, usually when the entire or half of the granules have been photobleached, indicates high mobility of the molecules suggesting liquid properties. In contrast, low or absence of recovery rather argues for solid or gel-like structures[30]. Performing FRAP on the different Mlp1 granules could inform us of their material nature.

The aliphatic alcohol 1,6-hexanediol has been used to differentiate liquid from solid assemblies in living cells[277]. Hexanediol treatment can rapidly dissolve liquid-like structures while solid or gel-like aggregates are largely resistant. We observed that hexanediol does not dissolve the foci already formed after heat shock or Nup60 depletion. However, we did not test whether hexanediol treatment during heat shock or concomitantly to Nup60 depletion could prevent Mlp1 granule formation, which would suggest that Mlp1 assemble first through liquid phase separation before they rigidify into solid assemblies. Overall, these results indicate that Mlp1 aggregates may have solid-like behavior. On the other hand, that Mlp1 localization at the periphery was disrupted by hexanediol treatment. This could argue for the stabilization of baskets through a liquid-liquid phase separation process. However, FG-Nups and structural Nups dissociate from the pore upon

hexanediol treatment, and basket destabilization may not be a direct result of the treatment but instead caused by a global destabilization of the pore sub-modules[36].

#### 5.4.2.1.2 Avoiding Mlp1 aggregation in normal conditions

If nuclear baskets are assembled through a phase separation process, how can cells prevent the fusion of basket into big granules and maintain their precise stoichiometry at the pore? Different studies have shown that RNA can buffer the phase separation of prion-like RNA binding proteins[40]. Those works proposed that transcripts in the nucleus represent a buffering system in which high RNA concentrations keep RBPs soluble and demonstrated that changes in RNA levels or RNA binding abilities of RBPs cause aberrant phase transitions and solid-like aggregates formation. Similarly, it has been shown that the FG-Nups assembling the phase in the central channel of the NPC can adopt multiple conformations from collapsed to completely extended[278,45]. It has been proposed that the various cargos and mRNPs passing through the pore "unfold" the FG filaments and maintain them in an extended conformation by competing with intra- and intermolecular interactions between the filaments themselves, leading to their collapsed conformation. Overall, our data suggest that in the absence of mRNPs and when pores cannot dock a basket, Mlp1 aggregates. Therefore, we can propose that mRNPs compete with Mlp1/2 multimerization. A pore offers a limited number of binding sites for basket formation, limiting the concentration of Mlps available to aggregate at the pore. Furthermore, the free fraction of Mlp1 in normal conditions would not reach the critical concentration to initiate granule formation. Contact with mRNPs competes with Mlp1 inter/intramolecular contacts at the pore, limiting their assembling into larger structures than baskets. Thus, because Mlp1 is engaged in mRNP export in a limited stoichiometry, the basket does not collapse on itself, and Mlp1 in the basket never aggregates. Therefore, transient contacts with mRNPs would prevent the collapsing of the system by participating in a fluid meshwork constantly in flux. According to this last scenario, removing the binding site for Mlp1 at the pore would favor Mlp1-Mlp1 contacts rather than mRNP-Mlp1 contacts leading to aggregate formation. Finally, we observed that PTMs could correlate with the aggregation of specific Mlp1 fragments. We have shown that the pore binding domain N-terminal

2 is phosphorylated upon heat shock. Therefore, this suggests that specific PTMs at the pore also modulate Mlp protein valency and, consequently, granule formation (Fig.26-27).

#### 5.4.2.2 Do baskets generate biophysical properties excluding them from the nucleolar phase?

We observed that Mlp1 granules were systematically excluded from nucleoli. Therefore, we wondered whether Mlp1 assemblies generate a set of biophysical properties systematically excluding them from the nucleolar phase. In the standard basket model, classically represented as a simple scaffold with a distal ring (Fig2), the access for cargos and mRNPs inside the basket is only limited by the steric hindrance; therefore, complexes are excluded from this sub-compartment depending on their size. In this view, the basket structure contains the same nucleoplasmic 'fluid' as the rest of the nucleus. The different concentrations of soluble nuclear components are balanced by diffusion across different basket elements. On the other hand, the essential hallmark of liquid-phase separation is its ability to exclude and concentrate specific factors depending on their biochemical properties. Importantly, some large molecules can penetrate these sub-compartments, while smaller proteins can be excluded. Liquid-like sub-compartments can thus generate a specific biochemical environment by concentrating and excluding specific components.

Upon assembly of an ectopic basket at the nucleolar rim, we observed an invagination in the nucleolar phase. It is legitimate to wonder whether this invagination represents a nucleolar exclusion zone caused by the steric hindrance of basket elements or whether basket components generate a set of local biochemical properties strictly incompatible with the nucleolar phase. On the other hand, the presence of ectopic baskets could correlate with an increased ectopic concentration of Nab2 (Fig.35). This may indicate that basket can differentiate between specific proteins and may argue for a model wherein the basket generates a set of biophysical properties, including and excluding specific factors.

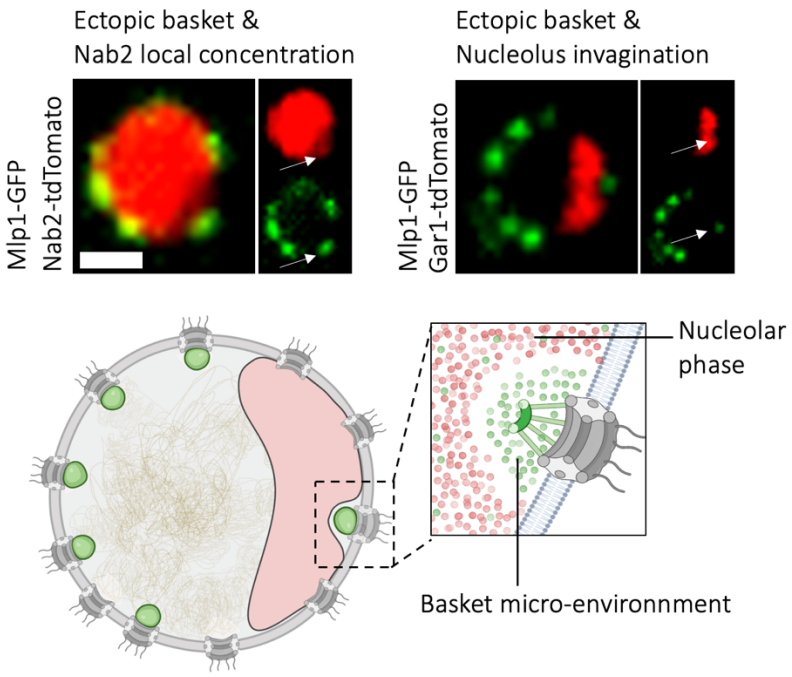


*Figure 35 Mlp proteins and their interactome could assemble a domain excluding some components of the nucleolar phase.*

*A relatively high Nab2 concentration and the absence of Gar1 correlate with the presence of an ectopic basket. In the model proposed here, Nab2 is a proxy for proteins forming the basket interactome, while Gar1 could represent the distribution of proteins participating in the formation of the nucleolar phase. In this scenario, a local NPC environment is cooperatively assembled by Mlp proteins, specific RBPs, and possibly mRNPs. This microenvironment generates a set of properties excluding the nucleolar phase components and favors the capture of the elements assembling it. Most of the time, the nucleolar phase would prevent the development of such compartments which formation is more favorable in the nucleoplasm (scale bars=1µm).*

The nucleolus/basket incompatibility may also be supported by other data presented in this work. Indeed, we reported in Chapter 3 of this thesis that when baskets relocate to the nucleolar periphery, the nucleolus was fragmented into internalized and spherical pseudo-nucleolar domains (Fig.26). The formation of small and spherical structures requires more energy (also termed interfacial tension) than the maintenance of long and relax interfaces. To put it simply: higher levels

of energy -or interfacial tension- are required to bend an interface between phases and form spherical structures (Fig36a,d). The energy of the interface is proportional to the non-miscibility between the components on the two sides of the interface[34,279,280]. Therefore, this property could explain why the nucleolar phase appears as several fragmented domains repelled towards the center of the nucleus as contacts between basket and nucleolus provide the interface tension to bend the nucleolar interface and assemble spherical compartments (Fig.36.b). This may indicate that the typical crescent-shaped nucleoli are not pushed toward the center of nuclei simply by steric hindrance caused by baskets but could be repelled by the proximity of high concentrations of Mlp1. This observation would suggest that baskets generate biophysical properties incompatible with the nucleolar phase. However, this phenotype is triggered by the relocation of transcripts into the nucleolus. Therefore, changes in nucleolar shape and fragmentation could also be caused by changes in the biophysical properties of the nucleolar phase itself saturated with poly(A) transcripts and associated proteins instead of being driven by the proximity of baskets. This could be tested by inducing the re-localization of poly(A) in the nucleolar phase and monitoring nucleoli's shape in Mlp1/2 depleted strains.

I presented in my thesis independent data that may also indicate an immiscibility between Mlp1 and nucleoli reported in section 4.3 (Fig.36c). Overexpression of Mlp1 can also induce the fragmentation of nucleoli into internalized spherical pseudo-nucleolar domains. This phenotype could be caused by the same biophysical properties driving the nucleolar deformation upon nucleolar basket formation. The interface between the nucleolar phase and the nucleoplasm saturated with Mlp1 fragments may increase the interface tension at the periphery of the nucleolus bending the interface and leading to the formation of spherical structures (Fig.36c). These cells are perfectly viable and normally divide, which questions to what extend ribosomal biogenesis is affected when nucleoli are internalized and fragmented. It has been shown that overexpression of Mlp1 and its C-terminal domain can induce the retention of poly(A) transcripts in the nucleoplasm[123]. It would, therefore, be interesting to examine whether the overexpression of Mlp1 fragments used in this project induces a similar retention phenotype and to which extent this participates in the formation of spherical pseudo-nucleolar domains.

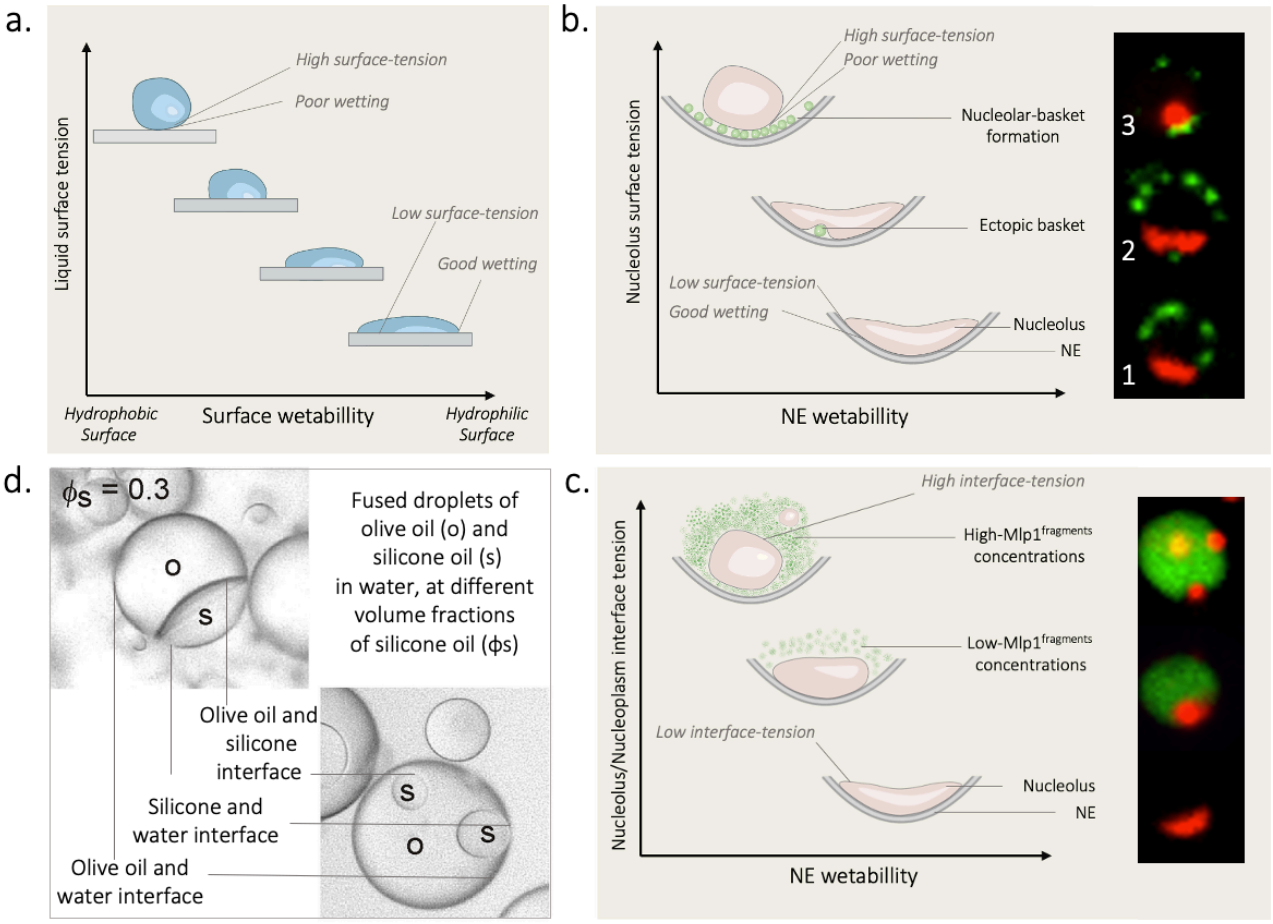


*Figure 36 Mlp1, the nucleoli, the NE, and the interface tension.*

*(a) Schematic representation of a hypothetical droplet on different surfaces. The affinity between the droplet and the surfaces decreases the surface tension (or surface energy) at the interface solid-liquid and allows the droplet to spread on the surface. Instead, a minimal degree of contact due to a low surface wettability corresponds to high surface energy allowing the formation of a spherical droplet*[280]*. (b) The wettability parameter could also be used to describe the interface between Mlp1s, nucleoli and the NE. While the nucleolus can 'wet' the NE (1), the presence of a basket at the interface decreases the ability of the nucleolar phase to maintain contact with the NE (2). The accumulation of multiple nucleolar baskets increases the surface tension and leads to the formation of the spherical nucleolus (3). (c) The interface between two soluble compartments behave similarly*

*to liquid-solid interacting surfaces. The contact between the nucleoplasmic fluid and the nucleolus generates relatively low energy (interface tension), and the interface appears concave, giving a crescent shape to nucleoli (4). The expression of Mlp1 fragments (here N-terminal 1) provides more energy to the interface, which becomes convex (5). When the energy of the interface reaches a certain threshold, possibly by increasing the concentration of Mlp1 fragments, the nucleolus acquires a spherical shape. d) Optical microscope images of fused droplets of olive oil (o) and silicone oil (s) in an aqueous media. Water limits the volume of the droplets encapsulating the silicon and the olive oil phases. In the top left image, the olive oil represents ~70% of the droplet volume. However, in the bottom right image, the proportion of olive oil is higher. In a limited volume, increasing the fraction of olive oil triggers the formation of spherical and internalized silicon compartments. This system could represent a very minimalistic model for what is observed in (c). The analogy could be relevant as both systems are composed of three interfaces mediating the formation of similar structures: the nucleolus and the spherical nucleolar domains, as well as the silicon phases forming spherical droplets or a crescent depending on the fraction occupied by the olive oil in the system*[279].

To go further, we could also interrogate the separation between the nucleoplasm as the place of mRNP biogenesis triggering the assembly of baskets and the nucleolus. The relatively low abundance of Nab2 in the nucleolus illustrates that, by enclosing two interactomes, the nucleolar and nucleoplasmic phases are distinct non-miscible compartments sharing a common space: the nucleus. Moreover, one could envision that upon inhibition of mRNP export, the equilibrium between the mRNP and ribosomal subunit compartments (the nucleolus and nucleoplasm, schematically) would be affected due to an excess of mRNPs in the nucleus. This proposition is very speculative but could be supported by the nucleolar "disintegration", and "fragmentation" observed upon Mex67 depletion [281,117]. Hence, it would be interesting to analyze more closely how and why the nucleolar phase is affected in such conditions. While possibly out of scope for this project, such investigations would further reinforce the idea that RNPs organize nuclear compartmentalization. Furthermore, it would also help to understand the distribution of baskets and their exclusion from nucleoli.

#### 5.4.2.3 Possible biological relevance for an Mlp1 assembled micro-environment

The nuclear basket has already been described as a phase-like compartment. The basket Nups Nup1, Nup2, Nup60 possess intrinsically disordered FG motifs and are believed to expand the phase-like compartment found in the central channel of the pore into the nucleoplasm[278] (Fig.37). Indeed, those Nups are predicted to assemble a non-cohesive network representing a selective phase protruding into the nucleoplasm[282,45]. It has been proposed that such microenvironments could participate in the phase-separated properties of transcriptional compartments such as transcription sites, enhancers, and super-enhancers [197]. In this scenario, the basket could concentrate chromatin and transcriptional regulators, and/or create an isolated hub generating selective permeability properties.

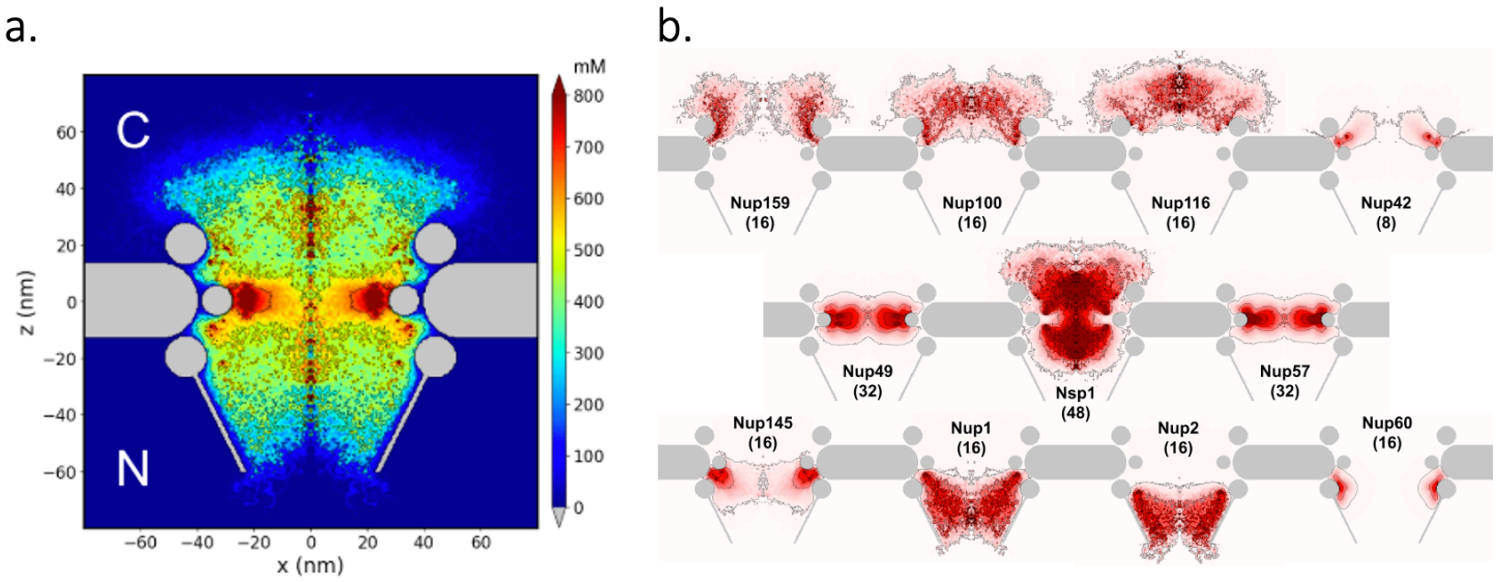


*Figure 37 Molecular model of the nuclear pore complex reveals FG-network with distinct territories occupied by different FG motifs.*

*(a) Color map of the mM concentration of all the amino acids inside the NPC with cooperative FG-pairing and cohesive spacer attraction. (b) An atlas of various FG-Nups of yeast NPC shown in color maps. From top to bottom, the three rows show the spatial distributions of the FG-Nups with their anchor positions located towards the cytoplasm, near the central inner ring, and towards the*

*nucleoplasm. The copy number of each individual Nup is indicated in the parenthesis. This model has been published in* [282].

Here, I propose a dual role for baskets; Mlp1 could alternatively facilitate the selective export in standard conditions and favor the retention upon stress. Such a micro-environment could provide selective access to the central channel of the pore. As described in the section where *in silico* models for selective export have been tested, mRNA quality control may be achieved by the cooperation of regulated weak and stochastic interactions with basket components[136,283]. The so-called "modulated-affinities" selection for export appears compatible with a phase-like microenvironment where molecules are trapped and retained depending on their ability to interact with the multiple partners concentrated at the basket. This is also compatible with the evolution of numerous export kinetics -facilitated or delayed - based on mRNP length and composition. Therefore, in normal conditions, baskets could simply represent a phenomenon where nuclear pore accessory factors tend to concentrate together with mRNPs to facilitate their export, or the last step of rearrangement before the transcripts access the pore channel. This model could account for the fact that Mlp1/2, similarly to other checkpoint proteins, are not essential under conditions where mRNP processing is undisturbed. On the other hand, the biophysical properties may allow the basket components to rearrange in granules when specific mRNA processing or stress conditions ask for a different export output, such as export of heat shock mRNA and the retention of unspliced or aberrant mRNPs.

Finally, we can speculate why evolution selected a basket scaffold displaying an apparent incompatibility with the nucleolus in yeast. Here we could propose that baskets participate in the functional asymmetry between nucleoplasm and nucleoli. Indeed, the strict exclusion between the nucleolar phase and Mlp assemblies (basket or granules) may indicate that the formation of a microenvironment that is non-miscible with the nucleolar phase enhances the segregation of mRNP export from the nucleolus. Hence, mRNPs reaching the periphery would participate in the formation of a domain together with Mlp1/2 triggering their own exclusion from the nucleolus. This could represent the primary function of Mlp protein in normal conditions, which captures and facilitates the bulk of mRNP export flux in the proper compartment, the nucleoplasm. This yeast-

specific organization may be necessary to optimize the nuclear compartmentalization and possibly the separation of mRNA and rRNA metabolism in a relatively limited nuclear volume compared to higher eukaryotes.

### 5.4.3 Suggestion for a simple model for basket positioning, persistence, and function

The strength of a "phase-like basket model" is that it could help us to understand both Mlp1 distribution and dynamics (Fig.38). By definition, phase-separated compartments are very efficient in capturing and retaining their interactomes [25,26,29]. This characteristic confers their quality of "self-assembling compartments". As discussed above, those structures are facilitated by multivalent interactions among the respective components. However, they are disfavored by the energetic cost for creating an interface between the two phases. The first contribution is proportional to the droplet volume, whereas the second is proportional to its surface. Thus, to be stable, droplets need to reach a critical size at which the energetic cost for creating an interface is exceeded by the energy gained from multivalent interactions within the droplet. This last statement could be the fundamental principle explaining the absence of baskets in nucleoli. The energetic cost to nucleate a basket would be simply too high to form nucleolar baskets or would require supersaturating concentration of RBPs such as what is observed mRNP relocate into the nucleolus.

However, nucleating a basket in the nucleoplasm may have a cost as well. This step can occur at nucleation sites, a pore, which can recruit and concentrate the respective components of the system: Mlps and mRNPs, to facilitate the compartment formation. Once baskets are large enough to be energetically favorable, they become stable. Here the stability may be reached when Mlp1/2 occupies all pore binding sites. On the other hand, if local concentrations of the different partners are too low, forming a basket is energetically unfavorable and Mlp1/2. In this case, free diffusing Mlps would bind a pore but form a non-stable and unproductive interaction. Instead, free Mlps tend to exchange onto pores where a basket is already established, sustaining the Mlp turnover. Therefore, a basket would represent a region where free diffusing Mlps have the highest probability of meeting their interactome and being retained. In this case, basket distribution,

observed by fluorescent microscopy, would follow a simple probabilistic pattern determined by the abundance of Mlp interactome, including other Mlps. Thus, one Mlp is more likely to multimerized onto pores already engaged in export, in contact with mRNPs, and rarely in the nucleolus. Following this logic, instead of nucleating new baskets on basket-less pores, Mlp1/2 rather maintains a turnover where one basket already exists. Thereby, the entire basket system would sustain self-assembling hotspots for mRNP maturation/export events at the nucleoplasmic periphery excluded from nucleoli.

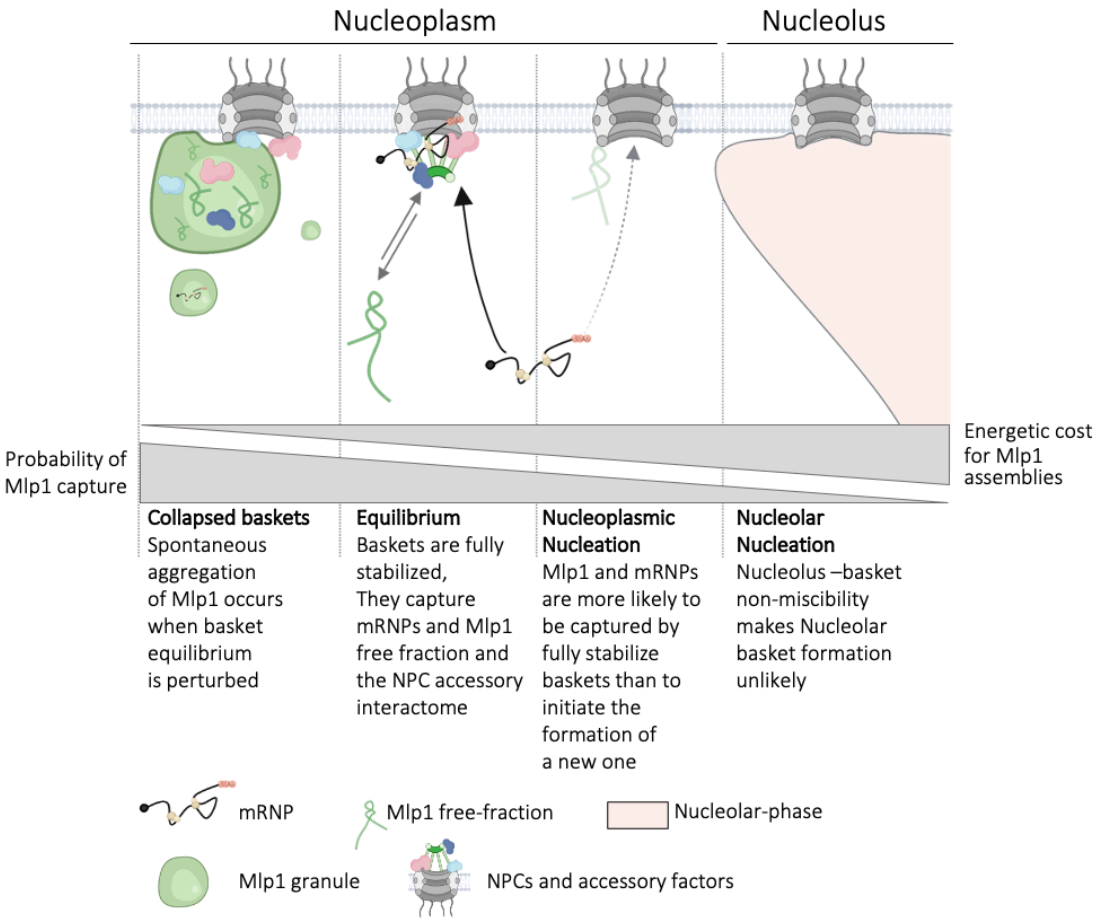


*Figure 38 A dynamic model for basket formation and localization.*

***Nucleolar nucleation:*** *Mlp1 and factors participating in basket formation do not reach the critical concentration to repel the nucleolar phase and initiate a basket assembly.* ***Nucleoplasmic nucleation:*** *Mlp1, mRNPs, and accessory proteins participating in basket formation can initiate the*

*formation of a basket without the hindrance of the nucleolar phase, however, they are more likely to be captured by a basket already stabilized where their interactome is more abundant.* ***Equilibrium****: The basket is fully assembled and is stabilized by the accessory interactome. They are maintained by the mRNP flow and the Mlp1/2 turnovers at the pore.* ***Collapsed baskets****: When some elements of the system are missing, such as mRNPs and a complete NPC nuclear platform, high valency of Mlp protein trigger the formation of Mlp1 granules: basket and part of its interactome aggregate.*

# 6. Conclusion

The vast majority of eukaryotes possess TPR/Mlp1/2 proteins or a functional homolog on the nucleoplasmic side of the pore. In higher eukaryotes and yeast cells, evidence shows that the basket-mediated positioning of chromatin at the periphery correlates with transcriptionally active state and possible transcriptional memory of their recent expression state. However, this picture is complicated by observations that NPCs and baskets can also mediate chromatin silencing.

Basket role in cell cycle regulation through the formation of the SPB and spindle assembly checkpoint to concentrate key mitotic regulators is evolutionary conserved in plants (*A. thaliana*) [284], fungi (*S. cerevisiae*[147]*, A. nidulans*[150]*, S. pombe*[285]), flies (*D. melanogaster*[151]*),* as well as in humans[286]. For example, the proteins Megator (*D. melanogaster*[151]*)* and NUA *(A. thaliana)*[284]*,* the TPR/Mlp1/2 counterparts, as well as TPR, form a fusiform structure called the mitotic spindle matrix surrounding the mitotic spindle, acting as a structural scaffold to coordinate the mitosis[148]. Therefore, in higher eukaryotes, basket proteins can assemble dynamic structures during mitotic progression. The role of baskets in mRNP export and possible proofreading mechanism and interaction with its partners TREX-2 and SAGA complex seems also conserved among eukaryotes. However, the dynamic of basket scaffolds, out of cell cycle regulation context, may have diverged during evolution, and Mlp1/2 behavior at the pore seems yeast specific.

In parallel with my project, we tested whether TPR-NPC interaction was dynamic with FRAP analysis and compared recovery rates to published data for the mammalian basket-associated proteins NUP50 and NUP153 known to exchange rapidly at the periphery. GFP-TPR showed a slow

recovery compared to the other basket proteins, with only about 20% recovery after 40min. Finally, we did not observe significant changes in TPR localization when we blocked Pol II elongation using 5,6-dichloro-1-B-D-ribofuranosylbenzimidazol (DRB) treatment or induced heat stress. Taken together, this suggested that the NPCs plasticity involving the basket scaffold is not conserved in humans. In addition, we searched for potential basket-less pores in human cells. TPR localization analysis compared to other Nups by IF did not reveal TPR-less NPCs in HEK 293 cells. Therefore, we can question which yeast-specific feature(s) required the evolution of a dynamic nuclear NPC platform. Multicellular organisms, especially mammals, may not be as sensitive as yeast to rapid environmental changes. Adjusting the pore composition and Mlp position could be a yeast-specific mechanism to adapt the mRNP export outcome rapidly.

Yeast has a substantially smaller nucleus than higher eukaryotes. The position of their prominent nucleoli at the nuclear rim is also a feature of their own, as mammalian cells usually possess two to three large internalized nucleoli. One interesting property of the basket scaffold in yeast is its incompatibility with the nucleolar phase. Therefore, one can surmise that the basket evolved in yeast to optimize, in a limited nuclear space, the exclusion of mRNPs export and the ribosomal subunits maturation in the nucleolus. This exclusion would require forming a specific structure -the basket-cooperatively assembled by Mlps, basket accessory factors, and mRNPs. This would suggest that by enhancing the formation of baskets, mRNAs facilitate their own capture at the nucleoplasmic periphery -excluded from nucleoli- and therefore, can organize their export in sub-nuclear spaces.

Typical sub-compartments or bodies such as PML and Cajal bodies, speckles, or paraspeckles described in metazoan cells, have not been identified in yeast. Their absence may be due to a lesser need for mRNP regulation and processing or can be the consequence of a lack of space available in nuclei to assemble such sub-compartments stably. Hence, we can suggest that these foci might be formed by a minimal number of factors in a transient manner creating local microenvironments to meet specific and temporary needs for mRNA regulation. Those bodies could only exist for a short time if induced, similarly as repair foci formed following double-strand breaks or stress granules[24]. Analogously, the existence and the abundancy of the micro-

environments organized by the baskets on pores can be adjusted by the intranuclear mRNA metabolism directly and may vary according to cell's needs.

*"All models are wrong, some are useful."*

(aphorism generally attributed to the statistician George Box, 1976[287])

Membrane-less organelles are usually described according to phase separation models characterizing their dynamics, their evolutions in larger structures, and their ability to capture their interactome while excluding specific components. This conceptual framework appeared useful for basket description as they are dynamic structures believed to exclude or concentrate different sets of proteins and able to form larges granules in precise conditions. Our model does not predict the physical nature of the basket micro-environment, which could correspond to a gel-like dense polymer meshwork or alternatively to a completely liquid-liquid phase-separated compartment. However, we predict that Mlp1 as an aggregation-prone multivalent polymer may have a central role in its formation and the set of properties it can generate, as illustrated by the Mlp1-nucleolar incompatibility. The first step for testing the model would probably be to reconstitute the phase *in vitro* with its main elements, as it has been done for the central pore channel phase assembled by FG-Nups or with nucleolar components. While this experiment may not reflect the exact biophysical properties of a compartment organized by Mlp1/2 *in vivo,* this would represent a first proof of principle for such function of basket scaffold and could potentially indicate what factors can enter or remain excluded from the basket-microenvironment.

# 7. References


1. Egyhiizi, E. Quantitation of Turnover and Export to the Cytoplasm of hnRNA Transcribed in the Balbiani Rings. *Cell* **7**, 507–515 (1976).
2. Gayon, J. De Mendel à l'épigénétique : histoire de la génétique. *Comptes Rendus - Biol.* **339**, 225–230 (2016).
3. Morange, M. Monod and the spirit of molecular biology. *Comptes Rendus - Biol.* **338**, 380–384 (2015).
4. F.Crick. Central Dogma of molecular biology. *Nat. Publ. Gr.* **228**, 726–734 (1970).
5. Darnell, J. E. Reflections on the history of pre-mRNA processing and highlights of current knowledge: A unified picture. *Rna* **19**, 443–460 (2013).
6. Franke, W. W., Scheer, U., Krohne, G. & Jarasch, E. D. The nuclear envelope and the architecture of the nuclear periphery. *J. Cell Biol.* **91**, (1981).
7. Stevens, B. J. & Swift, H. RNA transport from nucleus to cytoplasm in Chironomus salivary glands. *J. Cell Biol.* **31**, 55–77 (1966).
8. Mehlin, H., Daneholt, B. & Skoglund, U. Translocation of a specific premessenger ribonucleoprotein particle through the nuclear pore studied with electron microscope tomography. *Cell* **69**, 605–613 (1992).
9. Andrea M. Femino, Fredric S. Fay, Kevin Fogarty, R. H. S. Visualization of single RNA transcripts in situ. *Science (80. ).* **vol 280**, 580–595 (1998).
10. Singer, R. H. Reminiscences on my life with RNA: A self-indulgent perspective. *Rna* **21**, 508–509 (2015).
11. Lécuyer, Eric Yoshida, Hideki Parthasarathy, Neela Alm, Christina abak, Tomas Cerovina, Tanja Hughes, Timothy R. Tomancak, P. & Krause, H. M. Global Analysis of mRNA Localization Reveals a Prominent Role in Organizing Cellular Architecture and Function. *Cell* **131**, 174–187 (2007).
12. Yunger, S., Rosenfeld, L., Garini, Y. & Shav-Tal, Y. Single-allele analysis of transcription kinetics in living mammalian cells. *Nat. Methods* **7**, 631–633 (2010).
13. Bertrand, E. *et al.* Localization of ASH1 mRNA particles in living yeast. *Mol. Cell* **2**, 437–445 (1998).

14. Susan M Janicki, Toshiro Tsukamoto, Simone E Salghetti, William P Tansey, Ravi Sachidanandam, Kannanganattu V Prasanth, Thomas Ried, Yaron Shav-Tal, Edouard Bertrand, Robert H Singer, and D. Larson. From Silencing to Gene Expression: Real-Time Analysis in Single Cells. *Cell* **116(5)**, 683–698. (2004).
15. Hye Yoon Park, Hyungsik Lim, Young J. Yoon, Antonia Follenzi, Chiso Nwokafor, Melissa Lopez-Jones, Xiuhua Meng1, and Robert H. Singer. Visualization of Dynamics of Single Endogenous mRNA Labeled in Live Mouse Hye. *Science (80. ).* **343**, 422–424 (2014).
16. Grünwald, D. & Singer, R. H. In vivo imaging of labelled endogenous B-actin mRNA during nucleocytoplasmic transport. *Nature* **467**, 604–607 (2010).
17. Larson, D. R. Real-Time Observation of Transcription Initiation and Elongation. **332**, 475–478 (2011).
18. Kher, R. & Bacallao, R. L. *Imaging gene expression*. *methods in molecular biology* vol. 103 (2006).
19. Grimm, Jonathan B.English, Brian P.Chen, J. & Slaughter, Joel P.Zhang, Zhengjian, Revyakin, Andrey, Patel, Ronak, Macklin, John J., Normanno, Davide, Singer, Robert H.Lionnet, Timothée, Lavis, L. D. A general method to improve fluorophores for live-cell and single-molecule microscopy. *Nat. Methods* **12**, 244–250 (2015).
20. Wu, B., Eliscovich, C., Yoon, Y. J. & Singer, R. H. Translation dynamics of single mRNAs in live cells and neurons. *Science (80 ).* **352**, 1430–1435 (2016).
21. Niewidok, Benedikt Igaev, M. & da Graca, Abel Pereira Strassner, Andre Lenzen, Christine Richter, Christian P. Piehler, Jacob Kurre, Rainer Brandt, R. Single-molecule imaging reveals dynamic biphasic partition of RNA-binding proteins in stress granules. *J. Cell Biol.* **217**, 1303–1318 (2018).
22. Tuck, A. C. & Tollervey, D. A transcriptome-wide atlas of RNP composition reveals diverse classes of mRNAs and lncRNAs. *Cell* (2013) doi:10.1016/j.cell.2013.07.047.
23. Baejen, Carlo, Torkler, Phillipp, Gressel, Saskia, Essig, Katharina, Söding, Johannes, Cramer, P. Transcriptome Maps of mRNP Biogenesis Factors Define Pre-mRNA Recognition. *Mol. Cell* **55**, 745–757 (2014).
24. Miné-Hattab, J. & Taddei, A. Physical principles and functional consequences of nuclear

compartmentalization in budding yeast. *Curr. Opin. Cell Biol.* **58**, 105–113 (2019).

25. Iwashita, K., Handa, A. & Shiraki, K. Coacervates and coaggregates: Liquid–liquid and liquid–solid phase transitions by native and unfolded protein complexes. *Int. J. Biol. Macromol.* **120**, 10–18 (2018).
26. Feric, Marina, Vaidya, Nilesh, Harmon, T. S. & Mitrea, Diana M., Zhu, Lian, Richardson, Tiffany M., Kriwacki, Richard. W, Pappu, Rohit V.Brangwynne, C. P. Coexisting Liquid Phases Underlie Nucleolar Subcompartments. *Cell* **165**, 1686–1697 (2016).
27. Trinkle-Mulcahy, L. & Sleeman, J. E. The Cajal body and the nucleolus: "In a relationship" or "It's complicated"? *RNA Biol.* **14**, 739–751 (2017).
28. Lu, Huasong, Yu, Dan, Hansen, Anders S., Ganguly, Sourav, Liu, Rongdiao, Heckert, Alec, Darzacq, Xavier,Zhou, Q. Phase-separation mechanism for C-terminal hyperphosphorylation of RNA polymerase II. *Nature* **558**, 318–323 (2018).
29. Steven Boeynaems, Simon Alberti, Nicolas L. Fawzi5, Tanja Mittag6, Magdalini Polymenidou, Frederic Rousseau, Joost Schymkowitz, James Shorter, Benjamin Wolozin, Ludo Van Den Bosch, Peter Tompa, and M. F. Protein Phase Separation: A New Phase in Cell Biology. *Trends Cell Biol* **176**, 139–148 (2018).
30. Alberti, S., Gladfelter, A. & Mittag, T. Considerations and Challenges in Studying Liquid-Liquid Phase Separation and Biomolecular Condensates. *Cell* **176**, 419–434 (2019).
31. Erdel, F. & Rippe, K. Formation of Chromatin Subcompartments by Phase Separation. *Biophys. J.* **114**, 2262–2270 (2018).
32. Shin, Yongdae, Chang, Yi Che Lee, Daniel S.W. Berry, Joel Sanders, David W.Ronceray, Pierre Wingreen, Ned S. Haataja, Mikko Brangwynne, C. P. Liquid Nuclear Condensates Mechanically Sense and Restructure the Genome. *Cell* **175**, 1481-1491.e13 (2018).
33. Weber, S. C. Sequence-encoded material properties dictate the structure and function of nuclear bodies. *Curr. Opin. Cell Biol.* **46**, 62–71 (2017).
34. Berry, J., Brangwynne, C. P. & Haataja, M. Physical principles of intracellular organization via active and passive phase transitions. *Reports Prog. Phys.* **81**, (2018).
35. Schmidt, H. B. & Görlich, D. Transport Selectivity of Nuclear Pores, Phase Separation, and Membraneless Organelles. *Trends Biochem. Sci.* **41**, 46–61 (2016).

36. Shulga, N. & Goldfarb, D. S. Binding Dynamics of Structural Nucleoporins Govern Nuclear Pore Complex Permeability and May Mediate Channel Gating. *Mol. Cell. Biol.* **23**, 534–542 (2003).
37. Schmidt, H. B. rode. & Görlich, D. Nup98 FG domains from diverse species spontaneously phase-separate into particles with nuclear pore-like permselectivity. *Elife* **4**, 1–30 (2015).
38. Harmon, T. S., Holehouse, A. S., Rosen, M. K. & Pappu, R. V. Intrinsically disordered linkers determine the interplay between phase separation and gelation in multivalent proteins. *Elife* **6**, 1–31 (2017).
39. Garcia-Jove Navarro, Marina Kashida, Shunnichi Chouaib, Racha Souquere, S. & Pierron, Gérard Weil, D. G. RNA is a critical element for the sizing and the composition of phase-separated RNA–protein condensates. *Nat. Commun.* **10**, 1–13 (2019).
40. Shovamayee Maharana, Jie Wang, Dimitrios K. Papadopoulos, Doris Richter, Andrey Pozniakovsky, Ina Poser, Marc Bickle, Sandra Rizk, Jordina Guillén-Boixet, Titus M. Franzmann, Marcus Jahnel, Lara Marrone, Young-Tae Chang, S. A. RNA buffers the phase separation behavior of prion-like RNA binding proteins. *Science (80-. ).* **921**, 918–921 (2018).
41. Yamazaki, Tomohiro Souquere, Sylvie Chujo, Takeshi Kobelke, Simon Chong, Yee Seng Fox, Archa H. Bond, Charles S. Nakagawa, Shinichi Pierron, Gerard Hirose, T. Functional Domains of NEAT1 Architectural lncRNA Induce Paraspeckle Assembly through Phase Separation. *Mol. Cell* **70**, 1038-1053.e7 (2018).
42. Bensidoun, P., Zenklusen, D. & Oeffinger, M. Choosing the right exit: How functional plasticity of the nuclear pore drives selective and efficient mRNA export. *Wiley Interdiscip. Rev. RNA* 1–18 (2021) doi:10.1002/wrna.1660.
43. Strambio-De-Castillia, C., Niepel, M. & Rout, M. P. The nuclear pore complex: Bridging nuclear transport and gene regulation. *Nat. Rev. Mol. Cell Biol.* **11**, 490–501 (2010).
44. Kim, S. J. *et al.* Integrative structure and functional anatomy of a nuclear pore complex. *Nature* **555**, 475–482 (2018).
45. Vovk, Andrei Gu, Chad Opferman, Michael G.Kapinos, Larisa E. Lim, Roderick Y.H. Coalson, Rob D. Jasnow, David Zilman, A. Simple biophysics underpins collective conformations of

the intrinsically disordered proteins of the nuclear pore complex. *Elife* **5**, 1–29 (2016).

46. Ribbeck, K. & Görlich, D. Kinetic analysis of translocation through nuclear pore complexes. *EMBO J.* **20**, 1320–1330 (2001).
47. Culjkovic, B., Topisirovic, I., Skrabanek, L., Ruiz-Gutierrez, M. & Borden, K. L. B. eIF4E is a central node of an RNA regulon that governs cellular proliferation. *J. Cell Biol.* **175**, 415–426 (2006).
48. Zander, Gesa Hackmann, Alexandra Bender, Lysann Becker, Daniel Lingner, Thomas Salinas, Gabriela Krebber, H. MRNA quality control is bypassed for immediate export of stress-responsive transcripts. *Nature* **540**, 593–596 (2016).
49. Hackmann, Alexandra Wu, Haijia Schneider, Ulla Maria Meyer, Katja Jung, Klaus Krebber, H. Quality control of spliced mRNAs requires the shuttling SR proteins Gbp2 and Hrb1. *Nat. Commun.* **5**, 3123 (2014).
50. D.Zenklusen & M.Oeffinger. To the Pore and Through the Pore: A Story of mRNA Export Kinetics. *Biochim Biophys Acta* **23**, 1–7 (2012).
51. Tutucci, E. & Stutz, F. Keeping mRNPs in check during assembly and nuclear export. *Nat. Rev. Mol. Cell Biol.* **12**, 377–384 (2011).
52. Katahira, J. Nuclear export of messenger RNA. *Genes (Basel).* **6**, 163–184 (2015).
53. Wickramasinghe, V. O. & Laskey, R. A. Control of mammalian gene expression by selective mRNA export. *Nat. Rev. Mol. Cell Biol.* **16**, 431–442 (2015).
54. Oeffinger, Marlene, Wei, Karen E. Rogers, Richard DeGrasse, Jeffrey A. Chait, Brian T. Aitchison, John D. Rout, M. P. Comprehensive analysis of diverse ribonucleoprotein complexes. *Nat. Methods* **4**, 951–956 (2007).
55. Stäßer, Katja Masuda, Seiji Mason, Paul Pfannstiel, Jens Oppizzi, Marisa Rodriguez Navarro, Susana Rondón, Ana G. Aguilera, Andres Struhl, Kevin Reed, Robin Hurt, E. TREX is a conserved complex coupling transcription with messenger RNA export. *Nature* **417**, 304–308 (2002).
56. Katahira, J. MRNA export and the TREX complex. *Biochim. Biophys. Acta - Gene Regul. Mech.* **1819**, 507–513 (2012).
57. Mason, P. B. & Struhl, K. Distinction and relationship between elongation rate and

processivity of RNA polymerase II in vivo. *Mol. Cell* **17**, 831–840 (2005).

58. Rougemaille, Mathieu Dieppois, Guennaelle Kisseleva-Romanova, Elena Gudipati, Rajani Kanth Lemoine, Sophie Blugeon, Corinne Boulay, Jocelyne Jensen, Torben Heick Stutz, Françoise Devaux, Frédéric Libri, D. THO/Sub2p Functions to Coordinate 3′-End Processing with Gene-Nuclear Pore Association. *Cell* **135**, 308–321 (2008).
59. Saguez, C. *et al.* Nuclear mRNA Surveillance in THO/sub2 Mutants Is Triggered by Inefficient Polyadenylation. *Mol. Cell* **31**, 91–103 (2008).
60. Kim, M., Ahn, S. H., Krogan, N. J., Greenblatt, J. F. & Buratowski, S. Transitions in RNA polymerase II elongation complexes at the 3′ ends of genes. *EMBO J.* **23**, 354–364 (2004).
61. Johnson, S. A., Kim, H., Erickson, B. & Bentley, D. L. The export factor Yra1 modulates mRNA 3′ end processing. *Nat. Struct. Mol. Biol.* **18**, 1164–1171 (2010).
62. Gómez-González, Belén García-Rubio, María Bermejo, Rodrigo Gaillard, Hélène Shirahige, Katsuhiko Marín, Antonio Foiani, Marco Aguilera, A. Genome-wide function of THO/TREX in active genes prevents R-loop-dependent replication obstacles. *EMBO J.* **30**, 3106–3119 (2011).
63. Jimeno, S., Rondón, A. G., Luna, R. & Aguilera, A. The yeast THO complex and mRNA export factors link RNA metabolism with transcription and genome instability. *EMBO J.* **21**, 3526–3535 (2002).
64. Herold, Andrea, Teixeira, Luis Izaurralde, E. Genome-wide analysis of nuclear mRNA export pathways in Drosophila. *EMBO J.* **22**, 2472–2483 (2003).
65. Chávez, S., García-Rubio, M., Prado, F. & Aguilera, A. Hpr1 Is Preferentially Required for Transcription of Either Long or G+C-Rich DNA Sequences in Saccharomyces cerevisiae. *Mol. Cell. Biol.* (2001) doi:10.1128/mcb.21.20.7054-7064.2001.
66. Voynov, Vladimir Verstrepen, Kevin J. Jansen, An Runner, Vanessa M. Buratowski, Stephen Fink, G. R. Genes with internal repeats require the THO complex for transcription. *Proc. Natl. Acad. Sci. U. S. A.* **103**, 14423–14428 (2006).
67. Bonnet, A. & Palancade, B. Intron or no intron: A matter for nuclear pore complexes. *Nucleus* **6**, 455–461 (2015).
68. Bonnet, A., Bretes, H. & Palancade, B. Nuclear pore components affect distinct stages of

intron-containing gene expression. *Nucleic Acids Res.* **43**, 4249–4261 (2015).

69. Soucek, Sharon Zeng, Yi Bellur, Deepti L. Bergkessel, Megan Morris, Kevin J. Deng, Qiudong Duong, Duc Seyfried, Nicholas T. Guthrie, Christine Staley, Jonathan P. Fasken, Milo B. Corbett, A. H. Evolutionarily Conserved Polyadenosine RNA Binding Protein Nab2 Cooperates with Splicing Machinery To Regulate the Fate of Pre-mRNA. *Mol. Cell. Biol.* **36**, 2697–2714 (2016).
70. Taniguchi, I. & Ohno, M. ATP-Dependent Recruitment of Export Factor Aly/REF onto Intronless mRNAs by RNA Helicase UAP56. *Mol. Cell. Biol.* **28**, 601–608 (2008).
71. Andrew M. Ellisdon, Lyudmila Dimitrova, Ed Hurt, and M. S. Structural basis for the assembly and nucleic acid binding of the TREX-2 transcription-export complex. **19**, 328–336 (2012).
72. Carmody, S. R. & Wente, S. R. mRNA nuclear export at a glance. *J. Cell Sci.* **122**, 1933–1937 (2009).
73. Hautbergue, G. M., Hung, M. L., Golovanov, A. P., Lian, L. Y. & Wilson, S. A. Mutually exclusive interactions drive handover of mRNA from export adaptors to TAP. *Proc. Natl. Acad. Sci. U. S. A.* **105**, 5154–5159 (2008).
74. Cabal, Ghislain G. Genovesio, Auguste Rodriguez-Navarro, Susana Zimmer, Christophe Gadal, Olivier Lesne, Annick Buc, Henri Feuerbach-Fournier, Frank Olivo-Marin, Jean Christophe Hurt, E. C. N. SAGA interacting factors confine sub-diffusion of transcribed genes to the nuclear envelope. *Nature* **441**, 770–773 (2006).
75. Jani, Divyang Lutz, Sheila Marshall, Neil J. Fischer, Tamás Köhler, Alwin Ellisdon, Andrew M. Hurt, Ed Stewart, M. Sus1, Cdc31, and the Sac3 CID Region Form a Conserved Interaction Platform that Promotes Nuclear Pore Association and mRNA Export. *Mol. Cell* **33**, 727–737 (2009).
76. Umlauf, David Bonnet, Jacques Waharte, François Fournier, Marjorie Stierle, Matthieu Fischer, Benoit Brino, Laurent Devys, D. T. The human TREX-2 complex is stably associated with the nuclear pore basket. *J. Cell Sci.* **126**, 2656–2667 (2013).
77. Jani, D., Valkov, E. & Stewart, M. Structural basis for binding the TREX2 complex to nuclear pores, GAL1 localisation and mRNA export. *Nucleic Acids Res.* **42**, 6686–6697 (2014).

78. Jani, Divyang, Lutz, Sheila, Hurt, Ed, Laskey, Ronald A.Stewart, Murray Wickramasinghe, V. O. Functional and structural characterization of the mammalian TREX-2 complex that links transcription with nuclear messenger RNA export. *Nucleic Acids Res.* **40**, 4562–4573 (2012).

79. Wickramasinghe, Vihandha O. McMurtrie, Paul I.A. Mills, Anthony D. Takei, Yoshinori Penrhyn-Lowe, Sue Amagase, Yoko Main, Sarah Marr, Jackie Stewart, Murray Laskey, R. A. mRNA Export from Mammalian Cell Nuclei Is Dependent on GANP. *Curr. Biol.* **20**, 25–31 (2010).

80. Wickramasinghe, Vihandha O. Andrews, Robert Ellis, Peter Langford, Cordelia Gurdon, John B. Stewart, Murray Venkitaraman, Ashok R.Laskey, R. A. Selective nuclear export of specific classes of mRNA from mammalian nuclei is promoted by GANP. *Nucleic Acids Res.* **42**, 5059–5071 (2014).

81. Saguez, C., Olesen, J. R. & Jensen, T. H. Formation of export-competent mRNP: Escaping nuclear destruction. *Curr. Opin. Cell Biol.* **17**, 287–293 (2005).

82. Burkard, K. T. D. & Butler, J. S. A Nuclear 3′-5′ Exonuclease Involved in mRNA Degradation Interacts with Poly(A) Polymerase and the hnRNA Protein Npl3p. *Mol. Cell. Biol.* **20**, 604–616 (2000).

83. Libri, Domenico, Dower, Ken, Boulay, Jocelyne Thomsen, Rune Rosbash, Michael Jensen, T. H. Interactions between mRNA Export Commitment, 3′-End Quality Control, and Nuclear Degradation. *Mol. Cell. Biol.* **22**, 8254–8266 (2002).

84. Roth, K. M., Wolf, M. K., Rossi, M. & Butler, J. S. The Nuclear Exosome Contributes to Autogenous Control of NAB2 mRNA Levels. *Mol. Cell. Biol.* **25**, 1577–1585 (2005).

85. Fasken, M. B. & Corbett, A. H. Process or perish: Quality control in mRNA biogenesis. *Nat. Struct. Mol. Biol.* **12**, 482–488 (2005).

86. Tudek, Agnieszka, Schmid, Manfred, Makaras, Marius, Barrass, J. David Beggs, Jean D. Jensen, T. H. A Nuclear Export Block Triggers the Decay of Newly Synthesized Polyadenylated RNA. *Cell Rep.* **24**, 2457-2467.e7 (2018).

87. Battich, N., Stoeger, T. & Pelkmans, L. Control of Transcript Variability in Single Mammalian Cells. *Cell* **163**, 1596–1610 (2015).

88. Horvathova, Ivana Voigt, Franka Kotrys, Anna V.Zhan, YinxiuArtus-Revel, Caroline G.Eglinger, Jan Stadler, Michael B. Giorgetti, Luca Chao, J. A. The Dynamics of mRNA Turnover Revealed by Single-Molecule Imaging in Single Cells. *Mol. Cell* **68**, 615-625.e9 (2017).

89. Mor, A. *et al.* Dynamics of single mRNP nucleocytoplasmic transport and export through the nuclear pore in living cells. *Nat. Cell Biol.* **12**, 543–552 (2010).

90. Bahar Halpern, Keren, Caspi, Inbal Lemze, Doron Levy, Maayan Landen, Shanie Elinav, Eran Ulitsky, Igor Itzkovitz, S. Nuclear Retention of mRNA in Mammalian Tissues. *Cell Rep.* **13**, 2653–2662 (2015).

91. Calapez, Alexandre, Pereira, Henrique M.Calado, Angelo, Braga, José, Rino, J. & Carvalho, Célia, Tavanez, João Paulo Wahle, Elmar, Rosa, Agostinho C., Carmo-Fonseca, M. The intranuclear mobility of messenger RNA binding proteins is ATP dependent and temperature sensitive. *J. Cell Biol.* **159**, 795–805 (2002).

92. Molenaar, C., Abdulle, A., Gena, A., Tanke, H. J. & Dirks, R. W. Poly(A)+ RNAs roam the cell nucleus and pass through speckle domains in transcriptionally active and inactive cells. *J. Cell Biol.* **165**, 191–202 (2004).

93. Shav-tal, Yaron Darzacq, Xavier Shenoy, Shailesh M Fusco, Dahlene Susan, M Spector, David L Singer, Robert H Biology, S. Dynamics of Single mRNPs in Nuclei of Living Cells. **304**, 1797–1800 (2016).

94. Politz, J., Tuft, R. & Pederson, T. Movement of nuclear poly (A) RNA throughout the interchromatin space in living cells. *Curr. Biol.* **9**, 285–291 (1999).

95. Siebrasse, Jan Peter Veith, Roman Dobay, Akos Leonhardt, Heinrich Daneholt, Bertil Kubitscheck, U. Discontinuous movement of mRNP particles in nucleoplasmic regions devoid of chromatin. *Proc. Natl. Acad. Sci. U. S. A.* **105**, 20291–20296 (2008).

96. Casolari, J. M. *et al.* Genome-wide localization of the nuclear transport machinery couples transcriptional status and nuclear organization. *Cell* **117**, 427–439 (2004).

97. Kurshakova, Maria M. Krasnov, Alexey N. Kopytova, Daria V. Shidlovskii, Yulii V. Nikolenko, Julia V. Nabirochkina, Elena N. Spehner, Danièle Schultz, Patrick Tora, Làszlò Georgieva, S. G. SAGA and a novel Drosophila export complex anchor efficient transcription and mRNA

export to NPC. *EMBO J.* **26**, 4956–4965 (2007).

98. Schmid, Manfred Arib, Ghislaine Laemmli, Caroline Nishikawa, Junichi Durussel, Thérèse Laemmli, U. K. Nup-PI: The nucleopore-promoter interaction of genes in yeast. *Mol. Cell* **21**, 379–391 (2006).
99. Taddei, Angela Van Houwe, Griet Hediger, Florence Kalck, Veronique Cubizolles, Fabien Schober, Heiko Gasser, S. M. Nuclear pore association confers optimal expression levels for an inducible yeast gene. *Nature* **441**, 774–778 (2006).
100. Brickner, J. H. & Walter, P. Gene recruitment of the activated INO1 locus to the nuclear membrane. *PLoS Biol.* **2**, (2004).
101. Dieppois, G., Iglesias, N. & Stutz, F. Cotranscriptional Recruitment to the mRNA Export Receptor Mex67p Contributes to Nuclear Pore Anchoring of Activated Genes. *Mol. Cell. Biol.* **26**, 7858–7870 (2006).
102. Holstege, Frank C.P. Jennings, Ezra G. Wyrick, John J. Lee, Tong Ihn Hengartner, Christoph J. Green, Michael R. Golub, Todd R. Lander, Eric S. Young, R. A. Dissecting the regulatory circuitry of a eukaryotic genome. *Cell* **95**, 717–728 (1998).
103. Cabianca, D. S. & Gasser, S. M. Spatial segregation of heterochromatin: Uncovering functionality in a multicellular organism. *Nucleus* **7**, 301–307 (2016).
104. Scholz, Barbara A. Sumida, Noriyuki de Lima, Carolina Diettrich Mallet Chachoua, Ilyas Martino, Mirco Tzelepis, Ilias Nikoshkov, Andrej Zhao, Honglei Mehmood, Rashid Sifakis, Emmanouil G. Bhartiya, Deeksha Göndör, Anita Ohlsson, R. WNT signaling and AHCTF1 promote oncogenic MYC expression through super-enhancer-mediated gene gating. *Nat. Genet.* **51**, 1723–1731 (2019).
105. Harjes, U. One foot in the door: gene gating supports nuclear export of MYC mRNA. *Nat. Rev. Cancer* **20**, 2020 (2019).
106. Winey, M., Yarar, D., Giddings, T. H. & Mastronarde, D. N. Nuclear pore complex number and distribution throughout the Saccharomyces cerevisiae cell cycle by three-dimensional reconstruction from electron micrographs of nuclear envelopes. *Mol. Biol. Cell* **8**, 2119–2132 (1997).
107. Maul, Gerd G Deaven, L. Quantitative determination of nuclear pore complexes in cycling

cells with differing DNA content. *J. Cell Biol.* **73**, 748–760 (1977).

108. Saroufim, Mark Albert Bensidoun, Pierre Raymond, Pascal Rahman, Samir Krause, Matthew R. Oeffinger, Marlene Zenklusen, D. The nuclear basket mediates perinuclear mRNA scanning in budding yeast. *J. Cell Biol.* **211**, 1131–1140 (2015).
109. Rajanala, K. & Nandicoori, V. K. Localization of nucleoporin Tpr to the nuclear pore complex is essential for Tpr mediated regulation of the export of unspliced RNA. *PLoS One* **7**, (2012).
110. Frosst, P., Guan, T., Subauste, C., Hahn, K. & Gerace, L. Tpr is localized within the nuclear basket of the pore complex and has a role in nuclear protein export. *J. Cell Biol.* **156**, 617–630 (2002).
111. Lewis, A., Felberbaum, R. & Hochstrasser, M. A nuclear envelope protein linking nuclear pore basket assembly, SUMO protease regulation, and mRNA surveillance. *J. Cell Biol.* **178**, 813–827 (2007).
112. Niepel, M. *et al.* The nuclear basket proteins Mlp1p and Mlp2p are part of a dynamic interactome including Esc1p and the proteasome. *Mol. Biol. Cell* **24**, 3920–3938 (2013).
113. Goldberg, M. W. & Allen, T. D. High resolution scanning electron microscopy of the nuclear envelope: Demonstration of a new, regular, fibrous lattice attached to the baskets of the nucleoplasmic face of the nuclear pores. *J. Cell Biol.* **119**, 1429–1440 (1992).
114. Kim, Seung Joong Fernandez-Martinez, J., Nudelman, Ilona Shi, Yi Zhang, Wenzhu Raveh, Barak Herricks, Thurston Slaughter, Brian D. Hogan, Joanna A. Upla, P. & Chemmama, Ilan E. Pellarin, Riccardo Echeverria, Ignacia Shivaraju, Manjunatha Chaudhury, Azraa S. Wang, Junjie Williams, Rosemary Unruh, Jay R. Greenberg, Charles H.Jacobs, Erica Y. Yu, Zhiheng De La Cruz, M. Jason Mironska, Roxana Stokes, David L. Aitch, M. P. Integrative structure and functional anatomy of a nuclear pore complex. *Nature* **555**, 475–482 (2018).
115. Niepel, Mario Molloy, Kelly R. Williams, Rosemary Farrc, Julia C. Meinema, Anne C. Vecchietti, Nicholas Cristea, Ileana M. Chait, Brian T. Rout, Michael P. Strambio-De Castillia, C. The nuclear basket proteins Mlp1p and Mlp2p are part of a dynamic interactome including Esc1p and the proteasome. *Mol. Biol. Cell* **24**, 3920–3938 (2013).
116. Rajoo, S., Vallotton, P., Onischenko, E. & Weis, K. Stoichiometry and compositional

plasticity of the yeast nuclear pore complex revealed by quantitative fluorescence microscopy. *Proc. Natl. Acad. Sci. U. S. A.* **115**, E3969–E3977 (2018).

117. Benoıt Palancade, Michela Zuccolo, Sophie Loeillet, Alain Nicolas, A. & Doye, V. Pml39, a Novel Protein of the Nuclear Periphery Required for Nuclear Retention of Improper Messenger Ribonucleoparticles. *Mol. Biol. Cell* **16**, 5356–5372 (2005).
118. Iglesias, Nahid Tutucci, Evelina Gwizdek, Carole Vinciguerra, Patrizia Von Dach, Elodie Corbett, Anita H. Dargemont, Catherine Stutz, F. Ubiquitin-mediated mRNP dynamics and surveillance prior to budding yeast mRNA export. *Genes Dev.* **24**, 1927–1938 (2010).
119. Sydorskyy, Y. Srikumar, T. Jeram, S. M. Wheaton, S. Vizeacoumar, F. J. Makhnevych, T. Chong, Y. T. Gingras, A.-C. Raught, B. A Novel Mechanism for SUMO System Control: Regulated Ulp1 Nucleolar Sequestration. *Mol. Cell. Biol.* **30**, 4452–4462 (2010).
120. Folz, Hanne Nino, Carlos A. Taranum, Surayya Caesar, Stefanie Latta, Lorenz Waharte, François Salamero, Jean Schlenstedt, Gabriel Dargemont, C. SUMOylation of the nuclear pore complex basket is involved in sensing cellular stresses. *J. Cell Sci.* **132**, 1–11 (2019).
121. Walther, T. C. *et al.* The nucleoporin Nup153 is required for nuclear pore basket formation, nuclear pore complex anchoring and import of a subset of nuclear proteins. *EMBO J.* **20**, 5703–5714 (2001).
122. Buchwalter, A. L., Liang, Y. & Hetzer, M. W. Nup50 is required for cell differentiation and exhibits transcription-dependent dynamics. *Mol. Biol. Cell* **25**, 2472–2484 (2014).
123. Green, D. M., Johnson, C. P., Hagan, H. & Corbett, A. H. The C-terminal domain of myosin-like protein 1 (Mlp1p) is a docking site for heterogeneous nuclear ribonucleoproteins that are required for mRNA export. *Proc. Natl. Acad. Sci. U. S. A.* **100**, 1010–1015 (2003).
124. Grant, R. P. *et al.* Structure of the N-Terminal Mlp1-Binding Domain of the Saccharomyces cerevisiae mRNA-Binding Protein, Nab2. *J. Mol. Biol.* **376**, 1048–1059 (2008).
125. Fasken, M. B., Stewart, M. & Corbett, A. H. Functional significance of the interaction between the mRNA-binding protein, Nab2, and the nuclear pore-associated protein, mlp1, in mRNA export. *J. Biol. Chem.* **283**, 27130–27143 (2008).
126. Fasken, Milo B. Corbett, Anita H. Stewart, M. Structure–function relationships in the Nab2 polyadenosine-RNA binding Zn finger protein family. *Protein Sci.* **28**, 513–523 (2019).

127. Vinciguerra, P., Iglesias, N., Camblong, J., Zenklusen, D. & Stutz, F. Perinuclear Mlp proteins downregulate gene expression in response to a defect in mRNA export. *EMBO J.* **24**, 813–823 (2005).

128. Coyle, J. H., Bor, Y. C., Rekosh, D. & Hammarskjold, M. L. The Tpr protein regulates export of mRNAs with retained introns that traffic through the Nxf1 pathway. *Rna* **17**, 1344–1356 (2011).

129. Galy, Vincent Gadal, Olivier Fromont-Racine, Micheline Romano, Alper Jacquier, A. N. Nuclear Retention of Unspliced mRNAs in Yeast Is Mediated by Perinuclear Mlp1. *Cell* **116**, 63–73 (2004).

130. Benoît Palancade , Michela Zuccolo, Sophie Loeillet, Alain Nicolas, V. D. Pml39, a Novel Protein of the Nuclear Periphery Required for Nuclear Retention of Improper Messenger Ribonucleoparticles□. *Mol. Biol. Cell* **16**, 5356–5372 (2005).

131. Krull, Sandra Dörries, Julia Boysen, Björn Reidenbach, Sonja Magnius, Lars Norder, Helene Thyberg, Johan Cordes, V. C. Protein Tpr is required for establishing nuclear pore-associated zones of heterochromatin exclusion. *EMBO J.* **29**, 1659–1673 (2010).

132. Aksenova, Vasilisa Smith, Alexandra Lee, Hangnoh Bhat, Prasanna Esnault, Caroline Chen, Shane Iben, James Kaufhold, Ross Yau, Ka Chun Echeverria, Carlos Fontoura, Beatriz Arnaoutov, Alexei Dasso, M. Nucleoporin TPR is an integral component of the TREX-2 mRNA export pathway. *Nat. Commun.* **11**, 1–13 (2020).

133. Lee, Eliza S. Wolf, Eric J. Ihn, Sean S.J. Smith, Harrison W. Emili, Andrew Palazzo, A. F. TPR is required for the efficient nuclear export of mRNAs and lncRNAs from short and intron-poor genes. *Nucleic Acids Res.* **48**, 11645–11663 (2020).

134. Fazal, Furqan M. Han, Shuo Parker, Kevin R. Kaewsapsak, Pornchai Xu, Jin Boettiger, Alistair N. Chang, Howard Y. Ting, A. Y. Atlas of Subcellular RNA Localization Revealed by APEX-Seq. *Cell* **178**, 473-490.e26 (2019).

135. Fish, Lisa Navickas, Albertas Culbertson, Bruce Xu, Yichen Nguyen, Hoang C.B. Zhang, Steven Hochman, Myles Okimoto, Ross Dill, Brian D. Molina, Henrik Najafabadi, Hamed S. Alarcón, Claudio Ruggero, Davide Goodarzi, H. Nuclear TARBP2 Drives Oncogenic Dysregulation of RNA Splicing and Decay. *Mol. Cell* **75**, 967-981.e9 (2019).

136. Soheilypour, M. & Mofrad, M. R. K. Regulation of RNA-binding proteins affinity to export receptors enables the nuclear basket proteins to distinguish and retain aberrant mRNAs. *Sci. Rep.* **6**, 1–11 (2016).

137. Huang, Y., Yario, T. A. & Steitz, J. A. 2004A molecular link between SR protein dephosphorylation and mRNA export.Proceedings of the National Academy of Sciences of the United States of America.pdf. **101**, 2–6 (2004).

138. Reichert, V. L., Le Hir, H., Jurica, M. S. & Moore, M. J. 5′ Exon interactions within the human spliceosome establish a framework for exon junction complex structure and assembly. *Genes Dev.* **16**, 2778–2791 (2002).

139. Rodrigues, João P. Rode, Michaela Gatfield, David Blencowe, Benjamin J. Carmo-Fonseca, Maria Izaurralde, E. REF proteins mediate the export of spliced and unspliced mRNAs from the nucleus. *Proc. Natl. Acad. Sci. U. S. A.* **98**, 1030–1035 (2001).

140. Goldberg, M. W. & Allen, T. D. High resolution scanning electron microscopy of the nuclear envelope: Demonstration of a new, regular, fibrous lattice attached to the baskets of the nucleoplasmic face of the nuclear pores. *J. Cell Biol.* **119**, 1429–1440 (1992).

141. Maeshima, Kazuhiro Yahata, Kazuhide Sasaki, Yoko Nakatomi, Reiko Tachibana, Taro Hashikawa, Tsutomu Imamoto, Fumio Imamoto, N. Cell-cycle-dependent dynamics of nuclear pores: Pore-free islands and lamins. *J. Cell Sci.* **119**, 4442–4451 (2006).

142. Kittisopikul, M., Shimi, T., Tatli, M., Tran, J.R., Zheng, Y., Medalia, O., Jaqaman, K., Adam, S. A. & Goldman, R. D. Nuclear Lamins A/C and B1 Provide a Structural Framework That Organizes and Anchors Nuclear Pore Complexes. *bioRxiv* 2020.04.03.022798 (2020).

143. Xie, Wei Chojnowski, Alexandre Boudier, Thomas Lim, John S.Y. Ahmed, Sohail Ser, Zheng Stewart, Colin Burke, B. A-type Lamins Form Distinct Filamentous Networks with Differential Nuclear Pore Complex Associations. *Curr. Biol.* **26**, 2651–2658 (2016).

144. Kosova, Buket Panté, Nelly Rollenhagen, Christiane Podtelejnikov, Alexandre Mann, Matthias Aebi, Ueli Hurt, E. Mlp2p, a component of nuclear pore attached intranuclear filaments, associates with Nic96p. *J. Biol. Chem.* **275**, 343–350 (2000).

145. Strambio-de-Castillia, Caterina Blobel, Günter Rout, M. P. Proteins connecting the nuclear pore complex with the nuclear interior. *J. Cell Biol.* **144**, 839–855 (1999).

146. Fischer, Tamás Rodríguez-Navarro, Susana Pereira, Gislene Rácz, Attila Schiebel, Elmar Hurt, E. Yeast centrin Cdc31 is linked to the nuclear mRNA export machinery. *Nat. Cell Biol.* **6**, 840–848 (2004).

147. Niepel, M., Strambio-de-Castillia, C., Fasolo, J., Chait, B. T. & Rout, M. P. The nuclear pore complex-associated protein, Mlp2p, binds to the yeast spindle pole body and promotes its efficient assembly. *J. Cell Biol.* **170**, 225–235 (2005).

148. Gallardo, P., Salas-Pino, S. & Daga, R. R. A new role for the nuclear basket network. *Microb. Cell* **4**, 423–425 (2017).

149. Rajanala, Kalpana Sarkar, Anshuk Jhingan, Gagan Deep Priyadarshini, Raina Jalan, Manisha Sengupta, Sagar Nandicoori, V. K. Phosphorylation of nucleoporin Tpr governs its differential localization and is required for its mitotic function. *J. Cell Sci.* **127**, 3505–3520 (2014).

150. Colin P. De Souza,* Shahr B. Hashmi, T. N., Berl Oakley, and S. A. O. & *Department. Mlp1 Acts as a Mitotic Scaffold to Spatially Regulate Spindle Assembly Checkpoint Proteins in Aspergillus nidulans Colin. *Mol. Biol. Cell* **20**, 2673–2683 (2009).

151. Johansen, Jø. & Johansen, K. M. The spindle matrix through the cell cycle in Drosophila. *Fly (Austin).* **3**, 215–222 (2009).

152. Salas-Pino, S., Gallardo, P., Barrales, R. R., Braun, S. & Daga, R. R. The fission yeast nucleoporin Alm1 is required for proteasomal degradation of kinetochore components. *J. Cell Biol.* **216**, 3591–3608 (2017).

153. Tatebe, H. & Yanagida, M. Cut8, essential for anaphase, controls localization of 26S proteasome, facilitating destruction of cyclin and Cut2. *Curr. Biol.* **10**, 1329–1338 (2000).

154. Wilkinson, C. R. M., Penney, M., McGurk, G., Wallace, M. & Gordon, C. The 26S proteasome of the fission yeast Schizosaccharomyces pombe. *Philos. Trans. R. Soc. B Biol. Sci.* **354**, 1523–1532 (1999).

155. Kupiec, M. Biology of telomeres: Lessons from budding yeast. *FEMS Microbiol. Rev.* **38**, 144–171 (2014).

156. Pascual-Garcia, P. & Capelson, M. The nuclear pore complex and the genome: organizing and regulatory principles. *Curr. Opin. Genet. Dev.* **67**, 142–150 (2021).

157. Feuerbach, Frank Galy, Vincent Trelles-Sticken, Edgar Fromont-Racine, Micheline Jacquier, Alain Gilson, Eric Olivo-Marin, Jean Christophe Scherthan, H. N. Nuclear architecture and spatial positioning help establish transcriptional states of telomeres in yeast. *Nat. Cell Biol.* **4**, 214–221 (2002).

158. Galy, Vincent Olivo-Marin, Jean Christophe Scherthan, Harry Doye, Valerie Rascalou, N. N. Nuclear pore complexes in the organization of silent telomeric chromatin. *Nature* **403**, 108–112 (2000).

159. Mizuguchi, T., Barrowman, J. & Grewal, S. I. S. Chromosome domain architecture and dynamic organization of the fission yeast genome. *FEBS Lett.* **589**, 2975–2986 (2015).

160. Hediger, F., Neumann, F. R., Van Houwe, G., Dubrana, K. & Gasser, S. M. Live imaging of telomeres: yKu and Sir proteins define redundant telomere-anchoring pathways in yeast. *Curr. Biol.* **12**, 2076–2089 (2002).

161. Taddei, A. & Gasser, S. M. Structure and function in the budding yeast nucleus. *Genetics* **192**, 107–129 (2012).

162. Gasser, S. M., Hediger, F., Taddei, A., Neumann, F. R. & Gartenberg, M. R. The function of telomere clustering in yeast: The circe effect. *Cold Spring Harb. Symp. Quant. Biol.* **69**, 327–337 (2004).

163. Andrulis, Erik D. Zappulla, David C. Ansari, Athar Perrod, Severine Laiosa, Catherine V. Gartenberg, Marc R. Sternglanz, R. Esc1, a Nuclear Periphery Protein Required for Sir4-Based Plasmid Anchoring and Partitioning. *Mol. Cell. Biol.* **22**, 8292–8301 (2002).

164. Bühler, M. & Gasser, S. M. Silent chromatin at the middle and ends: Lessons from yeasts. *EMBO J.* **28**, 2149–2161 (2009).

165. Hediger, F., Dubrana, K. & Gasser, S. M. Myosin-like proteins 1 and 2 are not required for silencing or telomere anchoring, but act in the Tel1 pathway of telomere length control. *J. Struct. Biol.* **140**, 79–91 (2002).

166. Aguilera, Paula Whalen, Jenna Minguet, Christopher Churikov, Dmitri Freudenreich, Catherine Simon, Marie Noëlle Géli, V. The nuclear pore complex prevents sister chromatid recombination during replicative senescence. *Nat. Commun.* **11**, 1–13 (2020).

167. Clerici, M., Mantiero, D., Guerini, I., Lucchini, G. & Longhese, M. P. The Yku70-Yku80

complex contributes to regulate double-strand break processing and checkpoint activation during the cell cycle. *EMBO Rep.* **9**, 810–818 (2008).

168. Mekhail, K. & Moazed, D. The nuclear envelope in genome organization, expression and stability. *Nat. Rev. Mol. Cell Biol.* **11**, 317–328 (2010).
169. Freudenreich, C. H. & Su, X. A. Relocalization of DNA lesions to the nuclear pore complex. *FEMS Yeast Res.* **16**, 1–9 (2016).
170. D'Angelo Marcela Raices and Maximiliano d'Angelo. Nuclear Pore Complexes and Regulation of Gene Expression Marcela. *Opin. Cell Biol.* **46**, 26–32 (2018).
171. Krogan, Nevan J Lam, Mandy H Y Fillingham, Jeffrey Keogh, Michael-christopher Gebbia, Marinella Li, Joyce Datta, Nira Cagney, Gerard Buratowski, Stephen Emili, Andrew Greenblatt, Jack F Ms, O. Proteasome involvment in the Repair of DNA Double-Strand Breaks. **16**, 1027–1034 (2004).
172. Gudmundsdottir, K., Lord, C. J. & Ashworth, A. The proteasome is involved in determining differential utilization of double-strand break repair pathways. *Oncogene* **26**, 7601–7606 (2007).
173. Zhao, X., Wu, C. Y. & Blobel, G. Mlp-dependent anchorage and stabilization of a desumoylating enzyme is required to prevent clonal lethality. *J. Cell Biol.* **167**, 605–611 (2004).
174. Duheron, V., Nilles, N., Pecenko, S., Martinelli, V. & Fahrenkrog, B. Localisation of Nup153 and SENP1 to nuclear pore complexes is required for 53BP1-mediated DNA double-strand break repair. *J. Cell Sci.* **130**, 2306–2316 (2017).
175. Christopher D. Putnam, Anjana Srivatsan, Rahul V. Nene, Sandra L. Martinez, Sarah P. Clotfelter, Sara N. Bell1, Steven B. Somach, Jorge E.S. de Souza, Andre´ F. Fonseca, S. J. de S. & R. D. K. A genetic network that suppresses genome rearrangements in Saccharomyces cerevisiae and contains defects in cancers. *Nat. Commun.* **48**, 829–834 (2016).
176. García-Benítez, F., Gaillard, H. & Aguilera, A. Physical proximity of chromatin to nuclear pores prevents harmful R loop accumulation contributing to maintain genome stability. *Proc. Natl. Acad. Sci. U. S. A.* **114**, 10942–10947 (2017).
177. Bermejo, Rodrigo Capra, Thelma Jossen, Rachel Colosio, Arianna Frattini, Camilla

Carotenuto, Walter Cocito, Andrea Doksani, Ylli Klein, Hannah Gómez-González, Belén Aguilera, Andrés Katou, Yuki Shirahige, Katsuhiko Foiani, M. The replication checkpoint protects fork stability by releasing transcribed genes from nuclear pores. *Cell* **146**, 233–246 (2011).

178. El Kaderi, B., Medler, S., Raghunayakula, S. & Ansari, A. Gene looping is conferred by activator-dependent interaction of transcription initiation and termination machineries. *J. Biol. Chem.* **284**, 25015–25025 (2009).
179. Moabbi, A. M., Agarwal, N., El Kaderi, B. & Ansari, A. Role for gene looping in intron-mediated enhancement of transcription. *Proc. Natl. Acad. Sci. U. S. A.* **109**, 8505–8510 (2012).
180. Sun, J., Shi, Y. & Yildirim, E. The Nuclear Pore Complex in Cell Type-Specific Chromatin Structure and Gene Regulation. *Trends Genet.* **35**, 579–588 (2019).
181. O'Sullivan, Justin M. Tan-Wong, S. M. & Morillon, Antonin Lee, Barbara Coles, Joel Mellor, Jane Proudfoot, N. J. Gene loops juxtapose promoters and terminators in yeast. *Nat. Genet.* **36**, 1014–1018 (2004).
182. Tan-Wong, S. M., Wijayatilake, H. D. & Proudfoot, N. J. Gene loops function to maintain transcriptional memory through interaction with the nuclear pore complex. *Genes Dev.* **23**, 2610–2624 (2009).
183. Light, W. H., Brickner, D. G., Brand, V. R. & Brickner, J. H. Interaction of a DNA zip code with the nuclear pore complex promotes H2A.Z incorporation and INO1 transcriptional memory. *Mol. Cell* **40**, 112–125 (2010).
184. Yoshida, Takahito Shimada, Kenji Oma, Yukako Kalck, Véronique Akimura, Kazumi Taddei, Angela Iwahashi, Hitoshi Kugou, Kazuto Ohta, Kunihiro Gasser, Susan M. Harata, M. Actin-related protein Arp6 influences H2A.Z-dependent and -independent gene expression and links ribosomal protein genes to nuclear pores. *PLoS Genet.* **6**, 10–17 (2010).
185. Cho, U. H. & Hetzer, M. W. Nuclear Periphery Takes Center Stage: The Role of Nuclear Pore Complexes in Cell Identity and Aging. *Neuron* **106**, 899–911 (2020).
186. Ori, Alessandro Banterle, Niccolò Iskar, Murat Andrés-Pons, Amparo Escher, Claudia Khanh Bui, Huy Sparks, Lenore Solis-Mezarino, Victor Rinner, Oliver Bork, Peer Lemke, Edward A.

Beck, M. Cell type-specific nuclear pores: A case in point for context-dependent stoichiometry of molecular machines. *Mol. Syst. Biol.* **9**, (2013).

187. Raices, M. & D'Angelo, M. A. Nuclear pore complex composition: A new regulator of tissue-specific and developmental functions. *Nat. Rev. Mol. Cell Biol.* **13**, 687–699 (2012).
188. Rabut, G., Lénárt, P. & Ellenberg, J. Dynamics of nuclear pore complex organization through the cell cycle. *Curr. Opin. Cell Biol.* **16**, 314–321 (2004).
189. Makhnevych, T., Lusk, C. P., Anderson, A. M., Aitchison, J. D. & Wozniak, R. W. Cell Cycle Regulated Transport Controlled by Alterations in the Nuclear Pore Complex. *Cell* **115**, 813–823 (2003).
190. Joana Borlido, Stephen Sakuma, Marcela Raices, Florent Carrette, Roberto Tinoco, Linda M. Bradley, and M. A. D. Nuclear pore complex-mediated modulation of TCR signaling is required for naïve CD4+ T cell homeostasis. *Physiol. Behav.* **176**, 139–148 (2018).
191. Jacinto, Filipe V. Benner, Chris Hetzer, M. W. The nucleoporin Nup153 regulates embryonic stem cell pluripotency through gene silencing. *Genes Dev.* **29**, 1224–1238 (2015).
192. Zhang, Xianqin Chen, Shenghan Yoo, Shin Chakrabarti, Susmita Zhang, Teng Ke, Tie Oberti, Carlos Yong, Sandro L. Fang, Fang Li, Lin de la Fuente, Roberto Wang, Lejin Chen, Qiuyun Wang, Q. K. Mutation in Nuclear Pore Component NUP155 Leads to Atrial Fibrillation and Early Sudden Cardiac Death. *Cell* **135**, 1017–1027 (2008).
193. Parrott, Benjamin B. Chiang, Y. & Hudson, Alicia Sarkar, Angshuman Guichet, Antoine Schulz, C. Nucleoporin98-96 function is required for transit amplification divisions in the germ line of Drosophila melanogaster. *PLoS One* **6**, (2011).
194. Faria, Ana M.C. Levay, Agata Wang, Yaming Kamphorst, Alice O. Rosa, Magda L.P. Nussenzveig, Daniel R. Balkan, Wayne Chook, Yuh Min Levy, David E.Fontoura, B. M. A. The nucleoporin Nup96 is required for proper expression of interferon-regulated proteins and functions. *Immunity* **24**, 295–304 (2006).
195. Liang, Y., Franks, T. M., Marchetto, M. C., Gage, F. H. & Hetzer, M. W. Dynamic Association of NUP98 with the Human Genome. *PLoS Genet.* **9**, (2013).
196. Yonashiro, Ryo Sugiura, Ayumu Miyachi, Misako Fukuda, Toshifumi Matsushita, Nobuko Inatome, Ryoko Ogata, Yoshinobu Suzuki, Takehiro Dohmae, Naoshi Yanagi, S. The Mobile

FG Nucleoporin Nup98 Is a Cofactor for Crm1-dependent Protein Export. *Mol. Biol. Cell* **20**, 4524–4530 (2009).

197. Pascual-Garcia, P. & Capelson, M. Nuclear pores in genome architecture and enhancer function. *Curr. Opin. Cell Biol.* **58**, 126–133 (2019).
198. Sirri, V., Urcuqui-Inchima, S., Roussel, P. & Hernandez-Verdun, D. Nucleolus: The fascinating nuclear body. *Histochem. Cell Biol.* **129**, 13–31 (2008).
199. Haber, J. Role for perinuclear chromosome tethering in maintenance of genome stability Karim. *Nature* **456**, 667–670 (2013).
200. Delavoie, F., Soldan, V., Rinaldi, D., Dauxois, J. Y. & Gleizes, P. E. The path of pre-ribosomes through the nuclear pore complex revealed by electron tomography. *Nat. Commun.* **10**, (2019).
201. Carmody, S. R., Tran, E. J., Apponi, L. H., Corbett, A. H. & Wente, S. R. The Mitogen-Activated Protein Kinase Slt2 Regulates Nuclear Retention of Non-Heat Shock mRNAs during Heat Shock-Induced Stress. *Mol. Cell. Biol.* **30**, 5168–5179 (2010).
202. Azra Lari, Farzin Farzam, Pierre Bensidoun, Marlene Oeffinger, Daniel Zenklusen, David Grunwald2, B. M. Live-Cell Imaging of mRNP-NPC Interactions in Budding Yeast. *Physiol. Behav.* **176**, 139–148 (2017).
203. Aitchison, J. D. & Rout, M. P. The yeast nuclear pore complex and transport through it. *Genetics* **190**, 855–883 (2012).
204. Sood, V. & Brickner, J. H. Nuclear pore interactions with the genome. *Curr. Opin. Genet. Dev.* **25**, 43–49 (2014).
205. Dean, K. M. & Palmer, A. E. Advances in fluorescence labeling strategies for dynamic cellular imaging. *Nat. Chem. Biol.* **10**, 512–523 (2014).
206. Haim, L., Zipor, G., Aronov, S. & Gerst, J. E. A genomic integration method to visualize localization of endogenous mRNAs in living yeast. *Nat. Methods* **4**, 409–412 (2007).
207. Hocine, S., Raymond, P., Zenklusen, D., Chao, J. A. & Singer, R. H. Single-molecule analysis of gene expression using two-color RNA labeling in live yeast. *Nat. Methods* **10**, 119–121 (2013).
208. Zenklusen, D., Larson, D. R. & Singer, R. H. Single-RNA counting reveals alternative modes

of gene expression in yeast. *Nat. Struct. Mol. Biol.* **15**, 1263–1271 (2008).

209. Buxbaum, A. R., Haimovich, G. & Singer, R. H. In the right place at the right time: Visualizing and understanding mRNA localization. *Nat. Rev. Mol. Cell Biol.* **16**, 95–109 (2015).

210. Daigle, N. & Ellenberg, J. λN-GFP: An RNA reporter system for live-cell imaging. *Nat. Methods* **4**, 633–636 (2007).

211. Lange, Susanne Katayama, Yoshihiko Schmid, Maria Burkacky, Ondrej Brauchle, Christoph Lamb, Don C. Jansen, R. P. Simultaneous transport of different localized mRNA species revealed by live-cell imaging. *Traffic* **9**, 1256–1267 (2008).

212. Brodsky, A. S. & Silver, P. A. Pre-mRNA processing factors are required for nuclear export. *Rna* **6**, 1737–1749 (2000).

213. Urbanek, M. O., Galka-Marciniak, P., Olejniczak, M. & Krzyzosiak, W. J. 1083-1095 RNA imaging in living cells - Methods and applications. *RNA Biol.* **11**, 1083–1095 (2014).

214. Bajon, E., Laterreur, N. & Wellinger, R. J. A Single Templating RNA in Yeast Telomerase. *Cell Rep.* **12**, 441–448 (2015).

215. Lenstra, T. L., Coulon, A., Chow, C. C. & Larson, D. R. Single-Molecule Imaging Reveals a Switch between Spurious and Functional ncRNA Transcription. *Mol. Cell* **60**, 597–610 (2015).

216. Smith, Carlas Lari, Azra Derrer, C. P. & Ouwehand, Anette Rossouw, Ammeret Huisman, Maximiliaan Dange, Thomas Hopman, Mark Joseph, Aviva Zenklusen, Daniel Weis, Karsten Grunwald, David Montpetit, B. In vivo single-particle imaging of nuclear mRNA export in budding yeast demonstrates an essential role for Mex67p. *J. Cell Biol.* **211**, 1121–1130 (2015).

217. Lui, Jennifer Castelli, Lydia M. Pizzinga, Mariavittoria Simpson, Clare E. Hoyle, Nathaniel P. Bailey, Kathryn L. Campbell, Susan G. Ashe, M. P. Granules harboring translationally active mRNAs provide a platform for P-body formation following stress. *Cell Rep.* **9**, 944–954 (2014).

218. Halstead, James M. Lionnet, Timothée Wilbertz, Johannes H. Wippich, Frank Ephrussi, Anne Singer, Robert H. Chao, J. A. An RNA biosensor for imaging the first round of

translation from single cells to living animals. *Science (80-. ).* **347**, 1367–1370 (2015).

219. Chao, J. A., Patskovsky, Y., Almo, S. C. & Singer, R. H. Structural basis for the coevolution of a viral RNA-protein complex. *Nat. Struct. Mol. Biol.* **15**, 103–105 (2008).

220. Wu, B., Chao, J. A. & Singer, R. H. Fluorescence fluctuation spectroscopy enables quantitative imaging of single mRNAs in living cells. *Biophys. J.* **102**, 2936–2944 (2012).

221. Wu, Bin Miskolci, Veronika Sato, Hanae Tutucci, Evelina Kenworthy, Charles A. Donnelly, Sara K. Yoon, Young J. Cox, Dianne Singer, Robert H. Hodgson, L. Synonymous modification results in highfidelity gene expression of repetitive protein and nucleotide sequences. *Genes Dev.* **29**, 876–886 (2015).

222. Wu, B., Chen, J. & Singer, R. H. Background free imaging of single mRNAs in live cells using split fluorescent proteins. *Sci. Rep.* **4**, 11–13 (2014).

223. Lionnet, Timothée Czaplinski, Kevin Darzacq Xavier Shav-Tal, Yaron Wells, Amber L. Chao, Jeffrey A. Park, Hye Yoon De Turris, Valeria Lopez-Jones, Melissa Singer, R. H. A transgenic mouse for in vivo detection of endogenous labeled mRNA. *Nat. Methods* **8**, 165–170 (2011).

224. Garcia, J. F. & Parker, R. MS2 coat proteins bound to yeast mRNAs block 5′ to 3′ degradation and trap mRNA decay products: Implications for the localization of mRNAs by MS2-MCP system. *Rna* **21**, 1393–1395 (2015).

225. Amrani, N., Minet, M., Le Gouar, M., Lacroute, F. & Wyers, F. Yeast Pab1 interacts with Rna15 and participates in the control of the poly(A) tail length in vitro. *Mol. Cell. Biol.* **17**, 3694–3701 (1997).

226. Beelman, C. A. & Parker, R. Differential effects of translational inhibition in cis and in trans on the decay of the unstable yeast MFA2 mRNA. *J. Biol. Chem.* **269**, 9687–9692 (1994).

227. Güldener Ulrich, Heck Susanne, Fiedler, Thomas, Beinhauer Jens , Hegemann, J. H. A new efficient gene disruption cassette for repeated use in budding yeast. *Nucleic Acids Res.* **24**, 2519–2524 (1996).

228. Shulga, N., Mosammaparast, N., Wozniak, R. & Goldfarb, D. S. Yeast nucleoporins involved in passive nuclear envelope permeability. *J. Cell Biol.* **149**, 1027–1038 (2000).

229. Leslie, D. M., Timney, B., Rout, M. P. & Aitchison, J. D. Studying nuclear protein import in

yeast. *Methods* **39**, 291–308 (2006).

230. Lee, S., Lim, W. A. & Thorn, K. S. Improved Blue, Green, and Red Fluorescent Protein Tagging Vectors for S. cerevisiae. *PLoS One* **8**, 4–11 (2013).

231. Abrahamsson, Sara Chen, Jiji Hajj, Bassam Stallinga, Sjoerd Katsov, Alexander Y. Wisniewski, Jan Mizuguchi, Gaku Soule, Pierre Mueller, Florian Darzacq, Claire Dugast Darzacq, Xavier Wu, Carl Bargmann, Cornelia Agard, David A. Dahan, Maxime Gustafsson, M. G. L. Fast multicolor 3D imaging using aberration-corrected multifocus microscopy. *Nat. Methods* **10**, 60–63 (2013).

232. Smith, C. S. *et al.* Nuclear accessibility of ß-actin mRNA is measured by 3D single-molecule real-time tracking. *J. Cell Biol.* **209**, 609–619 (2015).

233. Mortensen, K. I., Churchman, L. S., Spudich, J. A. & Flyvbjerg, H. Optimized localization analysis for single-molecule tracking and super-resolution microscopy. *Nat. Methods* **7**, 377–381 (2010).

234. Thompson, R. E., Larson, D. R. & Webb, W. W. Precise nanometer localization analysis for individual fluorescent probes. *Biophys. J.* **82**, 2775–2783 (2002).

235. Ma, J. *et al.* High-resolution three-dimensional mapping of mRNA export through the nuclear pore. *Nat. Commun.* **4**, 1–9 (2013).

236. Larson, Daniel R. Fritzsch, Christoph Sun, Liang Meng, Xiuhau Lawrence, David S. Singer, R. H. Direct observation of frequency modulated transcription in single cells using light activation. *Elife* **2013**, 1–20 (2013).

237. Steinberg, Gero Schuster, Martin Theisen, Ulrike Kilaru, Sreedhar Forge, Andrew Martin Urdiroz, M. Motor-driven motility of fungal nuclear pores organizes chromosomes and fosters nucleocytoplasmic transport. *J. Cell Biol.* **198**, 343–355 (2012).

238. Alber, Frank Dokudovskaya, Svetlana Veenhoff, Liesbeth M. Zhang, Wenzhu Kipper, Julia Devos, Damien Suprapto, Adisetyantari Karni-Schmidt, Orit Williams, Rosemary Chait, Brian T. Sali, Andrej Rout, M. P. The molecular architecture of the nuclear pore complex. *Nature* **450**, 695–701 (2007).

239. Mi, L., Goryaynov, A., Lindquist, A., Rexach, M. & Yang, W. Quantifying Nucleoporin Stoichiometry Inside Single Nuclear Pore Complexes In vivo. *Sci. Rep.* **5**, 1–8 (2015).

240. Kiseleva, E., Goldberg, M. W., Allen, T. D. & Akey, C. W. Active nuclear pore complexes in Chironomus: Visualization of transporter configurations related to mRNP export. *J. Cell Sci.* **111**, 223–236 (1998).

241. Neumüller, Ralph A. Gross, Thomas Samsonova, Anastasia A. Vinayagam, Arunachalam Buckner, Michael Founk, Karen Hu, Yanhui Sharifpoor, Sara Rosebrock, Adam P. Andrews, Brenda Winston, Fred Perrimon, N. Conserved regulators of nucleolar size revealed by global phenotypic analyses. *Sci. Signal.* **6**, 1–31 (2013).

242. Aguilar, Lisbeth Carolina Paul, Biplab Reiter, Taylor Gendron, Louis Arul Nambi Rajan, Arvind Montpetit, Rachel Trahan, Christian Pechmann, Sebastian Oeffinger, Marlene Montpetit, B. Altered rRNA processing disrupts nuclear RNA homeostasis via competition for the poly(A)-binding protein Nab2. *Nucleic Acids Res.* **48**, 11675–11694 (2020).

243. Paul, B. & Montpetit, B. Altered RNA processing and export lead to retention of mRNAs near transcription sites and nuclear pore complexes or within the nucleolus. *Mol. Biol. Cell* **27**, 2742–2756 (2016).

244. Mészáros, Noémi Cibulka, Jakub Mendiburo, Maria Jose Romanauska, Anete Schneider, Maren Köhler, A. Nuclear Pore Basket Proteins Are Tethered to the Nuclear Envelope and Can Regulate Membrane Curvature. *Dev. Cell* **33**, 285–298 (2015).

245. Moore, M. S. J. and M. J. Pre-mRNA Splicing: Awash in a Sea of Proteins. *Mol. Cell,* **12**, 5–14, (2003).

246. Shao, Wei Ding, Zhan Zheng, Zeng Zhang Shen, Ji Jia Shen, Yu Xian Pu, Jia Fan, Yu Jie Query, Charles C. Xu, Y. Z. Prp5-Spt8/Spt3 interaction mediates a reciprocal coupling between splicing and transcription. *Nucleic Acids Res.* **48**, 5799–5813 (2020).

247. Carneiro, Tiago Celia Carvalho, Jose Braga, Jose Rino, Laura Milligan Tollervey, D. C.-F. M. Inactivation of Cleavage Factor I Components Rna14p and Rna15p Induces Sequestration of Small Nucleolar Ribonucleoproteins at Discrete. *Mol. Biol. Cell* **18**, 3250–3263 (2007).

248. Dziembowski, Andrzej Ventura, Ana Paula Rutz, Berthold Caspary, Friederike Faux, Céline Halgand, Frédéric Laprévote, Olivier Séraphin, B. Proteomic analysis identifies a new complex required for nuclear pre-mRNA retention and splicing. *EMBO J.* **23**, 4847–4856 (2004).

249. Panse, V. G., Küster, B., Gerstberger, T. & Hurt, E. Unconventional tethering of Ulp1 to the transport channel of the nuclear pore complex by karyopherins. *Nat. Cell Biol.* **5**, 21–27 (2003).

250. Fischer, Â Stra, Katja Rodriguez-navarro, Susana Oppizzi, Marisa Ihrig, Petra Lechner, Johannes Hurt, E. The mRNA export machinery requires the novel Sac3p–Thp1p complex to dock at the nucleoplasmic entrance of the nuclear pores. **21**, (2002).

251. Derrer, Carina Patrizia Mancini, Roberta Vallotton, Pascal Huet, Sébastien Weis, Karsten Dultz, E. The RNA export factor Mex67 functions as a mobile nucleoporin. *J. Cell Biol.* **218**, 3967–3976 (2019).

252. Christian Trahan, L.-C. A. M. O. Single-Step Affinity Purifi cation (ssAP) and Mass Spectrometry of Macromolecular Complexes in the Yeast S. cerevisiae Christian. *Yeast Funct. Genomics Methods Protoc.* **1361**, 391–404 (2016).

253. Zenklusen, D., Vinciguerra, P., Strahm, Y. & Stutz, F. The Yeast hnRNP-Like Proteins Yra1p and Yra2p Participate in mRNA Export through Interaction with Mex67p. *Mol. Cell. Biol.* **21**, 4219–4232 (2001).

254. Schmid, Manfred Olszewski, Pawel Pelechano, Vicent Gupta, Ishaan Steinmetz, Lars M. Jensen, T. H. The Nuclear PolyA-Binding Protein Nab2p Is Essential for mRNA Production. *Cell Rep.* **12**, 128–139 (2015).

255. Hector, R. E. *et al.* Dual requirement for yeast hnRNP Nab2p in mRNA poly(A) tail length control and nuclear export. *EMBO J.* **21**, 1800–1810 (2002).

256. Dunn, E. F., Hammell, C. M., Hodge, C. A. & Cole, C. N. Yeast poly(A)-binding protein, Pab1, and PAN, a poly(A) nuclease complex recruited by Pab1, connect mRNA biogenesis to export. *Genes Dev.* **19**, 90–103 (2005).

257. Minvielle-Sebastia, L., Preker, P. J., Wiederkehr, T., Strahm, Y. & Keller, W. The major yeast poly(A)-binding protein is associated with cleavage factor IA and functions in premessenger RNA 3′-end formation. *Proc. Natl. Acad. Sci. U. S. A.* **94**, 7897–7902 (1997).

258. Brown, C. E., Tarun, S. Z., Boeck, R. & Sachs, A. B. PAN3 encodes a subunit of the Pab1p-dependent poly(A) nuclease in Saccharomyces cerevisiae. *Mol. Cell. Biol.* **16**, 5744–5753 (1996).

259. Bensidoun, P., Raymond, P., Oeffinger, M. & Zenklusen, D. Imaging single mRNAs to study dynamics of mRNA export in the yeast Saccharomyces cerevisiae. *Methods* **98**, 104–114 (2016).

260. Magdalena Morawska, H. D. U. An expanded tool kit for the auxin-inducible degron system in budding yeast Magdalena. *Yeast* 191–198 (2008) doi:10.1002/yea.

261. Ling, Shuo-chien Polymenidou, Magdalini Cleveland, Don W Revyakin, Andrey Patel, Ronak Macklin, John J Normanno, Davide Robert, H. A general method to improve fluorophores for live-cell and single-molecule microscopy. *Nat. Methods* **79**, 244–250 (2015).

262. Rothbauer, Ulrich Zolghadr, Kourosh Muyldermans, Serge Schepers, Aloys Cardoso, M. Cristina Leonhardt, H. A versatile nanotrap for biochemical and functional studies with fluorescent fusion proteins. *Mol. Cell. Proteomics* **7**, 282–289 (2008).

263. Scott, Daniel D. Trahan, Christian Zindy, Pierre J. Aguilar, Lisbeth C. Delubac, Marc Y. Van Nostrand, Eric L. Adivarahan, Srivathsan Wei, Karen E. Yeo, Zenklusen, Daniel Oeffinger, M. Nol12 is a multifunctional RNA binding protein at the nexus of RNA and DNA metabolism. *Nucleic Acids Res.* **45**, 12509–12528 (2017).

264. Mishra, A., Sipma, W., Veenhoff, L. M., Van Der Giessen, E. & Onck, P. R. The effect of FG-nup phosphorylation on NPC selectivity: A one-bead-per-amino-acid molecular dynamics study. *Int. J. Mol. Sci.* **20**, (2019).

265. Darling, A. L. & Uversky, V. N. Intrinsic disorder and posttranslational modifications: The darker side of the biological dark matter. *Front. Genet.* **9**, 1–18 (2018).

266. Trahan, C. & Oeffinger, M. Targeted cross-linking-mass spectrometry determines vicinal interactomes within heterogeneous RNP complexes. *Nucleic Acids Res.* **44**, 1354–1369 (2016).

267. Cohen-Fix, O. & Askjaer, P. Cell biology of the Caenorhabditis elegans nucleus. *Genetics* **205**, 25–59 (2017).

268. Updike, D. L., Hachey, S. J., Kreher, J. & Strome, S. P granules extend the nuclear pore complex environment in the C. elegans germ line. *J. Cell Biol.* **192**, 939–948 (2011).

269. Randise-Hinchliff, Carlo Coukos, Robert Sood, Varun Sumner, Michael Chas Zdraljevic, Stefan Sholl, Lauren Meldi Brickner, Donna Garvey Ahmed, Sara Watchmaker, Lauren

Brickner, J. H. Strategies to regulate transcription factor-mediated gene positioning and interchromosomal clustering at the nuclear periphery. *J. Cell Biol.* **212**, 633–646 (2016).

270. Qu, Xiangping Lykke-Andersen, Søren Nasser, Tommy Saguez, Cyril Bertrand, Edouard Jensen, Torben Heick Moore, C. Assembly of an Export-Competent mRNP Is Needed for Efficient Release of the 3′-End Processing Complex after Polyadenylation. *Mol. Cell. Biol.* **29**, 5327–5338 (2009).
271. Zenklusen, D., Vinciguerra, P., Wyss, J.-C. & Stutz, F. Stable mRNP Formation and Export Require Cotranscriptional Recruitment of the mRNA Export Factors Yra1p and Sub2p by Hpr1p. *Mol. Cell. Biol.* **22**, 8241–8253 (2002).
272. Milligan, L., Torchet, C., Allmang, C., Shipman, T. & Tollervey, D. A Nuclear Surveillance Pathway for mRNAs with Defective Polyadenylation. *Mol. Cell. Biol.* **25**, 9996–10004 (2005).
273. Dheur, S., Nykamp, K. R., Viphakone, N., Swanson, M. S. & Minvielle-Sebastia, L. Yeast mRNA poly(A) tail length control can be reconstituted in vitro in the absence of Pab1p-dependent poly(A) nuclease activity. *J. Biol. Chem.* **280**, 24532–24538 (2005).
274. Hooks, K. B., Delneri, D. & Griffiths-Jones, S. Intron evolution in Saccharomycetaceae. *Genome Biol. Evol.* **6**, 2543–2556 (2014).
275. Rutz, B. & Séraphin, B. A dual role for BBP/ScSF1 in nuclear pre-mRNA retention and splicing. *EMBO J.* **19**, 1873–1886 (2000).
276. Dölker, N., Zachariae, U. & Grubmüller, H. Hydrophilic linkers and polar contacts affect aggregation of FG repeat peptides. *Biophys. J.* **98**, 2653–2661 (2010).
277. Lsptdixb, P. Hexandiol a chemical probe to investigate material properties of membrane less compartments. *matters*.
278. Yamada, Justin Phillips, Joshua L. Patel, Samir Goldfien, Gabriel Calestagne-Morelli, Alison Huang, Hans Reza, Ryan Acheson, Justin Krishnan, Viswanathan V. Newsam, Shawn Gopinathan, Ajay Lau, Edmond Y. Colvin, Michael E. Uversky, Vladimir N. Rexacha, M. F. A bimodal distribution of two distinct categories of intrinsically disordered structures with separate functions in FG nucleoporins. *Mol. Cell. Proteomics* **9**, 2205–2224 (2010).
279. Whitby, C. P. & Bahuon, F. Droplet fusion in oil-in-water Pickering emulsions. *Front. Chem.*

**6**, 1–6 (2018).

280. Jothi Prakash, C. G. & Prasanth, R. Approaches to design a surface with tunable wettability: a review on surface properties. *J. Mater. Sci.* **56**, 108–135 (2021).
281. Segref, Alexandra Sharma, Kishore Doye, Valérie Hellwig, Andrea Huber, Jochen Lührmann, Reinhard Hurt, E. Mex67p, a novel factor for nuclear mRNA export. Binds to both poly(A)+ RNA and nuclear pores. *EMBO J.* **16**, 3256–3271 (1997).
282. Huang, K., Tagliazucchi, M., Park, S. H., Rabin, Y. & Szleifer, I. Molecular model of the nuclear pore complex reveals a thermoreversible FG-network with distinct territories occupied by different FG motifs. *bioRxiv* 568865 (2019) doi:10.1101/568865.
283. Azimi, M., Bulat, E., Weis, K. & Mofrad, M. R. K. An agent-based model for mRNA export through the nuclear pore complex. *Mol. Biol. Cell* **25**, 3643–3653 (2014).
284. Ding, Dongfeng Muthuswamy, Sivaramakrishnan Meier, I. Functional interaction between the Arabidopsis orthologs of spindle assembly checkpoint proteins MAD1 and MAD2 and the nucleoporin NUA. *Plant Mol. Biol.* **79**, 203–216 (2012).
285. Zhang, Wanlu Neuner, Annett Rüthnick, Diana Sachsenheimer, Timo Lüchtenborg, Christian Brügger, Britta Schiebel, E. Brr6 and Brl1 locate to nuclear pore complex assembly sites to promote their biogenesis. *J. Cell Biol.* **217**, 877–894 (2018).
286. Sang, H. L., Sterling, H., Burlingame, A. & McCormick, F. Tpr directly binds to Mad1 and Mad2 and is important for the Mad1-Mad2-mediated mitotic spindle checkpoint. *Genes Dev.* **22**, 2926–2931 (2008).
287. Box, G. E. P. *Robustness in the Strategy of Scientific Model Building*. *Robustness in Statistics* (ACADEMIC PRESS, INC., 1979). doi:10.1016/b978-0-12-438150-6.50018-2.

# 8. Annex

## Annex-1 Choosing the right exit: How functional plasticity of the nuclear pore drives selective and efficient mRNA export

Pierre Bensidoun[1,2] | Daniel Zenklusen[2] | Marlene Oeffinger[1,2,3]

[1]Systems Biology, Institut de Recherches Cliniques de Montréal, Montréal, Canada

[2]Département de Biochimie et Médecine Moléculaire, Faculté de médecine, Université de Montréal, Montréal, Canada

[3]Faculty of Medicine, Division of Experimental Medicine, McGill University, Montréal, Canada

Published in WIRE RNA 2021

Received: 2 February 2021 | Revised: 30 March 2021 | Accepted: 4 April 2021

DOI: 10.1002/wrna.1660

ADVANCED REVIEW

WIREs RNA WILEY

# Choosing the right exit: How functional plasticity of the nuclear pore drives selective and efficient mRNA export

**Pierre Bensidoun**[1,2] | **Daniel Zenklusen**[2] | **Marlene Oeffinger**[1,2,3]

[1]Systems Biology, Institut de Recherches Cliniques de Montréal, Montréal, Canada

[2]Département de Biochimie et Médecine Moléculaire, Faculté de médecine, Université de Montréal, Montréal, Canada

[3]Faculty of Medicine, Division of Experimental Medicine, McGill University, Montréal, Canada

**Correspondence**
Daniel Zenklusen and Marlene Oeffinger, Département de Biochimie et Médecine Moléculaire, Faculté de Médecine, Université de Montréal, Montréal, Québec, Canada H3T 1J4.
Email: daniel.r.zenklusen@umontreal.ca (D.Z.); marlene.oeffinger@ircm.qc.ca (M.O.)

**Funding information**
Fonds de Recherche du Québec - Santé, Grant/Award Number: Chercheur Boursier Senior; Canadian Institutes of Health Research, Grant/Award Numbers: PJT148932, PJT153313, PJT168856; Natural Sciences and Engineering Research Council of Canada, Grant/Award Numbers: RGPIN-2020-06924, RGPIN-2020-06948

**Abstract**

The nuclear pore complex (NPC) serves as a central gate for mRNAs to transit from the nucleus to the cytoplasm. The ability for mRNAs to get exported is linked to various upstream nuclear processes including co-transcriptional RNP assembly and processing, and only export competent mRNPs are thought to get access to the NPC. While the nuclear pore is generally viewed as a monolithic structure that serves as a mediator of transport driven by transport receptors, more recent evidence suggests that the NPC might be more heterogenous than previously believed, both in its composition or in the selective treatment of cargo that seek access to the pore, providing functional plasticity to mRNA export. In this review, we consider the interconnected processes of nuclear mRNA metabolism that contribute and mediate export competence. Furthermore, we examine different aspects of NPC heterogeneity, including the role of the nuclear basket and its associated complexes in regulating selective and/or efficient binding to and transport through the pore.

This article is categorized under:

RNA Export and Localization > Nuclear Export/Import
RNA Turnover and Surveillance > Turnover/Surveillance Mechanisms
RNA Interactions with Proteins and Other Molecules > Protein-RNA Interactions: Functional Implications

**KEYWORDS**

export competency, export efficiency, export selectivity, gene gating, kinetic proofreading, Mlp1, mRNA export, NPC heterogeneity, nuclear basket, nuclear organization, nuclear pore complex, nuclear retention, TPR, TREX-2

## 1 | INTRODUCTION

Transit from the nucleus to the cytoplasm is a necessary step for mRNPs to reach their site of translation, and the nuclear pore complex (NPC) serves as the central gateway of nucleocytoplasmic transport. The NPC is a large macromolecular assembly that is embedded into the nuclear membrane. It is composed of around thirty proteins that assemble into an eight-fold symmetrical structure of different modules (Alber et al., 2007; Kim et al., 2018; Lin & Hoelz, 2019). Its central transport channel is lined with a class of nuclear pore proteins, called nucleoporins (nups), rich

Editor-in-chief: Jeff Wilusz

  

in phenylalanines and glycines (FG) that are part of intrinsically disordered domains responsible for creating a diffusion barrier and facilitate nucleocytoplasmic exchange mediated by specific transport receptors. Attached to the central framework of the NPC on the nuclear and cytoplasmic faces of the pore are structures that are thought to form regulatory platforms that modulate access and release of cargo—proteins and ribonucleoprotein complexes (RNPs). At the nuclear side of the NPC, the nuclear basket, an assembly made of long filamentous proteins (Mlp1/2 in *Saccharomyces cerevisiae* and TPR in metazoans), protrudes into the nuclear interior and is suggested to act as initial docking site for messenger RNAs (mRNAs) on their way to and through a nuclear pore (Ashkenazy-Titelman et al., 2020; Cordes et al., 1997; Strambio-de-Castillia et al., 1999).

The ability for a messenger ribonucleoprotein particle (mRNP) to reach a nuclear pore and get exported cannot, however, be seen as an isolated process and has been functionally linked to different upstream events that include the co-transcriptional assembly of mRNA with specific RNA-binding proteins (RBPs), splicing, 3′end processing, and polyadenylation, resulting in "export competent" mRNPs (Figure 1) (Björk & Wieslander, 2017; Singh et al., 2015; Stewart, 2019a; Xie & Ren, 2019). Moreover, the interaction of these "export competent" mRNPs with and their transport through the nuclear pore is further facilitated by transport receptors via adapter proteins deposited on mRNPs

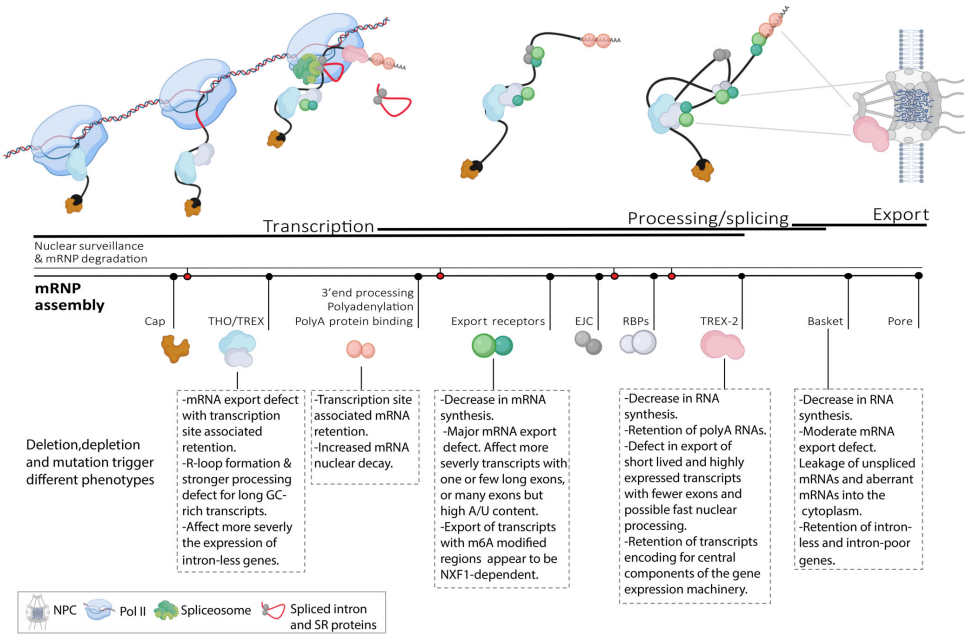


**FIGURE 1** Stages of the mRNP maturation, quality control and export pathway. Nascent mRNAs are capped and assembled with THO and TREX components that serve as adaptors for mRNA export receptors. Transcripts are generally spliced co-transcriptionally and associate with the exon junction complex (EJC), serine rich proteins (SR) as well as various RNA-binding proteins (RBPs), which enhance export kinetics by recruiting additional export receptors. Cleaved and polyadenylated transcripts associate with nuclear polyA-binding proteins and are released from the transcription sites. Export competent mRNPs can either associate with a pore through direct interactions between export receptors and the NPC, or TREX-2 mediated interactions between transcripts, the nuclear baskets and export receptors. It is assumed that cooperative interactions between the pore, the basket and RBPs ensure that only correctly processed transcripts have access to and translocate through the pore. Defects in capping, abortive transcription as well as inefficient splicing and/or polyadenylation can trigger mRNA degradation by the nuclear surveillance machineries, and several mRNP processing defects provide entry sites for 3′–5′ exosome decay (indicated by red dots). THO/TREX, TREX-2, export receptor and basket deficiencies do not affect transcripts or their export in the same manner, with pronounced transcription/export defects observed for specific subsets of transcripts

during late maturation steps. These transport receptors, in turn, mediate translocation through the nuclear pore by interaction with FG-nucleoporins lining the NPC (Scott et al., 2019).

Over the past two decades, genetic screens as well as proteomic and knock-down approaches have identified many of the proteins involved in these events in eukaryotes; the manifold nature of nuclear mRNPs and their components, the complexity of the mRNA maturation and export process have been described in several reviews (Ashkenazy-Titelman et al., 2020; Björk & Wieslander, 2017; Scott et al., 2019; Singh et al., 2015; Wegener & Müller-McNicoll, 2018; Wende et al., 2019). However, while it is evident that the coupling of mRNA transcription and processing to export may provide a robust strategy to ensure that only fully matured mRNPs leave the nucleus, what is less clear is the mechanism—or mechanisms—that enable an mRNP to get to a nuclear pore, remain at a pore, and, eventually, get exported through a pore.

mRNPs have to reach the periphery and interact with NPCs to initiate translocation and while "getting to a pore" is a passive process, binding of an mRNP to NPCs and gaining access to or staying at a nuclear pore are believed to be regulated and monitored by distinct quality control machineries to ensure that transcripts that have not yet completed splicing, or are incorrectly processed, are retained in the nucleus. In addition, cryptic transcripts and misprocessed mRNAs must be retained and/or degraded in the nucleus and a competitive model of export vs. retention and degradation has been proposed (Adivarahan & Zenklusen, 2019; Ashkenazy-Titelman et al., 2020; Grünwald & Singer, 2010; Lawrence & Singer, 1986; Shav-Tal et al., 2004). Yet considering all available data, the mechanisms that modulate access to the NPC are overall still poorly understood raising questions of how different components, not only of mRNPs but also the NPC, could regulate—or at least modulate—pore access and transport. Analyses of pre-mRNP maturation have shown that, despite an assumed common pathway, certain steps and RBPs may vary between subsets of transcripts based on their features (e.g., length, 3′UTR motifs, presence of intron, intron number or length, etc.) and/or cell types, suggesting that mRNP export competency might be based on different parameters and conditions (Williams et al., 2017). Furthermore, it is not known whether all mRNAs can exit the nucleus via all pores, or if a certain selectivity exists among transcripts or NPCs; either scenario would establish a variety of differential mechanisms to get to and through a pore.

Considering these open questions, this review focuses on how different components of the NPC and NPC-associated complexes have recently been shown to contribute to mRNP export by mediating between export selectivity and efficiency, posing the overarching question: What drives export?

## 2 | TO GET TO THE PORE: BALANCING mRNA RETENTION, DECAY, AND EXPORT

Gaining export competence is linked to many aspects of nuclear mRNP metabolism, including assembly, processing, quality control, and decay. The presence of an intron has long been known to stimulate expression of a transgene and this has largely been attributed to a splicing-dependent deposition of proteins on mRNA that, in turn, facilitate the recruitment of export receptors (Valencia et al., 2008; Woodward et al., 2016). Moreover, other steps of mRNP maturation have also been linked to export. One complex that illustrates the complexity of the functional connections between the various processes of the nuclear mRNA maturation pathway and export is the conserved Transcription and Export (TREX) complex, composed of the THO complex and the export factors Yra1/Ref2 (Aly/REF) and the RNA helicase Sub2/UAP56 (DDX39b). The THO components were initially characterized in yeast genetic screens aimed at identifying mutants showing transcription associated genome instability, a phenotype later linked to the accumulation of R-loops and now thought to be caused by defects in co-transcriptional mRNA folding and assembly (Aguilera & Klein, 1988; Heath et al., 2016; Pühringer et al., 2020; Schuller et al., 2020). Chromatin immunoprecipitation experiments in yeast further showed that THO components associate co-transcriptionally at all genes early during transcription, followed by association of Yra1 and Sub2 toward the 3′-ends of genes, suggesting a functional coupling of TREX, and possibly acquisition of export competence, to transcription termination and 3′-end processing (Gómez-González et al., 2011; Heath et al., 2016; Johnson et al., 2011; Kim et al., 2004; Rougemaille et al., 2008). Moreover, RNA fluorescence *in situ* hybridization experiments in yeast revealed an mRNA export defect in TREX complex mutants due to a failure in releasing transcripts from the site of transcription, whereas a nuclear accumulation of polyA RNA in nuclear speckles was observed upon depletion of TREX components in higher eukaryotes (Bonnet et al., 2015; Eshleman et al., 2016; Herold et al., 2003). The export phenotype is in part attributed to a problem in these mutants to recruit the mRNA export receptor Mex67/NFX1 required for mRNPs to interact with and translocate though the nuclear pore. However, part of the

observed phenotype is the targeting of the nuclear RNA surveillance machinery to retained mRNAs that may be either aberrant or their processing kinetically delayed. Nuclear exosome-mediated degradation is thought to provide a quality control platform to ensure that only correctly (and/or timely) processed transcripts will escape nuclear decay and are able to reach and traverse the nuclear pore (Hilleren et al., 2001; Roth et al., 2005; Saguez et al., 2005; Soucek et al., 2016; Vinciguerra et al., 2005). Those observations have led to a "kinetic proofreading" model for export where mRNPs can only spend a limited time in the nucleoplasm to avoid nuclear decay (Fasken & Corbett, 2005; Hilleren et al., 2001; Saguez et al., 2008; Tudek et al., 2019). In such a model, pre-mRNAs are potential targets for the nuclear exosome and its cofactors, which can recognize transcripts at various steps of the mRNA biogenesis pathway. Consequently, the nuclear exosome exerts a constant pressure on sub-optimally processed mRNAs, and rapid processing and export could thus explain, in part, how normal nascent mRNAs avoid degradation by the exosome. Cells could thus fine-tune their gene expression by modulating the export kinetics of some transcripts, balancing export and decay possibly in a cell-type-specific or condition-dependent manner.

While recent studies suggest the existence of regulatory processes modulating export efficiency, they also point towards a level of regulation that goes beyond the "kinetic proofreading" model. Bahar Halpern and colleagues have shown that in different tissues, specific mRNAs are nuclear retained without being targeted by the nuclear degradation machinery, and that such modulation of export kinetics allows buffering of cytoplasmic transcript levels from noise caused by transcriptional bursts (Bahar Halpern et al., 2015). In a parallel study, Battich et al demonstrated that export kinetics vary for different transcripts, which is also supported by live-cell imaging studies suggesting some mRNAs take up to two hours to be exported (Battich et al., 2015; Horvathova et al., 2017; Mor et al., 2010). Although mechanisms modulating export kinetics are not understood at this point, these studies demonstrate that longer nuclear residence times do not automatically lead to decay and can likely be a means of regulation, whereby transcripts may be protected—or distinguished—by the absence or presence of certain RBPs and/or sequence features such as RNA modifications.

The requirement for a decoupling of efficient export from mRNA degradation seems apparent, at least in higher eukaryotes, where mRNAs tend to spend longer time periods in the nucleus (Bahar Halpern et al., 2015; Battich et al., 2015; Horvathova et al., 2017; Mor et al., 2010; Shav-Tal et al., 2004). Moreover, lncRNAs, which share many features of mRNAs such as capping, various processing steps and polyadenylation, are often nuclear retained while some are also long-lived (Wegener & Müller-McNicoll, 2018). Hence, what regulates the stability of various types of nuclear RNAs is still uncertain and so is our understanding on whether slowly exported mRNAs and other types of stable nuclear transcripts share features that protect them from nuclear decay such as, for example, the binding of specific RBPs. There are different ways one could envision such regulation could be achieved; one is through the regulation of exosome activity as higher eukaryotes have evolved different exosome targeting complexes (Schmid & Jensen, 2018). Another is via spatial regulation, whereby mRNAs might be protected from degradation in specific nuclear sub-compartments. Regulated export of CTN-RNA/mCAT2 was shown to involve its localization to paraspeckles, whereas slowly exporting mRNAs in mouse tissues preferentially localized to nuclear speckles (Halpern et al., 2015; Prasanth et al., 2005; Wegener & Müller-McNicoll, 2018). However, whether localization in these compartments is the cause or the consequence of their retention, is still unclear. Overall, while many aspects of mRNA maturation—the processing events contributing to an export competent mRNP as well as the quality control pathways surveying this process—have been established, what mediates export efficiency and selective retention is still unknown. In particular, the role of nuclear organization but also of specific RBPs in this process is still poorly characterized, as it is uncertain whether mRNAs are retained because they never reach an NPC or are not able to translocate through the pore. It has also been speculated that parallel and partially overlapping pathways regulating mRNA maturation and export evolved to limit a potential take-over of the machineries by viruses. Indeed, numerous studies have reported that viral RNAs can hijack the host machinery to export their transcripts and even bypass mRNA surveillance for efficient access to and translocation through the pore (Bardina et al., 2009; Castelló et al., 2009; Kuss et al., 2013; Park et al., 2010; Porter & Palmenberg, 2008; von Kobbe et al., 2000; Vovk et al., 2016). (see BOX 1).

## 3 | PORE PROXIMITY: FACILITATING EXPORT BY TRANSCRIPTION SITE TETHERING AT THE PERIPHERY

As it has become evident that some transcripts are actively retained in the nucleus, or their export delayed, one might ask whether there are ways to increase export kinetics if necessary. Cells often have to respond quickly to external cues

**BOX 1 UNCONVENTIONAL EXPORT OF VIRAL RNAS**

Numerous viruses infecting eukaryotes such as the influenza virus, retroviruses, and most DNA viruses, need RNA Polymerase II as well as the intranuclear mRNA maturation machinery to synthesize and export their transcripts. To increase their coding capacity, viral mRNAs often harbor retained or partially spliced introns and long nontranslated regions with premature termination codons. Those features are the hallmark of incorrectly processed mRNAs and generally lead to nuclear retention and/or degradation instead of export. Viral strategies to escape nuclear surveillance are extremely diverse between and within viral families (see Gales et al., 2020; Sandri-Goldin, 2004; Yarbrough et al., 2014 for comprehensive reviews).

Overall, viral mRNPs exploit the nuclear mRNA export pathways of their different hosts. For this purpose, they form secondary structures which are, together with viral auxiliary proteins, recognized by host canonical export machineries such as TREX, TREX-2 or export receptors. One example is the causative agent of acquired immunodeficiency syndrome (AIDS), the HIV-1 retrovirus; it encodes auxiliary proteins expressed from more than forty different RNA isoforms and the elucidation of the temporal dynamic of viral transcript expression has been key to understand how HIV-1 mRNAs escape nuclear host surveillance (Ocwieja et al., 2012). The very first exported mRNAs mimic the features of host transcripts and are capped, spliced, and polyadenylated allowing them to be exported through canonical host pathways. One of these encodes for the auxiliary protein REV (Regulator of expression of viral). REV is then imported into the nucleus, where it recognizes a secondary mRNA structure, RRE (Rev responsive element) present on intron-containing viral transcripts. REV contains nuclear export signals (NES) enabling the protein to recruit the export receptor CRM1 and trigger the exit of viral transcripts from the nucleus. Therefore, the RRE–REV–CRM1 complex is crucial for the selective nuclear export of partially spliced and unspliced viral mRNAs but not for fully spliced RNA isoforms (Mahiet & Swanson, 2016). In addition, recruiting the canonical mRNA export machinery onto viral transcripts may present an advantage: impairing the immune response by competing with host mRNA export that is required to establish an effective cellular immune response.

Compromising export of host transcripts represents a general widespread viral strategy (for review see Kuss et al., 2013). Some viruses such as the vesicular stomatitis virus expresses the matrix protein VSV M, which is able to target NUP98 and the NPC-associated protein Gle2. VSV M localizes to the nuclear rim and forms a complex with these two proteins, occupying the Gle2 RNA binding motif, hence competing with host mRNP binding and blocking export of host bulk mRNAs (von Kobbe et al., 2000).

Alternatively, some viruses can also affect the host mRNA export pathway directly by remodeling NPCs. Enteroviruses encode for a protease PV 2A responsible for the cleavage of FG-domains of specific nups such as NUP153, NUP98, and NUP62 (Castelló et al., 2009; Park et al., 2010). While PV 2A expression has a weak effect on the distribution of constitutively synthesized mRNAs, it instead blocks the transport of some induced cellular mRNAs soon after their expression, compromising mainly the expression of host genes involved in the immune response. Cardio viruses target similar nups as enteroviruses but instead encode a "leader protein" causing hyperphosphorylation of NUP62, NUP153, NUP214, and NUP98 and resulting in slow-down of host mRNA over viral mRNA export, the latter occurring potentially via interactions with different subsets of nucleoporins (Bardina et al., 2009; Porter & Palmenberg, 2008).

Studying mechanisms of viral mRNA export has considerably improved our understanding of canonical nuclear export pathways and their components for the selective nuclear export of unspliced and partially spliced viral mRNAs but not for fully spliced RNA isoforms. Notably, the first NES was discovered in HIV-1 REV protein and are now known to be crucial for the export of many proteins and cargoes (Fischer et al., 1995). Continuing to study the varied ways of viral take-over of the host mRNA transport machinery is likely to provide additional insights into how pore and nuclear transport plasticity can be established.

that result in gene expression changes requiring increased efficiency of mRNA maturation steps, including export. However, single molecule microscopy experiments have shown that nuclear mRNAs diffuse by Brownian motion with velocities that vary significantly depending on whether mRNAs traverse crowded domains of the nucleus such as chromatin-dense regions; hence such diffusion process might not be considered efficient, in particular in higher eukaryotes

with large nuclei (Calapez et al., 2002; Grünwald & Singer, 2010; Molenaar et al., 2004; Politz et al., 1998; Shav-Tal et al., 2004; Siebrasse et al., 2008). One way to speed up this process would be to bring genes closer to the nuclear periphery. The presence of transcription sites at the nuclear periphery has been described in yeast and, to some extent, in flies, where actively transcribed genes are often found to be tethered to NPCs (Brickner & Walter, 2004; Casolari et al., 2004; Kurshakova et al., 2007; Schmid et al., 2006; Sood & Brickner, 2014; Taddei et al., 2006). In *Saccharomyces cerevisiae*, activation of genes induced by various external stimuli, including the *INO1*, *GAL1*, *HXK1* and *HSP104* genes among others, induces re-localization of the gene loci to the nuclear periphery (Brickner & Walter, 2004; Cabal et al., 2006; Dieppois et al., 2006; Schmid et al., 2006; Taddei et al., 2006). Different mechanisms of gene tethering at the pore have been proposed, including specific NPC-chromatin interactions as well as genes being moved to the periphery by export receptors associating with nascent transcripts, while simultaneously able to interact with the NPC (Brickner & Walter, 2004; Cabal et al., 2006; Dieppois et al., 2006; Schmid et al., 2006; Taddei et al., 2006). However, in a small nucleus such as that of yeast, it is unclear whether gene tethering represents a significant kinetic advantage for mRNAs to be efficiently exported, compared to mRNAs transcribed within the nuclear interior that will reach the periphery within less than a second. Transcribing genes at the NPC might nevertheless provide an advantage if access to pores is competitive, or to avoid the hostile nuclear environment as proposed by the kinetic proofreading model, limiting the need for surveillance under conditions where rapid export of specific mRNAs is important. Moreover, gene tethering might contribute to other aspects of gene regulation such as transcriptional memory, as shown for the *INO* genes, or genome stability by preventing R-loop formation (Brickner et al., 2007; García-Benítez et al., 2017; Sood & Brickner, 2014).

While gene tethering of active genes is frequent in lower eukaryotes and flies, the process seems less widespread in mammals, where the nuclear periphery is generally associated with heterochromatin. However, gene gating has been described in mammals as a means to establish differential mRNA export-dynamic (Capelson et al., 2010; Ibarra et al., 2016; Scholz et al., 2019). Scholtz et al. revealed a gene gating strategy involving an oncogenic super-enhancer (OSE) that facilitated efficient export of transcripts generated by the MYC oncogene (Scholz et al., 2019) (Figure 2). The study found that, in certain cancer cells, transcriptionally active MYC alleles clustered with an OSE at nuclear pores, which correlated with higher cytoplasmic MYC transcript levels. This increase was in part attributed to expedited mRNA escape from the nuclear degradation machinery when MYC was transcribed at NPCs. It will be interesting to see whether this process, which resembles a concept of kinetic proofreading as previously described in yeast, is also more widespread in higher eukaryotes (Fasken & Corbett, 2005; Hilleren et al., 2001; Saguez et al., 2008; Tudek et al., 2019).

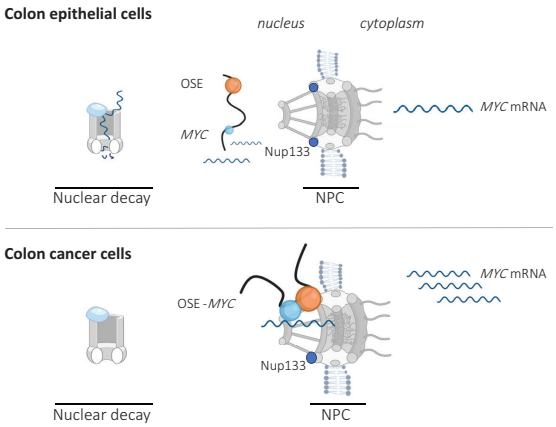


**FIGURE 2** Chromatin re-organization and NPC-tethering in human colon cancer cells enhances MYC mRNA export rates. Reduction of the MYC-OSE distance correlates with a localization of MYC loci at nuclear pores. OSE-mediated gene gating favors nucleocytoplasmic transport of MYC mRNA over nuclear decay and results in increased levels of cytoplasmic MYC mRNAs

## 4 | PROVIDING ACCESS: THE ROLE OF THE NUCLEAR BASKET AND ITS ASSOCIATED PROTEINS

At the nuclear periphery, regions of low chromatin density are believed to form "nucleoplasmic-channel pathways" that facilitate the diffusion of mRNAs towards nuclear pores (Ashkenazy-Titelman et al., 2020; Blobel, 1985; Politz et al., 1999; Shav-Tal et al., 2004; Veith et al., 2010). The nuclear basket, an assembly at the nuclear face of the NPC, has been linked to establishing "chromatin exclusion zones" close to nuclear pores and is the first structure mRNPs encounter upon reaching the periphery (Krull et al., 2010; Niepel et al., 2013; Strambio-De-Castillia et al., 2010) (Figure 3a). The main structural components of the nuclear basket are long filamentous coiled-coil proteins, Mlp1 and Mlp2 in yeast, and TPR in humans, which, similar to the overall NPC architecture, assemble in an eight-fold symmetry at the outer ring of the NPC and protrude into the nuclear interior forming a basket-like structure of ~60-80 nm (Ashkenazy-Titelman et al., 2020; Buchwalter et al., 2018; Cordes et al., 1997; Strambio-de-Castillia et al., 1999). The C-terminal regions of Mlp/TPR are thought to shape the top of the basket forming a distal ring, which has been shown in early electron microscopy studies to serve as an entry point for mRNPs to the nuclear pore (Mehlin et al., 1992). In addition to the structural components, the basket also contains the FG-nups, Nup1, Nup2, Nup60 in yeast, and NUP153 and NUP50 in metazoans, which may facilitate the binding of transport receptors to the nuclear basket (Lin & Hoelz, 2019).

Over the past two decades, multiple roles have been attributed to the nuclear basket in the context of nuclear export, which can be interpreted in the light of both efficiency and selectivity. Single-particle tracking approaches in humans and yeast have shown that mRNPs scan the nuclear periphery prior to export, and in yeast, prolonged scanning has been linked to the presence of the nuclear basket (Figure 3b) (Grünwald & Singer, 2010; Mor et al., 2010; Saroufim et al., 2015; Siebrasse et al., 2008). Deletion of Mlp1, the truncation of its C-terminal region as well as mutations in the polyA-binding protein Nab2, which interacts directly with Mlp1, all affect periphery-scanning by mRNPs and result in a frequent release of mRNPs back into the nucleoplasm (Saroufim et al., 2015). This suggests that the basket may participate in increasing the residence time of mRNPs at the periphery and that scanning presents a probabilistic efficiency model whereby mRNPs "test out" nuclear pores and are either able to bind to baskets efficiently, or not. Alternatively, scanning could also be part of a competitive efficiency model, in which mRNPs search for pores that allow transport, i.e., are not too crowded, and thus enable binding to their basket. Lastly, it could also present a form of selectivity, where certain mRNPs can only access and bind to selected pores. Regardless of the model, scanning appears to represent a rate-limiting step in all of them and its underlying mechanisms and biological purpose remain yet to be uncovered.

For many years, the main role of the basket has been envisioned as stage for overall mRNA export surveillance and quality control (Figure 3c). Yet export of bulk mRNA was only affected to varying degrees upon deletion of Mlp/TPR in different organisms. Deletion of Mlp1/2 and TPR resulted in the leakage of un-spliced and aberrant mRNAs into the cytoplasm, implicating the basket in export selectivity and retention, if not overall quality control (Coyle et al., 2011; Galy et al., 2004; Green et al., 2003; Rajanala & Nandicoori, 2012); and while these data have defined the role of the basket as a nuclear gatekeeper, more recent work in human cells has not found a role for the basket in regulating the retention of unspliced mRNAs in the nucleus (Aksenova et al., 2020; Lee et al., 2020; Zuckerman et al., 2020).

Genome-wide studies investigating the effect of TPR depletion using either a siRNA knock-down approach or an auxin-inducible degron system combined with cell fractionation and RNA-seq, suggest a role for the nuclear basket in facilitating mRNA export rather than retention (Aksenova et al., 2020; Lee et al., 2020). TPR depletion resulted in the nuclear accumulation of mRNAs primarily expressed from short, intron-less and intron-poor genes such as those encoding for ribosomal protein genes and histones; export of longer mRNAs, however, appeared to be less dependent on TPR. An mRNA retention phenotype upon TPR depletion was confirmed using RNA FISH, and, moreover, retained transcripts preferentially localized to nuclear speckles, a phenotype previously observed upon deletion of other factors implicated in mRNA export, including those of the basket-associated Transcription and export-2 (TREX-2) complex (Aksenova et al., 2020; Lee et al., 2020; Umlauf et al., 2013).

Initially identified in yeast as a complex bridging transcription and mRNA export independent of THO and/or TREX, TREX-2 localizes to the nuclear periphery and shares a subunit with the transcriptional co-activator complex SAGA (Figure 3d**)** (Cabal et al., 2006; Fischer et al., 2002; Stewart, 2019b). Interaction between SAGA and TREX-2 was shown to facilitate the association of actively transcribing genes with nuclear pores, therefore, suggesting a functional link for TREX-2 as mediator of these two processes (Cabal et al., 2006; Jani et al., 2009; Umlauf et al., 2013). TREX-2, consisting of the scaffold protein Sac3 in yeast or GANP in humans, yThp1/hPCID2, ySus1/hENY2, yCdc31/hCETN2

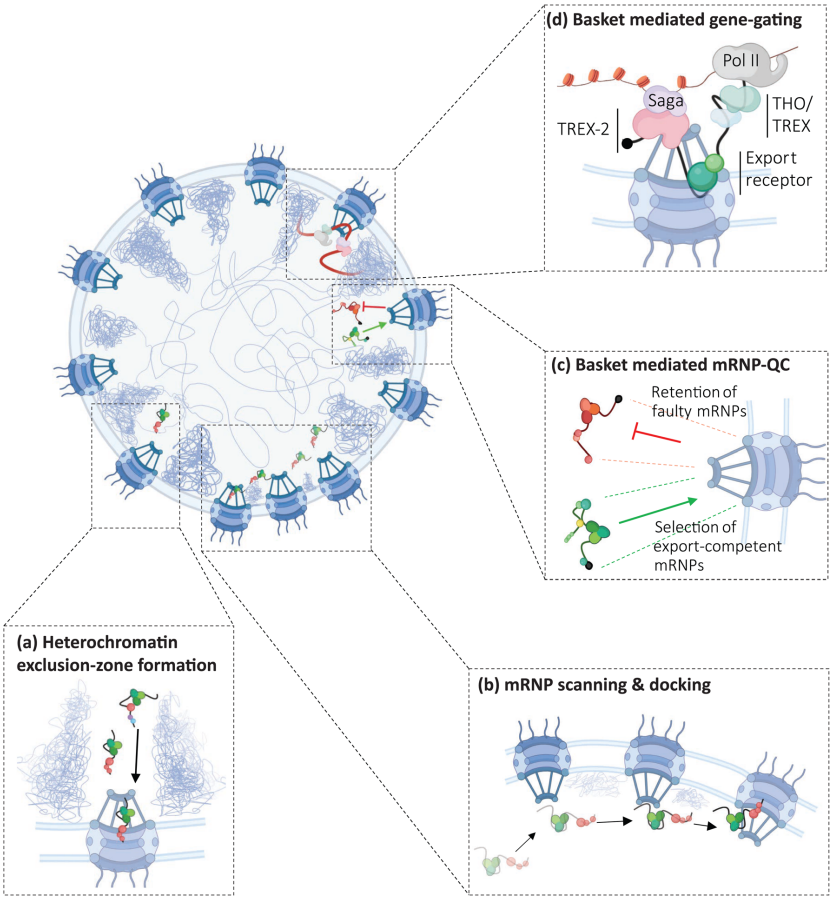


**FIGURE 3** The nuclear basket may participate in different steps of selective mRNP export. (a) In metazoans, the basket has been linked to the formation of chromatin exclusion zones believed to be used as channels by mRNPs to access the nuclear pore. (b) mRNPs scan the nuclear periphery prior to export, and in yeast, this scanning behavior has been linked to the presence of the basket core component Mlp1 and its interaction with polyA-binding proteins, which are suggested to increase residence time of mRNPs at the periphery and to facilitate binding/docking to the pore (c). The nuclear basket is believed to act as gatekeeper for aberrant mRNAs. However, at this point it is unclear whether the basket interacts with RBPs to recognize mature and export competent mRNPs or if aberrant transcripts are retained at the basket either to be matured or targeted for exosome-mediated decay. (d) The basket proteins Mlp1 and TPR were shown to be important for gene gating, or tethering, of actively transcribed genes at the nuclear periphery; in this model, transcription at the periphery is suggested to provide and advantage for mRNA export that may be based on selectivity and/or efficiency. Tethering genes at the NPC was shown to involve TREX2/SAGA and/or export receptors associating with nascent transcripts

and hCETN3, and ySem1/hDSS1, is highly conserved across higher eukaryotes and has also been linked to export in metazoans (Stewart, 2019b). In humans, TREX-2 components stably associate with the NPC at the nuclear basket and their localization requires TPR (Aksenova et al., 2020; Umlauf et al., 2013). Moreover, genome-wide gene expression profiling upon GANP depletion suggests a functional overlap between TREX-2 and the nuclear basket, specifically TPR. Similar to depletions of TPR, loss of GANP resulted only in a partial defect of mRNA export leading to the retention of

a selective subset of transcripts that showed significant overlap to mRNAs retained upon TPR depletion (Aksenova et al., 2020; Umlauf et al., 2013). While the number of mRNAs retained upon depletion of TREX-2 components varied between different studies, which may be due to differing experimental set-ups, there was an overall trend correlating specific transcript features with retention in cells depleted of GANP and/or TPR: short length and low intron/exon numbers (0–3) (Aksenova et al., 2020; Lee et al., 2020; Umlauf et al., 2013; Zuckerman et al., 2020). These observations raise once again questions about the role of the basket, as well as of Mlp/TPR as central basket component, in mRNA export. If, as these data indicate, the nuclear basket is required for the export of a subset of transcripts that contain specific features, is its role driven by providing selectivity, or contributing to transport efficiency?

Transcripts whose export depends on TPR—and TREX-2—appear to contain common features, which would point towards a role of the basket in selective transport. However, it is important to note that while one of these features is low number of introns, it is not—as previously thought—the mere presence or absence of introns, suggesting the basket may not be primarily a designated gatekeeper for unspliced pre-mRNAs. While mediating selective transport could still be one of its roles, nevertheless, features such as short transcript length could also indicate that some mRNAs require the nuclear basket to be efficiently exported; short mRNAs and those that have undergone only one to two splicing events may represent less complex RNPs lacking components to facilitate efficient binding to and transport through the pore. If we consider mRNP scanning of the nuclear periphery as part of a probabilistic process towards successful binding to the pore through specific RBP:pore interactions, it is possible that shorter transcripts require the basket to facilitate such a binding event. Consistent with such a notion, recent APEX2 data found short mRNAs enriched with NPCs, which was suggested to be due to a lower number of NPC-interacting factors on these transcripts that would mediate efficient translocation (Fazal et al., 2019). Moreover, a relationship between length and number of RBPs is also consistent with *in silico* predictions that suggest basket-mediated mRNA quality control to be a length-dependent mechanism (Soheilypour & Mofrad, 2016); see Box 2).

Besides length, specific motifs have recently been implicated in the basket-mediated retention and quality control of a selected subset of transcripts in metazoans. The protein TARBP2 was shown to bind a subset of pre-mRNAs, the TARBP2 regulon, via GC-rich structural *cis*-regulatory RNA elements resulting in m6A-mediated intron retention and exosome mediated decay (Fish et al., 2019). Transcriptomic and proteomic data link this surveillance process to TPR and, possibly, the nuclear basket, which would be in line with the proposed function of the nuclear basket as surveillance platform (Coyle et al., 2011; Galy et al., 2004; Rajanala & Nandicoori, 2012).

The decision of mRNA export is ultimately determined by the ability of mRNPs to efficiently access and get translocated through a nuclear pore, and several works have shown that the nuclear basket is likely to play an important role in this process. Overall, however, the data so far does not provide a clear picture of whether there is a single central function for the basket mediating pore access. Instead, it rather suggests a multitude of functions that may include transcript surveillance as well as facilitating efficient access to the pore. The mechanistic aspects of any of these processes remain unknown.

## 5 | A PECULIAR CASE OF NPC HETEROGENEITY: BASKET-LESS NUCLEOLAR PORES IN YEAST

The yeast *Saccharomyces cerevisiae* presents a good model organism to study basket function as it contains two sets of nuclear pores, one that contains baskets, and another that is basket-less (Galy et al., 2004). The nucleolus in yeast is sequestered to one side of the nucleus forming a crescent shaped membrane-less compartment that is adjacent to the nuclear membrane, occupying around one third of the nuclear volume. Nuclear pores adjacent to the nucleolus do not contain baskets as they are lacking the basket scaffold proteins Mlp1 and Mlp2 (Galy et al., 2004; Niepel et al., 2013) (Figure 4a). The functional relevance for the presence of two types of nuclear pores is still unclear, however, it suggests a specific role for the basket that is limited to aspects of RNA metabolism that occur in the nucleoplasm. Moreover, in contrast to higher eukaryotes where TPR is stably associated with the NPC, Mlp1 and Mlp2 association with the NPC appears to be somewhat more dynamic (Niepel et al., 2013; Niño et al., 2016). In addition, in yeast, nucleoplasmic pores lose their baskets upon heat-shock when Mlp1/2 sequester into the nucleoplasm and assemble intranuclear granules (Carmody et al., 2010). Those granules were shown to contain polyA RNAs and selected RBPs, including Nab2 and

**BOX 2 LESSONS FROM IN SILICO PREDICTIONS: DOES LENGTH MATTER?**

Numerous research groups have used biochemical and biophysical data combined with computational simulations to understand how the central channel of the NPC can serve as a selective yet permeable barrier. Generally, those studies have applied reductionist approaches using a minimal number of key physical variables to understand biophysical principles driving complex mechanisms such as the collective behaviors of intrinsically disordered domains of FG-nups during the translocation of cargo through the nuclear pore (Schmidt & Görlich, 2015; Vovk et al., 2016). In their recent work, Soheilypour and Mofrab have used a modeling approach for complex systems to develop a minimal model of mRNA quality control mechanism (Soheilypour & Mofrad, 2016). The authors based their simulations on the current model for quality control, in which RBPs serve as adaptors for recruitment of export receptors (NXF1/NXT1 or Mex67/Mtr2) and the nuclear basket protein Mlp/TPR interacts with RBPs to act as a checkpoint verifying mRNP maturity and export competence. It has been shown that while splicing is not an absolute requirement for interaction between export receptors and mRNAs, export receptors do have a higher affinity for RBPs bound to spliced mRNAs (Hackmann et al., 2014; Huang et al., 2004; Reichert et al., 2002; Rodrigues et al., 2001). Therefore, RBPs bound to un-spliced mRNAs could still recruit export receptors, yet with lower affinities. Using 2.2 kb-long spliced or unspliced mRNAs (designated here as "normal" and "aberrant," respectively) as models of average transcripts, with a mean of nine expected RBP binding sites, a simulation tested export specificity based on only one RPB and export receptors without including Mlp/TPR. By varying the affinity between RBP and export receptors (high for "normal" and low for "aberrant" mRNAs) "normal" mRNAs exhibited a percentage of simulated successful export events three times above that of "aberrant" mRNAs suggesting that a different interaction affinity between RBPs and export receptors can be sufficient to retain "aberrant" mRNAs. However, "aberrant" mRNAs were not retained when the number of RBP binding sites on the mRNA was increased to twelve.

Another simulation modeled quality control efficiency based on the interaction between Mlp/TPR and RBPs, including variations of RBP:Mlp/TPR affinities, demonstrating that interactions between Mlp/TPR and RBPs efficiently distinguished "aberrant" from "normal" mRNAs even if mRNAs contained twelve RBP binding sites. Moreover, in this model, export selectivity was conserved even for low range RBP: Mlp/TPR affinity. Lastly, simulations using shorter mRNAs (∼500nts) with similar densities of RBP binding sites showed that while short "normal" mRNAs were exported efficiently, the quality control mechanism was not as efficient as for longer mRNAs. While these computational simulations present only a minimalistic model of mRNA quality control, the data suggest that mRNA quality control involving the nuclear basket could be a length-dependent mechanism.

Yra1, suggesting that they may serve as storage structures for a subset of mRNPs during heat stress. As such, Mlp granule formation might serve to remove baskets from the nuclear pore to facilitate rapid export of heat-shock mRNAs foregoing quality control steps believed to occur at the nuclear basket under normal conditions. A simultaneous dissociation of the mRNA export receptor Mex67 from bulk mRNA and its association with heat-shock mRNAs for rapid export suggests not only a by-passing of basket-mediated quality control but also that yeast cells have acquired a mechanism to efficiently export selective mRNAs under these conditions (Figure 4b) (Zander et al., 2016). Moreover, this demonstrates that nuclear pores lacking a basket are capable of efficient transport, which is further emphasized by the observation that cells carrying double deletions of *mlp1/mlp2* are viable and only exhibit a mild mRNA export defect (Galy et al., 2004; Powrie et al., 2011). Furthermore, double deletion of *mlp1/mlp2* results in the leakage of unspliced transcripts into the cytoplasm promoting a potential role for the basket in mRNA surveillance of intron-containing transcripts in yeast (Galy et al., 2004). This is further supported by genetic interactions that connect mRNA processing, quality control, and the nuclear basket components, overall pointing towards a role for the yeast nuclear basket in selective transport insofar as only fully matured and export-competent mRNAs can access the NPC under normal conditions (Vinciguerra et al., 2005).

The absence of baskets along the nucleolar periphery may, on the other hand, suggest either a lack of necessity as mRNPs are not exported through these pores, or, conversely, selectivity. The nucleolus is the site of ribosome biogenesis and, hence, it is conceivable that nucleolar pores may be solely used for export of pre-ribosomal subunits, either due to

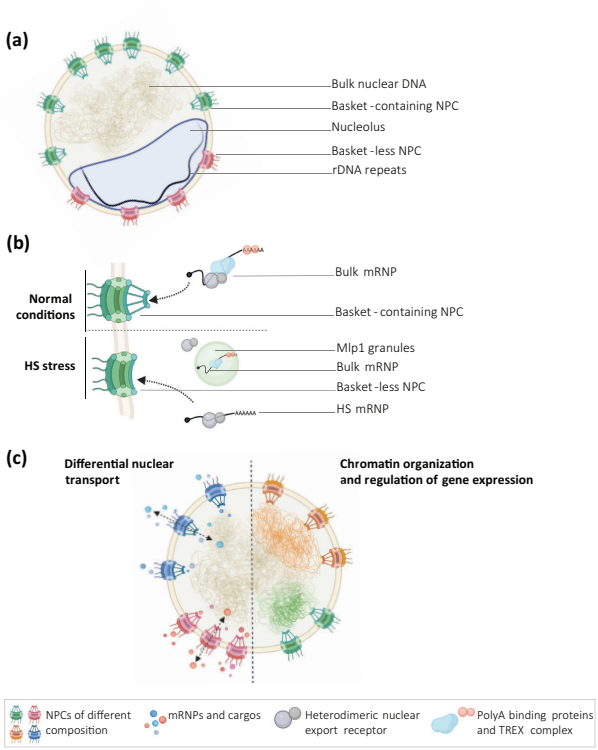


**FIGURE 4** Nuclear pore heterogeneity. (a) In the yeast *Saccharomyces cerevisiae*, basket-containing pores occupy the nucleoplasmic periphery, while nuclear pores along the nuclear membrane adjacent to the nucleolus lack a basket structure; in particular, the basket core components Mlp1 and Mlp2. (b) Upon heat-shock of yeast cells, Mlp1 detaches from nuclear pores and assembles into nucleoplasmic granules. These granules also contain the bulk of sequestered mRNAs as well as TREX components and polyA-binding proteins such as Nab2. While export receptors dissociate from bulk mRNPs upon heat shock, they facilitate the export of heat-shock transcripts in a basket-independent manner. (c) Potential models for NPC heterogeneity have been proposed in higher eukaryotes, which could be required to establish nuclear sub-domains with specific chromatin organization, regulate the transport of specific cargos in a topological dependent manner or, similar to yeast, occupy specific regions along the nuclear periphery (adapted from D'Angelo et al., 2012)

their proximity to sites of ribosome assembly promoting efficiency of transport and ribosome production (Woolford & Baserga, 2013), or due to size limitations of pre-ribosomes. One argument for the latter is that the distal ring that provides entry to the central channel of the pore is only ~25 nm in diameter (Beck et al., 2004); while, in yeast, that would be wide enough for a pre-40S subunit, pre-60S subunits are ~35 nm in diameter (Klinge & Woolford, 2018; Schäfer et al., 2006; Schmeing et al., 2009). Therefore, these subunits would either have to undergo structural rearrangement to fit through the basket opening or be exported via pores that do not contain a basket. Recent EM data, however, has shown that pre-ribosomal subunits can also be exported through nucleoplasmic pores indicating that nucleolar pores are not specialized for pre-ribosome export, although the precise mechanism of their transport remains unclear (Delavoie et al., 2019). In addition, single-particle microscopy studies of CLB2 mRNA revealed that this mRNA is infrequently exported through nucleolar pores (Saroufim et al., 2015). Overall, the purpose of basket-less nuclear pores in the yeast nucleolus remains to be determined.

## 6 | DIFFERENT CELL, DIFFERENT NPC: NUCLEAR PORE HETEROGENEITY IN METAZOANS

NPC components are conserved across eukaryotes, however, different studies examining nuclear pore composition showed differential expression of peripheral and inner ring nups in distinct cell types and during development (Cho & Hetzer, 2020; D'Angelo et al., 2012; Ori et al., 2013; Rabut et al., 2004; Raices & D'Angelo, 2012; Sun et al., 2019). Additional observations that cells may be differentially affected by mutations in different nups suggests that NPC composition as well as nucleoporin function may not be universal across cell types but that, instead, fine-tuning of gene regulation could be mediated through selective coupling of transcription and export via subsets of nucleoporins, or selective export driven by changes in NPC composition and post-translational modifications of specific NPC subunits (Cho & Hetzer, 2020; Makhnevych et al., 2003; Ori et al., 2013; Raices & D'Angelo, 2012; Sun et al., 2019).

In $CD4^{+}$T lymphocytes, lack of NUP210 impaired T cell receptor signaling and negatively affected T cell homeostasis (Borlido et al., 2018) while depletion of NUP153 in mouse embryonic stem cells led to derepression of developmental genes and loss of pluripotency (Jacinto et al., 2015). Mutation of NUP155 in human and mouse models was shown to negatively affect export of HSP70 mRNA in cardiomyocytes (Zhang et al., 2008). In *Drosophila*, NUP96-98 levels were observed to affect mRNA export selectivity during oocyte and germline differentiation (Parrott et al., 2011); and in mice, cell-cycle dependent variation in NUP96 levels were linked to regulation of cell cycle progression in mitosis through modulation of nuclear export of certain mRNAs, among which are key cell cycle regulators (Chakraborty et al., 2008; Faria et al., 2006). All these studies illustrate a context-dependent role for nucleoporins in selective gene regulation through export. This suggests the stoichiometry of certain nucleoporins in the NPC itself may vary in a cell type- or cell cycle-specific manner to regulate the function of the nuclear pore. Moreover, many nucleoporins have acquired nucleoplasmic functions including transcription regulation and genome organization providing another functional link between transcription, export and gene regulation in general (Liang et al., 2013; Makhnevych et al., 2003; Oka et al., 2010; Rajoo et al., 2018); these functions have been reviewed in more detail elsewhere (Pascual-Garcia & Capelson, 2019; Sun et al., 2019).

While the mechanistic details are still lacking, overall the data challenge the paradigm that the NPC is a structure of ubiquitous composition but rather show that NPC heterogeneity, i.e., nuclear pores with different compositions and distinct functions in mRNA export, genome organization and/or transcriptional memory, can modulate gene expression and cell fate in a cell-type-specific manner, providing an additional layer of regulation (Raices & D'Angelo, 2012). As such, an image of the NPC as a plastic structure emerges where different types of pores might co-exist within the same nucleus which exhibit different properties and specialized functions to either mediate efficient and/or selective access to the pore, or to stimulate selective transcription in a topology-dependent manner (Figure 4c).

## 7 | CONCLUDING REMARKS

The last decade has once again placed the role of the nuclear pore in mRNA transport in the spotlight, dispelling notions of a monolithic transport channel and gatekeeper while revealing it to be a multilayered platform that plays an active role in the regulation of mRNA export. In particular, an unanticipated plasticity of the NPC appears to give rise to a functional heterogeneity of the nuclear pore that allows for targeted mediation of selective upstream mRNA maturation events across different cell types, but even within the same nucleus. Basket-less NPCs in yeast are one clear example of NPC plasticity, here, both in structure and function; NPC accessory factors, such as TREX-2 components, impart functional plasticity to pores; multiplicitous roles of differentially expressed nucleoporins as well as transiently NPC-tethered chromatin drive mRNA export kinetics under certain conditions. All these examples of NPC plasticity may constitute in themselves microenvironments that drive mRNA export by balancing –or distinguishing– requirements for selectivity and/or efficiency with quality control. What these recent studies have also brought to the fore, however, is the lack of our mechanistic understanding of mRNA export, particularly the events that lead up to and enable translocation of an mRNP to the cytoplasm. Future studies will have to further elucidate the conditions under which NPC plasticity is established, its mechanisms, as well as how exactly it contributes to the multitude of tasks of the pore—beyond those of a mere transport channel.

## ACKNOWLEDGMENTS

D.Z. holds an FRS-Q Chercheur Boursier Senior and is supported by funding from the Canadian Institutes of Health Research (CIHR) (PJT148932 and PJT168856) and National Science and Engineering Research Council (NSERC) (RGPIN-2020-06948). M.O. is supported by funding from the CIHR (PJT153313 and PJT168856) and NSERC (RGPIN-2020-06924). Figures have been created with Biorender.com (License #DD20C0D9-0001).

## CONFLICT OF INTEREST

The authors have declared no conflicts of interest for this article.

## AUTHOR CONTRIBUTIONS

**Pierre Bensidoun:** Writing-original draft; writing-review & editing. **Daniel Zenklusen:** Supervision; writing-review & editing. **Marlene Oeffinger:** Supervision; writing-review & editing.

## DATA AVAILABILITY STATEMENT

Data sharing is not applicable to this article as no new data were created or analyzed in this study.

## ORCID

*Pierre Bensidoun* https://orcid.org/0000-0002-0659-225X
*Daniel Zenklusen* https://orcid.org/0000-0002-0067-0093
*Marlene Oeffinger* https://orcid.org/0000-0001-6427-1393

## RELATED WIREs ARTICLES

mRNA export and cancer
ALREX-elements and introns: two identity elements that promote mRNA nuclear export
Intron retention in viruses and cellular genes: Detention, border controls and passports
Nuclear quality control of RNA polymerase II transcripts
Dynamics and kinetics of nucleo-cytoplasmic mRNA export

## REFERENCES

Adivarahan, S., & Zenklusen, D. (2019). Lessons from (pre-)mRNA Imaging. *Advances in Experimental Medicine and Biology*, *1203*, 247–284.
Aguilera, A., & Klein, H. L. (1988). Genetic control of intrachromosomal recombination in *Saccharomyces cerevisiae*. I. Isolation and genetic characterization of hyper-recombination mutations. *Genetics*, *119*, 779–790.
Aksenova, V., Smith, A., Lee, H., Bhat, P., Esnault, C., Chen, S., Iben, J., Kaufhold, R., Yau, K. C., Echeverria, C., et al. (2020). Nucleoporin TPR is an integral component of the TREX-2 mRNA export pathway. *Nature Communications*, *11*, 4577.
Alber, F., Dokudovskaya, S., Veenhoff, L. M., Zhang, W., Kipper, J., Devos, D., Suprapto, A., Karni-Schmidt, O., Williams, R., Chait, B. T., et al. (2007). The molecular architecture of the nuclear pore complex. *Nature*, *450*, 695.
Ashkenazy-Titelman, A., Shav-Tal, Y., & Kehlenbach, R. H. (2020). Into the basket and beyond: the journey of mRNA through the nuclear pore complex. *The Biochemical Journal*, *477*, 23–44.
Bahar Halpern, K., Caspi, I., Lemze, D., Levy, M., Landen, S., Elinav, E., Ulitsky, I., & Itzkovitz, S. (2015). Nuclear retention of mRNA in mammalian tissues. *Cell Reports*, *13*, 2653–2662.
Bardina, M. V., Lidsky, P. V., Sheval, E. V., Fominykh, K. V., van Kuppeveld, F. J. M., Polyakov, V. Y., & Agol, V. I. (2009). Mengovirus-induced rearrangement of the nuclear pore complex: Hijacking cellular phosphorylation machinery. *Journal of Virology*, *83*, 3150–3161.
Battich, N., Stoeger, T., & Pelkmans, L. (2015). Control of transcript variability in single mammalian cells. *Cell*, *163*, 1596–1610.
Beck, M., Förster, F., Ecke, M., Plitzko, J. M., Melchior, F., Gerisch, G., Baumeister, W., & Medalia, O. (2004). Nuclear pore complex structure and dynamics revealed by cryoelectron tomography. *Science*, *306*, 1387–1390.
Björk, P., & Wieslander, L. (2017). Integration of mRNP formation and export. *Cellular and Molecular Life Sciences*, *74*, 2875–2897.
Blobel, G. (1985). Gene gating: a hypothesis. *Proceedings of the National Academy of Sciences of the United States of America*, *82*, 8527–8529.
Bonnet, A., Bretes, H., & Palancade, B. (2015). Nuclear pore components affect distinct stages of intron-containing gene expression. *Nucleic Acids Research*, *43*, 4249–4261.
Borlido, J., Sakuma, S., Raices, M., Carrette, F., Tinoco, R., Bradley, L. M., & D'Angelo, M. A. (2018). Nuclear pore complex-mediated modulation of TCR signaling is required for naïve CD4+ T cell homeostasis. *Nature Immunology*, *19*, 594–605.
Brickner, D. G., Cajigas, I., Fondufe-Mittendorf, Y., Ahmed, S., Lee, P.-C., Widom, J., & Brickner, J. H. (2007). H2A.Z-mediated localization of genes at the nuclear periphery confers epigenetic memory of previous transcriptional state. *PLoS Biology*, *5*, e81.

Brickner, J. H., & Walter, P. (2004). Gene recruitment of the activated INO1 locus to the nuclear membrane. *PLoS Biology*, *2*, e342.

Buchwalter, A., Kaneshiro, J. M., & Hetzer, M. W. (2018). Coaching from the sidelines: the nuclear periphery in genome regulation. *Nature Reviews. Genetics*, *20*, 1.

Cabal, G. G., Genovesio, A., Rodriguez-Navarro, S., Zimmer, C., Gadal, O., Lesne, A., Buc, H., Feuerbach-Fournier, F., Olivo-Marin, J.-C., Hurt, E. C., et al. (2006). SAGA interacting factors confine sub-diffusion of transcribed genes to the nuclear envelope. *Nature*, *441*, 770.

Calapez, A., Pereira, H. M., Calado, A., Braga, J., Rino, J., Carvalho, C., Tavanez, J. P., Wahle, E., Rosa, A. C., & Carmo-Fonseca, M. (2002). The intranuclear mobility of messenger RNA binding proteins is ATP dependent and temperature sensitive. *The Journal of Cell Biology*, *159*, 795–805.

Capelson, M., Liang, Y., Schulte, R., Mair, W., Wagner, U., & Hetzer, M. W. (2010). Chromatin-bound nuclear pore components regulate gene expression in higher eukaryotes. *Cell*, *140*, 372–383.

Carmody, S. R., Tran, E. J., Apponi, L. H., Corbett, A. H., & Wente, S. R. (2010). The mitogen-activated protein kinase Slt2 regulates nuclear retention of non-heat shock mRNAs during heat shock-induced stress. *Molecular and Cellular Biology*, *30*, 5168–5179.

Casolari, J. M., Brown, C. R., Komili, S., West, J., Hieronymus, H., & Silver, P. A. (2004). Genome-wide localization of the nuclear transport machinery couples transcriptional status and nuclear organization. *Cell*, *117*, 427–439.

Castelló, A., Izquierdo, J. M., Welnowska, E., & Carrasco, L. (2009). RNA nuclear export is blocked by poliovirus 2A protease and is concomitant with nucleoporin cleavage. *Journal of Cell Science*, *122*, 3799–3809.

Chakraborty, P., Wang, Y., Wei, J.-H., van Deursen, J., Yu, H., Malureanu, L., Dasso, M., Forbes, D. J., Levy, D. E., Seemann, J., et al. (2008). Nucleoporin levels regulate cell cycle progression and phase-specific gene expression. *Developmental Cell*, *15*, 657–667.

Cho, U. H., & Hetzer, M. W. (2020). Nuclear periphery takes center stage: the role of nuclear pore complexes in cell identity and aging. *Neuron*, *106*, 899–911.

Cordes, V. C., Reidenbach, S., Rackwitz, H.-R., & Franke, W. W. (1997). Identification of protein p270/Tpr as a constitutive component of the nuclear pore complex–attached intranuclear filaments. *The Journal of Cell Biology*, *136*, 515–529.

Coyle, J. H., Bor, Y.-C., Rekosh, D., & Hammarskjold, M.-L. (2011). The Tpr protein regulates export of mRNAs with retained introns that traffic through the Nxf1 pathway. *RNA*, *17*, 1344–1356.

D'Angelo, M. A., Gomez-Cavazos, J. S., Mei, A., Lackner, D. H., & Hetzer, M. W. (2012). A change in nuclear pore complex composition regulates cell differentiation. *Developmental Cell*, *22*, 446–458.

Delavoie, F., Soldan, V., Rinaldi, D., Dauxois, J.-Y., & Gleizes, P.-E. (2019). The path of pre-ribosomes through the nuclear pore complex revealed by electron tomography. *Nature Communications*, *10*, 497.

Dieppois, G., Iglesias, N., & Stutz, F. (2006). Cotranscriptional recruitment to the mRNA export receptor Mex67p contributes to nuclear pore anchoring of activated genes. *Molecular and Cellular Biology*, *26*, 7858–7870.

Eshleman, N., Liu, G., McGrath, K., Parker, R., & Buchan, J. R. (2016). Defects in THO/TREX-2 function cause accumulation of novel cytoplasmic mRNP granules that can be cleared by autophagy. *RNA*, *22*, 1200–1214.

Faria, A. M. C., Levay, A., Wang, Y., Kamphorst, A. O., Rosa, M. L. P., Nussenzveig, D. R., Balkan, W., Chook, Y. M., Levy, D. E., & Fontoura, B. M. A. (2006). The nucleoporin Nup96 is required for proper expression of interferon-regulated proteins and functions. *Immunity*, *24*, 295–304.

Fasken, M. B., & Corbett, A. H. (2005). Process or perish: Quality control in mRNA biogenesis. *Nature Structural & Molecular Biology*, *12*, 482–488.

Fazal, F. M., Han, S., Parker, K. R., Kaewsapsak, P., Xu, J., Boettiger, A. N., Chang, H. Y., & Ting, A. Y. (2019). Atlas of subcellular RNA localization revealed by APEX-Seq. *Cell*, *178*, 473–490.

Fischer, T., Sträßer, K., Rácz, A., Rodriguez-Navarro, S., Oppizzi, M., Ihrig, P., Lechner, J., & Hurt, E. (2002). The mRNA export machinery requires the novel Sac3p-Thp1p complex to dock at the nucleoplasmic entrance of the nuclear pores. *The EMBO Journal*, *21*, 5843–5852.

Fischer, U., Huber, J., Boelens, W. C., Mattajt, L. W., & Lührmann, R. (1995). The HIV-1 Rev activation domain is a nuclear export signal that accesses an export pathway used by specific cellular RNAs. *Cell*, *82*, 475–483.

Fish, L., Navickas, A., Culbertson, B., Xu, Y., Nguyen, H. C. B., Zhang, S., Hochman, M., Okimoto, R., Dill, B. D., Molina, H., et al. (2019). Nuclear TARBP2 drives oncogenic dysregulation of RNA splicing and decay. *Molecular Cell*, *75*, 967–981.e9.

Gales, J. P., Kubina, J., Geldreich, A., & Dimitrova, M. (2020). Strength in diversity: Nuclear export of viral RNAs. *Viruses*, *12*, 1014.

Galy, V., Gadal, O., Fromont-Racine, M., Romano, A., Jacquier, A., & Nehrbass, U. (2004). Nuclear retention of unspliced mRNAs in yeast is mediated by perinuclear Mlp1. *Cell*, *116*, 63–73.

García-Benítez, F., Gaillard, H., & Aguilera, A. (2017). Physical proximity of chromatin to nuclear pores prevents harmful R loop accumulation contributing to maintain genome stability. *Proceedings of the National Academy of Sciences of the United States of America*, *114*, 10942–10947.

Gómez-González, B., García-Rubio, M., Bermejo, R., Gaillard, H., Shirahige, K., Marín, A., Foiani, M., & Aguilera, A. (2011). Genome-wide function of THO/TREX in active genes prevents R-loop-dependent replication obstacles. *The EMBO Journal*, *30*, 3106–3119.

Green, D. M., Johnson, C. P., Hagan, H., & Corbett, A. H. (2003). The C-terminal domain of myosin-like protein 1 (Mlp1p) is a docking site for heterogeneous nuclear ribonucleoproteins that are required for mRNA export. *Proceedings of the National Academy of Sciences of the United States of America*, *100*, 1010–1015.

Grünwald, D., & Singer, R. H. (2010). In vivo imaging of labelled endogenous β-actin mRNA during nucleocytoplasmic transport. *Nature*, *467*, 604.

Hackmann, A., Wu, H., Schneider, U.-M., Meyer, K., Jung, K., & Krebber, H. (2014). Quality control of spliced mRNAs requires the shuttling SR proteins Gbp2 and Hrb1. *Nature Communications*, *5*, 3123.

Halpern, K. B., Tanami, S., Landen, S., Chapal, M., Szlak, L., Hutzler, A., Nizhberg, A., & Itzkovitz, S. (2015). Bursty gene expression in the intact mammalian liver. *Molecular Cell*, *58*, 147–156.

Heath, C. G., Viphakone, N., & Wilson, S. A. (2016). The role of TREX in gene expression and disease. *The Biochemical Journal*, *473*, 2911–2935.

Herold, A., Teixeira, L., & Izaurralde, E. (2003). Genome-wide analysis of nuclear mRNA export pathways in Drosophila. *The EMBO Journal*, *22*, 2472–2483.

Hilleren, P., McCarthy, T., Rosbash, M., Parker, R., & Jensen, T. H. (2001). Quality control of mRNA 3′-end processing is linked to the nuclear exosome. *Nature*, *413*, 538.

Horvathova, I., Voigt, F., Kotrys, A. V., Zhan, Y., Artus-Revel, C. G., Eglinger, J., Stadler, M. B., Giorgetti, L., & Chao, J. A. (2017). The dynamics of mRNA turnover revealed by single-molecule imaging in single cells. *Molecular Cell*, *68*, 615–625.e9.

Huang, Y., Yario, T. A., & Steitz, J. A. (2004). A molecular link between SR protein dephosphorylation and mRNA export. *Proceedings of the National Academy of Sciences of the United States of America*, *101*, 9666–9670.

Ibarra, A., Benner, C., Tyagi, S., Cool, J., & Hetzer, M. W. (2016). Nucleoporin-mediated regulation of cell identity genes. *Genes & Development*, *30*, 2253–2258.

Jacinto, F. V., Benner, C., & Hetzer, M. W. (2015). The nucleoporin Nup153 regulates embryonic stem cell pluripotency through gene silencing. *Genes & Development*, *29*, 1224–1238.

Jani, D., Lutz, S., Marshall, N. J., Fischer, T., Köhler, A., Ellisdon, A. M., Hurt, E., & Stewart, M. (2009). Sus1, Cdc31, and the Sac3 CID region form a conserved interaction platform that promotes nuclear pore association and mRNA export. *Molecular Cell*, *33*, 727–737.

Johnson, S. A., Kim, H., Erickson, B., & Bentley, D. L. (2011). The export factor Yra1 modulates mRNA 3′ end processing. *Nature Structural & Molecular Biology*, *18*, 1164.

Kim, M., Ahn, S., Krogan, N. J., Greenblatt, J. F., & Buratowski, S. (2004). Transitions in RNA polymerase II elongation complexes at the 3′ ends of genes. *The EMBO Journal*, *23*, 354–364.

Kim, S. J., Fernandez-Martinez, J., Nudelman, I., Shi, Y., Zhang, W., Raveh, B., Herricks, T., Slaughter, B. D., Hogan, J. A., Upla, P., et al. (2018). Integrative structure and functional anatomy of a nuclear pore complex. *Nature*, *555*, 475.

Klinge, S., & Woolford, J. L. (2018). Ribosome assembly coming into focus. *Nature Reviews. Molecular Cell Biology*, *20*, 116–131.

Krull, S., Dörries, J., Boysen, B., Reidenbach, S., Magnius, L., Norder, H., Thyberg, J., & Cordes, V. C. (2010). Protein Tpr is required for establishing nuclear pore-associated zones of heterochromatin exclusion. *The EMBO Journal*, *29*, 1659–1673.

Kurshakova, M. M., Krasnov, A. N., Kopytova, D. V., Shidlovskii, Y. V., Nikolenko, J. V., Nabirochkina, E. N., Spehner, D., Schultz, P., Tora, L., & Georgieva, S. G. (2007). SAGA and a novel Drosophila export complex anchor efficient transcription and mRNA export to NPC. *The EMBO Journal*, *26*, 4956–4965.

Kuss, S. K., Mata, M. A., Zhang, L., & Fontoura, B. M. A. (2013). Nuclear imprisonment: Viral strategies to arrest host mRNA nuclear export. *Viruses*, *5*, 1824–1849.

Lawrence, J. B., & Singer, R. H. (1986). Intracellular localization of messenger RNAs for cytoskeletal proteins. *Cell*, *45*, 407–415.

Lee, E. S., Wolf, E. J., Ihn, S. S. J., Smith, H. W., Emili, A., & Palazzo, A. F. (2020). TPR is required for the efficient nuclear export of mRNAs and lncRNAs from short and intron-poor genes. *Nucleic Acids Research*, *48*, 11645–11663.

Liang, Y., Franks, T. M., Marchetto, M. C., Gage, F. H., & Hetzer, M. W. (2013). Dynamic association of NUP98 with the human genome. *PLoS Genetics*, *9*, e1003308.

Lin, D. H., & Hoelz, A. (2019). The structure of the nuclear pore complex (an update). *Annual Review of Biochemistry*, *88*, 1–59.

Mahiet, C., & Swanson, C. M. (2016). Control of HIV-1 gene expression by SR proteins. *Biochemical Society Transactions*, *44*, 1417–1425.

Makhnevych, T., Lusk, C. P., Anderson, A. M., Aitchison, J. D., & Wozniak, R. W. (2003). Cell cycle regulated transport controlled by alterations in the nuclear pore complex. *Cell*, *115*, 813–823.

Mehlin, H., Daneholt, B., & Skoglund, U. (1992). Translocation of a specific premessenger ribonucleoprotein particle through the nuclear pore studied with electron microscope tomography. *Cell*, *69*, 605–613.

Molenaar, C., Abdulle, A., Gena, A., Tanke, H. J., & Dirks, R. W. (2004). Poly(A)+ RNAs roam the cell nucleus and pass through speckle domains in transcriptionally active and inactive cells. *The Journal of Cell Biology*, *165*, 191–202.

Mor, A., Suliman, S., Ben-Yishay, R., Yunger, S., Brody, Y., & Shav-Tal, Y. (2010). *Dynamics of single mRNP nucleocytoplasmic transport and export through the nuclear pore in living cells*.

Niepel, M., Molloy, K. R., Williams, R., Farr, J. C., Meinema, A. C., Vecchietti, N., Cristea, I. M., Chait, B. T., Rout, M. P., & Strambio-De-Castillia, C. (2013). The nuclear basket proteins Mlp1p and Mlp2p are part of a dynamic interactome including Esc1p and the proteasome. *Molecular Biology of the Cell*, *24*, 3920–3938.

Niño, C. A., Guet, D., Gay, A., Brutus, S., Jourquin, F., Mendiratta, S., Salamero, J., Géli, V., & Dargemont, C. (2016). Posttranslational marks control architectural and functional plasticity of the nuclear pore complex basket. *The Journal of Cell Biology*, *212*, 167–180.

Ocwieja, K. E., Sherrill-Mix, S., Mukherjee, R., Custers-Allen, R., David, P., Brown, M., Wang, S., Link, D. R., Olson, J., Travers, K., et al. (2012). Dynamic regulation of HIV-1 mRNA populations analyzed by single-molecule enrichment and long-read sequencing. *Nucleic Acids Research*, *40*, 10345–10355.

Oka, M., Asally, M., Yasuda, Y., Ogawa, Y., Tachibana, T., & Yoneda, Y. (2010). The Mobile FG Nucleoporin Nup98 Is a Cofactor for Crm1-dependent Protein Export. *Molecular Biology of the Cell*, *21*, 1885–1896.

Ori, A., Banterle, N., Iskar, M., Andrés-Pons, A., Escher, C., Bui, H. K., Sparks, L., Solis-Mezarino, V., Rinner, O., Bork, P., et al. (2013). Cell type-specific nuclear pores: a case in point for context-dependent stoichiometry of molecular machines. *Molecular Systems Biology*, *9*, 648.

Park, N., Skern, T., & Gustin, K. E. (2010). Specific cleavage of the nuclear pore complex protein Nup62 by a viral protease. *The Journal of Biological Chemistry*, *285*, 28796–28805.

Parrott, B. B., Chiang, Y., Hudson, A., Sarkar, A., Guichet, A., & Schulz, C. (2011). Nucleoporin98-96 Function Is required for transit amplification divisions in the germ line of *Drosophila melanogaster*. *PLoS One*, *6*, e25087.

Pascual-Garcia, P., & Capelson, M. (2019). Nuclear pores in genome architecture and enhancer function. *Current Opinion in Cell Biology*, *58*, 126–133.

Politz, J. C., Browne, E. S., Wolf, D. E., & Pederson, T. (1998). Intranuclear diffusion and hybridization state of oligonucleotides measured by fluorescence correlation spectroscopy in living cells. *Proceedings of the National Academy of Sciences of the United States of America*, *95*, 6043–6048.

Politz, J. C., Tuft, R. A., Pederson, T., & Singer, R. H. (1999). Movement of nuclear poly(A) RNA throughout the interchromatin space in living cells. *Current Biology*, *9*, 285–291.

Porter, F. W., & Palmenberg, A. C. (2008). Leader-induced phosphorylation of nucleoporins correlates with nuclear trafficking inhibition by cardioviruses. *Journal of Virology*, *83*, 1941–1951.

Powrie, E. A., Zenklusen, D., & Singer, R. H. (2011). A nucleoporin, Nup60p, affects the nuclear and cytoplasmic localization of ASH1 mRNA in *S. cerevisiae*. *RNA*, *17*, 134–144.

Prasanth, K. V., Prasanth, S. G., Xuan, Z., Hearn, S., Freier, S. M., Bennett, C. F., Zhang, M. Q., & Spector, D. L. (2005). Regulating gene expression through RNA nuclear retention. *Cell*, *123*, 249–263.

Pühringer, T., Hohmann, U., Fin, L., Pacheco-Fiallos, B., Schellhaas, U., Brennecke, J., & Plaschka, C. (2020). Structure of the human core transcription-export complex reveals a hub for multivalent interactions. *eLife*, *9*, e61503.

Rabut, G., Lénárt, P., & Ellenberg, J. (2004). Dynamics of nuclear pore complex organization through the cell cycle. *Current Opinion in Cell Biology*, *16*, 314–321.

Raices, M., & D'Angelo, M. A. (2012). Nuclear pore complex composition: a new regulator of tissue-specific and developmental functions. *Nature Reviews. Molecular Cell Biology*, *13*, 687.

Rajanala, K., & Nandicoori, V. K. (2012). Localization of nucleoporin Tpr to the nuclear pore complex is essential for Tpr mediated regulation of the export of unspliced RNA. *PLoS One*, *7*, e29921.

Rajoo, S., Vallotton, P., Onischenko, E., & Weis, K. (2018). Stoichiometry and compositional plasticity of the yeast nuclear pore complex revealed by quantitative fluorescence microscopy. *Proceedings of the National Academy of Sciences of the United States of America*, *115*, 201719398.

Reichert, V. L., Hir, H. L., Jurica, M. S., & Moore, M. J. (2002). 5′ exon interactions within the human spliceosome establish a framework for exon junction complex structure and assembly. *Genes & Development*, *16*, 2778–2791.

Rodrigues, J. P., Rode, M., Gatfield, D., Blencowe, B. J., Carmo-Fonseca, M., & Izaurralde, E. (2001). REF proteins mediate the export of spliced and unspliced mRNAs from the nucleus. *Proceedings of the National Academy of Sciences of the United States of America*, *98*, 1030–1035.

Roth, K. M., Wolf, M. K., Rossi, M., & Butler, J. S. (2005). The nuclear exosome contributes to autogenous control of NAB2 mRNA levels. *Molecular and Cellular Biology*, *25*, 1577–1585.

Rougemaille, M., Dieppois, G., Kisseleva-Romanova, E., Gudipati, R. K., Lemoine, S., Blugeon, C., Boulay, J., Jensen, T. H., Stutz, F., Devaux, F., et al. (2008). THO/Sub2p functions to coordinate 3′-end processing with gene-nuclear pore association. *Cell*, *135*, 308–321.

Saguez, C., Olesen, J. R., & Jensen, T. H. (2005). Formation of export-competent mRNP: escaping nuclear destruction. *Current Opinion in Cell Biology*, *17*, 287–293.

Saguez, C., Schmid, M., Olesen, J. R., Ghazy, M. A. E.-H., Qu, X., Poulsen, M. B., Nasser, T., Moore, C., & Jensen, T. H. (2008). Nuclear mRNA surveillance in THO/sub2 mutants is triggered by inefficient polyadenylation. *Molecular Cell*, *31*, 91–103.

Sandri-Goldin, R. M. (2004). Viral regulation of mRNA export. *Journal of Virology*, *78*, 4389–4396.

Saroufim, M.-A., Bensidoun, P., Raymond, P., Rahman, S., Krause, M. R., Oeffinger, M., & Zenklusen, D. (2015). The nuclear basket mediates perinuclear mRNA scanning in budding yeast. *The Journal of Cell Biology*, *211*, 1131–1140.

Schäfer, T., Maco, B., Petfalski, E., Tollervey, D., Böttcher, B., Aebi, U., & Hurt, E. (2006). Hrr25-dependent phosphorylation state regulates organization of the pre-40S subunit. *Nature*, *441*, 651–655.

Schmeing, T. M., Voorhees, R. M., Kelley, A. C., Gao, Y.-G., Murphy, F. V., Weir, J. R., & Ramakrishnan, V. (2009). The crystal structure of the ribosome bound to EF-Tu and asminoacyl-tRNA. *Science*, *326*, 688–694.

Schmid, M., Arib, G., Laemmli, C., Nishikawa, J., Durussel, T., & Laemmli, U. K. (2006). Nup-PI: The nucleopore-promoter interaction of genes in yeast. *Molecular Cell*, *21*, 379–391.

Schmid, M., & Jensen, T. H. (2018). Controlling nuclear RNA levels. *Nature Reviews. Genetics*, *19*, 518–529.

Schmidt, H. B., & Görlich, D. (2015). Nup98 FG domains from diverse species spontaneously phase-separate into particles with nuclear pore-like permselectivity. *eLife*, *4*, e04251.

Scholz, B. A., Sumida, N., de Lima, C. D. M., Chachoua, I., Martino, M., Tzelepis, I., Nikoshkov, A., Zhao, H., Mehmood, R., Sifakis, E. G., et al. (2019). WNT signaling and AHCTF1 promote oncogenic MYC expression through super-enhancer-mediated gene gating. *Nature Genetics*, *51*, 1723–1731.

Schuller, S. K., Schuller, J. M., Prabu, J. R., Baumgärtner, M., Bonneau, F., Basquin, J., & Conti, E. (2020). Structural insights into the nucleic acid remodeling mechanisms of the yeast THO-Sub2 complex. *eLife*, *9*, e61467.

Scott, D. D., Aguilar, L. C., Kramar, M., & Oeffinger, M. (2019). The biology of mRNA: Structure and function. *Advances in Experimental Medicine and Biology*, *1203*, 33–81.

Shav-Tal, Y., Darzacq, X., Shenoy, S. M., Fusco, D., Janicki, S. M., Spector, D. L., & Singer, R. H. (2004). Dynamics of single mRNPs in nuclei of living cells. *Science*, *304*, 1797–1800.

Siebrasse, J.P., Veith, R., Dobay, A., Leonhardt, H., Daneholt, B., &Kubitscheck, U. (2008). *Discontinuous movement of mRNP particles in nucleoplasmic regions devoid of chromatin*.

Singh, G., Pratt, G., Yeo, G. W., & Moore, M. J. (2015). The clothes make the mRNA: Past and present trends in mRNP fashion. *Annual Review of Biochemistry*, *84*, 1–30.

Soheilypour, M., & Mofrad, M. R. K. (2016). Regulation of RNA-binding proteins affinity to export receptors enables the nuclear basket proteins to distinguish and retain aberrant mRNAs. *Scientific Reports UK*, *6*, 35380.

Sood, V., & Brickner, J. H. (2014). Nuclear pore interactions with the genome. *Current Opinion in Genetics & Development*, *25*, 43–49.

Soucek, S., Zeng, Y., Bellur, D. L., Bergkessel, M., Morris, K. J., Deng, Q., Duong, D., Seyfried, N. T., Guthrie, C., Staley, J. P., et al. (2016). Evolutionarily conserved polyadenosine RNA binding protein Nab2 cooperates with splicing machinery to regulate the fate of pre-mRNA. *Molecular and Cellular Biology*, *36*, 2697–2714.

Stewart, M. (2019a). Polyadenylation and nuclear export of mRNAs. *The Journal of Biological Chemistry*, *294*, 2977–2987.

Stewart, M. (2019b). Subcellular biochemistry. *Sub-Cellular Biochemistry*, *93*, 461–470.

Strambio-de-Castillia, C., Blobel, G., & Rout, M. P. (1999). Proteins connecting the nuclear pore complex with the nuclear interior. *The Journal of Cell Biology*, *144*, 839–855.

Strambio-De-Castillia, C., Niepel, M., & Rout, M. P. (2010). The nuclear pore complex: bridging nuclear transport and gene regulation. *Nature Reviews. Molecular Cell Biology*, *11*, 490.

Sun, J., Shi, Y., & Yildirim, E. (2019). The nuclear pore complex in cell type-specific chromatin structure and gene regulation. *Trends in Genetics*, *35*, 579–588.

Taddei, A., Houwe, G. V., Hediger, F., Kalck, V., Cubizolles, F., Schober, H., & Gasser, S. M. (2006). Nuclear pore association confers optimal expression levels for an inducible yeast gene. *Nature*, *441*, 774.

Tudek, A., Schmid, M., & Jensen, T. H. (2019). Escaping nuclear decay: the significance of mRNA export for gene expression. *Current Genetics*, *65*, 473–476.

Umlauf, D., Bonnet, J., Waharte, F., Fournier, M., Stierle, M., Fischer, B., Brino, L., Devys, D., & Tora, L. (2013). The human TREX-2 complex is stably associated with the nuclear pore basket. *Journal of Cell Science*, *126*, 2656–2667.

Valencia, P., Dias, A. P., & Reed, R. (2008). Splicing promotes rapid and efficient mRNA export in mammalian cells. *Proceedings of the National Academy of Sciences of the United States of America*, *105*, 3386–3391.

Veith, R., Sorkalla, T., Baumgart, E., Anzt, J., Häberlein, H., Tyagi, S., Siebrasse, J. P., & Kubitscheck, U. (2010). Balbiani ring mRNPs diffuse through and bind to clusters of large intranuclear molecular structures. *Biophysical Journal*, *99*, 2676–2685.

Vinciguerra, P., Iglesias, N., Camblong, J., Zenklusen, D., & Stutz, F. (2005). Perinuclear Mlp proteins downregulate gene expression in response to a defect in mRNA export. *The EMBO Journal*, *24*, 813–823.

von Kobbe, C., van Deursen, J. M. A., Rodrigues, J. P., Sitterlin, D., Bachi, A., Wu, X., Wilm, M., Carmo-Fonseca, M., & Izaurralde, E. (2000). Vesicular stomatitis virus matrix protein inhibits host cell gene expression by targeting the nucleoporin Nup98. *Molecular Cell*, *6*, 1243–1252.

Vovk, A., Gu, C., Opferman, M. G., Kapinos, L. E., Lim, R. Y., Coalson, R. D., Jasnow, D., & Zilman, A. (2016). Simple biophysics underpins collective conformations of the intrinsically disordered proteins of the Nuclear Pore Complex. *eLife*, *5*, e10785.

Wegener, M., & Müller-McNicoll, M. (2018). Nuclear retention of mRNAs—Quality control, gene regulation and human disease. *Seminars in Cell & Developmental Biology*, *79*, 131–142.

Wende, W., Friedhoff, P., & Sträßer, K. (2019). The biology of mRNA: Structure and function. *Advances in Experimental Medicine and Biology*, *1203*, 1–31.

Williams, T., Ngo, L. H., & Wickramasinghe, V. O. (2017). Nuclear export of RNA: Different sizes, shapes and functions. *Seminars in Cell & Developmental Biology*, *75*, 70–77.

Woodward, L. A., Mabin, J. W., Gangras, P., & Singh, G. (2016). The exon junction complex: a lifelong guardian of mRNA fate. *WIREs RNA*, *8*, e1411.

Woolford, J. L., & Baserga, S. J. (2013). Ribosome biogenesis in the yeast *Saccharomyces cerevisiae*. *Genetics*, *195*, 643–681.

Xie, Y., & Ren, Y. (2019). Mechanisms of nuclear mRNA export: A structural perspective. *Traffic*, *20*, 829–840.

Yarbrough, M. L., Mata, M. A., Sakthivel, R., & Fontoura, B. M. A. (2014). Viral subversion of nucleocytoplasmic trafficking. *Traffic*, *15*, 127–140.

Zander, G., Hackmann, A., Bender, L., Becker, D., Lingner, T., Salinas, G., & Krebber, H. (2016). mRNA quality control is bypassed for immediate export of stress-responsive transcripts. *Nature*, *540*, 593.

Zhang, X., Chen, S., Yoo, S., Chakrabarti, S., Zhang, T., Ke, T., Oberti, C., Yong, S. L., Fang, F., Li, L., et al. (2008). Mutation in nuclear pore component NUP155 leads to atrial fibrillation and early sudden cardiac death. *Cell*, *135*, 1017–1027.

Zuckerman, B., Ron, M., Mikl, M., Segal, E., & Ulitsky, I. (2020). Gene architecture and sequence composition underpin selective dependency of nuclear export of long RNAs on NXF1 and the TREX complex. *Molecular Cell*, *79*, 251–267.

**How to cite this article:** Bensidoun P, Zenklusen D, Oeffinger M. Choosing the right exit: How functional plasticity of the nuclear pore drives selective and efficient mRNA export. *WIREs RNA*. 2021;e1660. https://doi.org/10.1002/wrna.1660

# Annex-2 The nuclear basket mediates perinuclear mRNA scanning in budding yeast

Mark-Albert Saroufim,[1] Pierre Bensidoun,[1,2] Pascal Raymond,[1] Samir Rahman,[1] Matthew R. Krause,[4] Marlene Oeffinger,[1,2,3] and Daniel Zenklusen[1]

[1]Departement de Biochimie et Medecine Moleculaire, Faculte de Medecine, Universite de Montreal, H3T 1J4 Montreal, Quebec, Canada
[2]Institut de Recherches Cliniques de Montreal, H2W 1R7 Montreal, Quebec, Canada
[3]Faculty of Medicine, Division of Experimental Medicine and [4]Montreal Neurological Institute, McGill University, H3A 2B4 Montreal, Quebec, Canada

Published in JCB (2015)

THE JOURNAL OF CELL BIOLOGY

# The nuclear basket mediates perinuclear mRNA scanning in budding yeast

Mark-Albert Saroufim,[1] Pierre Bensidoun,[1,2] Pascal Raymond,[1] Samir Rahman,[1] Matthew R. Krause,[4] Marlene Oeffinger,[1,2,3] and Daniel Zenklusen[1]

[1]Departement de Biochimie et Medecine Moleculaire, Faculte de Medecine, Universite de Montreal, H3T 1J4 Montreal, Quebec, Canada
[2]Institut de Recherches Cliniques de Montreal, H2W 1R7 Montreal, Quebec, Canada
[3]Faculty of Medicine, Division of Experimental Medicine and [4]Montreal Neurological Institute, McGill University, H3A 2B4 Montreal, Quebec, Canada

After synthesis and transit through the nucleus, messenger RNAs (mRNAs) are exported to the cytoplasm through the nuclear pore complex (NPC). At the NPC, messenger ribonucleoproteins (mRNPs) first encounter the nuclear basket where mRNP rearrangements are thought to allow access to the transport channel. Here, we use single mRNA resolution live cell microscopy and subdiffraction particle tracking to follow individual mRNAs on their path toward the cytoplasm. We show that when reaching the nuclear periphery, RNAs are not immediately exported but scan along the nuclear periphery, likely to find a nuclear pore allowing export. Deletion or mutation of the nuclear basket proteins *MLP1/2* or the mRNA binding protein Nab2 changes the scanning behavior of mRNPs at the nuclear periphery, shortens residency time at nuclear pores, and results in frequent release of mRNAs back into the nucleoplasm. These observations suggest a role for the nuclear basket in providing an interaction platform that keeps RNAs at the periphery, possibly to allow mRNP rearrangements before export.

## Introduction

The export of mRNAs from the nucleus to the cytoplasm is one of many steps along the gene expression pathway and is fundamental for mRNAs to meet with ribosomes for translation in the cytoplasm (Oeffinger and Zenklusen, 2012). Export to the cytoplasm occurs through the nuclear pore complex (NPC), a large macromolecular complex embedded in the nuclear membrane (Aitchison and Rout, 2012). On the nuclear side of the NPC, eight protein filaments protrude from the central scaffold into the nucleoplasm and converge in a distal ring to form the nuclear basket (Beck et al., 2004). The nuclear basket is therefore the first structure messenger RNPs (mRNPs) encounter when reaching the nuclear periphery. Furthermore, mRNA quality control steps are suggested to occur at the nuclear basket, pointing toward a function of the basket as both a gatekeeper and physical barrier (Galy et al., 2004; Vinciguerra et al., 2005). These steps are thought to involve structural rearrangements of mRNPs induced by the local modification of RNA binding proteins and their release from the mRNA before export (Daneholt, 2001; Müller-McNicoll and Neugebauer, 2013). Although exhibiting a weak RNA export phenotype, deletion of nuclear basket proteins does not abolish mRNA export but leads to the increased leakage of partially processed mRNAs to the cytoplasm, suggesting that at least some of these rearrangements are not essential for the transport process per se, but for ensuing proper mRNP maturation, its regulation, and possibly influencing export kinetics (Kosova et al., 2000; Galy et al., 2004; Vinciguerra et al., 2005; Fasken et al., 2008; Powrie et al., 2011).

The myosin-like proteins Mlp1p and Mlp2p are structural components of the basket and are essential for basket integrity; the deletion of Mlps results in basketless pores (Strambio-de-Castillia et al., 1999; Kosova et al., 2000; Niepel et al., 2013). Mlps are composed of a long N-terminal coiled-coil domain and a C-terminal unstructured head domain. The C-terminal region of Mlp1p interacts with the nuclear polyA RNA-binding protein Nab2, a known adapter protein for the mRNA export receptor Mex67, possibly providing an interaction platform for mRNPs at the nuclear basket (Green et al., 2003; Fasken et al., 2008; Grant et al., 2008). In addition to Nab2, Mex67 binds other adapter proteins mediating the interaction between the export receptor and mRNA, including the RNA binding protein Yra1 (Strässer and Hurt, 2000; Stutz et al., 2000; Iglesias et al., 2010). In contrast to Nab2, which accompanies mRNAs to the cytoplasmic side of the NPC, Yra1 is released from the mRNA before translocation to the cytoplasm, a process stimulated by the E3 ubiquitin ligase Tom1 (Duncan et al., 2000; Iglesias et al., 2010). Whether these steps require a potential scaffolding function of the nuclear basket and how the nuclear basket influences the export process has not yet

Correspondence to Daniel Zenklusen: daniel.r.zenklusen@umontreal.ca

Abbreviations used in this paper: mRNP, messenger RNP; NPC, nuclear pore complex; SD, synthetic defined minimal medium; smFISH, single-molecule FISH; SSC, saline sodium citrate; WT, wild type.



The Rockefeller University Press $30.00
J. Cell Biol. Vol. 211 No. 6 1131–1140
www.jcb.org/cgi/doi/10.1083/jcb.201503070

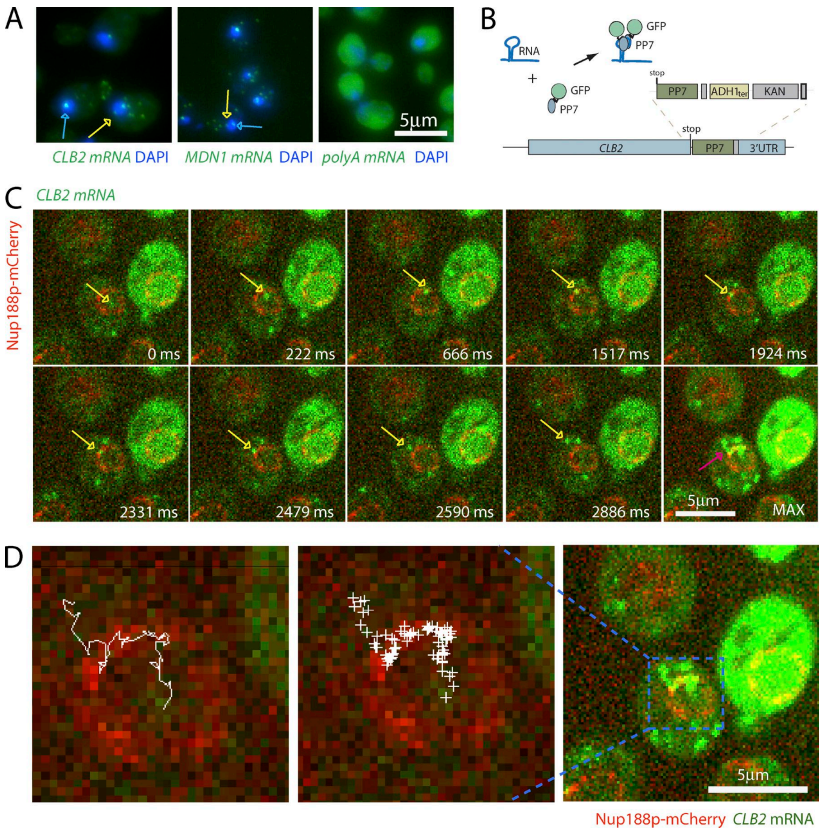


Figure 1. **mRNAs scan the nuclear periphery before export to the cytoplasm.** (A) Localization of *CLB2*, *MDN1*, and polyA mRNA by FISH suggests a rate-limiting step at the nuclear periphery. Blue arrows show sites of transcription. Yellow arrows show single mRNAs. DNA is stained with DAPI (blue). (B) Cartoon illustrating the mRNA labeling strategy using PP7 stem loops. (C) Live cell imaging of *CLB2* mRNA. Individual frames from video acquired in 37-ms intervals. MAX shows the maximum intensity projection of all frames. mRNA is shown in green and NPC in red. The yellow arrows show single tracked mRNA in each frame. The purple arrow outlines the same RNA path in the MAX projected image. (D) Track of nuclear *CLB2* mRNA from C and Video 1. The RNA position in each frame was determined using 2D Gaussian fitting and was superimposed onto a single frame of Video 1 (middle). Left panel shows connected positions to visualize the path from the nucleus to the cytoplasm.

been studied in vivo, largely the result of the lack of experimental tools allowing us to analyze such events. Here, we use single-molecule resolution microscopy to investigate the role of the nuclear basket in mRNA export and reveal general features of mRNA export in budding yeast.

## Results and discussion

Nuclear mRNPs in mammalian cells reach the nuclear periphery by diffusion (Shav-Tal et al., 2004; Grünwald and Singer, 2010; Mor et al., 2010). Because of the large size of mammalian cell nuclei, mRNPs spend a significant amount of time in the nucleus. Yeast nuclei are much smaller (~1.5–2 µm in diameter), and, if diffusing freely in the yeast nucleus, mRNPs will reach the periphery quickly, suggesting that mRNA export in yeast is a fast process (Oeffinger and Zenklusen, 2012). Supporting this notion, FISH, using either probes recognizing polyA RNA or probes to specific mRNAs, shows that mRNAs are rarely observed in the nucleus apart from the site of transcription (Fig. 1 A). Interestingly, when observed in the nucleoplasm, mRNAs are generally excluded from the nucleolus and are most frequently found at the nuclear periphery (Fig. 1 A), suggesting a rate-limiting step at the NPC.

Insertion of PP7 RNA step loops to the 3′ UTR of *MDN1* mRNA allows the detection and tracking of individual mRNAs in yeast (Hocine et al., 2013). To investigate nuclear mRNP movement and to follow the path of single mRNAs toward

the cytoplasm, we labeled *MDN1* and the cell cycle–regulated *CLB2* mRNAs with 12xPP7 stem loops in a strain in which the nuclear pore protein Nup188 was labeled with mCherry (Fig. 1, B and C). Insertion of the PP7 stem loops neither affected growth nor altered mRNA or proteins expression levels, suggesting that PP7 tagging does not affect general mRNA metabolism (Fig. S1). To optimize the signal to noise ratio for single mRNA detection, the PP7-GFP fusion was expressed from an *ADE3* promoter, resulting in low expression levels of free PP7-GFP. This setup allows the detection of individual mRNAs in real time using spinning disk confocal microscopy (Fig. 1, C and D). mRNAs were imaged in a single imaging plane in 37-ms intervals, allowing image acquisition for ∼500 frames (18 s) before signals were bleached. Fig. 1 C, Fig. S2, and Video 1 show that, consistent with what was previously observed by FISH, *CLB2* and *MDN1* mRNAs are mainly cytoplasmic, move rapidly within the cytoplasm, and are frequently lost from the imaging plane. As *CLB2* and *MDN1* are transcribed at low frequency, nuclear mRNAs are rare, and if observed, only a single *CLB2* and *MDN1* mRNA is present in the nucleus at most times. When detecting nuclear mRNPs, they spend little time in the nuclear interior and quickly reach the nuclear periphery, consistent with FISH data showing only few RNAs in the nuclear interior. At the periphery, mRNAs are often not immediately exported, but slide along the nuclear envelope (Fig. 1 C). Infrequently, mRNAs lose their association with the periphery and are released back into the nucleoplasm, but then quickly reassociate with the periphery. Export events are difficult to observe, possibly often occurring outside of the imaging plane. mRNPs are also generally excluded from the nucleolus, although infrequently residence in the nucleolus can be observed (Fig. S2, A and B; and Videos 2 and 3). Nucleolar localization is more frequent for *MDN1* mRNA, possibly because of the gene's localization close to the ribosomal DNA repeats. Interestingly, *MDN1* mRNPs can get trapped in the nucleolus and exit through pores adjacent to the nucleolus (Fig. S2 C and Video 4). To better visualize the path of nuclear mRNAs, we applied a spot detection and tracking software and plotted all nuclear positions, as well as the mRNP track in a single image. As illustrated for the *CLB2* mRNA in Fig. 1 D, mRNPs can scan a large region of the nuclear periphery before being exported.

Obtaining nuclear tracks for mRNAs expressed at low levels is challenging. To facilitate nuclear mRNA detection, we constructed a reporter strain where the *GLT1* gene is regulated by the inducible *GAL1* promoter and labeled with 24xPP7 stem loops in its 5′ UTR (Fig. 2 A). This allows for visualizing RNAs while being synthetized, released into the nucleoplasm, and then exported to the cytoplasm (Fig. 2 A). Images were acquired at early times of induction before RNAs accumulate in high numbers in the cytoplasm. When RNAs are released from the site of transcription into the nucleoplasm, we observe a similar mRNA behavior for *GLT1* mRNAs as for the *CBL2* and *MDN1* mRNAs, spending most of their time in the nucleus scanning the periphery before being exported to the cytoplasm (Fig. 2 B and Video 5).

To quantify mRNA behavior at the periphery, we measured the duration of continuous mRNA movement at the nuclear periphery before mRNAs were either released back into the nucleoplasm, lost from the imaging plane, or exported to the cytoplasm. Perinuclear localization was scored by the overlap of the mRNA signal with the nuclear pore labeled with Nup188-mCherry/dTomato signal. The three mRNAs showed a similar behavior, with approximately two thirds of the mRNAs continuously moving along the nuclear periphery for <500 ms, whereas the remaining RNAs could be observed at the periphery for up to a second, with few RNAs showing longer continuous scanning. We refer to continuous movement at the periphery as scanning that could represent mRNPs moving between pores where transient interactions with NPCs result in increased residence time at the periphery. To better characterize mRNP scanning, we next measured the distances covered by mRNAs during scanning.

Localizing single molecules by Gaussian fitting allows the localization of mRNAs with subdiffraction resolution (Thompson et al., 2002). We first measured the movement of the *GLT1* locus marked by nascent *GLT1* RNAs (Fig. 2 A, blue arrows). The locus is often found at the nuclear periphery, consistent with observations that the endogenous *GAL1* locus associates with the NPC (Casolari et al., 2004; Cabal et al., 2006). Measuring the distance of the center of the nascent RNA spot between two consecutive frames (jump distance) showed that the locus moved <100 nm between frames (Fig. 2 C, middle). This also suggests that if a single mRNA is bound to an NPC, we expect mRNA jump distances similar to that of nascent RNAs. We will therefore consider NPC binding interchangeable with restricted movement similar to the movement of a perinuclear locus. Analyzing the behavior of the peripheral *MDN1*, *CLB2*, and *GLT1* mRNAs showed that the mRNAs moved a range of distances within 37 ms, varying from 50 to 500 nm. Comparing mRNP movement to the movement of transcription sites shows that only a small portion of mRNPs exhibit jump distances consistent with mRNPs bound to NPCs between 37-ms frames (Fig. 2 C, middle).

Electron microscopy has shown that although neither evenly distributed nor regularly spaced from each other, NPCs do not cluster in close proximity to each other (Winey et al., 1997). Furthermore, a peak density in the distance distribution between the center of two pores of ∼240 nm was observed, with a large fraction of pores even further apart from each other. This suggests that spacing between individual baskets is in most cases farther than 120 nm (Winey et al., 1997). Furthermore, with an NPC diameter of ∼100 nm, the mean distance between two pores is therefore greater than the pore diameter. To determine if scanning mRNPs stay associated with individual pores for multiple consecutive frames, we measured the time span in which individual mRNAs move <100 nm between two consecutive frames. Fig. 2 (C, right) shows that a significant fraction of mRNAs show restricted movement for up to 250 ms, consistent with possible interactions of mRNPs with the NPC during scanning. Such interactions might require the interaction of mRNP components and the NPC and might be responsible for the retention of mRNPs at the periphery during scanning.

### The nuclear basket components Mlp1/2 are required for scanning

The nuclear basket is the first structure mRNPs encounter when reaching an NPC. The filamentous Mlp1p and Mlp2p proteins are structural components of the basket, and EM studies showed that their deletion leads to basketless NPCs (Krull et al., 2010; Niepel et al., 2013). Surprisingly, MLPs are not essential for viability, and their deletion only leads to a mild growth and mRNA export defect, which is more pronounced in diploid strains (Fig. S3; Strambio-de-Castillia et al., 1999; Kosova et al., 2000; Green et al., 2003; Powrie et al., 2011). Their presence at the NPC, however, is required for quality control pro-

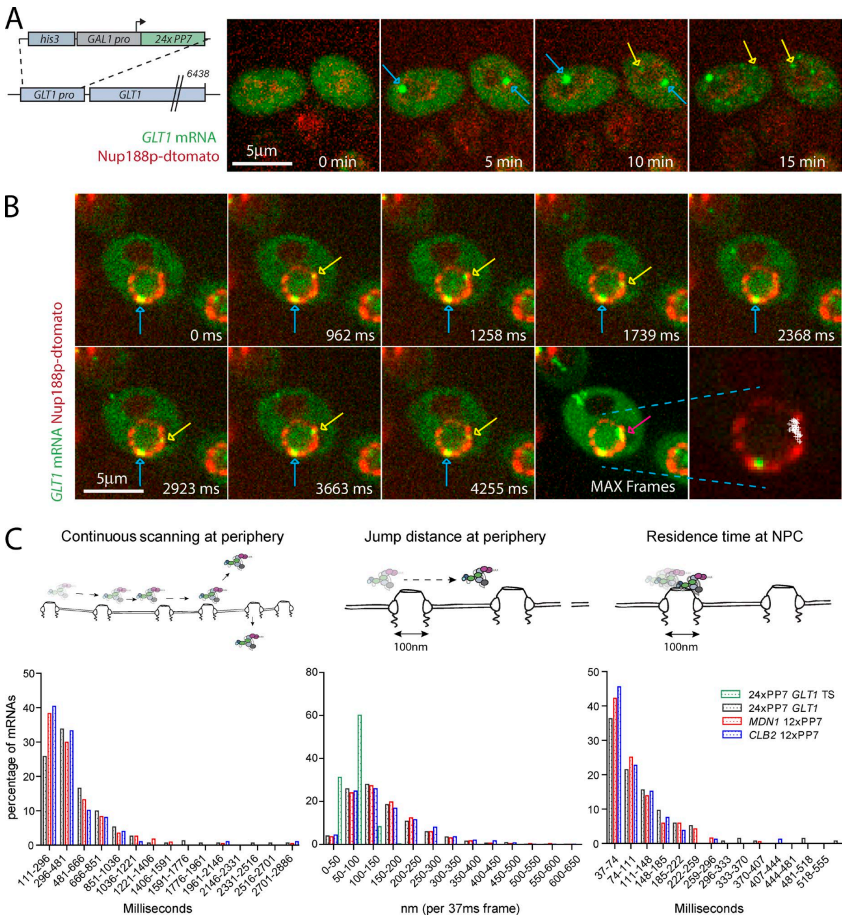


Figure 2. **Jump distances of scanning RNAs suggest movement between pores.** (A) Kinetics of *24PP7-GLT1* mRNA expression upon induction by galactose. Cartoon outlining the *GAL1pro-24PP7-GLT1* reporter (left). Single images of *24PP7-GLT1* mRNA (green) and NPC (red) for indicated time points after the addition of galactose (right). Blue arrows show sites of transcription where multiple nascent mRNAs are associated with the *GAL1pro-24PP7-GLT1* locus. Yellow arrows show single mRNAs. (B) Live cell tracking of scanning *24PP7-GLT1* mRNAs. Individual frames from a video acquired in 37-ms intervals. Lower right panel shows all nuclear positions of a single RNA superimposed onto a single frame. Blue arrows show sites of transcription, and yellow and purple arrows show the tracked mRNA in individual frames and MAX projected image, respectively. (C) Characterization of perinuclear mRNA scanning for *CLB2-12xPP7*, *MDN1-12xPP7*, and *GAL1pro-24PP7-GLT1* mRNAs. Timescales of continuous mRNP scanning (left), jump distance at the periphery (middle), and timescales of restricted movements (right) are shown. Jump distances for the *GAL1pro-24PP7-GLT1* transcription sites are shown in green. 156 (*GLT1*), 171 (*MDN1*), and 104 (*CLB2*) tracks were analyzed. See text for details.

cesses that ensure that only mature mRNPs are exported to the cytoplasm, and they could therefore serve as an interaction platform for different processes to occur at the nuclear periphery. To determine whether the basket is required for perinuclear mRNP scanning, we tracked mRNPs in a strain where *MLP1* and *MLP2* genes were deleted. Fig. 3 B and Video 6 show a *GLT1* mRNA being released from the site of transcription and diffusing to the nuclear periphery. At the periphery, however, the mRNA does not scan for a prolonged period of time, but is quickly released back into the nucleoplasm. Plotting all positions of the nuclear mRNA while in the imaging plane (5.5-s acquisition period) shows that the mRNA spends more time in the nuclear interior than at the periphery, different than mRNAs in a wild-type (WT) background. Moreover, >60% of mRNPs are released back into the nucleoplasm after a <300-ms residence time at the periphery and do not scan for prolonged amounts

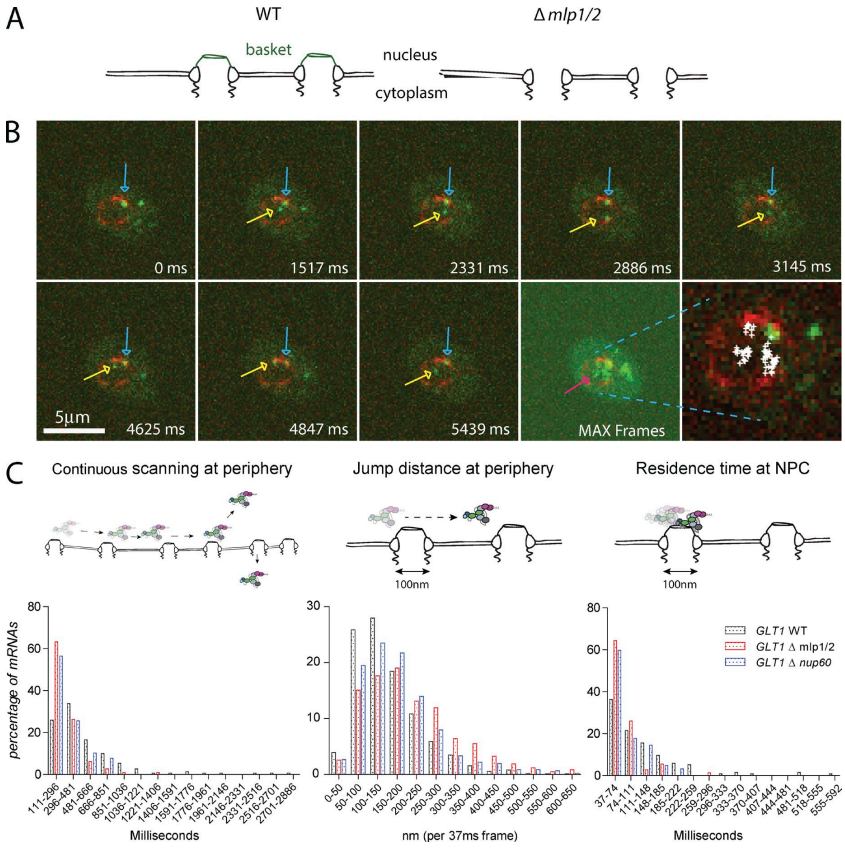


Figure 3. **The nuclear basket is required for perinuclear scanning.** (A) Cartoon illustrating the phenotype of *mlp1/2* deletion leading to basketless pores. (B) Live cell RNA imaging of *GAL1pro-24PP7-GLT1* mRNA shows reduced residence time at the nuclear periphery. Individual frames from a video acquired in 37-ms intervals. Lower right panel shows all nuclear positions of a single RNA superimposed onto a single frame. Blue arrows show sites of transcription, and yellow and purple arrows show the tracked mRNA in individual frames and MAX projected image, respectively. (C) Characterization of perinuclear mRNA scanning for *GAL1pro-24PP7-GLT1* mRNAs in WT *Δmlp1/2* and *Δnup60*. Timescales of continuous mRNP scanning (left), jump distance at the periphery (middle), and timescales of restricted movements (right) are shown. 156 (WT), 105 (*ΔMLP1/2*), and 76 (*ΔNUP60*) tracks were analyzed. See text for details. $P < 0.05$, comparing WT versus mutants using a randomized ANOVA followed by posthoc tests.

of time as observed in WT cells (Fig. 3 C), suggesting a role for the basket in maintaining mRNPs at the periphery. Measuring the jump distance at the periphery shows that mRNPs in basketless cells move longer distances within 37 ms compared with WT, further underlying a role for the basket in restricting the movement of mRNPs at the periphery. Similarly, lack of the basket significantly reduces the number of static frames at the periphery. Deletion of *NUP60*, a nucleoporin involved in the anchoring of Mlp's at the pore, causes similar mRNP behavior to *MLP1/2* deletion. These data suggest that the nuclear basket is required to restrict mRNP movement at the periphery as well as to retain mRNPs at the periphery. The weak mRNA export phenotype of these mutants might result in part from the more frequent release of mRNAs from the nuclear periphery back into the nucleoplasm. However, most mRNAs are likely exported, probably with some delay, as RNAs accumulate in the cytoplasm (Fig. S3, A and B; Fischer et al., 2002; Powrie et al., 2011). Alternatively, a part of mRNAs released from the periphery might get degraded in the nucleus.

### mRNP interactions with the basket stimulate scanning

Loss of the nuclear basket has been shown to change the chromatin environment at the nuclear periphery; regions close to the NPC, usually chromatin free, show dense chromatin compared with a WT strain (Krull et al., 2010; Niepel et al., 2013). The

phenotypes observed in a *ΔMLP1/2* background could therefore, at least in part, be the result of a change in physical properties of the nuclear periphery. Furthermore, lack of the basket could allow mRNPs to diffuse more freely at the periphery, resulting in the larger jump distances observed. Alternatively, these phenotypes could be caused by a change in specific interactions between mRNP components and the basket. The nuclear polyA binding protein Nab2 directly interacts with the C-terminal region of Mlp1 (Green et al., 2003; Fasken et al., 2008; Grant et al., 2008). Nab2 also interacts with the mRNA export receptor Mex67, and the interaction between Nab2 and Mlp1 is likely among the first between the mRNP and the nuclear basket. Furthermore, a single amino acid substitution in Nab2 (Nab2 F73D) was shown to affect the interaction of Nab2p with the C terminus of Mlp1p (Fasken et al., 2008; Grant et al., 2008). To determine whether a Nab2–Mlp1 interaction is required for mRNP scanning at the periphery, we determined mRNP movement in a strain where the C-terminal region of Mlp1 was deleted. In addition to providing an interaction surface for Nab2, the C-terminal region also contains the NLS required to target it to the nucleus. To assure that this C-terminal deletion is targeted to the NPC, we replaced the C-terminal domain of Mlp1p starting at position 4,470 by an exogenous NLS and two copies of mCherry (Fig. 4 B). Furthermore, to test whether the phenotypes observed in the C-terminal deletion are not caused by a change in the overall composition of the basket, we purified Mlp1-associated proteins from an Mlp1–protein A–tagged strain or a strain where the Mlp1 C terminus (Mlp1-ΔC) was replaced by NLS–protein A (Oeffinger et al., 2007b). Fig. 4 C and Table S2 show that Mlp1 and Mlp1-ΔC both copurify basket and NPC components with the same efficiency, suggesting that basket integrity is not disrupted.

Investigation of mRNP movement in an Mlp1-ΔC strain showed reduced continuous mRNP scanning at the periphery, although to a lesser extent than an *MLP1/2* deletion. Furthermore, jump distances at the periphery are similar to the deletion strain, suggesting that the interaction between the mRNP and the basket, dependent on the C terminus of Mlp1, is required to restrict mRNP movement (Fig. 4 D). Deleting the C terminus also led to a reduction in extended NPC interactions. In addition, the Nab2 F73D mutant showed a similar phenotype to the Mlp1-ΔC, suggesting that the Nab2-dependent interaction between the mRNP and the C terminus of Mlp1 is required for perinuclear scanning and that the phenotypes observed in *MLP1/2* deletions are not the result of the physical absence of the basket at the nuclear periphery.

### Tom1 stimulates mRNP binding to the NPC

Although mRNP composition likely varies for different mRNAs, various RNA-binding proteins are thought to be present on most, if not all, mRNAs (Oeffinger and Zenklusen, 2012). We tested whether different nonessential mRNP-associated factors affect perinuclear scanning, including the nuclear cap binding complex (CBC), Pml1 and Pml39, proteins involved in mRNA quality control at the NPC, and the Tom1 E3 ubiquitin ligase (Palancade et al., 2005; Iglesias et al., 2010; Müller-McNicoll and Neugebauer, 2014). Tom1 modifies the mRNP component Yra1, inducing its release from the mRNP before mRNA translocation to the cytoplasm. Neither deletion of the CBC component *CBP80* nor deletions of either *PML1* or *PML39* affected *GLT1* mRNP behavior at the periphery (unpublished data). However, deletion of *TOM1* led to a strong reduction in the number of static mRNPs at the periphery, similar to an *MLP1/2* deletion, whereas scanning times and jump distances were only marginally affected (Fig. 4 E and Fig. S3, C and D). This suggests that Tom1-mediated removal of Yra1 from the mRNP might facilitate binding of mRNPs to the NPC.

The single-molecule tracking data presented here suggest an additional role for the nuclear basket in providing a platform that facilitates mRNPs to stay at the nuclear periphery in the case that they are not immediately exported. mRNP scanning has previously been observed in higher eukaryotes, and here we show that specific interactions of the mRNP with the C-terminal domain of Mlp1 is implicated in maintaining RNAs at the periphery (Grünwald and Singer, 2010). One apparent question is why mRNPs show such a behavior and are not directly exported. One possibility is that rearrangements on the mRNP have to occur before translocation, possibly as part of a quality control mechanism, and that these processes do not take place during the first contact with the periphery. It is also possible that not all pores are available for export, either because of specialized pores or, more likely, because pores might be occupied transporting other molecules; in rapidly growing cells, nucleocytoplasmic transport might get saturated and pore access might be limited. It will be interesting to determine whether different scanning and export rates could be observed for different mRNAs, or under different environmental conditions where nucleocytoplasmic transport is less active, such as the *GFA1* mRNA, which is induced upon cell wall stress and does not show extensive scanning (see Smith et al. in this issue).

## Materials and methods

#### Strains and plasmids

Yeast strains were constructed using standard genetic techniques (Amberg et al., 2005) and are listed in Table S1. GAL1p-24xPP7-*GLT1*–containing strains were constructed by replacing the endogenous *GLT1* promoter with a DNA fragment containing a histidine selectable marker, the *GAL1* promoter followed by 24xPP7 stem loops using homologous recombination *CLB2*-12xPP7, and *MDN1*-12xPP7 strains were constructed by inserting 12xPP7 stem loops into the 3′ UTR of *CLB2* and *MDN1*, respectively, by homologous recombination using a PCR product amplified from pDZ617 (pKAN 12xPP7 V4-*ADH1* terminator) and pDZ645 (pKAN mCherry-12xPP7 V4-*ADH1* terminator). *CLB2* and *MDN1* 3′ UTRs were reconstituted by removing the *ADH1* using CRE recombinase. Nup188 was C-terminal tagged with dTomato or 2xmCherry by homologous recombination using a PCR fragment amplified from pDZ264 (pKAN tdTomato) and from pDZ585 (pKan 2xmCherry), respectively. *Haploid ΔMLP1/2* deletion strains were obtained from M. Rout (The Rockefeller University, New York, NY; Niepel et al., 2013). *CBC80*, *TOM1*, *PML1*, and *PML39* knockout strains were constructed by homologous recombination using a PCR fragment amplified from plasmid pFA6-hphNT1. *nab2F73D* strains were constructed by homologous recombination using a PCR fragment inserting the mutant allele and a selection marker replacing the WT allele. Integration of the mutation was confirmed by sequencing. PP7-PS-2xeGFP fusion protein was expressed from either the *MET25* (pDZ514 or pDZ529) or *ADE3* (pDZ536) promoter. Mlp1 C-terminal deletion was obtained by a C-terminal in-frame integration of a PCR-derived fragment encoding NLS–protein A or NLS-2xmCherry. Correct integration was verified by PCR, Western blot (rabbit anti–protein A antibody; P1291; Sigma-Aldrich), and/or fluorescence microscopy.

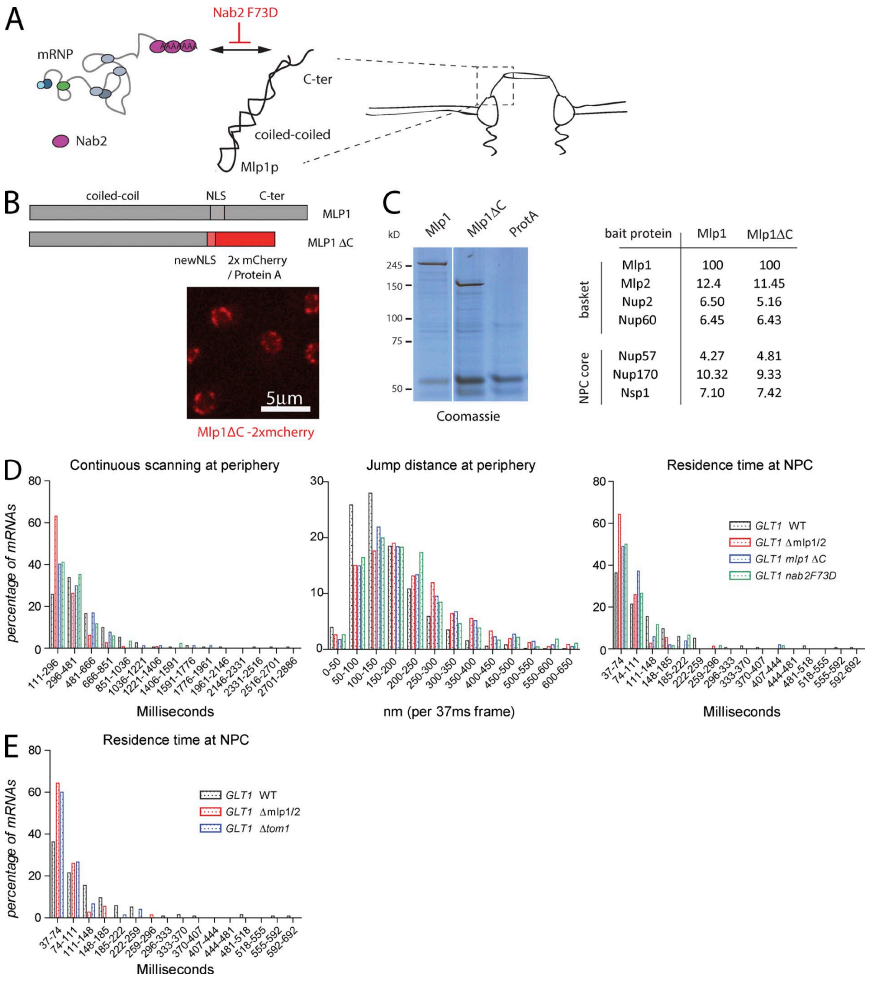


Figure 4. **mRNP–NPC interactions mediate perinuclear scanning.** (A) Cartoon describing the relationship between the nuclear polyA RNA binding protein Nab2 and the C-terminal domain of Mlp1p. (B) Localization of the Mlp1ΔC-2xmCherry fusion protein to the nuclear periphery. See text for details. (C) Deletion of the C terminus of Mlp1 does not affect basket integrity. Coomassie-stained gel separating protein complexes isolated by single-step affinity purification using Mlp1-ProtA, Mlp1ΔC-ProtA, or ProtA as baits. White line indicates that intervening lanes have been spliced out. Table with normalized peptide counts of copurified proteins as determined by mass spectrometry. Only selected NPC components are shown; for full list, see Table S2. (D) Quantification of *GAL1pro-24PP7-GLT1* mRNP scanning behavior in *mlp1ΔC* and *nab2F73D*. 156 (WT), 75 (Mlp1-ΔC), and 85 (Nab2 F73D) tracks were analyzed. (E) Frequency of static frames at the periphery for *GAL1pro-24PP7-GLT1* mRNPs in *Δtom1* strain. $P < 0.05$, comparing WT versus mutants using a randomized ANOVA followed by posthoc tests, except WT versus Mlp1ΔC for scanning.

### Cell synchronization

Cell synchronization to enrich for Clb2 was performed as previously described (Oeffinger et al., 2007a). In brief, cells were grown in synthetic media, arrested in 10-µM α-factor, released into synthetic media, and collected 70 min after release. A harvested cell pellet equivalent to 20 cell ODs was taken up in 6× Laemmli buffer and glass beads, lysed by vortexing and heating cycles, and separated on an SDS-PAGE gel, followed by Western blotting using a rabbit anti-mCherry (PA534974; Invitrogen) and mouse anti-GAPDH antibody (125247; Abcam).

### Single-molecule FISH

Single-molecule FISH (smFISH) was essentially performed as described in Rahman and Zenklusen (2013). *MDN1* and *CLB2* probes were described previously and are listed in Table S3 (mix of 48 for *MDN1*, 40 for *CLB2* 20-nt-long oligos containing 3′ amine synthetized by Biosearch Technologies, Inc., and labeled postsynthesis cy5 and cy3, respectively; Castelnuovo et al., 2013; Messier et al., 2013). polyA RNA was detected using a 35-nt dT DNA probe containing 10 locked nucleic acid nucleosides (synthetized by Exiqon) labeled postsynthesis with cy5 (Table S3). Cells were grown in synthetic defined minimal medium (SD)–uracil and 2% glucose at 30°C overnight to mid-log phase ($OD_{600}$ = 0.6–0.8) and fixed with 4% paraformaldehyde (Electron Microscopy Science) for 30 min at room temperature. Cells were subsequently washed three times with Buffer B (1.2-M sorbitol and 100-mM $KHPO_4$, pH 7.5) and stored overnight at 4°C in Buffer B. Cells were then digested with lyticase (dissolved in 1× PBS to 25,000 U/ml and stored at −20°C; Sigma-Aldrich). Digested cells were plated on poly-L-lysine–treated coverslips and stored in 70% ethanol at −20°C. For hybridization, cells were removed from 70% ethanol, washed twice with 2× saline sodium citrate (SSC), and hydrated in 10% formamide/2× SSC. 10 ng of labeled probe per hybridization (*MDN1* cy5, *CLB2* cy3, and dT LNA cy5) was resuspended in 10% (vol/vol) formamide, 2× SSC, 1 mg $ml^{-1}$ BSA, 10-mM ribonucleoside vanadyl complex (New England Biolabs, Inc.), 5-mM $NaHPO_4$, pH 7.5, 0.5 mg $ml^{-1}$ *Escherichia coli* tRNA, and 0.5 mg $ml^{-1}$ single-stranded DNA and denatured at 95°C for 3 min. Cells were then hybridized for 3 h in the dark at 37°C (20-ng probe per sample). Cells were then washed in 10% formamide/2× SSC at 37°C twice for 30 min, followed by a quick wash in 1× PBS at room temperature. The coverslips were then mounted on glass slides using Prolong gold with DAPI mounting medium (Invitrogen). Images were acquired with a 100× NA 1.3 oil objective on a microscope (Axio Imager Z2; Carl Zeiss) equipped with a charge-coupled device camera (AxioCam mRm; Carl Zeiss) and the following filter sets: 488050–9901-000 (Cy5; Carl Zeiss), SP102 v1 (Cy3; Chroma Technology Corp.), SP103 v2 (Cy3.5; Chroma Technology Corp.), and 488049–9901-000 (DAPI; Carl Zeiss). 3D datasets were generated by acquiring multiple 200-nm z stacks spanning the entire volume of cells using acquisition software (Zen; Carl Zeiss). For mRNA counting, 3D datasets were reduced to 2D datasets by applying a maximum projection function in Fiji. RNA signals were detected and quantified using a spot localization algorithm based on 2D Gaussian fitting that was implemented with custom-made software for the interactive data language platform (ITT Visual Information Solutions) as previously described (Zenklusen et al., 2008). Cellular segmentation was performed manually in Fiji.

### Preparing cells for live cell imaging

Yeast were grown at 30°C in SD with 3% raffinose or SD with 2% glucose to an $OD_{600}$ of 0.4–0.6. For galactose induction, galactose was added to a final concentration of 3%. For imaging, 100-µl cell suspension was added to a 96-well glass-bottom plate (MGB096-1-2-LG-L; Brooks Life Science Systems) previously coated with concanavalin A (Con A) and concentrated on the bottom of the well by centrifugation. Wells were coated by adding 100 µl of 1 mg/ml Con A (Sigma-Aldrich) for 10 min before unbound Con A is removed and the Con A activated by adding 100 µl of 50-mM $CaCl_2$/50-mM $MnSO_4$ for 10 min. The solution was then removed, washed once with 100 µl $ddH_2O$, and air dried.

### Image acquisition and analysis

Images were acquired on a spinning disk confocal microscope (Observer SD; Carl Zeiss) using a 100×/1.43 NA objective (Carl Zeiss), 488-nm (100 mW) and 561-nm (40 mW) excitation laser lines, and Semrock single bandpass filters for GFP (525 nm/50 nm) and RFPs (617 nm/73 nm). Images were captured using an electron-multiplying charge-coupled device camera (Evolve 512; Photometrics) using Zen blue software. Image sequences were performed by first acquiring a single image of a red fluorescent signal, followed by 500 37-ms frames of GFP channel acquisition. Composite images of NPC and mRNA signals (single NPC image was used for the entire length of the video) were assembled in ImageJ. Only videos with nuclear RNAs were analyzed, and mRNAs showing cytoplasmic scanning were excluded from the analysis. For measuring times of continuous scanning at the periphery, jump distances, and number of static frames, only tracks where RNAs colocalize with the nuclear periphery were used. For each strain, perinuclear mRNAs from 20 cells were tracked. Most cells showed mRNAs associate with the periphery multiple times, either because scanning mRNAs moved RNAs out of the imaging plane and then back in, the tracking algorithm missed more than two frames, or mRNAs were released from the periphery to the nuclear interior, resulting in multiple tracks originating from the same mRNA. Only tracks where mRNAs are observed for at least three frames were used in the analysis, and short associations of mRNAs with the periphery in mutant strains (less than three frames) did not lead to scored tracks, resulting in less tracks observed for mutants compared with WT strains. Plots represent the frequency distribution from data of all perinuclear tracks. The total number of tracks analyzed are as follows: GAL-*GLT1* (156), *MDN1* (171), and *CLB2* (104) in WT (Fig. 2 C), GAL-*GLT1* in *ΔMLP1/2* (105), and *ΔNUP60* (76; Fig. 3 C), Mlp1-ΔC (75), Nab2 F73D (85; Fig. 4 D), and *ΔTOM1* (95; Figs. 4 E and S3).

Spot detection using a 2D Gaussian mask fitting algorithm and particle tracking was performed using "localize" as previously described (Coulon et al., 2014). Statistical analysis was performed using Excel (Microsoft), Prism (GraphPad Software), and R software (The R Foundation). Jump distances were calculated using coordinates from the spot detection algorithm using the equation from Excel:

$$D = \sqrt{(x_2 - x_1)^2 + (y_2 - y_1)^2},$$

where $x_1$ and $y_1$ are the coordinates at t = 0, and $x_2$ and $y_2$ are the coordinates of the same mRNA at t = 0 + 1 (37 ms). Superimposing all mRNA positions observed in a single cell was done in MATLAB using the coordinates obtained from the tracking software. Statistical significance comparing the distributions of mRNA behavior was performed using randomized ANOVA, performed in R (Horthorn et al., 2008). Where appropriate, posthoc tests were subsequently performed using randomized *t* tests. P-values were corrected for multiple comparisons using the Holm-Bonferroni method; adjusted p-values <0.05 were considered statistically significant.

### NPC purification and mass spectrometry

Affinity purification was performed as previously described (Oeffinger et al., 2007b). In brief, cells were grown to late log phase, frozen by immersion in liquid nitrogen, and mechanically ground using a planetary ball mill (Retsch). 1 g of cell powder was thawed in 9 ml of extraction buffer (1× tributyltin, 50-mM NaCl, 1-mM DTT, 0.5% Triton X-100, 0.5% of solution P, and 0.02% Antifoam), homogenized with a Polytron for 25 s, and cleared by centrifugation at 4,000 *g* for 5 min. Each lysate was incubated for 30 min with magnetic beads coated with IgG (Dynabeads M-280 sheep anti–rabbit IgG), washed extensively, and resuspended in 50 µl of 20-mM Tris-HCl, pH 8.0. Proteins were digested on beads at 37°C using 1 µg trypsin (Pierce Trypsin Protease, MS Grade) for 16 h and blocked by the addition of 2 µl of 50% formic acid and peptides analyzed by mass spectrometry. Prey proteins were

semiquantitatively analyzed by spectral counting, normalized against the bait counts, and compared.

### Online supplemental material

Fig. S1 shows that the insertion of PP7 stem loops does not alter *MDN1* and *CLB2* mRNA and protein expression levels. Fig. S2 shows *MDN1* and *CLB2* mRNAs scanning the nuclear periphery outside of the nucleolus (A and B) or an *MDN1* mRNA trapped in the nucleolus and getting exported to the cytoplasm though NPCs in the nucleolus. Fig. S3 illustrates *MLP1/2* deletion growth and mRNA export phenotype and mRNP behavior at the nuclear periphery in a *TOM1* deletion strain. Video 1 shows *CLB2* mRNA scanning the nuclear periphery from Fig. 1. Video 2 shows that *CLB2* mRNA scanning the nuclear periphery occurs outside of the nucleolus as shown in Fig. S2 A. Videos 3 and 4 show *MDN1* mRNA scanning the nuclear periphery outside of the nucleolus or being trapped in the nucleolus as shown in Fig. S2 (B and C, respectively). Videos 5–7 show galactose-induced nuclear *GLT1* mRNAs in WT (Fig. 3 A), *Δmlp1/2* (Fig. 3 B), and *Δtom1* (Fig. S3). Table S1 shows yeast strains used in this study. Table S2 is provided as an Excel spreadsheet and summarizes the proteins identified by mass spectrometry purified using Mlp1-ProtA or Mlp1ΔC-ProtA as baits (Fig. 4, B and C). Table S3 is provided as an Excel spreadsheet and lists the smFISH probes. Online supplemental material is available at http://www.jcb.org/cgi/content/full/jcb.201503070/DC1.


### Acknowledgments

We thank Seckin Sinan Isik for help with MATLAB and Mike Rout for the *MLP1/2* deletion strain.

This work is supported by a discovery grant from the Natural Sciences and Engineering Research Council, the Canadian Institute for Health Research (MOP-232642), and the Canadian Foundation for Innovation (awarded to D. Zenklusen). D. Zenklusen holds a Fonds de Recherche du Quebec (FRSQ) Chercheur Boursier Junior I. M. Oeffinger holds a Canadian Institute for Health Research New Investigator Award and an FRSQ Chercheur Boursier Junior I and is supported by a grant from the Canadian Institute for Health Research (MOP-106628).

The authors declare no competing financial interests.

Submitted: 16 March 2015
Accepted: 9 November 2015


## References


Aitchison, J.D., and M.P. Rout. 2012. The yeast nuclear pore complex and transport through it. *Genetics.* 190:855–883. http://dx.doi.org/10.1534/genetics.111.127803

Amberg, D., D. Burke, and J. Strathern. 2005. Methods in Yeast Genetics: A Cold Spring Harbor Laboratory Course Manual. Cold Spring Harbor Laboratory Press, Cold Spring Harbor, NY. 230 pp.

Beck, M., F. Förster, M. Ecke, J.M. Plitzko, F. Melchior, G. Gerisch, W. Baumeister, and O. Medalia. 2004. Nuclear pore complex structure and dynamics revealed by cryoelectron tomography. *Science.* 306:1387–1390. http://dx.doi.org/10.1126/science.1104808

Cabal, G.G., A. Genovesio, S. Rodriguez-Navarro, C. Zimmer, O. Gadal, A. Lesne, H. Buc, F. Feuerbach-Fournier, J.C. Olivo-Marin, E.C. Hurt, and U. Nehrbass. 2006. SAGA interacting factors confine sub-diffusion of transcribed genes to the nuclear envelope. *Nature.* 441:770–773. http://dx.doi.org/10.1038/nature04752

Casolari, J.M., C.R. Brown, S. Komili, J. West, H. Hieronymus, and P.A. Silver. 2004. Genome-wide localization of the nuclear transport machinery couples transcriptional status and nuclear organization. *Cell.* 117:427–439. http://dx.doi.org/10.1016/S0092-8674(04)00448-9

Castelnuovo, M., S. Rahman, E. Guffanti, V. Infantino, F. Stutz, and D. Zenklusen. 2013. Bimodal expression of PHO84 is modulated by early termination of antisense transcription. *Nat. Struct. Mol. Biol.* 20:851–858. http://dx.doi.org/10.1038/nsmb.2598

Coulon, A., M.L. Ferguson, V. de Turris, M. Palangat, C.C. Chow, and D.R. Larson. 2014. Kinetic competition during the transcription cycle results in stochastic RNA processing. *eLife.* 3. http://dx.doi.org/10.7554/eLife.03939

Daneholt, B. 2001. Assembly and transport of a premessenger RNP particle. *Proc. Natl. Acad. Sci. USA.* 98:7012–7017. http://dx.doi.org/10.1073/pnas.111145498

Duncan, K., J.G. Umen, and C. Guthrie. 2000. A putative ubiquitin ligase required for efficient mRNA export differentially affects hnRNP transport. *Curr. Biol.* 10:687–696. http://dx.doi.org/10.1016/S0960-9822(00)00527-3

Fasken, M.B., M. Stewart, and A.H. Corbett. 2008. Functional significance of the interaction between the mRNA-binding protein, Nab2, and the nuclear pore-associated protein, Mlp1, in mRNA export. *J. Biol. Chem.* 283:27130–27143. http://dx.doi.org/10.1074/jbc.M803649200

Fischer, T., K. Strässer, A. Rácz, S. Rodríguez-Navarro, M. Oppizzi, P. Ihrig, J. Lechner, and E. Hurt. 2002. The mRNA export machinery requires the novel Sac3p–Thp1p complex to dock at the nucleoplasmic entrance of the nuclear pores. *EMBO J.* 21:5843–5852. http://dx.doi.org/10.1093/emboj/cdf590

Galy, V., O. Gadal, M. Fromont-Racine, A. Romano, A. Jacquier, and U. Nehrbass. 2004. Nuclear retention of unspliced mRNAs in yeast is mediated by perinuclear Mlp1. *Cell.* 116:63–73. http://dx.doi.org/10.1016/S0092-8674(03)01026-2

Grant, R.P., N.J. Marshall, J.-C. Yang, M.B. Fasken, S.M. Kelly, M.T. Harreman, D. Neuhaus, A.H. Corbett, and M. Stewart. 2008. Structure of the N-terminal Mlp1-binding domain of the *Saccharomyces cerevisiae* mRNA-binding protein, Nab2. *J. Mol. Biol.* 376:1048–1059. http://dx.doi.org/10.1016/j.jmb.2007.11.087

Green, D.M., C.P. Johnson, H. Hagan, and A.H. Corbett. 2003. The C-terminal domain of myosin-like protein 1 (Mlp1p) is a docking site for heterogeneous nuclear ribonucleoproteins that are required for mRNA export. *Proc. Natl. Acad. Sci. USA.* 100:1010–1015. http://dx.doi.org/10.1073/pnas.0336594100

Grünwald, D., and R.H. Singer. 2010. In vivo imaging of labelled endogenous β-actin mRNA during nucleocytoplasmic transport. *Nature.* 467:604–607. http://dx.doi.org/10.1038/nature09438

Hocine, S., P. Raymond, D. Zenklusen, J.A. Chao, and R.H. Singer. 2013. Single-molecule analysis of gene expression using two-color RNA labeling in live yeast. *Nat. Methods.* 10:119–121. http://dx.doi.org/10.1038/nmeth.2305

Horthorn, T., K. Hornik, M.A. van de Wiel, and A. Zeileis. 2008. Implementing a class of permutation tests: the coin package. *J. Stat. Softw.* 28:1–23.

Iglesias, N., E. Tutucci, C. Gwizdek, P. Vinciguerra, E. Von Dach, A.H. Corbett, C. Dargemont, and F. Stutz. 2010. Ubiquitin-mediated mRNP dynamics and surveillance prior to budding yeast mRNA export. *Genes Dev.* 24:1927–1938. http://dx.doi.org/10.1101/gad.583310

Kosova, B., N. Panté, C. Rollenhagen, A. Podtelejnikov, M. Mann, U. Aebi, and E. Hurt. 2000. Mlp2p, a component of nuclear pore attached intranuclear filaments, associates with nic96p. *J. Biol. Chem.* 275:343–350. http://dx.doi.org/10.1074/jbc.275.1.343

Krull, S., J. Dörries, B. Boysen, S. Reidenbach, L. Magnius, H. Norder, J. Thyberg, and V.C. Cordes. 2010. Protein Tpr is required for establishing nuclear pore-associated zones of heterochromatin exclusion. *EMBO J.* 29:1659–1673. http://dx.doi.org/10.1038/emboj.2010.54

Messier, V., D. Zenklusen, and S.W. Michnick. 2013. A nutrient-responsive pathway that determines M phase timing through control of B-cyclin mRNA stability. *Cell.* 153:1080–1093. http://dx.doi.org/10.1016/j.cell.2013.04.035

Mor, A., S. Suliman, R. Ben-Yishay, S. Yunger, Y. Brody, and Y. Shav-Tal. 2010. Dynamics of single mRNP nucleocytoplasmic transport and export through the nuclear pore in living cells. *Nat. Cell Biol.* 12:543–552. http://dx.doi.org/10.1038/ncb2056

Müller-McNicoll, M., and K.M. Neugebauer. 2013. How cells get the message: dynamic assembly and function of mRNA-protein complexes. *Nat. Rev. Genet.* 14:275–287. http://dx.doi.org/10.1038/nrg3434

Müller-McNicoll, M., and K.M. Neugebauer. 2014. Good cap/bad cap: how the cap-binding complex determines RNA fate. *Nat. Struct. Mol. Biol.* 21:9–12. http://dx.doi.org/10.1038/nsmb.2751

Niepel, M., K.R. Molloy, R. Williams, J.C. Farr, A.C. Meinema, N. Vecchietti, I.M. Cristea, B.T. Chait, M.P. Rout, and C. Strambio-De-Castillia. 2013. The nuclear basket proteins Mlp1p and Mlp2p are part of a dynamic interactome including Esc1p and the proteasome. *Mol. Biol. Cell.* 24:3920–3938. http://dx.doi.org/10.1091/mbc.E13-07-0412

Oeffinger, M., and D. Zenklusen. 2012. To the pore and through the pore: a story of mRNA export kinetics. *Biochim. Biophys. Acta.* 1819:494–506. http://dx.doi.org/10.1016/j.bbagrm.2012.02.011

Oeffinger, M., A. Fatica, M.P. Rout, and D. Tollervey. 2007a. Yeast Rrp14p is required for ribosomal subunit synthesis and for correct positioning of the mitotic spindle during mitosis. *Nucleic Acids Res.* 35:1354–1366. http://dx.doi.org/10.1093/nar/gkl824

Oeffinger, M., K.E. Wei, R. Rogers, J.A. DeGrasse, B.T. Chait, J.D. Aitchison, and M.P. Rout. 2007b. Comprehensive analysis of diverse ribonucleoprotein complexes. *Nat. Methods.* 4:951–956. http://dx.doi.org/10.1038/nmeth1101

Palancade, B., M. Zuccolo, S. Loeillet, A. Nicolas, and V. Doye. 2005. Pml39, a novel protein of the nuclear periphery required for nuclear retention of improper messenger ribonucleoparticles. *Mol. Biol. Cell.* 16:5258–5268. http://dx.doi.org/10.1091/mbc.E05-06-0527

Powrie, E.A., D. Zenklusen, and R.H. Singer. 2011. A nucleoporin, Nup60p, affects the nuclear and cytoplasmic localization of ASH1 mRNA in *S. cerevisiae*. *RNA.* 17:134–144. http://dx.doi.org/10.1261/rna.1210411

Rahman, S., and D. Zenklusen. 2013. Single-molecule resolution fluorescent in situ hybridization (smFISH) in the yeast *S. cerevisiae*. *Methods Mol. Biol.* 1042:33–46. http://dx.doi.org/10.1007/978-1-62703-526-2_3

Shav-Tal, Y., X. Darzacq, S.M. Shenoy, D. Fusco, S.M. Janicki, D.L. Spector, and R.H. Singer. 2004. Dynamics of single mRNPs in nuclei of living cells. *Science.* 304:1797–1800. http://dx.doi.org/10.1126/science.1099754

Smith, C., A. Lari, C.P. Derrer, A. Ouwehand, A. Rossouw, M. Huisman, T. Dange, M. Hopman, A. Joseph, D. Zenklusen, et al. 2015. In vivo single-particle imaging of nuclear mRNA export in budding yeast. *J. Cell Biol.* http://dx.doi.org/10.1083/jcb.201503135

Strambio-de-Castillia, C., G. Blobel, and M.P. Rout. 1999. Proteins connecting the nuclear pore complex with the nuclear interior. *J. Cell Biol.* 144:839–855. http://dx.doi.org/10.1083/jcb.144.5.839

Strässer, K., and E. Hurt. 2000. Yra1p, a conserved nuclear RNA-binding protein, interacts directly with Mex67p and is required for mRNA export. *EMBO J.* 19:410–420. http://dx.doi.org/10.1093/emboj/19.3.410

Stutz, F., A. Bachi, T. Doerks, I.C. Braun, B. Séraphin, M. Wilm, P. Bork, and E. Izaurralde. 2000. REF, an evolutionary conserved family of hnRNP-like proteins, interacts with TAP/Mex67p and participates in mRNA nuclear export. *RNA.* 6:638–650. http://dx.doi.org/10.1017/S1355838200000078

Thompson, R.E., D.R. Larson, and W.W. Webb. 2002. Precise nanometer localization analysis for individual fluorescent probes. *Biophys. J.* 82:2775–2783. http://dx.doi.org/10.1016/S0006-3495(02)75618-X

Vinciguerra, P., N. Iglesias, J. Camblong, D. Zenklusen, and F. Stutz. 2005. Perinuclear Mlp proteins downregulate gene expression in response to a defect in mRNA export. *EMBO J.* 24:813–823. http://dx.doi.org/10.1038/sj.emboj.7600527

Winey, M., D. Yarar, T.H. Giddings Jr., and D.N. Mastronarde. 1997. Nuclear pore complex number and distribution throughout the *Saccharomyces cerevisiae* cell cycle by three-dimensional reconstruction from electron micrographs of nuclear envelopes. *Mol. Biol. Cell.* 8:2119–2132. http://dx.doi.org/10.1091/mbc.8.11.2119

Zenklusen, D., D.R. Larson, and R.H. Singer. 2008. Single-RNA counting reveals alternative modes of gene expression in yeast. *Nat. Struct. Mol. Biol.* 15:1263–1271. http://dx.doi.org/10.1038/nsmb.1514

# Annex-3 Live-Cell Imaging of mRNP-NPC Interactions in Budding Yeast

Azra Lari[1], Farzin Farzam[2], Pierre Bensidoun[3,4], Marlene Oeffinger[3,4,5], Daniel Zenklusen[3], David Grunwald[2], Ben Montpetit[6,7]

[1]Department of Cell Biology, University of Alberta, Edmonton, Canada.

[2]RNA Therapeutics Institute, University of Massachusetts Medical School, Worcester, MA, USA.

[3]Département de Biochimie et Médecine Moléculaire, Université de Montréal, Montréal, QC, Canada.

[4]Institut de Recherches Cliniques de Montréal, Montréal, QC, Canada.

[5]Faculty of Medicine, Division of Experimental Medicine, McGill University, Montréal, QC, Canada. [6]Department of Cell Biology, University of Alberta, Edmonton, Canada.

[7]Department of Viticulture and Enology, University of California, Davis, Davis, CA, USA.

Published in Methods Mol Biology 2019

HHS Public Access
Author manuscript
*Methods Mol Biol*. Author manuscript; available in PMC 2020 July 30.

Published in final edited form as:
*Methods Mol Biol*. 2019 ; 2038: 131–150. doi:10.1007/978-1-4939-9674-2_9.

# Live-Cell Imaging of mRNP-NPC Interactions in Budding Yeast

**Azra Lari**[1], **Farzin Farzam**[2], **Pierre Bensidoun**[3,4], **Marlene Oeffinger**[3,4,5], **Daniel Zenklusen**[3], **David Grunwald**[2], **Ben Montpetit**[6,7]

[1]Department of Cell Biology, University of Alberta, Edmonton, Canada.

[2]RNA Therapeutics Institute, University of Massachusetts Medical School, Worcester, MA, USA.

[3]Département de Biochimie et Médecine Moléculaire, Université de Montréal, Montréal, QC, Canada.

[4]Institut de Recherches Cliniques de Montréal, Montréal, QC, Canada.

[5]Faculty of Medicine, Division of Experimental Medicine, McGill University, Montréal, QC, Canada.

[6]Department of Cell Biology, University of Alberta, Edmonton, Canada.

[7]Department of Viticulture and Enology, University of California, Davis, Davis, CA, USA.

## Abstract

Single-molecule resolution imaging has become an important tool in the study of cell biology. Aptamer-based approaches (e.g., MS2 and PP7) allow for detection of single RNA molecules in living cells and have been used to study various aspects of mRNA metabolism, including mRNP nuclear export. Here we outline an imaging protocol for the study of interactions between mRNPs and nuclear pore complexes (NPCs) in the yeast *S. cerevisiae*, including mRNP export. We describe in detail the steps that allow for high-resolution live-cell mRNP imaging and measurement of mRNP interactions with NPCs using simultaneous two-color imaging. Our protocol discusses yeast strain construction, choice of marker proteins to label the nuclear pore complex, as well as imaging conditions that allow high signal-to-noise data acquisition. Moreover, we describe various aspects of postacquisition image analysis for single molecule tracking and image registration allowing for the characterization of mRNP-NPC interactions.

### Keywords

mRNP export; Nuclear pore complex; NPC; Live-cell imaging; Single molecule; Budding yeast; *S. cerevisiae*; Fluorescent imaging; PP7; Superregistration

## 1 Introduction

Transport from the nucleus to the cytoplasm is required for messenger ribonucleic acids (mRNAs) to assemble with ribosomes in the cytoplasm for translation. mRNAs in complex with associated proteins are referred to as messenger ribonucleoprotein particles (mRNPs).

ben.montpetit@ucdavis.edu.
Azra Lari, Farzin Farzam and Pierre Bensidoun contributed equally to this work.

Export of mRNPs occurs through nuclear pore complexes (NPCs), large protein assemblies imbedded in the double membrane lipid bilayer of the nuclear envelope [1]. Built from ~30 nucleoporin proteins (Nups), NPCs form an eight-fold symmetrical assembly that can be divided into three functionally distinct domains. A central scaffold anchors the NPC into the nuclear envelope and forms the central transport channel that allows nucleocytoplamic exchange. Attached to the central scaffold are a number of asymmetrically distributed Nups on the nuclear and cytoplasmic side of the NPC. The cytoplasmic asymmetric Nups play a role in mRNP release after translocation through the central channel, a process that requires the dynamic association of the DEAD-box protein Dbp5 (DDX19b in humans) with the NPC [2]. On the nuclear side, long filamentous proteins, Mlp1/Mlp2 (TPR in humans), protrude into the nucleoplasm converging in a distal ring structure called the nuclear basket. Mlp1/2, as well as basket associated proteins, interact with mRNPs through associated RNA binding proteins (RBPs) to provide a docking site for mRNPs, thereby regulating access to the central transport channel [3,4]. Upon entering the central channel, translocation is not rate limiting, with mRNAs reaching the other side of the nuclear pore within tens of milliseconds [5–8].

The yeast *S. cerevisiae* has been a valuable model system to study mRNA transport. The combination of proteomic and genetic approaches were instrumental to identify most players in this process and in the development of current models describing mRNP export [9–11]. However, how this process is coordinated in space and time, or coupled to upstream and downstream events in gene expression, is still largely unexplored. Live cell single molecule microscopy is an important tool to study this process, and when combined with the power of yeast genetics, has the potential to reveal mechanistic details about this process [4, 6, 12]. However, studying mRNP export using high resolution single molecule microscopy is technically challenging. For example, the size of an NPC in relation to diffraction limited imaging makes it difficult to assign the position of a single mRNP to a subregion of the NPC. Gaussian fitting does allow for subdiffraction localization of single mRNPs, but mRNP signals have to be aligned to a reference nuclear pore signal acquired in a different channel. Moreover, a yeast cell possesses a 200 nm thick cell wall that induces significant light scattering affecting signal-to-noise ratio and therefore localization precision.

Of the various methods allowing for RNA visualization in cells, including molecular beacons and, more recently, variants of Cas9 and Cas13, not all methods allow for single molecule detection in a living cell under fast imaging regimes [13]. The PP7 and MS2 RNA labeling approaches are currently the most robust method for single molecule resolution mRNA imaging. These aptamer-based approaches use the high affinity and specificity of bacteriophage capsid proteins (CP) to bind to an RNA stem-loop that can be inserted into mRNAs of interest. Fusion of the CP to a fluorescent protein allows for the tagged RNA to be fluorescently marked and multimerizing CP binding sites increases signal-to-noise ratio, with 12–24 repeats being typically used for mRNA labeling and detection in yeast [4, 6, 14–17].

To track mRNP-NPC interactions and export events, NPCs are visualized by the labeling of specific nuclear pore proteins using fluorescent proteins. mRNP export is then measured using a microscope setup that allows simultaneous acquisition of both mRNP and NPC

signals using laser illumination and sensitive EMCCD cameras for detection. Because of the spectral shift associated with imaging two channels, measuring the interaction of an mRNP with an NPC, and in particular a subregion of the NPC, requires precise registration of the two imaging channels. This is achieved by a combination of mechanical alignment and image processing using a common signal detected on both cameras [5]. Moreover, mRNP movement must be tracked in each frame using Gaussian fitting with information regarding mRNP movement in prior and subsequent frames used to identify mRNP export events.

In this chapter, we describe a detailed protocol to image mRNP transport with high spatial and temporal resolution by combining the PP7 mRNA labeling strategy with ultrafast image acquisition and image registration allowing the study mRNP export in real time.

## 2 Materials

### 2.1 Yeast Strains and Plasmids

1. *Saccharomyces cerevisiae* BY4743 with genotype *MAT*a/α *his3*Δ*1/his3*Δ*1 leu2*Δ*0/leu2*Δ*0 LYS2/lys2*Δ*0 met15*Δ*0/MET15 ura3*Δ*0/ura3*Δ*0* (EUROSCARF).
2. pDZ417–24xPP7-loxP-KanMX-loxP is used as a template for PCR to generate product to integrate stem loops into target gene (T7 promoter, integrating plasmid) [14].
3. pSH47 (pRS416-GAL1-Cre) used to express Cre recombinase (GAL1 promoter, URA3 CEN plasmid) [18].
4. Nuclear pore complex protein tagged using pFA6a-3xmKATE-caURA3 (pKW4019) [19].
5. GFP-PP7-CP is integrated using pMET25-GFP-PP7-CP plasmid (MET25 promoter, LEU2 integrating plasmid) (pKW3616) [19].

### Media and Solutions

1. *20% Dextrose stock solution:* Dissolve 200 g of dextrose (D-(+)- glucose) in 800 mL of ultrapure water. Stir to dissolve and then autoclave. Store at room temperature.
2. *YEPD liquid medium (Yeast Extract Peptone Dextrose):* Dissolve 10 g of yeast extract and 20 g of peptone to 880 mL of ultrapure water. Stir to dissolve and then autoclave. Allow medium to cool and then add 100 mL of dextrose stock solution. Store at room temperature.
3. *250 mg/ml G418 stock solution:* Dissolve 2.5 g of G418 into 10 mL of ultrapure water. Store at –20 °C in 1 mL aliquots.
4. *YEPD + G418 solid medium (Yeast Extract-Peptone-Dextrose with G418*): Prepare YEPD medium described above and add 20 g of agar before autoclaving (agar will not dissolve until autoclaved). Allow solution to cool enough to be handled but not solidified (~65 °C), and then add 100 mL of the dextrose stock solution and 1 mL of the G418 stock solution. Pour medium (25 mL) into petri

dishes, allow to solidify at room temperature, and then dry for ~3 days (1 L of medium will make ~40 plates). Store at 4 °C.

5. *SC -Ura liquid or solid medium (synthetic complete medium lacking uracil*): Dissolve 6.7 g of yeast nitrogenous base (without amino acids, with ammonium sulfate), and -Uracil dropout supplement in 900 mL of ultrapure water. Stir to dissolve and then autoclave. Allow medium to cool and then add 100 mL of dextrose stock solution. Store at room temperature. To make solid medium add 20 g of Agar and prepare as described above for YEPD plates. Store at 4 °C.

6. *20% Galactose stock solution:* Dissolve 200 g of D-galactose in 800 mL of ultrapure water. Stir to dissolve and then autoclave. Store at room temperature.

7. *SC - Ura +GAL liquid medium (synthetic complete medium lacking uracil with 2% galactose*): Prepare SC-Ura liquid medium as described above, but substitute glucose with a 100 mL of the galactose stock solution.

8. *2 mg/mL Uracil stock solution*: Dissolve 1 g of uracil in 500 mL of ultrapure water. Stir to dissolve and then autoclave. Store at room temperature.

9. *SC + 5-FOA solid medium (synthetic complete medium with 5-fluoroorotic acid*): Dissolve 6.7 g of yeast nitrogenous base (without amino acids, with ammonium sulfate), and complete dropout supplement in 700 mL of ultrapure water. Stir to dissolve and then add 20 g of agar and autoclave. Allow medium to cool (~65 °C) and then add 100 mL of dextrose stock solution and 200 mL of 5-FOA solution (1 g of 5-FOA dissolved in 5 mL of uracil stock solution and 195 mL of ultrapure water heated to 50 °C before adding the 5-FOA). Pour medium (25 mL) into petri dishes, allow to solidify at room temperature, and then dry for ~3 days (1 L of medium will make ~40 plates). Store at 4 °C.

10. *SC -Leu liquid medium (synthetic complete medium lacking leucine*): Dissolve 6.7 g of yeast nitrogenous base (without amino acids, with ammonium sulfate), and -Leucine dropout supplement in 900 mL of ultrapure water. Stir to dissolve and then autoclave. Allow medium to cool and then add 100 mL of dextrose stock solution. Store at room temperature.

11. *Sporulation medium:* Dissolve 10 g of potassium acetate and 1 g of yeast extract in 997.5 mL of ultrapure water. Stir to dissolve and autoclave. Allow to cool and then add 2.5 mL of dextrose stock solution. Store at room temperature.

12. *15 g/L Methionine stock solution:* Dissolve 15 g of methionine in 1 L of ultrapure water. Stir to dissolve and then filter-sterilize (0.22 μm filter). Store at room temperature.

13. *SC-Leu +Met liquid medium (synthetic complete medium lacking leucine supplemented with methionine):* Prepare SC-Leu medium as described above and supplement with 1 mL of methionine stock solution.

14. *SC-Leu +Met + 1.2 M Sorbitol (synthetic complete medium lacking leucine supplemented with methionine and sorbitol*): Dissolve 6.7 g of yeast nitrogenous base (without amino acids, with ammonium sulfate), and -Leucine dropout

supplement, and 218.6 g of sorbitol to an adjusted volume of 900 mL of ultrapure water. Stir to dissolve and then autoclave. Allow medium to cool and then add 100 mL of dextrose stock solution and 1 mL of methionine stock solution. Store at room temperature.

15. *1 M DTT stock solution:* Dissolve 1.5 g of DTT in 10 mL of ultrapure water. Filter to sterilize (0.22 $\mu$m filter), and store at −20 °C in 1 mL aliquots.

16. *1 M Tris-HCl buffer pH 9.5 stock solution:* Dissolve 121.14 g of Tris base in 800 mL of ultrapure water. Adjust pH to 9.5 with concentrated HCl. Stir to dissolve and adjust volume to 1 L. Autoclave and store at room temperature.

17. *1 M magnesium chloride ($MgCl_2$) stock solution:* Dissolve 9.52 g of magnesium chloride in 100 mL of ultrapure water. Filter to sterilize (0.22 $\mu$m filter) and store at room temperature.

18. *20 mg/mL zymolyase (20 T) stock solution*: dissolve 20 mg of zymolyase in 1 mL of spheroplast buffer (below). Aliquot and store at −20 °C.

19. *Spheroplast buffer (1.2 M sorbitol, 50 mM $KPO_4$ pH 7.4, 1 mM $MgCl_2$, 250 $\mu$g/mL zymolyase)*: Dissolve 218.6 g of sorbitol, 3.03 g of potassium phosphate monobasic ($K_2HPO_4$), and 1.035 g of potassium phosphate dibasic ($KH_2PO_4$) in an adjusted volume of 999 mL of ultrapure water. Stir to dissolve and add 1 mL of magnesium chloride stock solution. Filter to sterilize (0.22 $\mu$m filter) and store at room temperature. Before use for spheroplasting, add zymolyase to a final concentration of 250 $\mu$g/mL.

20. *Concanavalin A solution (ConA):* Dissolve 10 mg of ConA in 10 mL of a solution of 5 mM manganese chloride, 5 mM calcium chloride, and 5 mM Tris-HCl buffer pH 7 in ultrapure water. Store in 1 mL aliquots at −20 °C.

### 2.3 Consumables

1. Toothpicks to inoculate yeast cultures.
2. Petri dishes for agar plates.
3. PCR tubes.
4. 35 mm glass bottom plates for imaging.
5. Focus check beads (e.g., FocalCheck Microspheres or similar).
6. Diffraction limited multicolor fluorescent beads (e.g., Tetra-Speck Microspheres or similar)

### 2.4 Equipment

1. PCR machine.
2. Micropipettes.
3. Test tubes for liquid yeast cultures.
4. Incubators with rotators/shakers for yeast growth.

5. Autoclave.
6. Spectrophotometer to measure yeast growth.
7. Centrifuge.
8. Tetrad dissection microscope.

## 3. Methods

Standard yeast growth and transformation methods are followed as described previously [20, 21].

### 3.1 Tagging of an Endogenous Nuclear Pore Complex (NPC) Component with a Fluorescent Protein

To track mRNPs in relation to NPCs, a protein constituent of the complex must be fluorescently tagged. We do this as the first step in strain construction, since once the strain is verified, the same strain can be used for the subsequent tagging of genes of interest with the PP7 cassette. Yeast PCR-based tagging methods are followed to C-terminally tag the component of interest [22], which is only briefly described below.

1. Design oligos containing a sequence homologous to the end of the coding region of the target protein (*see* Note 1).
2. Use oligos and template plasmid (e.g., pKW4019) to generate a PCR product that can be transformed into the BY4743 yeast strain (*see* Note 2).
3. Test resulting transformants by PCR, western blotting, and/or microscopy for proper expression and localization of the tagged protein.

### 3.2 Tagging of an Endogenous Gene with the 24xPP7 Stem Loop Cassette

A detailed method to tag genes with an aptamer-based RNA-tag has been recently described in detail by Tutucci et al. [23]. Refer to this method for detailed instructions for each step including oligo design, PCR, and transformation conditions (*see* Note 3).

1. Amplify the 24xPP7 stem loop cassette from plasmid pDZ617 with oligos each containing 40 base pairs of homologous sequence to the 3′-UTR region of the target gene (*see* Notes 4–6).
2. Grow the yeast strain expressing the fluorescent NPC marker overnight, dilute, and grow to mid-log phase. Transform cells with the PCR product, allow cells to recover in liquid medium, and then plate on YEPD plates supplemented with 200 $\mu$g/mL G418 to select for transformants.
3. Select multiple transformants and confirm integration of the PP7 cassette in the correct location of the genome by PCR, as well as continued presence and expression of the NPC marker.
4. Transform two or more strains with the correct insertion with plasmid pSH47 and select for transformants on synthetic medium lacking uracil (SC-Ura) plates. Multiple transformants should then be grown overnight in SC-Ura supplemented

with 2% galactose to allow for expression of Cre recombinase. Cells are then plated for single colonies on YEPD and tested for growth on G418 to identify colonies that do not grow on G418 due to excision of the selectable marker from the 3′-UTR region of the target gene. Loss of the pSH47 plasmid can be selected by growing cells on medium containing 5-FOA.

5. Genomic DNA PCR can be used to confirm both the genomic location of the loops, as well as the size of the 24xPP7 cassette to ensure the cassette is full length. At this step, also confirm the presence and expression of the NPC marker once again.

6. To generate a haploid strain expressing both the mRNA with PP7 stem loops and the NPC marker, sporulate the diploid heterozygous strain by growing cells for ~5 days (or until tetrads are formed) in 5 mL of sporulation medium.

7. To dissect and isolate tetrads follow the protocol previously described by Amberg et al. [24]. If insertion of the PP7 loops, tagging of the NPC component, or the combination of the two impact fitness of the cell, this is often observed here through a reduction is spore viability and/or slow growth of the haploids containing the cassette and NPC marker.

8. Analyze resulting haploid strains for presence of both the 24xPP7 tagged gene and fluorescently tagged NPC component to isolate haploids of each mating type. These two strains can subsequently be mated to generate a diploid strain homozygous for both the 24xPP7 cassette and NPC marker (*see* Note 7).

9. Analyze resulting 24xPP7 and NPC tagged strains to confirm functionality of the tagged mRNA and Nup protein (*see* Note 8).

### 3.3 Expression of the PP7 Coat Protein

1. Digest ~1 $\mu$g of the pMET-GFP-PP7-CP containing plasmid, transform into the verified haploid or homozygous diploid strains carrying the 24xPP7 cassette and NPC marker, and select for transformants on SC-Leu (*see* Notes 2 and 9).

2. Test multiple transformants for CP expression and the presence of fluorescently marked mRNPs using a fluorescence microscope under careful growth conditions in liquid culture using SC-Leu supplemented with 150 mg/liter of methionine (Met) and grown until early-log phase ($O.D_{600}$ of 0.1–0.3) at 25 °C. Single mRNP particles are often visible as is a general diffuse cell fluorescence from the free PP7-CP (Fig. la and Notes 10 and 11).

### 3.4 Growth and Preparation of Budding Yeast Cells for Imaging and Data Collection

The protocol below uses spheroplasting to remove the yeast cell wall for the purpose of reducing light scatter, which improves signal-to-noise ratios for imaging rapid events (e.g., mRNP export). This may not be required for events that are longer lived (*see* Note 12). The protocol below can be shortened by omitting **steps 2–4**, which will not require sorbitol to be added to the medium in **steps 7** and **8**.

1. Grow cells overnight at 25 °C in SC-Leu+Met, being careful to not allow the cultures to reach saturation by the following morning. Dilute the culture into fresh SC-Leu+Met medium to an $O.D_{600}$ of 0.05 and grow at 26 °C for at least three doublings to ~$O.D_{600}$ of 0.4.
2. Collect 2.0 O.Ds of cells by centrifugation, wash one time with water, and resuspend in 50 mM Tris-HCl, pH 9.5 and 10 mM DTT at room temperature for 15 min.
3. Collect cells again by centrifugation and resuspend in 0.3 mL of spheroplast buffer and incubate at 26 °C for 45 min, while rotating.
4. Collect cells by centrifuging at 500 *g* for 2 min and gently resuspending the cells with 1 mL of synthetic complete medium supplemented with 1.2 M sorbitol.
5. During **steps 2–4**, coat the glass surface of a 35 mm glass bottom dish (MatTek or similar) with ~0.25 mL of the Concanavalin A solution for 5 min and then remove by pipetting and allow to dry.
6. Add 1 mL of spheroplasted cells to the ConA-coated plate and slowly move the plate to coat the glass bottom with the liquid. Allow cells to adhere to the glass surface for ~5 min, or in a swinging bucket centrifuge, spin the plate at 500 *g* for 2 min to adhere the cells to the glass bottom. This requires that the plate and lid be secured to the rotor. We use tape for this, being careful to prevent the dish glass imaging surface from coming in contact with the tape adhesive.
7. Remove unadhered cells by removing the culture liquid in the plate and gently washing the adhered cells and plate with 1 mL of fresh medium with sorbitol.
8. Add 2 mL of fresh SC +sorbitol and incubate the plates in the microscope room for ~30 min to allow the cells to recover from stresses induced by spheroplasting and plating (*see* Note 13).

### 3.5 Live-Cell Two-Color Imaging Setup and Data Acquisition

For imaging mRNP export events a custom microscope has been used, as described below. Commercial single and dual color imaging systems may also be used to collect data detailing NPC-mRNP interactions on different time scales depending on the instrument (Fig. 2).

1. Imaging is performed on a custom-built dual channel microscope setup using a ×60 1.3 NA silicone oil immersion objective (refractive index 1.405; Olympus) (*see* Note 14). The objective is combined with 500-mm focal length tube lenses, resulting in an effective x167 magnification and a back projected pixel size of 95.8-nm on sample plane. The primary emission beam path is split onto two electron-multiplying charge-coupled devices (DU897 BI; iXon; Andor Technology) by a dichroic mirror (z543rdc Chroma). For excitation of fluorescent proteins, solid-state 514-nm and 561-nm laser lines (SE; Cobolt) are used and intensity and on/off are controlled by an acoustooptic tunable filter (AA Opto-Electronics). Laser lines are merged into a mono mode optical fiber

(Qioptiq). The output of the fiber is collimated and delivered through the back port of a stand (IX71) and reflected toward the objective by a dichroic mirror (z514–561-1064rpc, Chroma). Alignment onto the optical axis of the objective is achieved with a 4-axis controlled support for the collimator. An adjustable size iris is used to restrict the illumination to an area of approximately 25-$\mu$m in diameter. The intensity profile in this area has a flatness of about 5%. Each laser is utilized with a shutter (Uniblitz) controlled from the imaging software. To allow reasonably fast switching (100-ms) between high and low power settings with the 561-nm line, a motorized filter wheel with appropriate neutral density filters is placed behind the shutter and before the merging dichroic of the laser module. The notch filters 514.5-nm and 568-nm (Semrock) are used to prevent excitation light from entering the emission path. The latter filter is rotated by 17 degrees with respect to the normal to achieve blocking 561-nm scattered light (*see* Note 15). Mirrors and adjustable custom built camera holders are used to impose control on five degrees of freedom (x, y, z, $\phi$-and $\theta$-angle) and prealign both CCDs. CCDs are synchronized by a start signal generated by one CCD that is directly delivered to the second CCD. The offset between the two CCDs was determined to be three orders of magnitude below the integration time (2.1 ± 0.2 ns/frame/ms). The microscope is equipped with a heated stage inset (Warner Scientific) and an objective heater (Bioptechs) (*see* Note 16).

2. After initial coarse alignment, use fluorescent focus check beads and diffraction limited multicolor beads for fine mechanical alignment. To do the fine mechanical alignment, image fluorescent beads on both cameras in both channels to compare alignment. Adjust positions by changing the x,y,z of the camera holders so that beads have the same location on both cameras. To check the tilt of the camera plane, prepare a bead sample of uniform distribution that is not saturated and check the focus at center vs. the edges for each camera separately. If you see a difference, change the $\phi$-and $\theta$-angles on the camera holders accordingly.

3. Find cells for imaging taking care to limit bleaching. First, use transmitted light and the whole camera field of view to position 1–3 cells in the active imaging area focused on what is judged to be the middle of the cell(s). Use the reddest channel in the experiment to set the focus for the equatorial plane, as described here this is the NPC marker channel. Images need to be recorded in the equatorial plane of the yeast nucleus to minimize false-positive detection of mRNAs that diffuse above or below the nucleus. Using maximal signal amplification (for EMCCDs) and the lowest possible laser power setting that produces a very noisy live image, adjust focus to image the equatorial plane of the cell nucleus. Start automated imaging protocol for registration image and tracking data (**step #4**).

4. Perform simultaneous imaging on two channels using sub-frames (approximately two-fifths of each camera chip, e.g., 200 × 200 pixel) on both cameras at a frame rate of 67 Hz, equaling a time resolution of 15-ms. For each cell, acquire four datasets, two in each color. First, record a registration image for 375-ms, save,

and 500-ms later, record the tracking dataset for 7.5 s (500 frames) in parallel for both channels. Time values refer to published work and may need to be adjusted for new experiments and the imaging system used; hence, the given values present a starting point for optimization. Imaging sub-frames is critical for data collection at fast rates, allows for cells to be selected that are present in the same imaging plane, and acquired images can be rapidly screened during data collection to determine if the dataset should be saved for analysis or discarded due to signal quality or lack of signal (i.e., cells in which no mRNAs are expressed). Finally, a small imaging area also makes it easier to fulfill the 5% intensity flatness criteria (**step #1** above).

### 3.6 Super-Registration and Colocalization Precision

All image processing and visual analysis is done using FIJI or ImageJ [25, 26]. Custom Plugins for registration and particle tracking are available upon request.

1. Superregistration is achieved by a combination of precise mechanical alignment and image processing using transformations based on the registration signal that is detected on both cameras (Fig. 3a) (*see* Note 17).
2. In the registration images, make the NPC signal visible in both channels by using x10 more excitation power from the 561-nm laser than for the tracking videos. Using the sensitivity of the EM CCD cameras and the surface reflection of the dichroic, the NPC signal will be visible in both the mRNP (one image taken for 375 ms) and the NPC channel (25 images taken in 375 ms, and the mean time projected for analysis). Fine register the mRNP and NPC channels postexperimentally by shifting the NPC channel registration image onto the mRNA channel registration image to calculate the parameters to be used for registration of the tracking videos [27]. To make this alignment more robust, filter the mRNP channel with a Gaussian kernel (1.5 pixel width) before registration. Save RGB images of the two registration images before and after registration and evaluate if the correlation factor of the linear shift is better than 0.95 (*see* Note 18).
3. Determine registration precision by calculating the remaining offset between the imaging data from the two cameras after linear translation (*see* Note 19).
4. Create two copies of each tracking video (NPC and mRNP channel); one is the raw data for quantitative image analysis and the other is enhanced for visual inspection (*see* Note 20).
5. Test each dataset for drift during acquisition by generating 10 mean projections of 50 frames of the NPC signal that are normalized and fused into a color-coded hyperstack. If the color separation in the resulting stack indicates drift, these datasets should be discarded.

### 3.7 Tracking mRNPs and Analyzing mRNP–NPC Interactions

1. Data analysis is performed using a custom manual-tracking interface within FIJI, in which the filtered and raw data are presented simultaneously and a particle of interest is tracked by consecutively clicking through image frames. The maximal displacement from frame to frame is displayed in the tracking channel to identify situations where two particles can be interchanged. In such cases, tracking is stopped.
2. Identify mRNP signals visually in either the filtered or raw images. To do a 2D Gaussian fit, find the center of mass within 5 pixels around the signal and click the position to identify the coordinate for the fit. All fits should be done in the raw data, with all fit parameters and initiation parameters reported to the user for inspection [5].
3. To enhance images for visual inspection, use a running mean and a subtraction of a Laplacian filter for the NPC marker channel and a Laplacian filter for the mRNP channel. The kernel size should be set relative to the theoretical width of the emission point spread function, adjust the contrast in the final RGB videos after processing. After filtering, apply the transition matrix to the NPC marker channel to overlay it onto the mRNP channel.
4. During manual tracking, assign a descriptive state to the particle in each frame based on the distance from the NE using the following guidelines: nuclear diffusive or cytoplasmic diffusive if the distance is >250 nm, nuclear docked or cytoplasmic docked if the distance is between 250 and 100 nm, and transition if the distance is <100 nm. The dynamic behavior of the particle (i.e., the direction and distance the particle moved with respect to the NE) in prior and subsequent frames should also be used to inform state decisions (Fig. 3b).
5. Using these descriptors, perform an analysis in MATLAB (MathWorks) using routines to search for specific events (e.g., export or scanning) based on these five states [6] (*see* Note21).
6. Estimate dwell times using two methods; the dwell time fit based on the histogram (exponential distribution) and an MLE based on the assumption that the data follow an exponential distribution [28, 29] (*see* Note 22).

## 4. Notes

1. When choosing a nuclear pore complex component to tag with a fluorescent protein, it is important to consider both the stability and localization of the protein within the NPC. For example, some Nups are dynamic and known to localize to other structures within the cell, which may complicate analysis. Currently, we use Ndc1 and Nup188. Additionally, not every NPC component can be tagged without impacting function, which should be considered when choosing a Nup to tag. We have observed that tagging of Nup49, previously used in various studies as an NPC marker, shows a weak poly(A)-RNA accumulation

phenotype and should therefore be avoided as an NPC marker (unpublished observations).

2. For high single-to-noise ratio, fluorophore choice should be optimized or chosen carefully. Ideally fluorophores with improved brightness and photostability should be used. Examples of enhanced fluorescent proteins include the far-red variant mKATE or GFP variants such as mNeonGreen [30, 31]. Fluorescent tagging of more than one NPC component may also result in brighter signals; however, some combinations of double tagged Nups are known to result in NPC dysfunction, and it is important to test various combinations for fitness defects [32]. Currently, dye-based labeling systems are less suited for this application (e.g., Spinach & Mango) due to the inability to fuse multiple dye binding aptamers and achieve signals that are bright enough to allow robust single mRNP detection.

3. Tutucci et al. have outlined a method for detection of mRNAs using a reengineered MS2 aptamer-based RNA tagging system [23]. Here, we use a stem loop tagging system derived from the *Pseudomonas* phage PP7, however the same methods described by Tutucci et al. can be followed to generate PP7 stem loop tagged strains. Furthermore, a shorter version of the PP7 repeat cassette containing 12 copies has been used successfully to track single mRNPs [4].

4. Integration of the stem loops into the 3′-UTRis preferred over the 5′-UTRregion of the target gene as it is less likely to impact expression of the gene (insertion into the 5′-UTR can affect mRNA translation and mRNA stability). In the 3'-UTR, stem loops can be inserted just after the stop codon with the endogenous terminator sequence or an exogenous terminator sequence can be used.

5. In order to allow single mRNP tracking in living cells, the target mRNA must be expressed at a low copy number (less than 20 transcripts per cell), as this will minimize issues related to differentiating signals from multiple mRNPs from frame to frame. Inducible reporter systems (e.g., *GAL1* promoter) can also be utilized to control expression of the target mRNA, but single mRNP tracking will only be possible at early stages of induction, as transcript levels will increase rapidly and spatial separation of individual mRNPs becomes challenging [33].

6. Amplification of the repetitive stem loop sequence by PCR can be more difficult when compared to other templates. Tutucci et al. outline a method using Taq DNA polymerase for MS2 stem loop amplification [23]. We have had success using a high-fidelity DNA polymerase such as Phusion (*New England Biolabs*).

7. Diploid strains are preferred due to the larger size of the cell nucleus, but this does require generation of homozygous diploid strains by isolating both haploid mating types and mating the strains.

8. Addition of the 24xPP7 cassette will disrupt the 3′-UTR and add a significant amount of sequence to the mRNA transcript, which may impact expression, stability, and functionality. Therefore, we target essential genes, as nonfunctional transcripts will result in lethality that will be observed during tetrad dissection.

Growth of the tagged strain should also be compared to the parental strain under multiple conditions to verify that there are no growth defects as a result of the addition of the PP7 stem loops when combined with the fluorescent NPC marker. Additionally, single-molecule FISH (smFISH), RT-qPCR, and/or northern blotting experiments should be used to determine expression level and proper decay of the modified mRNA, especially due to the fact that the 24xPP7 cassette can alter mRNA decay or accumulate in cells as partial decay products, [23, 34–36].

**9.** Integration of the PP7-CP coding sequence into the yeast genome is not required and PP7-CP can be expressed on a CEN plasmid instead [6, 23, 33]. However, integration of the PP7-CP cassette provides homogenous expression of the protein and less frequent aggregation of the CP. Aggregation of the CP is a common issue that causes formation of bright foci that will preclude imaging and tracking of single mRNA particles (Fig. 1a, b).

**10.** Expression of the PP7-CP is driven by the *MET25* promoter, which is expressed under conditions of low available methionine. Leaky expression from this promoter is sufficient to produce enough PP7-CP required for live-cell imaging in medium containing methionine; therefore, the strain is grown in synthetic medium supplemented with methionine. Conditions with low amounts or no methionine result in high expression of the PP7-CP, which can produce CP aggregates and a high background that masks signals from individual mRNP particles. Constitutive low expression by using an *ADE3* promoter has also been shown to allow robust single mRNA detection [4].

**11.** It is important to keep cells in exponential growth phase and to not allow cells to reach saturation phase of growth (O. $D_{600} > 1$) in liquid media, as this is accompanied by an increase in PP7-CP expression/aggregation and yeast autofluorescence (Fig. 1a, b).

**12.** Spheroplasting to remove the yeast cell wall decreases light scatter and significantly increases the signal-to-noise ratio of the tagged Nup and mRNA fluorescent signals [6]. However, be careful when handling the cells after digestion. DO NOT VORTEX or pipette the cells too vigorously at or beyond this point. The cells are fragile and susceptible to lysis.

**13.** After removal of the cell wall and recovery of the cells in fresh medium supplemented with sorbitol, there are ~30–60 min for imaging before the cell regrows enough of the cell wall to begin to significantly scatter light and decrease signal-to-noise ratios.

**14.** Use of a 1.3 NA objective enables imaging of ~60% of the yeast nuclear volume within a single focal plane. This allows for tracking of mRNPs for an increased number of frames.

**15.** A dedicated 561 nm NOTCH filter is commercially available from several sources.

16. Any heating system that fits the microscope will be suitable for this imaging setup.

17. Two-color colocalization by wide-field microscopy lacks the resolution to determine whether two molecules are close enough to be in physical contact or simply nearby by chance due to chromatic aberrations in the objective lens. A robust methodology can be used to generate an internal registration signal from each cell imaged that can be used to register spectrally different channels relative to each other to achieve spatial precision below the optical resolution limit. This methodology, superregistration, can be used to correct for chromatic aberration in the objective lens across the entire image field to within 10 nm, which is capable of determining whether two molecules are physically close enough to interact or not [5].

18. Registration can fail because of aberrations caused by heterogeneity in spheroplasting. We have found the failure rate to occur at a frequency of ~50%. In successful cases the resulting registration precision is determined to be 0.14 pixel.

19. To determine registration precision, NPC positions from both imaging channels must be fitted. To do this, apply a linear transformation matrix to match the NPC positions on the mRNP channel with the NPC channel [27]. We use a linear translation since we need to match the features only in 2D and on the XY plane. The transformation is needed since the quality of the registration data does not reach the level of individual nuclear pores [5]. The SD using this method is in the order of the mean.

20. Always display raw data images next to the enhanced images during visual analysis when tracking, and double check all traces of interest in the raw dataset to prevent a false-positive identification of an event as a result of image processing.

21. This classification can be made because the localization precision of single molecules follows a Gaussian distribution described by $\theta - {}^{\Lambda}\theta \sim N(0, C(\theta))$, where $\theta = (x, y, I, bg)$, ${}^{\Lambda}\theta$ is the corresponding MLE, and $C(\theta)$ is CRLB [37].

22. Due to imaging in a single focal plane, the number of mRNP-NPC interactions that will be observed is greatly reduced. Therefore, two methods are used to estimate mRNP dwell times.

## Acknowledgments

We would like to acknowledge the laboratories of Drs. Robert Singer and Karsten Weis for reagents and support of previous works related to the methods described here. A.L. was supported by a Natural Sciences and Engineering Research Council Canada Graduate Scholarship; D.Z. is supported by the Canadian Institutes of Health (Project Grant-366682), Fonds de recherche du Québec—Santé (Chercheur-boursier Junior 2), Canada Foundation for Innovation, and the Natural Sciences and Engineering Research Council; D.G. by a National Institute of General Medical Sciences award (5R01GM123541); B.M. and D.G. by a National Institute of General Medical Sciences award (5R01GM124120). The content is solely the responsibility of the authors and does not necessarily represent the official views of the National Institutes of Health.

## References


1. Kim SJ, Fernandez-Martinez J, Nudelman I et al. (2018) Integrative structure and functional anatomy of a nuclear pore complex. Nature 555:475 [PubMed: 29539637]
2. Folkmann A, Noble K, Cole C (2011) Dbp5, Gle1-IP6, and Nup159: a working model for mRNP export. Nucleus 2(6):540–548 [PubMed: 22064466]
3. Green DM, Johnson CP, Hagan H, Corbett AH (2003) The C-terminal domain of myosin-like protein 1 (Mlp1p) is a docking site for heterogeneous nuclear ribonucleoproteins that are required for mRNA export. Proc Natl Acad Sci U S A 100:1010–1015. 10.1073/pnas.0336594100 [PubMed: 12531921]
4. Saroufim M-A, Bensidoun P, Raymond P et al. (2015) The nuclear basket mediates perinuclear mRNA scanning in budding yeast. J Cell Biol 211:1131–1140. 10.1083/jcb.201503070 [PubMed: 26694838]
5. Grünwald D, Singer RH (2010) In vivo imaging of labelled endogenous β-actin mRNA during nucleocytoplasmic transport. Nature 467:604–607. 10.1038/nature09438 [PubMed: 20844488]
6. Smith C, Lari A, Derrer CP et al. (2015) In vivo single-particle imaging of nuclear mRNA export in budding yeast demonstrates an essential role for Mex67p. J Cell Biol 211:1121–1130. 10.1083/jcb.201503135 [PubMed: 26694837]
7. Siebrasse JP, Kaminski T, Kubitscheck U (2012) Nuclear export of single native mRNA molecules observed by light sheet fluorescence microscopy. Proc Natl Acad Sci U S A 109:9426–9431. 10.1073/pnas.1201781109 [PubMed: 22615357]
8. Mor A, Suliman S, Ben-Yishay R et al. (2010) Dynamics of single mRNP nucleocytoplasmic transport and export through the nuclear pore in living cells. Nat Cell Biol 12:543–552. 10.1038/ncb2056 [PubMed: 20453848]
9. Niño CA, Hérissant L, Babour A, Dargemont C (2013) mRNA nuclear export in yeast. Chem Rev 113:8523–8545. 10.1021/cr400002g [PubMed: 23731471]
10. Floch AG, Palancade B, Doye V (2014) Fifty years of nuclear pores and nucleocytoplasmic transport studies: multiple tools revealing complex rules. Methods Cell Biol 122C:1–40. 10.1016/B978-0-12-417160-2.00001-1
11. Oeffinger M, Zenklusen D (2012) To the pore and through the pore: a story of mRNA export kinetics. Biochim Biophys Acta 1819:494–506. 10.1016/j.bbagrm.2012.02.011 [PubMed: 22387213]
12. Heinrich S, Derrer CP, Lari A et al. (2017) Temporal and spatial regulation of mRNA export: single particle RNA-imaging provides new tools and insights. BioEssays 39 10.1002/bies.201600124
13. Pichon X, Lagha M, Mueller F, Bertrand E (2018) A growing toolbox to image gene expression in single cells: sensitive approaches for demanding challenges. Mol Cell 71:468–480. 10.1016/J.MOLCEL.2018.07.022 [PubMed: 30075145]
14. Hocine S, Raymond P, Zenklusen D et al. (2013) Single-molecule analysis of gene expression using two-color RNA labeling in live yeast. Nat Methods 10:119–121. 10.1038/nmeth.2305 [PubMed: 23263691]
15. Bertrand E, Chartrand P, Schaefer M et al. (1998) Localization of AsH1 mRNA particles in living yeast. Mol Cell 2:437–445. 10.1016/S1097-2765(00)80143-4 [PubMed: 9809065]
16. Larson DR, Zenklusen D, Wu B et al. (2011) Real-time observation of transcription initiation and elongation on an endogenous yeast gene. Science 332:475–478. 10.1126/science.1202142 [PubMed: 21512033]
17. Tutucci E, Vera M, Biswas J et al. (2018) An improved MS2 system for accurate reporting of the mRNA life cycle. Nat Methods 15:81–89. 10.1038/nmeth.4502 [PubMed: 29131164]
18. Güldener U, Heck S, Fielder T et al. (1996) A new efficient gene disruption cassette for repeated use in budding yeast. Nucleic Acids Res 24:2519–2524 [PubMed: 8692690]
19. Chan LY, Mugler CF, Heinrich S et al. (2018) Non-invasive measurement of mRNA decay reveals translation initiation as the major determinant of mRNA stability. elife 7 10.7554/eLife.32536
20. Sherman BF, Sherman MF, Enzymol M (2003) Getting started with yeast. Contents 41:3–41

21. Gietz RD, Woods RA (2002) Transformation of yeast by lithium acetate/single-stranded carrier DNA/polyethylene glycol method. Methods Enzymol 350:87–96. 10.1016/S0076-6879(02)50957-5 [PubMed: 12073338]
22. Longtine MS, McKenzie A 3rd, Demarini DJ et al. (1998) Additional modules for versatile and economical PCR-based gene deletion and modification in Saccharomyces cerevisiae. Yeast 14:953–961. 10.1002/(SICI)1097-0061(199807)14:10<953::AID-YEA293>3.0.CO;2-U [PubMed: 9717241]
23. Tutucci E, Vera M, Singer RH (2018) Single-mRNA detection in living S. cerevisiae using a re-engineered MS2 system. Nat Protoc 13:2268–2296. 10.1038/s41596-018-0037-2 [PubMed: 30218101]
24. Amberg DC, Burke DJ, Strathern JN (2006) Tetrad dissection. Cold Spring Harb Protoc 2006:pdb.prot4181 10.1101/pdb.prot4181
25. Schindelin J, Arganda-Carreras I, Frise E et al. (2012) Fiji: an open-source platform for biological-image analysis. Nat Methods 9:676–682. 10.1038/nmeth.2019 [PubMed: 22743772]
26. Schneider CA, Rasband WS, Eliceiri KW (2012) NIH Image to ImageJ: 25 years of image analysis. Nat Methods 9:671–675 [PubMed: 22930834]
27. Preibisch S, Saalfeld S, Tomancak P (2009) Globally optimal stitching of tiled 3D microscopic image acquisitions. Bioinformatics 25:1463–1465. 10.1093/bioinformatics/btp184 [PubMed: 19346324]
28. Colquhoun D, Hawkes AG (1982) On the stochastic properties of bursts of single ion channel openings and of clusters of bursts. Philos Trans R Soc Lond Ser B Biol Sci 300:1–59 [PubMed: 6131450]
29. Kubitscheck U, Grünwald D, Hoekstra A et al. (2005) Nuclear transport of single molecules. J Cell biol 168:233–243. 10.1083/jcb.200411005 [PubMed: 15657394]
30. Shaner NC, Lambert GG, Chammas A et al. (2013) A bright monomeric green fluorescent protein derived from Branchiostoma lanceolatum. Nat Methods 10:407 [PubMed: 23524392]
31. Shcherbo D, Merzlyak EM, Chepurnykh TV et al. (2007) Bright far-red fluorescent protein for whole-body imaging. Nat Methods 4:741 [PubMed: 17721542]
32. Ryan KJ, McCaffery JM, Wente SR(2003) The Ran GTPase cycle is required for yeast nuclear pore complex assembly. J Cell Biol 160:1041–1053. 10.1083/jcb.200209116 [PubMed: 12654904]
33. Bensidoun P, Raymond P, Oeffinger M, Zenklusen D (2016) Imaging single mRNAs to study dynamics of mRNA export in the yeast Saccharomyces cerevisiae. Methods 98:104–114. 10.1016/j.ymeth.2016.01.006 [PubMed: 26784711]
34. Trcek T, Rahman S, Zenklusen D (2018) Measuring mRNA decay in budding yeast using single molecule FISH. Methods Mol Biol 1720:35–54. 10.1007/978-1-4939-7540-2_4 [PubMed: 29236250]
35. Garcia JF, Parker R (2015) MS2 coat proteins bound to yeast mRNAs block 5′ to 3′ degradation and trap mRNA decay products: implications for the localization of mRNAs by MS2-MCP system. RNA 21:1393–1395. 10.1261/rna.051797.115 [PubMed: 26092944]
36. Heinrich S, Sidler CL, Azzalin CM, Weis K (2017) Stem-loop RNA labeling can affect nuclear and cytoplasmic mRNA processing. RNA 23:134–141. 10.1261/rna.057786.116 [PubMed: 28096443]
37. Sengupta SK, Kay SM (1995) Fundamentals of statistical signal processing: estimation theory. Technometrics 37:465 10.2307/1269750

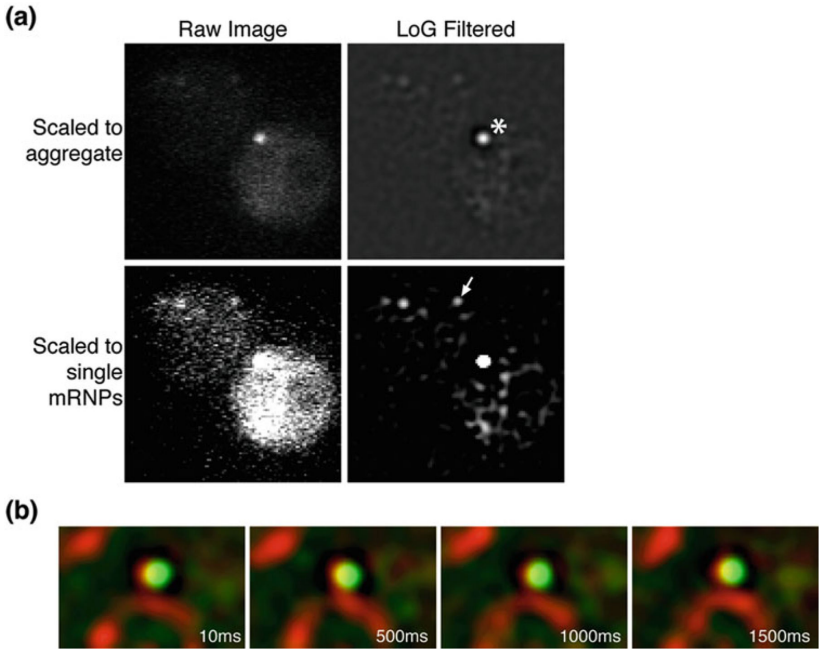


**Fig. 1.**

(**a**) Fluorescent images showing a cell in which PP7-CP has formed a bright aggregate. Raw and Laplacian filtered images are shown, each scaled to show the presence of the aggregate (asterisk) and single mRNP (arrow). Scaling to observe single mRNPs leads to difficulty in tracking single due to the presence of a bright foci. (**b**) Merged and registered images showing the bright PP7-CP aggregate in panel (**a**) persists in the same location through the imaging series, whereas single mRNPs are usually dynamic. Green channel = CP, red channel = nuclear pore complexes (NPCs)

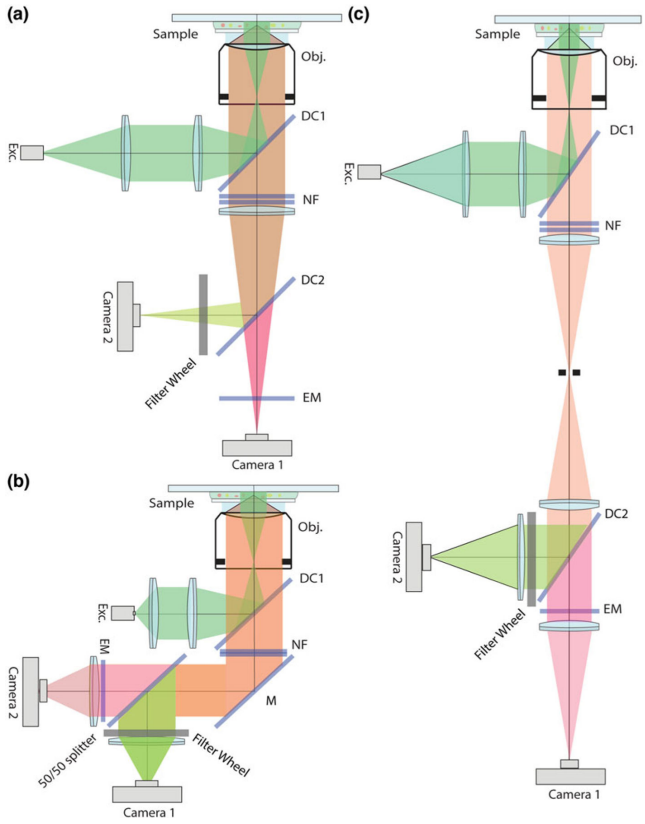


**Fig. 2.**

Optical design of the custom-built microscope. (**a**) Optical setup described previously in Grunwald et al. [5]. (**b**) Optical setup described here for data acquisition and described previously by Smith et al. [6]. (**c**) Optical setup to use as an adapter for imaging with commercial microscopes

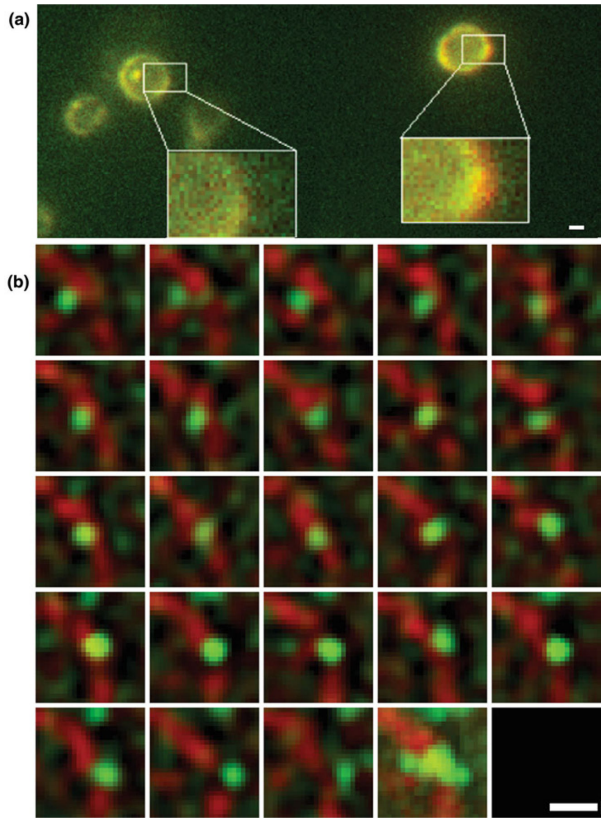


**Fig. 3.**

(**a**) Example of the color overlay used for registration. Using an RGB scheme, images before and after registration are overlaid to visualize the shift in nuclear envelope position in each cell. This method aids in quantification of whether the correlation factor for the linear shift is higher than the set threshold for 0.95 or not. The red pixels shown help to visualize the shift. (**b**) Example of an mRNP export event through selected frames of a tracking dataset. Second to last square shows all frames merged. Green = CP and red = nuclear pore complexes (NPCs). Scale bars = 1 $\mu$m